PCT

INTERNATIONAL APPLICATION PUBLISHED UNDER THE PATENT COOPERATION TREATY (PCT)

(54) Title: VERTICAL ADAPTIVE ANTENNA ARRAY FOR A DISCRETE MULTITONE SPREAD SPECTRUM COMMUNICATIONS SYSTEM

(57) Abstract

Two or more antenna elements are arranged in the vertical direction to give vertical spatial adaptivity to a wireless discrete multitone spread spectrum communications system. The system is based on a combination of Discrete Multitone Spread Spectrum (DMT–SS) and multi–element adaptive antenna array technologies. This enables the automatic positioning of a beam in the vertical direction to position nulls where interferers are located on the same azimuth but are separated in elevation.

VERTICAL ADAPTIVE ANTENNA ARRAY FOR A DISCRETE MULTITONE SPREAD SPECTRUM COMMUNICATIONS SYSTEM

5

Field of the Invention

This invention involves improvements to a wireless a discrete multitone spread spectrum communications system.

The invention disclosed herein is related to the copending US patent application by

10   S. Alamouti, D. Michaelson, E. Casas, E. Hoole, G. Veintimilla, H. Zhang, M. Hirano, and P. Poon, entitled "Method for Frequency Division Duplex Communications in a Personal Wireless Access Network", serial number   , filed on the same day as the instant patent application, assigned to AT&T, and incorporated herein by reference.

15   ## Background of the Invention

Wireless communications systems, such as cellular and personal communications systems, operate over limited spectral bandwidths. They must make highly efficient use of the scarce bandwidth resource to provide good service to a large population of users.

20   Code Division Multiple Access (CDMA) protocol has been used by wireless communications systems to efficiently make use of limited bandwidths. The protocol uses a unique code to distinguish each user's data signal from other users' data signals. Knowledge of the unique code with which any specific information is transmitted, permits the separation and reconstruction of each user's message at the receiving end of the

25   communication channel.

The personal wireless access network (PWAN) system described below, uses a form of the CDMA protocol known as discrete multitone spread spectrum (DMT-SS) to provide efficient communications between a base station and a plurality of remote units. (The term "discrete multitone stacked carrier (DMT-SS)" also refers to this protocol.) In

30   this protocol, the user's data signal is modulated by a set of weighted discrete frequencies or tones. The weights are spreading codes that distribute the data signal over many discrete tones covering a broad range of frequencies. The weights are complex numbers with the real component acting to modulate the amplitude of a tone while the complex component of the weight acts to modulate the phase of the same tone. Each tone in the

35   weighted tone set bears the same data signal. Plural users at the transmitting station can use the same tone set to transmit their data, but each of the users sharing the tone set has a

different set of spreading codes. The weighted tone set for a particular user is transmitted to the receiving station where it is processed with despreading codes related to the user's spreading codes, to recover the user's data signal. For each of the spatially separated antenna array elements at the receiver, the received multitone signals are transformed from time domain signals to frequency domain signals. Despreading weights are assigned to each frequency component of the signals received by each antenna array element. The values of the despreading weights are combined with the received signals to obtain an optimized approximation of individual transmitted signals characterized by a particular multitone set and transmitting location. The PWAN system has a total of 2560 discrete tones (carriers) equally spaced in 8 MHZ of available bandwidth in the range of 1850 to 1990 MHZ. The spacing between the tones is 3.125 kHz. The total set of tones are numbered consecutively from 0 to 2559 starting from the lowest frequency tone. The tones are used to carry traffic messages and overhead messages between the base station and the plurality of remote units. The traffic tones are divided into 32 traffic partitions, with each traffic channel requiring at least one traffic partition of 72 tones.

In addition, the PWAN system uses overhead tones to establish synchronization and to pass control information between the base station and the remote units. A Common Link Channel (CLC) is used by the base to transmit control information to the Remote Units. A Common Access Channel (CAC) is used to transmit messages from the Remote Unit to the Base. There is one grouping of tones assigned to each channel. These overhead channels are used in common by all of the remote units when they are exchanging control messages with the base station.

In the PWAN system, Time Division Duplexing (TDD) is used by the base station and the remote unit to transmit data and control information in both directions over the same multi-tone frequency channel. Transmission from the base station to the remote unit is called forward transmission and transmission from the remote unit to the base station is called reverse transmission. The time between recurrent transmissions from either the remote unit or the base station is the TDD period. In every TDD period, there are four consecutive transmission bursts in each direction. Data is transmitted in each burst using multiple tones. The base station and each remote unit must synchronize and conform to the TDD timing structure and both the base station and the remote unit must synchronize to a framing structure. All remote units and base stations must be synchronized so that all remote units transmit at the same time and then all base stations transmit at the same time. When a remote unit initially powers up, it acquires synchronization from the base station so that it can exchange control and traffic messages within the prescribed TDD time format. The remote unit must also acquire frequency and phase synchronization for the

DMT-SS signals so that the remote is operating at the same frequency and phase as the base station.

The PWAN system provides for base station beam steering in the horizontal plane. Interference sources that are located in substantially the same horizontal plane as the base station antenna array can have their effects reduced by steering the received sensitivity direction away from that source. A corresponding horizontal shift can be made in the transmitted beam direction to avoid creating interference at the location of the interfering source. In effect, nulls are steered onto the interfering sources. However, a problem arises when there are interfering sources located in the same radial direction from the base station as a remote unit but are separated in the vertical plane. Such sources cannot be adequately minimized by the PWAN system as the beam and null resolution attained in the horizontal plane is insufficient.

Summary of the Invention

This problem is solved, in accordance with the invention, by providing two or more antenna arrays, here called subarrays arranged in the vertical direction to give spatial adaptivity in the vertical plane to the wireless discrete multitone spread spectrum communications system. The PWAN system is based on a combination of Discrete Multitone Spread Spectrum (DMT-SS) and multi-element adaptive antenna array technologies. The inventors have discovered that the spatial and spectral processing of the DMT--SS signals received or transmitted from the base station antenna array is independent of the type of antenna array utilized. This processing maximized the overall signal -to-interference level of a base station's coverage area. Using vertically-separated subarrays (composed of horizontal antenna elements) enables the base station to position beams on remote units in the vertical plane as well as position nulls on interferers located at the same azimuth angle as the remote but which are separated in elevation angle. This additional vertical plane adaptivity will enhance the PWAN system's overall performance and improve the signal-to-interference level.

The invention is a highly bandwidth-efficient communications method to enable vertical and horizontal receive beam steering, that includes the following steps. The base station receives a first spread signal at a base station having a multi-subarray antenna array with a first plurality of subarrays arranged in a spaced vertical direction and a second plurality of subarray elements arranged in a spaced horizontal direction. The first spread signal comprises a first data signal spread over a plurality of discrete tones in accordance

with a remote spreading code assigned to a remote unit for a first time period. The base station adaptively despreads the received signal by using first despreading codes that are based on the characteristics of the received signals at the first plurality of subarrays of the array. The vertical displacement of the subarrays enables the base station to perform

5   vertical, receive beam steering. In addition, the base station adaptively despreads the signal received by using second despreading codes that are based on the characteristics of the received signals at the second plurality of subarray elements of the array. The horizontal displacement of the subarray elements enables the base station to perform horizontal, receive beam steering.

10   The invention also enables transmit beam steering in the vertical and horizontal directions. The method includes the following additional steps. The base station spreads a second data signal with first spreading codes derived from the first despreading codes, that distributes the second data signal over a plurality of discrete tones and the first plurality subarrays of the array, forming a first spectrally spread signal that is spatially

15   spread vertically. The vertical displacement of the subarray enables the base station to perform vertical, transmit beam steering. The base station also spreads the second data signal with second spreading codes derived from the second despreading codes, that distributes the second data signal over the plurality of discrete tones and the second plurality subarray elements of the array, forming a second spectrally spread signal that is

20   spatially spread horizontally. The horizontal displacement of the subarray enables the base station to perform horizontal, transmit beam steering. The base station then transmits the first and second spread signals during a second time period.

        The invention has advantageous applications in the field of wireless communications, such as cellular communications or personal communications, where

25   bandwidth is scarce compared to the number of the users and their needs. Such applications may be effected in mobile, fixed, or minimally mobile systems.

Brief Description of the Drawings

        In the drawings:

30   FIGURE 1A shows a linear antenna array at a base station where the signal processor distinguishes two discrete monotone signals received from two remote units that are placed far from one another.

        FIGURE 1B shows a vertical and horizontal, two dimensional antenna array at the base station, in accordance with the invention, where the signal processor distinguishes

35   two discrete monotone signals received from the two remote units X and Y that are separated from one another in the vertical plane.

FIGURE 1C shows the linear antenna array at the base station of FIGURE 1A, where the signal processor processes two discrete monotone signals for transmission to two remote units that are displaced from one another.

FIGURE 1D shows the vertical and horizontal, two dimensional antenna array at the base station of FIGURE 1B, in accordance with the invention, where the signal processor processes two discrete monotone signals for transmission to two remote units that are separated from one another in the vertical plane.

FIGURE 2 shows an alternate embodiment of the vertical and horizontal, two dimensional antenna array at the base station of FIGURE 1B and FIGURE 1D, in accordance with the invention, the elements of each subarray are disposed around a cylinder.

FIGURE 3A is a tutorial diagram illustrating an example of pure spectral diversity, showing how a receiver distinguishes two sets of discrete multitone signals from two transmitters that are placed close to one another, in accordance with the PWAN system.

FIGURE 3B is a tutorial diagram illustrating an example of pure spatial diversity, showing how a receiver distinguishes two discrete monotone signals from two transmitters that are placed far from one another, in accordance with the PWAN system.

FIGURE 3C is a tutorial diagram illustrating an example of both spectral and spatial diversity, showing how a receiver distinguishes two discrete multitone signals from two transmitters that are placed far from one another, in accordance with the PWAN system.

FIGURE 3D is a high-level schematic representation of an implementation of the PWAN system in a fixed wireless communication system.

FIGURE 3E is a simplified representation of multitone transmission.

FIGURE 3F is a simplified representation of the use of a discrete multitone spread spectrum signal format.

FIGURE 4 is a simplified representation of the matrix formalism used in an implementation of the PWAN system.

FIGURE 5 is a simplified representation of the matrix formalism, used in an implementation of the PWAN system, that includes the effects of channel response.

FIGURE 6 is a simplified representation of DMT-SS using an exemplary higher order QAM modulation format.

FIGURE 7 is a timing diagram that illustrates the general time division duplex signal and protocol used in an embodiment of the PWAN system.

FIGURE 8 is a signal processing flow diagram that depicts the main signal processing steps used in an embodiment of the PWAN system to provide for high bandwidth efficiency.

FIGURE 9 is a signal processing flow diagram that illustrates a method used to spread the encoded carrier signal.

FIGURE 10 is a three-dimensional plot of the signal to interference plus noise ratio versus code weights and spatial weights applied to the transmitted and received signals.

FIGURE 11 is a perspective cut away view showing an embodiment of a base station antenna.

FIGURE 12 is a perspective cut away view showing a second embodiment of a base station antenna.

FIGURE 13 graphically depicts the null steering aspect of the present PWAN system.

FIGURE 14 is a schematic representation of an inverse frequency channelized spreader implementation.

FIGURE 15 is a schematic representation of a frequency channelized despreader implementation.

FIGURE 16 is a plot of antenna gain versus angular direction.   -

FIGURE 17 is a highly simplified block diagram that illustrates one particular application of the highly bandwidth-efficient communications network of the present PWAN system.

FIGURE 18 is a list of the possible operational frequency bands of a specific embodiment of the PWAN system.

FIGURE 19 shows the RF Band/Sub-band organization of the airlink of a specific embodiment of the PWAN system.

FIGURE 20 shows the tones within each sub-band of a specific embodiment of the PWAN system

FIGURE 21 shows the traffic partitions in a specific embodiment of the PWAN system

FIGURE 22 shows the tone mapping to the ith traffic partition

FIGURE 23 shows the overhead tone Mapping to Channels for the ith Sub-band Pair

FIGURE 24 shows the Division of Tone Space to Traffic and Overhead Tones

FIGURE 25 shows the time Division Duplex format for Base and Remote Unit Transmissions

FIGURE 26 shows Details of the Forward and Reverse Channel Time Parameters

FIGURE 27 shows the TDD Parameter Values

FIGURE 28 shows the Physical Layer Framing Structure

FIGURE 29 shows the Phase A Sub-band Pair Assignment Within a Cell

FIGURE 30 shows the Phase-A Sub-band Pair Assignment Across Cells

FIGURE 31 is a Functional Block Diagram for the Upper Physical Layer of Base Transmitter for High Capacity Mode

FIGURE 32 is a Data Transformation Diagram for the High Capacity Forward Channel Transmissions

FIGURE 33 is a Functional Block Diagram for the Upper Physical Layer of Base Transmitter for Medium Capacity Mode

FIGURE 34 is a Data Transformation Diagram for the Medium Capacity Forward Channel Transmissions

FIGURE 35 is a Functional Block Diagram for the Upper Physical Layer of Base Transmitter for Low Capacity Mode

FIGURE 36 is a Data Transformation Diagram for the Low Capacity Forward Channel Transmissions

FIGURE 37 is a representation of the Triple DES Encryption Algorithm

FIGURE 38 depicts a Feed Forward Shift Register Implementation of Rate 3/4, 16PSK Trellis Encoder for High Capacity Mode

FIGURE 39 depicts a Feed Forward Shift Register Implementation of Rate 3/4, 16QAM Trellis Encoder for High Capacity Mode

FIGURE 40 shows the Signal Mappings for Rate 3/4, 16QAM and 16PSK Trellis Encoding Schemes Employed in High Capacity Mode

FIGURE 41 shows the Signal Mappings for Rate 3/4, Pragmatic 16 QAM and 16 PSK Trellis Encoding Schemes Employed in High Capacity Mode

FIGURE 42 depicts a Feed Forward Shift Register Implementation of Rate 2/3, 8PSK Trellis Encoder for Medium Capacity Mode

FIGURE 43 depicts a Feed Forward Shift Register Implementation of Rate 2/3 8QAM Trellis Encoder for Medium Capacity Mode

FIGURE 44 shows the Signal Mappings for Rate 2/3, 8QAM and 8PSK Trellis Encoding Schemes Employed in Medium Capacity Mode

FIGURE 45 shows the Signal Mappings for Rate 2/3, 8QAM and 8PSK Trellis Encoding Schemes Employed in Medium Capacity Mode

FIGURE 46 depicts a Feed Forward Shift Register Implementation of Rate « Convolutional Encoder for Low Capacity Mode

FIGURE 47 shows the Signal Mapping for Rate «, QPSK Pragmatic Trellis Encoding Scheme Employed in Low Capacity Mode

FIGURE 48 shows the Gray-Coded Mapping for Rate «, QPSK Pragmatic Trellis Encoding Scheme Employed in Low Capacity Mode

FIGURE 49 shows the Base Mapping of Elements of Received Weight Vectors to Antenna Elements and Tones

FIGURE 50 is a Block Diagram Representation of CLC Physical Layer Format

FIGURE 51 shows the QPSK Signal Mapping for the CLC Channel

FIGURE 52 is a representation of the CLC Interleaving Rule

FIGURE 53 shows the Tone Mapping of (4 x 4) Interleaved Matrix Elements

FIGURE 54 is a Block Diagram Representation of BRC Physical Layer Format

FIGURE 55 shows the Tone Mapping of the (4 x 4) Interleaved Matrix Elements

FIGURE 56 is a representation of a Broadcast Channel Beam Sweep

FIGURE 57 is a Functional Block Diagram of the Upper Physical Layer of Remote Unit Transmitter for High Capacity Mode

FIGURE 58 is a Data Transformation Diagram for the High Capacity Reverse Channel Transmissions

FIGURE 59 is a Functional Block Diagram for the Upper Physical Layer of Remote Unit Transmitter for Medium Capacity Mode

FIGURE 60 is a Data Transformation Diagram for the Medium Capacity Reverse Channel Transmissions

FIGURE 61 is a Functional Block Diagram for the Upper Physical Layer of Remote Unit Transmitter for Low Capacity Mode

FIGURE 62 is a Data Transformation Diagram for the Low Capacity Reverse Channel Transmissions

FIGURE 63 shows the Remote Unit Tone Mapping of Received Weight Vector Elements

FIGURE 64 is a Block Diagram Representation of the CAC Physical Layer Format

FIGURE 65 shows the BPSK Signal Mapping for the CAC Channel

FIGURE 66 depicts the CAC Interleaving Rule

FIGURE 67 shows the Tone Mapping of the (8 x 2) Interleaved Matrix Elements

FIGURE 68 is a Functional Block Diagram for the Lower Physical Layer of Base Transmitter

FIGURE 69 shows Tone Mapping into DFT Bins

FIGURE 70 shows Tone Mapping into DFT Bins

FIGURE 71 is a block diagram that illustrates the main structural and functional elements of the bandwidth on demand communications network of the present PWAN system.

FIGURE 72 is a functional block diagram that illustrates the main functional elements of the high bandwidth remote access station.

FIGURE 73 is a functional block diagram that shows the main functional components of the high bandwidth base station.

FIGURE 74 is an overall system schematic block diagram that shows the main structural and functional elements of one implementation of the highly bandwidth-efficient communication system in greater detail.

FIGURES 75A depict the digital architecture within an exemplary remote access terminal.

FIGURES 75B depict the digital architecture within an exemplary remote access terminal.

FIGURE 76 is a software block diagram that indicates the general processing steps performed by each of the digital signal processing chips within the digital signal processing architecture of FIGURES 75A and 75B.

FIGURES 77A-77D are block diagrams that show in detail the digital architecture of the LPA cards of FIGURES 75A and 75B.

FIGURES 78A-78C are block diagrams that detail the digital architecture used to support the main digital signal processing chips on the interface card of FIGURES 75A and 75B.

FIGURES 79A-79D are a schematic block diagram that depicts the overall digital signal processing architectural layout within an exemplary base station of the present PWAN system.

FIGURE 80 is a schematic block diagram showing a dual band radio frequency transceiver that may advantageously be used in the high bandwidth remote access station shown in FIGURE 74.

FIGURE 80A is a schematic block diagram showing the main internal functional elements of the synchronization circuitry shown in FIGURE 80.

FIGURE 81 is a schematic block diagram depicting a dual band radio frequency transceiver that may advantageously be implemented within the high bandwidth base station shown in FIGURE 74.

FIGURE 81A is a simplified schematic block diagram showing the main internal components of the frequency reference circuit shown in FIGURE 81.

FIGURE 82 is a schematic block diagram of a dual band radio frequency transmitter of a type that may advantageously be implemented within a base station constructed in accordance with the present PWAN system.

FIGURE 83 depicts the bandwidth allocation method performed by the bandwidth demand controller of FIGURE 74.

FIGURE 84A and FIGURE 84B show an alternate embodiment of the PWAN system, where the spectral processing and the spatial processing are separated. The spatial weights are computed independently for each carrier frequency.

Figure 85 is an illustrative flow chart of an embodiment of the adaptive solution of spectral and spatial weights.

Detailed Description of the Preferred Embodiment

The invention is a highly bandwidth-efficient communications method to enable vertical and horizontal receive beam steering, that includes the following steps. The base
5   station receives a first spread signal at a base station having a multi-subarray antenna array with a first plurality of antenna elements arranged in a spaced vertical direction and a second plurality of subarray elements arranged in a spaced horizontal direction. The first spread signal comprises a first data signal spread over a plurality of discrete tones in accordance with a remote spreading code assigned to a remote unit for a first time period.
10 The base station adaptively despreads the received signal by using first despreading codes that are based on the characteristics of the received signals at the first plurality of subarrays of the array. The vertical displacement of the subarrays enables the base station to perform vertical, receive beam steering. In addition, the base station adaptively despreads the signal received by using second despreading codes that are based on the
15 characteristics of the received signals at the second plurality of subarray elements of the array. The horizontal displacement of the subarray elements enables the base station to perform horizontal, receive beam steering.

The invention also enables transmit beam steering in the vertical and horizontal directions. The method includes the following additional steps. The base station spreads
20 a second data signal with first spreading codes derived from the first despreading codes, that distributes the second data signal over a plurality of discrete tones and the first plurality of subarrays of the array, forming a first spectrally spread signal that is spatially spread vertically. The vertical displacement of the subarrays enables the base station to perform vertical, transmit beam steering. The base station also spreads the second data
25 signal with second spreading codes derived from the second despreading codes, that distributes the second data signal over the plurality of discrete tones and the second plurality of subarray elements of the array, forming a second spectrally spread signal that is spatially spread horizontally. The horizontal displacement of the subarray elements enables the base station to perform horizontal, transmit beam steering. The base station
30 then transmits the first and second spread signals during a second time period.

The invention uses pilot tones to make successively more precise estimates of the despreading codes. This process begins in an initialization period, when the base station receives a pilot spread signal comprising a known data signal spread over a plurality of discrete tones. The signal processor in the base station correlates the known data signal
35 from the pilot spread signal with a reference known data signal and forms the despreading codes. For the vertically displaced subarrays, a first despreading code is estimated that is

based on the characteristics of the received signals at the subarrays , where a given element of the first despreading code corresponds to a given one of the vertical antenna elements and a given one of the discrete tones. In a similar manner, for the horizontally displaced elements of each subarray,, the signal processor correlates the known data signal

5   from the pilot spread signal with the reference known data signal and forms the second despreading code that is based on the characteristics of the received signals at the subarray elements. A given element of the despreading code corresponds to a given one of the subarray elements and a given one of the discrete tones.

FIGURE 1A shows a linear antenna array at a base station where the signal

10   processor distinguishes two discrete monotone signals received from two remote units that are placed far from one another. Transmitting remote unit X receives an input data signal shown as a white data signal from a first sender. The first sender is assigned a unique code of "1" that is used by the encoder at remote unit X to encode the white data signal. In this example, there is only one tone at remote unit X. The encoder encodes the

15   white data signal onto a single discrete frequency or tone: Tone 1. The white data signal is copied onto the tone. The magnitude of a code digit value is converted by the encoder into a corresponding magnitude phase delay in positioning the copy of the white signal onto the discrete tone. A phase delay corresponding to a code digit value of 1 is shown as positioning the copy of the white signal on its discrete tone at the time T1. (This example

20   introduces the reader to the invention's feature of spectral spreading by portraying the phase encoding of the signal as a time delay modulation.) FIGURE 1A also shows transmitting remote unit Y receiving an input data signal shown as a black data signal from a second sender. Remote unit Y is geographically distant from remote unit X. In this example, the second sender is assigned the same unique code of "1" at that for the first

25   sender. Thus, the black data signal is also copied onto the first discrete tone 1. A phase delay corresponding to a code digit value of 1 is shown as positioning the copy of the black signal onto its discrete tone at the time T1. Both remote units X and Y have used the same tone and phase to transmit their respective data. In this example, we rely on the diverse geographic locations of remote units X and Y to distinguish the signals transmitted

30   from the two remote units. This is an example of spatial diversity. The two signals from remote unit X and remote unit Y are diverse because the phases of their tones will appear arrive at different times at a receiver.

This spatial diversity is detected by the receiving base station Z of FIGURE 1A, in accordance with one aspect of the PWAN system. The direction of transmission from the

35   remote units to the base station is referred to herein as the reverse channel and occurs in the reverse interval of a time division duplex (TDD) period. FIGURE 1A shows the

receiving base station Z receiving the discrete monotone signals on its four antennas A, B, C, and D over reverse channels from the remote units X and Y in. The signals are processed by a signal processor computer using the PWAN spatial and spectral despreading codes and stored in a memory. The memory at the receiving base station Z is organized so that each bin is associated with one of the four antennas at the receiving base station and with one tone out of a possible plurality of four tones. If there were four possible tones, then each antenna A, B, C, and D would have four bins in the memory. As before, each bin is further divided into four sub-bins for each of the four possible phases, T1, T2, T3, and T4. FIGURE 1A shows how the bins and sub-bins in the memory of base station Z store the patterns of the white data received on the four antennas A, B, C, and D from remote unit X. The base station computes updated values for its despreading weights based on the most recent data received on the reverse channel, as is described below for the PWAN system.

FIGURE 1A also shows how the bins and sub-bins in the memory of base station Z store the patterns of the black data received on the four array elements A, B, C, and D from remote unit Y. The signal processor at base station Z uses the process of spatial despreading, in accordance with one aspect of the PWAN system, to distinguish the white data from the black data. The first user's unique code "1" and the relative phase delays in the arrival of the white data to the four array elements A, B, C, and D is used here to form a first spatial despreading code to extract the white data form all of the signals received by array elements A, B, C, and D. The second user's unique code "1"and the relative phase delays in the arrival of the black data to the four antennas A, B, C, and D is used here to form a second spatial despreading code to extract the black data from all of the signals received by element A.

FIGURE 1B shows a vertical and horizontal, two dimensional antenna array at the base station, in accordance with the invention, where the signal processor distinguishes two discrete monotone signals received from the two remote units X and Y that are separated from one another in the vertical plane. The remote unit X is at a relatively high elevation angle and remote unit Y is at a relatively low elevation angle. Both remote units are positioned off-axis from the normal to the plane of the antenna array. In accordance with the invention, array elements A and D have been arranged to be vertically displaced and antenna elements B and C have been arranged to be horizontally displaced. Transmitting remote unit X receives an input data signal shown as a white data signal from a first sender. The first sender is assigned a unique code of "1" that is used by the encoder at remote unit X to encode the white data signal. In this example, there is only one tone at remote unit X. The encoder encodes the white data signal onto a single discrete frequency

or tone: Tone 1. The white data signal is copied onto the tone. The magnitude of a code digit value is converted by the encoder into a corresponding magnitude phase delay in positioning the copy of the white signal onto the discrete tone. A phase delay corresponding to a code digit value of 1 is shown as positioning the copy of the white

5 signal on its discrete tone at the time T1. FIGURE 1B also shows transmitting remote unit Y receiving an input data signal shown as a black data signal from a second sender. Remote unit Y is separated from remote unit X in the vertical plane. In this example, the second sender is assigned the same unique code of "1" at that for the first sender. Thus, the black data signal is also copied onto the first discrete tone 1. A phase delay

10 corresponding to a code digit value of 1 is shown as positioning the copy of the black signal onto its discrete tone at the time T1. Both remote units X and Y have used the same tone and phase to transmit their respective data. In this example, we rely on the diverse elevation angles of remote units X and Y to distinguish the signals transmitted from the two remote units. This is an example of vertical plane spatial diversity. The

15 two signals from remote unit X and remote unit Y are diverse because the phases of their tones will appear arrive at different times at array elements A and D. Since the pair of horizontal antenna elements B and C are positioned midway in the vertical direction between vertical array elements A and D, the two signals from remote unit X and remote unit Y will appear arrive at the pair B and C at a different time than when they arrive at

20 vertically displaced array elements A and D. Since array element C is closer to the remote units than is array element B, the signals from a given .emote unit will arrive at C sooner than they will arrive at B. The delay in the arrival times at the respective horizontal elements B and C gives the horizontal azimuth of the remote unit relative to the vertical plane passing perpendicularly through the axis of the horizontally displaced pair B and C.

25 This two dimensional spatial diversity is detected by the receiving base station Z of FIGURE 1B in the same manner as it is for the linear antenna array of FIGURE 1A, in accordance with the invention.

FIGURE 1B shows the receiving base station Z receiving the discrete monotone signals on its four array elements A, B, C, and D from the remote units X and Y. The

30 signals are processed by the signal processor computer using the PWAN spatial and spectral despreading codes and stored in the memory in the same way as was described for the linear antenna array of FIGURE 1A. The base station computes updated values for its despreading weights based on correlation estimates with the most recent data received on the reverse channel, as is described below for the PWAN system. The memory at the

35 receiving base station Z is organized so that each bin is associated with one of the four array elements at the receiving base station and with one tone out of a possible plurality of

four tones.   As before, each bin is further divided into four sub-bins for each of the four
possible phases, T1, T2, T3, and T4. FIGURE 1B shows how the bins and sub-bins in the
memory of base station Z store the patterns of the white data received on the four
vertically and horizontally separated array elements A, B, C, and D from remote unit X.
5   FIGURE 1B also shows how the bins and sub-bins in the memory of base station Z store
the patterns of the black data received on the four spatially separated array elements A, B,
C, and D from remote unit Y. The signal processor at base station Z uses the process of
spatial despreading, in accordance with one aspect of the PWAN system, to distinguish the
white data from the black data. The first user's unique code "1" and the relative phase
10   delays in the arrival of the white data to the four array elements A, B, C, and D is used
here to form a first spatial despreading code to extract the white data from all of the
signals received by array elements A, B, C, and D. The second user's unique code "1"and
the relative phase delays in the arrival of the black data to the four array elements A, B, C,
and D is used here to form a second spatial despreading code to extract the black data
15   from all of the signals received by array element A.

It can be seen by a comparison of FIGURE 1A and FIGURE 1B that there is a
similarity in the processing of spatially diverse signals of a linear antenna array and the
processing of spatially diverse signals from a vertical and horizontal two dimensional
antenna array, when they are encoded and decoded as has been described in accordance
20   with one aspect of the PWAN system.

FIGURE 1C shows the linear antenna array at a base station of FIGURE 1A,
where the signal processor processes two discrete monotone signals for transmission to
two remote units that are displaced from one another. Transmission from the base station
to the remote unit is called the forward channel and occurs in the forward interval of a
25   time division duplex (TDD) period. The base station Z performs transmit beam forming,
adjusting the phases of transmission from the respective array elements, to direct the signal
to the desired remote unit. For example, the signal processor, using the PWAN spatial
and spectral spreading codes, arranges the white data signals to be sent to remote unit X,
by beginning transmission from that array element that is the farthest from remote unit X.
30   The transmit spreading weights are a scaled version of the received despreading weights
computed using the respective array element inputs with each of the respective receive
frequencies. The spreading weights are computed and are applied to forward channel
bursts after a short delay.   In this example, the signal processor arranges base station's
memory shown in FIGURE 1C to have array element D transmitting white data at time
35   T1, array element C transmitting at time T2, array element B transmitting at time T3, and
array element A transmitting at time T4.   These relative phases for the respective

transmitted white data signals add together and form a beam that is directed to the remote unit X. A similar arrangement is produced by the signal processor, using the PWAN spatial and spectral spreading codes, to transmit the black data to remote station Y. In this example, the signal processor arranges base station's memory shown in FIGURE 1C

5   to have array element A transmitting black data at time T1, array element B transmitting at time T2, array element C transmitting at time T3, and array element D transmitting at time T4. These relative phases for the respective transmitted black data signals add together and form a beam that is directed to the remote unit Y.

FIGURE 1D shows the vertical and horizontal, two dimensional antenna array at

10   the base station of FIGURE 1B, in accordance with the invention, where the signal processor processes two discrete monotone signals for transmission to two remote units that are separated from one another in the vertical plane. The base station Z performs transmit beam forming, adjusting the phases of transmission from the respective array elements, to direct the signal to the desired remote unit. The remote unit X is at a

15   relatively high elevation angle and remote unit Y is at a relatively low elevation angle. Both remote units are positioned off-axis from the normal to the plane of the antenna array. In accordance with the invention, array elements A and D have been arranged to be vertically displaced and array elements B and C have been arranged to be horizontally displaced.. Since the pair of horizontally displaced array elements B and C are positioned

20   midway in the vertical direction between vertically displaced array elements A and D, the two signals transmitted to remote unit X and remote unit Y will be timed for transmission from the pair B and C at a different instant than the time for transmission from array elements A and D. Since array element C is closer to the remote units than is array element B, the signals transmitted to a given remote unit are transmitted from element B at

25   an earlier instant than they are transmitted from element C. The difference in the transmission instant from B and C corresponds to the horizontal azimuth of the remote unit relative to the vertical plane passing perpendicularly through the axis of the pair B and C. This two dimensional spatial diversity is controlled by PWAN spatial and spectral spreading codes at the transmitting base station Z of FIGURE 1D in the same manner as it

30   is for the linear antenna array of FIGURE 1C, in accordance with the invention.

For example, the signal processor, using the PWAN spatial and spectral spreading codes, arranges the white data signals to be sent to remote unit X, by beginning transmission from that array element that is the farthest from remote unit X. The transmit spreading weights are a scaled version of the received weights using the respective array

35   inputs with each of the respective receive frequencies. The spreading weights are applied to forward channel bursts after a short delay. In this example, the signal processor

arranges base station's memory shown in FIGURE 1D to have antenna D transmitting white data at time T1, element B transmitting at time T2, element C transmitting at time T3, and element D transmitting at time T4. These relative phases for the respective transmitted white data signals add together and form a beam that is directed to the remote

5   unit X. A similar arrangement is produced by the signal processor, using the PWAN spatial and spectral spreading codes, to transmit the black data to remote station Y. In this example, the signal processor arranges base station's memory shown in FIGURE 1D to have element A transmitting black data at time T1, element B transmitting at time T2, element C transmitting at time T3, and element D transmitting at time T4. These relative

10   phases for the respective transmitted black data signals add together and form a beam that is directed to the remote unit Y.

It can be seen by a comparison of FIGURE 1C and FIGURE 1D that there is a similarity in the processing of spatially diverse signals of a linear antenna array and the processing of spatially diverse signals from a vertical and horizontal two dimensional

15   antenna array, when they are encoded and decoded as has been described in accordance with the PWAN system described below.

FIGURE 2 shows an alternate embodiment of the vertical and horizontal, two dimensional antenna array at the base station of FIGURE 1B and FIGURE 1D, in accordance with the invention, where the antenna subarrays are cylindrical. Subarrays

20   elements A and D are arranged along the vertical axis and can be made up of subarrays arranged in a cylindrical symmetry about the vertical axis. Subarrays elements B and C are arranged in a cylindrical symmetry about the vertical axis. The arrangement of elements A, B, C, and D provides the vertical and horizontal, two dimensional antenna array in a similar manner as has been described for the antenna elements of FIGURE 1B

25   and FIGURE 1D. The vertical arrangement of the subarrays elements A and D enables the base station to perform vertical, receive and transmit beam steering. The horizontal orientation of the subarray elements B and C enables the base station to perform horizontal, receive and transmit beam steering. Although FIGURE 2 shows three cylindrical subarrays, the invention can also be embodied as two cylindrical arrays, with

30   the upper subarray containing both B and C type elements and the bottom subarray contain both C and B type elements. Although FIGURE 2 shows three cylindrical arrays of subarrays, the invention can also be embodied as four or more cylindrical subarrays, with at least one of the vertically displaced subarrays containing B and C type elements. The vertical spacing of the subarrays A and D and the horizontal spacing of the subarray

35   elements B and C can be chosen in accordance with the desired width of the transmitted beam and the desired range of electromagnetic wavelengths to be communicated.

The resultant invention forms beams in both the horizontal and vertical planes. It solves the problem of forming a beam to a first subscriber when there is a second subscriber located on the same horizontal azimuth but at a different elevation. The directed beam is formed using the PWAN system's spatial and spectral spreading and despreading codes so as to maximize the signal to interference and noise ratio.

Detailed Description of the PWAN system

In what follows, aspects of the principles of the PWAN system will be discussed in a tutorial illustrating an example of pure spectral diversity, an example of pure spatial diversity, and an example of mixed spectral and spatial diversity. This will be followed by a discussion of the PWAN system in a high-level overview that will include an explanation of the waveform used in the practice of an aspect of this PWAN system. This will be followed by a description of more specific "details of the PWAN system," and then by a detailed description of a "specific embodiment of the PWAN system."

HIGH LEVEL OVERVIEW OF THE PWAN system

Introduction

This PWAN system is based, in part, on the realization that there is an analogy between the mathematical description of beams formed by multi-element adaptive, or phased, antenna arrays and the mathematical description of signals that are formatted according to certain multiple access schemes, such as the exemplary DMT-SS. Based on this realization, applicants have been able to simplify the calculations necessary when a plurality of multiple access techniques are combined. Using this PWAN system, one may more effectively use a limited bandwidth region of the electromagnetic spectrum to service a large number of users. Techniques that may be combined in accordance with the teachings of this PWAN system include SDMA using multi-element antenna arrays, DMT-SS, and higher order modulation formats such as higher order QAM.

FIGURE 3A is a tutorial diagram illustrating an example of pure spectral diversity, showing how a receiver distinguishes two sets of discrete multitone signals from two transmitters that are placed close to one another, in accordance with one aspect of the PWAN system. Transmitting station X receives an input data signal shown as a white data signal from a first sender. The first sender is assigned a unique code of "1234" that is used by the encoder at station X to encode the white data signal. In accordance with one aspect of the PWAN system, the encoder uses a discrete multitone spread spectrum protocol to encode the white data signal onto four discrete frequencies or tones: Tone 1, Tone 2, Tone 3, and Tone 4. The white data signal is copied onto each of the four tones.

The first digit of the code is assigned to the first discrete tone 1. The second digit of the code is assigned to the second discrete tone 2, and so forth. The magnitude of a code digit value is converted by the encoder into a corresponding magnitude phase delay in positioning the copy of the white signal onto the discrete tone. A phase delay

5   corresponding to a code digit value of 1 is shown as positioning the copy of the white signal on its discrete tone at the time T1. A phase delay corresponding to a code digit value of 2 is shown as positioning the copy of the white signal on its discrete tone one unit later in time at T2, and so forth. The encoder at station X is shown in FIGURE 3A as converting the first sender's unique code of "1234" into positioning four copies of the

10   white data at the phases T1, T2, T3, and T4 for Tone 1, Tone 2, Tone 3, and Tone 4, respectively. This process is spectral spreading and the unique code is a spectral spreading code.

FIGURE 3A also shows transmitting station Y receiving an input data signal shown as a black data signal from a second sender. The second sender is assigned a

15   unique code of "4321" that is used by the encoder at station Y to encode the black data signal. In accordance with one aspect of the PWAN system, the encoder at station Y uses a discrete multitone spread spectrum protocol to encode the black data signal onto the same four discrete frequencies or tones: Tone 1, Tone 2, Tone 3, and Tone 4. The black data signal is copied onto each of the four tones. The first digit of the code is assigned to

20   the first discrete tone 1. The second digit of the code is assigned to the second discrete tone 2, and so forth. The magnitude of a code digit value is converted by the encoder at station Y into a corresponding magnitude phase delay in positioning the copy of the black signal onto the discrete tone. A phase delay corresponding to a code digit value of 1 is shown as positioning the copy of the black signal onto its discrete tone at the time T1. A

25   phase delay corresponding to a code digit value of 2 is shown as positioning the copy of the black signal on its discrete tone one unit later in time at T2, and so forth. The encoder at station Y is shown in FIGURE 3A as converting the second sender's unique code of "4321" into positioning four copies of the black data at the phases T1, T2, T3, and T4 for Tone 4, Tone 3, Tone 2, and Tone 1, respectively. This process is another

30   example of spectral spreading and the second user's unique code is also a spectral spreading code.

FIGURE 3A shows the transmitters at stations X and Y being positioned close to one another, so that the transmitted signals from them are not significantly different in their spatial characteristics. The transmitted signals from the two stations X and Y also

35   have the same four discrete frequencies or tones: Tone 1, Tone 2, Tone 3, and Tone 4. However, the transmitted signals from the two stations X and Y are distinguishable by the

phases of their tones, each having a pattern representing the unique code assigned to either the first or the second senders. This is an example of spectral diversity. The two signals from station X and station Y are diverse because the encoded phases of their tones are diverse. This spectral diversity is detected by the receiving station Z of FIGURE 3A, in

5   accordance with one aspect of the PWAN system.

FIGURE 3A shows the receiving station Z receiving the discrete multitone signals on its antenna A from the stations X and Y. The signals are processed by a signal processor computer and stored in a memory. The memory at the receiving station Z is organized into sections called bins. Each bin is associated with one antenna at the

10   receiving station and with one tone of the multitone set. The antenna A has four bins in the memory, one each for Tone 1, Tone 2, Tone 3, and Tone 4. Each bin is further divided into four sub-bins for each of the four possible phases, T1, T2, T3, and T4. FIGURE 3A shows how the bins and sub-bins in the memory of station Z store the patterns of the white data received from station X and the black data received from station

15   Y. The signal processor at station Z uses the process of spectral despreading, in accordance with one aspect of the PWAN system, to distinguish the white data from the black data. The first user's unique code "1234" is used here as a first spectral despreading code to extract the white data form all of the signals received by antenna A. The second user's unique code "4321" is used here as a second spectral despreading code to extract

20   the black data from all of the signals received by antenna A. After the following discussion of spatial diversity in FIGURE 3B, the reader will come to appreciate that there is a similarity in the processing of spatially diverse signals and the processing of spectrally diverse signals, when they are encoded and decoded as has been described in accordance with one aspect of the PWAN system.

25   FIGURE 3B is a tutorial diagram illustrating an example of pure spatial diversity, showing how a receiver distinguishes two discrete monotone signals from two transmitters that are placed geographically far from one another, in accordance with one aspect of the PWAN system. Transmitting station X receives an input data signal shown as a white data signal from a first sender. The first sender is assigned a unique code of "1" that is used by

30   the encoder at station X to encode the white data signal. In this example, there is only one tone at station X. The encoder encodes the white data signal onto a single discrete frequency or tone: Tone 1. The white data signal is copied onto the tone. The magnitude of a code digit value is converted by the encoder into a corresponding magnitude phase delay in positioning the copy of the white signal onto the discrete tone. A phase delay

35   corresponding to a code digit value of 1 is shown as positioning the copy of the white signal on its discrete tone at the time T1. FIGURE 3B also shows transmitting station Y

receiving an input data signal shown as a black data signal from a second sender. Station Y is geographically distant from station X. In this example, the second sender is assigned the same unique code of "1" at that for the first sender. Thus, the black data signal is also copied onto the first discrete tone 1. A phase delay corresponding to a code digit value of

5   1 is shown as positioning the copy of the black signal onto its discrete tone at the time T1. Both stations X and Y have used the same tone and phase to transmit their respective data. In this example, we rely on the diverse geographic locations of stations X and Y to distinguish the signals transmitted from the two stations.   This is an example of spatial diversity. The two signals from station X and station Y are diverse because the phases of

10   their tones will appear arrive at different times at a receiver. This spatial diversity is detected by the receiving station Z of FIGURE 3B, in accordance with one aspect of the PWAN system.   FIGURE 3B shows the receiving station Z receiving the discrete monotone signals on its four antennas A, B, C, and D from the stations X and Y. The signals are processed by a signal processor computer and stored in a memory.   The

15   memory at the receiving station Z is organized so that each bin is associated with one of the four antennas at the receiving station and with one tone out of a possible plurality of four tones. If there were four possible tones, then each antenna A, B, C, and D would have four bins in the memory.   As before, each bin is further divided into four sub-bins for each of the four possible phases, T1, T2, T3, and T4. FIGURE 3B shows how the bins

20   and sub-bins in the memory of station Z store the patterns of the white data received on the four antennas A, B, C, and D from station X.   FIGURE 3B also shows how the bins and sub-bins in the memory of station Z store the patterns of the black data received on the four antennas A, B, C, and D from station Y. The signal processor at station Z uses the process of spatial despreading, in accordance with one aspect of the PWAN system, to

25   distinguish the white data from the black data. The first user's unique code "1" and the relative phase delays in the arrival of the white data to the four antennas A, B, C, and D is used here to form a first spatial despreading code to extract the white data form all of the signals received by antennas A, B, C, and D. The second user's unique code "1"and the relative phase delays in the arrival of the black data to the four antennas A, B, C, and D is

30   used here to form a second spatial despreading code to extract the black data from all of the signals received by antenna A.   It can be seen by a comparison of FIGURE 3A and FIGURE 3B that there is a similarity in the processing of spatially diverse signals and the processing of spectrally diverse signals, when they are encoded and decoded as has been described in accordance with one aspect of the PWAN system.

35   FIGURE 3C is a tutorial diagram illustrating an example of both spectral and spatial diversity, showing how a receiver distinguishes two discrete multitone signals from

two transmitters that are placed geographically far from one another, in accordance with one aspect of the PWAN system. Transmitting station X receives an input data signal shown as a white data signal from a first sender. The first sender is assigned a unique code of "3333" that is used by the encoder at station X to encode the white data signal. In accordance with one aspect of the PWAN system, the encoder uses the discrete multitone spread spectrum protocol to encode the white data signal onto four discrete frequencies or tones: Tone 1, Tone 2, Tone 3, and Tone 4. The white data signal is copied onto each of the four tones. The magnitude of a code digit value is converted by the encoder into a corresponding magnitude phase delay in positioning the copy of the white signal onto the discrete tone. The encoder at station X performs spectral encoding in FIGURE 3C when it converts the first sender's unique code of "3333" into positioning four copies of the white data at the phases T1 T2, T3, and T4 for Tone 1, Tone 2, Tone 3, and Tone 4, respectively. The station X is shown in FIGURE 3C as being equidistant from the four receiving antennas A, B, C, and D of station Z. Thus, the signals arrive at each antenna at the same time. This relative positioning of the sending station X and the receiving station Z can be viewed as imparting a spatial encoding to the first user's white data. The white data is therefore both spatially and spectrally encoded. In accordance with one aspect of the PWAN system, the first sender's unique code "3333" and the relative phase delays in the arrival of the white data to the four antennas A, B, C, and D is used at station Z to form a first, combined spectral and spatial despreading code to extract the white data form all of the signals received by antennas A, B, C, and D.

FIGURE 3C shows transmitting station Y located at a geographic position with respect to station Z so that signals from station Y are received at different times by the four antennas A, B, C, and D at station Z. Station Y receives an input data signal shown as a black data signal from a second sender. The second sender is assigned a unique code of "1111" that is used by the encoder at station Y to encode the black data signal. In accordance with one aspect of the PWAN system, the encoder uses the discrete multitone spread spectrum protocol to spectrally encode the black data signal onto four discrete frequencies or tones: Tone 1, Tone 2, Tone 3, and Tone 4. The black data signal is copied onto each of the four tones. The magnitude of a code digit value is converted by the encoder into a corresponding magnitude phase delay in positioning the copy of the black signal onto the discrete tone. The encoder at station Y is shown in FIGURE 3C as converting the second sender's unique code of "1111" into positioning four copies of the black data at the phases T1, T1, T1, and T1 for Tone 1, Tone 2, Tone 3, and Tone 4, respectively. Since station Y is shown in FIGURE 3C as not being equidistant from the four receiving antennas A, B, C, and D of station Z, the signals arrive at each antenna

different times. This relative positioning of the sending station Y and the receiving station
Z can be viewed as a spatial encoding of the second user's black data. The black data is
both spatially and spectrally encoded. The second sender's unique code of "1111" and the
relative phase delays in the arrival of the black data to the four antennas A, B, C, and D is

5 used at station Z to form a second, combined spectral and spatial despreading code to
extract the black data form all of the signals received by antennas A, B, C, and D. Thus,
in accordance with one aspect of the PWAN system, signals from both station X and from
station Y can be simultaneously processed by combined spectral and spatial despreading
codes to distinguish both spatially diverse signals and spectrally diverse signals, when they

10 are encoded and decoded as has been described in these examples.

An exemplary communication system in which the PWAN system may be
implemented is shown in FIGURE 3D. In this FIGURE, the various elements marked 11
are exemplary fixed remote terminals serving users, while the boxes marked 12 are the
base stations associated with certain of those remote terminals. It should be noted that in

15 this context the term "fixed" remote terminals applies not only to remote terminals that do
not move during use, but may also apply to terminals that are mobile, so long as they are
serviced by one base station during a call. Other "fixed" embodiments may include motion
between cells during a call and motion at less than 10 or 5 miles per hour. Additional
remote terminals and base stations are also shown.

20 The remotes and base stations are connected by exemplary airlinks, 13. The base
stations may be connected to a "wireless network controller" 14, which then connects to
the wider telecommunications network, 15. Connections between the base station and the
network controller and between the controller and the telephone network, may be wired
or wireless.

25 An aspect of the PWAN system is centered about the exemplary airlinks, 13, that
connect the base stations and the remotes. These airlinks use scarce bandwidth resources
and are advantageously operated in a highly bandwidth efficient mode so as to
accommodate a large number of users.

The Airlink

30 Discrete Multitone Transmission

The airlink, shown as 13 in FIGURE 3D, involves a multitude of complex
transmission techniques. The first is an embodiment of multitone transmission that we call
"discrete multitone (DMT)". In this technique, a signal is transmitted over discrete carrier
frequencies, shown in FIGURE 3E as 21. Specific tones can be assigned to specific users,

35 as shown in the FIGURE. As discussed above, the tones may be spaced at a frequency of
$1/T$, where T is the symbol rate, so that they are "orthogonal" - i.e., they do not interfere

23

with one another - as in OFDM. Each tone can carry different data, but for the purposes of this discussion, at least some of the various tones assigned to a specific user will be assumed to be carrying redundant information to realize the advantages of frequency diversity. Such redundant transmission over a range of frequencies allows recovery of the

5 signal even if some frequencies are subject to severe interference -- a problem of particular interest in the embodiment of this PWAN system that involves fixed remotes. As mentioned above, certain implementations of this signal format enables analysis that can be effected using fast Fourier transform calculational techniques

DMT-SS

10 In an aspect of this PWAN system, bandwidth efficiency is increased by spreading the signal over a set of weighted tones, with each user being assigned a specific set of tones and weights. This technique, is depicted in FIGURE 3. In this FIGURE, identical data is sent over the four tones identified as 1, 2, 3, and 4. User 1 is to be sent a "+1." User 2 is to be sent a "+1." User 3 is to be sent a "+1." User 4 is to be sent a "-1." The

15 same tones are used to send information to the four different users by using different "weights" for each user. These weights may be viewed as user-specific codes, and we may refer to them as weights, codes or weight-codes. In this heuristic example, the amplitude of a particular tone is obtained by multiplying the data value by the weight-code value for that combination of user and tone. For example, the weight-code of the second user is [1

20 -1 1 -1], meaning that for the second user the amplitude of the first tone is the data value times +1, the value for the second tone is the data value times -1. etc. For example, the value of the second tone for the second user is the data value, +1, multiplied by the weight-code value for the second user's second tone, -1, to yield a -1, as shown in the second position of the second line. This process is called "spreading" since it effects the

25 spreading of the data across the tone set.

The various tone values are added to obtain the composite spectrum, shown on the last line of the FIGURE, that is then transmitted. Upon receipt of the spread data, the data is "despread", i.e., the data to be sent to the various users is obtained, by multiplying the composite spectrum by the inverse of a particular user's weight-code. This can be

30 performed simultaneously for all users by using appropriate matrix techniques.

It is helpful to bear in mind the difference between this "discrete multitone spread spectrum (DMT-SS)" technique and well known embodiments of the classical spread spectrum technique. In DIRECT SEQUENCE SPREAD SPECTRUM, each data symbol is multiplied by a series of code pulses. This spreads the data over a much wider region of

35 the spectrum. In FREQUENCY HOP SPREAD SPECTRUM, the data is transmitted over different regions of the spectrum during different time slots, in accordance with a

pre-defined hopping code. In the DMT-SS used in this invention, the signal is modulated by a set of weighted discrete frequencies, not over a continuous broad frequency range, as in direct sequence.

It should be appreciated, that although depicted in this example as a set of real
5   numbers, the spreading codes advantageously comprise a vector wherein each vector is a complex number.

Matrix Representation of the "Coding" Process

Exemplary, high level equipment arrangements used in the "spreading" and
10   "despreading" is represented schematically in FIGURE 4. In this FIGURE, 41 is the data, D, that is to modulate a DMT-SS signal. At 42, the various DMT-SS carriers are encoded as depicted previously in FIGURE 3. The mathematical description of the spreading operation is shown in formula 43, where SD is the "spread data," CM is the "code matrix," and D is the "data." The detailed matrix operation is shown in formula 44, where 45 is the
15   data vector array representing the data of FIGURE 3, 46 is the code matrix of that FIGURE, and 47 is the composite spectrum or spread data vector array.

When the spread data, SD, is received, it is "despread" by means of the vector operation shown in 60, where SD is the received "spread data," CM^{-1} is the inverse of the code matrix and DD is the "despread data," that, as required, is reflective of the original
20   data. This vector operation is shown in detail in 48, where 49 is the received spread data, 50 is the inverse of the code matrix, and 51 is the despread data. It is important to note for the discussion in the next section on the effects of SDMA, that the size of this code matrix is determined by the total number of tones that are used.

As will be discussed below in the section on "Specific Details of the Invention," it
25   is not necessary to use orthogonal codes. In fact, in most embodiments of this invention the codes are usually only linearly independent, and the effects of cross talk between users with different codes is treated using a "code nulling" process that results automatically from the practice of one aspect of this invention.

Use of SDMA in "Coded" Multitone Transmission

30   An important aspect of the invention involves the realization that the mathematical description of a certain processed spectrally processed signals, such as DMT-SS signals, is analogous to the mathematical description of a signal spatially processed by a multi-element adaptive antenna array. Accordingly, the mathematical description of such
35   spectrally processed signals may simultaneously describe spatial processing by a multi-element adaptive antenna array by simply increasing the size of the DMT-SS matrix to

take into account the number of antenna elements in the antenna array.   The dimensionality of the combined "spectral/spatial matrix" that comprises the spreading weights by which each tone is multiplied, is then equal to the number of tones multiplied by the number of energized antenna elements.

5   As noted in the Summary of the Invention, the mathematical formalism that describes an aspect of this invention treats both code and antenna aspects of the received signal similarly.   The signal processing may therefore automatically result not only in codes that have minimal cross talk with other coded signals, but also in the formation of beams that yield minimal interference from users illuminated by different beams.   These

10   advantages are usually derived separately and are known as code nulling and null steering respectively.   They will be explained in greater detail below in the section on "Specific Details of the Invention."

Channel Response, Equalization, and Signal Extraction

15   The discussion to this point has not involved any description of the effects of channel response.   Distortions due to the channel response can be introduced into the formalism by means of a "channel response" matrix, shown in FIGURE 5.   In this FIGURE, the received data "RD", shown in 52, is no longer equal to the spread data as in FIGURE 4, but is now distorted by a channel response "CR.".   The received data is then

20   the product of the spread data and the channel response, as shown in 52.   This effect is shown in 53, with the exemplary numbers used in FIGURE 3.   As shown, the despread data, 54, now do not have the original data values, but rather values that are distorted by the channel response.   In order to correct this distortion, the code despread matrix must include terms that "equalize" the channel distortion.

25   In an embodiment of the invention, this channel response vector is determined by transmitting a pilot signal and noting its distortion by the channel ("pilot driven equalization").   In another embodiment, the effect of channel response is "equalized" by simply adaptively calculating a "despread matrix" that maximizes the ratio of signal-to-noise-and-interference associated with the transmitted data (data driven equalization).

30   The calculated optimum system parameters may include a mathematical representation of the channel response.   These channel response parameters may then be used by either the base or the remote to "equalize" the channel distortion.   These parameters may be used by the either side of the link because, at least for short periods of time, the channel is reciprocal in time.   Of course, these calculations may be equally well done at some more

35   central location rather than at the remote.   What is central to this aspect of the invention is that certain calculations can be reused.   Accordingly, despread weights used on the receive

26

signals can be reused, with only minimal modifications, to spread signals on the next transmission - a process called retrodirectivity. Additionally, it may be possible to reuse, at the remotes, the weights that are calculated at the base station.

Of course, the calculation of optimum system parameters, and the adaptive
5   extraction of the data associated with each user from the combined signal, is done taking into account all of the system signals that are seen by the base and transmitted by the base. Accordingly, the remotes may calculate their own despread weights to take into account the interfering signals that they receive, which are not received by the base station. Simplification may be achieved by using a fixed beam pattern for the remotes, rather than
10 calculating beam weights, since the remote knows where the fixed base is and need not reoptimize its beam weights once its beam pattern is fixed.

Modulation Formats

Although, to this point, we have shown the signal as either zeros or ones, it is clear
15 that the carrier may be modulated in any one of a number of signal modulation formats, such as higher order QAM. In such an exemplary format, the composite spectrum will be as shown heuristically in FIGURE 6. In this FIGURE, the tone sets, as shown in FIGURE 2, are displayed on the x-axis. The different codes used for the various tone sets are shown on the z-axis. Finally, the constellations associated with QAM modulation are
20 shown on the y-axis as circles. The particular constellation point that is energized is represented by a closed circle. The composite spectrum, obtained by "collapsing" the z-axis, is shown x-z dimension. The blur represents the composite of all of the energized constellations of a particular tone.

25 Time Division Duplex

In an embodiment of the invention, the bandwidth-efficient transmission techniques used in the invention are combined in a Time Division Duplex (TDD) configuration, i.e., a configuration in which the channel is divided into time slots with uplink and downlink transmission occurring alternately in adjoining time slots. A simplistic TDD configuration
30 is shown in FIGURE 7. As shown in the FIGURE, during alternate time slots, information is sent uplink (from base station to remote) and then downlink (remote to base station). The guard time is selected to allow for the delay time due to multi-path. All remotes and base stations may be synchronized so that all remotes transmit at the same time and then all base stations transmit at the same time. Well known GPS techniques
35 may be used for such synchronization.

As indicated above, the use of TDD, and the assumption of a channel response that varies slowly compared to a TDD period, permits the interchangeable use of spread and despread weights, at least during contiguous receive and transmit cycles at a given location. Likewise it may be possible to reuse, at a second location, the larger part of the "spread/despread matrix" calculated at a first location. For example, it may be possible to use at the remotes the weights - from which each users information can be extracted - that were calculated at a base station during a previous TDD period by maximizing the signal-to-noise-and-interference ratio for the signals received at the base. In this embodiment, the base sends to its remotes their appropriate "channel equalized codes" or "weights" using the TDD format. The remotes may perform at least some weight recalculation, but may rely on some of the weight analysis performed at the base station. In this way the larger part of the calculation may be done at the base stations or at some other location removed from the remote locations. This reduces the cost and complexity of the more numerous remotes considerably.

Of course, to implement this aspect of the invention, optimization parameters must be relatively constant during the time period of one uplink and one downlink time slot. Thereafter newly calculated optimization parameters may be determined, and sent to the remotes, on a periodic basis.

Bandwidth on Demand

As noted above, the invention is particularly well adapted to providing variable bandwidth on demand. The provision of such additional bandwidth is effected by simply assigning more tones or codes to the requesting user, or by transmitting in a higher order modulation format.

EXEMPLARY DETAILS OF THE INVENTION
The Analogy Between DMT-SS and Adaptive Antenna Array Processing

The aspect of this invention that involves the use of spectral multiple access techniques that are mathematically analogous to the mathematical description of adaptive antenna array signals can be better understood in the context of heuristic FIGURE 14. In that FIGURE, 10 is the mathematical description of Discrete Multitone Spread Spectrum (DMT-SS). In 10, a baseband signal, d(t) is multiplied by a spreading code comprising a set of tone frequencies and associated carrier weights, g_k. It should be appreciated that this is different than Direct Sequence Spread Spectrum where the baseband signal is multiplied by a PN code, rather than by a set of weighted carriers. The expression of 10 can be rewritten in block form, as in 20. Here the weighting operation associated with g_k

has been separated from the exponential operation, that we characterize in the FIGURE as an "inverse frequency channelizer", for example an inverse FFT. In a point central to this aspect of the invention, applicants have recognized that this representation is analogous to that of an adaptive antenna array - where a baseband signal is multiplied by an aperture

5   vector.

The DMT-SS despreading operation is shown in heuristic FIGURE 15 and it also is found by applicants to be analogous to similar expressions for adaptive antenna array processing. In 10, a wideband signal x(t) is passed through a bandpass filter, BPF, and then multiplied by a despreading code, w(t) nominally the inverse of the spreading code of

10   FIGURE 15, to get the original signal, d(t). By calculating the despreader weights appropriately, for example to maximize signal to noise, we can automatically correct for channel distortion and other interfering signals. In 20, the despreading operation is again separated from the exponential coefficients, as in FIGURE 14. Here the received signal, x(t) is represented as equal to the sum of an interference term, i(t) and the transmitted

15   signal, s(t) multiplied by a distortion term h(t). From FIGURE 14, the transmitted signal s(t) is equal to g times d(t), giving equation 30 in FIGURE 15. Applicants have recognized that this equation is analogous to that describing the output of an adaptive antenna array.

In accordance with an aspect of this invention, this analogy between DMT-SS and

20   adaptive antenna array processing leads to the possibility of combining both spatial and spectral expressions in ᴏᴺᴇ mathematical expression that can be solved in one unified spectral/spatial calculation. This also leads to the further discovered analogy between null steering in adaptive antenna arrays and code nulling in CDMA in general, and in DMT-SS in particular. In accordance with another aspect of the invention, instead of setting the

25   despread weights to previously estimated spectral spreading and beam steering weights, we adaptively calculate the despread weights to maximize some general measure of signal quality - either characteristics measured directly from the channel or obtained from a blind adaptive operation or a combination of the two.

30   Time Division Duplex

The TDD signaling protocol used in an embodiment of the airlink is depicted in FIGURE 7. It should be noted that two 5 MHz frequency bands separated by 80 MHz are depicted in FIGURE 7. In one embodiment, the same data is transmitted over both 5 MHz bands to reduce multi-path fading effects. The 80 MHz separation between the two

35   bands ensures that the same multi-path fade does not interfere with both bands. In addition, the 5 MHz frequency band is divided into four 1 MHz sub-bands, with the lower

and upper 500 Hz of each 5 MHz band being designated as guard bands. The four 1 MHz sub-bands in the lower 5 MHz band are matched with corresponding sub-bands in the upper 5 MHz band. So, for example, the first sub-band in the lower 5 MHz band shares is duplicated in the first sub-band in the upper 5 MHz band, etc.

5   In one preferred embodiment, the transmission period from the base station to the remotes and from the remotes to the base station (T_{symbol}) is approximately equal to 340 microseconds. The guard time (T_{guard}) between transmission and reception is approximately 35 microseconds, in one embodiment, while the total revisit time ($T_{revisit}$) is approximately 750 microseconds. As has been mentioned, and as will be discussed in 10   greater detail below, it is important that $T_{revisit}$ be less than the amount of time in which significant changes are likely to occur over the air channel, in order to ensure that essentially the same channel characteristics are observed within any selected interval of length $T_{revisit}$.

       The guard time, T_{guard}, between the forward and reverse bursts must be sufficiently 15   large to allow significant attenuation of multi-path reflections. Base-to-base interference necessitates sufficient guard time between forward and reverse transmission bursts. In an embodiment of the invention four forward bursts are transmitted without any intervening reverse bursts and then four reverse bursts are transmitted. The guard time between the four bursts is much smaller than the guard time at the end of the four bursts. This reduces 20   the base-to-base interference.

High Level View of the Signal Processing

       FIGURE 8 is a signal flow diagram that generally illustrates the signal processing steps performed in one embodiment of the invention on an audio, video, voice or data 25   signal transmitted over the air interface between the base station and the remotes. As shown in FIGURE 8, a signal (that may comprise audio, video, voice or data) is supplied from a communication link to an input terminal 1010. This signal is then packetized in digital format as indicated by a block 1011. The signal is packetized so that the entire signal can be sent in a single packet during the transmission time T_{packet}. As indicated 30   within block 1012, the packetized signal is subsequently quadrature amplitude modulation (QAM) encoded and error encoded (using, for example, well known Reed-Solomon and/or trellis encoding techniques). Of course, it should be understood that in other advantageous embodiments of the invention, binary phase shift keying (BPSK) or M-ary phase shift keying (MPSK) may be employed as an alternative modulation technique to 35   QAM.

The mapper 1012 outputs a complex number representative of an n-bit binary value based upon the mapping scheme. For example, if 16 QAM is used, then the encoder 1012 will output a four-bit binary value, one of 16 possible values since $2^4=16$. Likewise if 256 QAM is used, then the encoder 1012 will output one of 256 complex values representing an eight-bit binary value since $2^8=256$. The bits that enter the mapper may have been forward error correction encoded to protect against channel errors.

The encoded signal is then spread over a portion of the frequency band as indicated within a block 1013. In accordance with an embodiment of the invention, the DMT-SS spreading technique is used to spread the encoded signal over several frequency tones within the total frequency spectrum. The method used to spread the encoded carrier signal is described in greater detail immediately below with reference to the signal processing flow diagram of FIGURE 9.

Parallel Data Transmission Using Multitones

The division and transmission of a signal over a number of carriers - Parallel Transmission - is discussed, for example, in a paper entitled "Analysis and Simulation of a Digital Mobile Channel Using Orthogonal Frequency Division Multiplexing," by Leonard J. Cimini, Jr., IEEE Transactions on Communications Vol. Com 33, No. 7, July 1985. Briefly, Parallel Transmission is a signal processing technique that converts a serial data stream into a parallel data stream, and modulates different discrete carrier tones with each of the parallel data streams.

For example, consider a set of carriers (called a tone set) that includes four tones. A serial data stream is then divided into four parallel data streams by taking every fourth symbol and assigning it to a particular one of the tones. So, for example, the first, fifth, and ninth symbols are assigned to the first tone; the second, sixth, and tenth symbols are assigned to the second tone, etc. Accordingly, the first tone in the tone set will be set to an amplitude and phase corresponding to the symbol values output onto the first parallel data stream, the second tone in the tone set will be set to an amplitude and phase corresponding to the symbol values output onto the second parallel data stream, etc. In a particularly advantageous embodiment of the invention, the spacing between the tones is carefully selected to provide orthogonal frequency division multiplexing (OFDM).

A PN code method of implementing such a modulation scheme, is depicted in FIGURE 9 As indicated above, the data in the parallel data streams may be the same or different data. The major advantage of this technique is that it can be shown that such a processed signal is effectively the Fourier transform of the original data stream, and that a bank of coherent demodulators is effectively an inverse Fourier transform. In an aspect of

the invention, these technique is used to obtain the calculational advantages of FFT and IFFT processing

DMT-SS Details

5   In an exemplary embodiment of the invention, the total bandwidth allocation for the airlink is 10 MHz. in the range of 1850 to 1990 MHz. The total bandwidth is divided into two 5 MHz bands called the Lower RF band and the Upper RF band. The separation between the lowest frequency in the Lower RF Band and the lowest frequency in the Upper RF Band (DF) is 80 MHz. The base frequency (f_{base})for the network is defined as

10   the lowest frequency of the Lower RF Band.

The Lower and Upper RF Bands are further subdivided into sub-bands. The first and last 0.5 MHz of each band are designated as guard bands and are hence unused. The remaining 4 MHz in each band is then subdivided into 4 Sub-bands sequentially numbered from 0 to 3. Each Sub-band contains a set of frequencies in the Lower RF Band and

15   another set of frequencies in the Upper RF Band. The extension L indicates the set within the Lower RF Band and U indicates the set within the Upper RF Band.

In one embodiment there are a total of 2560 frequency tones equally spaced in the 8 MHz of available bandwidth. There are 1280 tones in each Band, and 640 tones in each Sub-band (320 frequencies in the lower band and 320 frequencies in the upper band). The

20   spacing between the tones (Df) is simply 8 MHz divided by 2560 that translates to 3.125 KHz. The tones may be further organized into Tone Sets each with four tones, and Tone Partitions, each with 20 Tone Sets. Alternatively the tones may be organized into Tone Clusters each with 20 tones, and Traffic Partitions, each with 4 Tone Clusters. A traffic channel requires at least one traffic partition. Control and access channels may be

25   interspersed among the traffic channels in the 5 MHz slots. As will be discussed further below, data is redundant over a tone set.

The organization of the tones also permits standardization of tone assignments to users so as to permit the contemplated calculations in an orderly fashion. For example, each user may be assigned only multiples of traffic partitions. The division of the total

30   transmission band into sub-bands also allows for lower sampling rates and less intensive DSP requirements (since the processed band is spread over a significantly smaller bandwidth). In addition, the partitions provide a convenient division for reducing the dimensionality of received vectors. This could be accomplished by combining selected tone set values (i.e., the corresponding tone set values in each cluster set). Although this

35   involves a reduction in the number of degrees of freedom, such a tradeoff can be advantageous in systems wherein the maximum number of degrees of freedom are not

necessary to accurately decode the data. Thus, by reducing the dimensionality of the tone set vector, the processing cost is significantly reduced.

As indicated above, to ensure that the signals modulated onto the separate tones do not mutually interfere by overlapping with other tones the tones set are spaced at
5   intervals of 1/T, the symbol rate. Of course, some distortion occurs during transmission so that some interference may occur which may be removed with additional error correcting techniques.

The Use of DMT-SS

10   As noted above, the signals may be initially spread over assigned tones using appropriate codes or weights. These codes may be orthogonal within a given spatial cell, and may be randomly assigned to the same tone bins within adjacent spatial cells. Thus, spreading codes may be reused in adjacent spatial cells and also may have a random correlation between adjacent spatial cells. Although the initial code assignments made by
15   the base station may be orthogonal, it will be understood that in response to the weight adjustments made during adaptive equalization, the spreading codes will typically evolve, or adapt, to non-orthogonal codes after the communications network has been active for some time. As will be discussed in greater detail below, the criterion for the spreading codes used within a given spatial cell is advantageously linear independence rather than
20   orthogonality. The random correlation of spreading codes in adjacent spatial cells is compensated for by means of an automatically implemented code nulling technique that nulls out correlated portions of the transmitted signals using linear weighting.

Once the spreading codes associated with the DMT-SS modulation technique have been assigned to the encoded data signals, as represented by the block 1013 of FIGURE 8,
25   the processed signals are linearly summed, as indicated by a summing block 1025. A similar signal processing procedure is used on other incoming signals as indicated by the blocks 1021-1023, that correspond to the blocks 1011-1013. These signals are summed within the summer 1025 and assigned to carrier frequencies within the 5 MHz sub-bands shown in FIGURE 7, as indicated by a block 1030.
30   As noted above, during the course of adaptive equalization, the codes typically become non-orthogonal in order to maximize the SINR throughout the overall communications network 100. However, in order to retain the maximum number of degrees of freedom throughout the communications system 100, it is preferable to maintain linear independence of the complex spreading vectors throughout a given spatial
35   cell. Linearly independent complex vectors are those that cannot be expressed as a sum or scalar multiple of any combination of the other complex vectors in the system. Thus, by

preserving linear independence among the spreading codes, a matrix set of linear equations can be derived that allows each of the system variables (i.e., data symbols) to be uniquely decoded. Insofar as the spreading codes become more linearly dependent, the ability to discriminate amongst data symbols becomes more difficult. However, in some

5   applications, band pass filter values are established in the beginning and thereafter the system must operate within those constraints.

The spread signals are linearly added on a carrier-by-carrier basis to obtain the overall DMT-SS waveform. In order to despread this signal, the received signal is detected and converted into matrix form. The received vector is multiplied by a scaling

10   factor (that is proportional to the number of bits in the spreading code), and a matrix comprised of the spreading codes. The resultant vector provides the despread data symbols as an output. From this example, it can be induced that as many data bits can be distinctly despread as there are bits in the spreading codes, so long as the spreading codes remain linearly independent

15   Returning to the spreading of the data, once the encoded, spread-spectrum signals have been assigned to the frequency carrier bands, the signal may be transformed from the discrete frequency domain to the analog time domain using an inverse fast Fourier transform (IFFT) and an analog to digital converter. By using an IFFT and an FFT to provide for OFDM, multiple modulators are not required, as is well known in the art. This

20   is because the calculations relating to the DMT-SS modulation technique are less intensive in the frequency domain than in the time domain. For this reason, the bulk of the signal processing is preferably performed in the frequency domain (with the exception of the modem operations of, for example, encryption, filtering, etc.) and is transformed to the time domain as one of the last steps before transmission.

25   Depending upon bandwidth considerations, signals from the same user are assigned one or more spreading codes and one or more traffic partitions. The assignment of different spreading codes and additional traffic partitions to provide additional bandwidth for a requesting user unit (a unit that communicates via one of the remotes) is particularly elegant (in comparison with bandwidth allocation using TDMA) from an

30   implementation standpoint. This is because the allocation of new spreading codes and tone sets is mathematically simple and merely requires a numerical change to the despreading vector (for the reassignment of a new tone set) or an increase or decrease of the bandwidth of a bandpass filter on the receiving side (for the reassignment of a new tone set).

35

Advantages Associated with DMT-SS

        The use of DMT-SS is highly advantageous in the system of the present invention. For example, the use of DMT-SS allows the channel characteristics to be evaluated at discrete points that can be exactly represented in matrix form as a complex vector. Thus,

5   because selected tones within each tone set can be designated as pilots distributed throughout the frequency band, a simple evaluation of a finite number of complex values results in an accurate channel estimation. Furthermore, theoretically, the channel distortion can be exactly compensated at the discrete tone frequencies by a simple complex conjugate multiplication. That is, since discrete tones are used, it is not necessary

10 to know the entire channel response between the tones since the channel only affects operations at the exact points of the tone set frequencies. If the channel is defined at these discrete points, the received tones need only be multiplied by the appropriate complex, amplitude and phase to equalize the channel. This means that exact equalization is accomplished by a simple complex multiplication. This channel equalization calculation

15 may be subsumed in the calculation of despread/spread weights that improve or optimize characteristics of the signal such as the signal to noise and interference ratio.

        Also, the use of DMT-SS ensures that the equalization of antenna array time dispersion is very simple. In multiple element antenna arrays, a time delay is observed between receptions of a waveform by the spatially separated sensors when the wave

20 impinges on the array. In a very wide band system, this delay creates dispersion. However, by using DMT-SS, the dispersion can be represented by discrete values of a scaleable vector since the response is only evaluated at discrete points of the frequency.

        Furthermore, each user on the system could operate with a different QAM (or other M-ary) constellation size. This is because the symbols are not spread over the entire

25 bandwidth as in direct sequence spread spectrum. Rather, in DMT-SS the symbols are spread over frequency bins of various sizes so that each user can have the optimum size QAM constellation (i.e., the highest order allowable in a given SINR). This increases the overall system capacity since the system is not restricted to the lowest common denominator (i.e., the QAM or M-ary constellation size at which all channels can operate).

30 In addition, at lower constellation sizes a lower signal-to-noise ratio is required to demodulate the signal, and this lower signal-to-noise ratio requirement can be used to extend the range of the base station that provides additional system flexibility. Finally, the packet size could also be varied in conjunction with the QAM constellation size to manage interference levels.

35   The use of DMT-SS modulation also provides several unexpected advantages when used in combination with certain communication technologies. First of all, since

DMT-SS spreading allows for flexible spreading bandwidths and gain factors (i.e., a given signal can be spread over as much bandwidth as desired), it is particularly advantageous for exploiting the spectral diversity of the channel. That is, since the channel has certain bands with better response than other bands, signals can be selectively spread over the

5   more desirable bands.

In addition, DMT-SS also allows for the use of code-nulling to greatly improve the reuse capacity of the communication link beyond the reuse capacity of conventional CDMA. Since DMT-SS is used instead of direct sequence or frequency hopping, selected portions of the spreading code can be nulled within the despreader. Thus, only those

10   portions of the spreading code which are not common with the interfering spreading codes will be despread. Furthermore, DMT-SS is particularly advantageous when implemented within a variable bandwidth system since the allocation of bandwidth is highly flexible in such a system, and can be implemented by the appropriate assignment of additional tones to the requesting user. In summary, DMT-SS provides a solution that nulls the interfering

15   signals.

Finally, DMT-SS is advantageous as applied to a multi-element antenna array system where matrix calculations comprise the bulk of the processing operations. As is well known in the art, as the dimensionality of a matrix grows, the calculation operations necessary to invert the covariant matrix increases as the cube of the matrix dimensionality.

20   Thus, the processing power increases as the cube of the matrix dimensionality and, consequently, so does the cost of the processing circuitry. Thus, in order to avoid skyrocketing costs, it is advantageous to limit the dimensionality of the matrices used to perform the spreading and despreading calculations. Since in a multi-element antenna array system it is sometimes desirable to change the number of antenna sensor elements to

25   enhance the beam forming capability of the system, such a system would normally incur an increase in matrix dimensionality (since each sensor corresponds to an element in the matrix). However, in a DMT-SS system, if sensors are added to the antenna array, the dimensionality of the matrix can be preserved by reducing the number of tones in each tone set.

30   This preservation of matrix dimensionality is possible because the mathematical formalism used when performing amplitude and phase weighting of the signal on each of the sensors is substantially similar to the formalism used when performing amplitude and phase weighting of each of the tones in a tone set. Thus, an analogy exists between the multiple sensors in an antenna array and the multiple tones in a tone set. Consequently,

35   the same matrix can be used to determine weights for both sensor elements and tones, so that if the number of sensor elements increases, the number of tones can be decreased to

compensate (i.e., preserve the same matrix dimensionality), and vice versa. Furthermore, essentially the same SINR is preserved in such a system since the degrees of freedom lost in the number of tones is regained in the number of beams. In contrast, direct sequence spread spectrum could not change the number of tones as beams are added since there are

5   no tones to add or subtract. Thus, the cost of such a system would increase enormously relative to the cost of the system of the present invention as capacity is increased. Specifically, the cost of the present invention increases approximately proportionally with the capacity, while the cost of another system using, for example, direct sequence spread spectrum, increases as the cube of the capacity.

10   Once the signal has been DMT-SS modulated, the signal is output to the antenna for transmission. Control circuitry within the base station keeps track of the location of the user terminals in communication with the base station, so that the appropriate signals are directed to the appropriate user units (i.e., by means of antenna beam-forming discussed below).

15

Beam Forming

In accordance with one aspect of the present invention, adaptive antenna arrays are used in conjunction with a beam forming algorithm to achieve spatial diversity within each spatial cell and implement SDMA. That is, signals output by the antennas are directionally

20   formed by selectively energizing different antenna sensors with different signal gains so that remote terminals in one portion of a spatial cell are able to communicate with the base station while other remote terminals in a different portion of the spatial cell may communicate with the same base station, even if they are using the same tone set and code. It should be understood that in the fixed implementation of the current invention,

25   i.e., where the remote access terminals do not move substantially during communication with the base station, usually staying within a spatial cell during communication, the beam forming algorithm used in the airlink need not account for mobile remote units leaving and entering the spatial cell. In one advantageous embodiment, each spatial cell is partitioned into four sectors where each sector transmits and receives over one of the four sub-band

30   pairs.

As set forth above, the beam forming method of the present invention, like the use of codes, should not be conceived as separate from the overall adaptive equalization method of the present invention. Rather, the method used to selectively energize the antenna sensors (during transmission) or selectively weight the signals received on the

35   different sensor elements (during reception) is subsumed into the overall method used to

37

maximize SINR. The relation of the beam forming method to the overall maximization of SINR method will be described in greater detail below.

Code-Nulling

5   The use of spread-spectrum technology (particularly DMT-SS) and directional antennas within the preferred airlink of the present invention allows for several error cancellation benefits, including effects that are analogous to code nulling and null steering, by means of linear weighting in code and space.

Code-nulling is used to discriminate between non-orthogonal signals emanating 10   from adjacent spatial cells. Again, the code-nulling method should be understood in the context of the maximization of SINR method of the present invention. That is, the code-nulling method should be considered as the portion of the method that maximizes SINR with respect to the code domain. This way of understanding the code-nulling method will be described in further detail with respect to FIGURE 10.

15   It should be understood that if signals generated within the same spatial cell or beam all have orthogonal spreading codes, code-nulling is typically not necessary since the orthogonality is sufficient to ensure that there is no cross modulation. However, as mentioned above, the spreading codes used within a particular spatial cell may not be orthogonal, although they are preferably linearly independent. Furthermore, the 20   transceivers within the neighboring spatial cells may employ spreading codes that have a random correlation with the spreading codes used in the local spatial cell.

By adjusting the spreading weights associated with each communications channel the base station is able to cross-correlate these signals on the same tone set to subtract out interference due to "neighboring" signals. In one embodiment, the base station has the 25   spreading codes used to spread different signals assigned to the same tone set, so that this information can be used to initially calculate the appropriate weights for nulling out interference from other codes.

As discussed above, when the spreading codes used to spread distinct data signals are orthogonal, the spread data can be precisely recovered during despreading. However, 30   when the spreading codes are not orthogonal (as is the case with spreading codes that are used in neighboring spatial cells), cross modulation may result so that the data signals are not able to be precisely distinguished by simple despreading (i.e., despreading without code-nulling).

In order to compensate for this phenomenon, code-nulling weights used in the 35   despreader are multiplied by the received signal vector. By nulling out the cross modulation present in the received signal, the appropriate values of the data bits are

output by the receiver. As long as the complex spreading weights are linearly independent, and the SNR is sufficiently high, the exact symbol values can be discriminated by this method. It will be appreciated that the code-nulling procedure above is inherently implemented during derivation of the overall weights that maximize the

5   SINR.

Null-Steering

In addition to code-nulling, an exemplary directional antenna shown in FIGURES 11 and 12 with no spectral spreading, forms signals including null regions (i.e., regions

10   where the antenna attenuates incoming signals or where there is a very low antenna gain). These null regions can be formed in a pattern so that the nulls are directed towards known interferers (e.g., interfering signal sources or interfering multi-path reflectors). In this manner, interfering signals are de-emphasized in the spatial domain. As will be discussed in greater detail below, the use of null-steering in conjunction with code-nulling is highly

15   advantageous.

In accordance with one aspect of the present invention, significant processing time and sophistication can be saved since significant similarity exists between the methods for performing null-steering and code-nulling. Specifically, the mathematical formalism used to achieve null-steering is analogous to the formalism used to achieve code-nulling.

20   According to this analogy, just as the tones in a tone set are multiplied by complex weights to alter the amplitude and phase of the tones, so are the gain and relative phase of signals output and received by the antenna elements altered by a set of multiplicative weights. This multiplication by complex weights can be expressed in a matrix form for both code nulling - a spectral concept - and null steering - a spatial concept. Thus, the calculations

25   performed in the spectral code domain correspond formally to the calculations performed in the spatial domain. Consequently, null steering can be performed in a system using code-nulling simply by adding an extra dimension to the matrices used for calculating the complex weights and multiplying the signals by these weights.

FIGURE 10 generally depicts how weights calculated in both the code and spatial

30   domain are used to maximize the SINR. It should be noted that FIGURE 10 is primarily a conceptual representation and is not meant to convey the actual processing steps that occur in the method of maximizing SINR. As shown in FIGURE 10, a three dimensional graph plots the relationship among code, space, and SINR. Specifically, the code and spatial domains are shown in one plane, while the SINR is plotted perpendicular to the

35   plane defined by the code and spatial domains. The SINR is plotted on a scale of 0 to 1

where a value of 0 indicates that the signal consists entirely of noise and interference while a value of 1 indicates that the signal consists entirely of the signal of interest.

The code domain axis of the graph represents the various weighting values that can be applied to each of the tones, while the spatial domain axis of the graph represents the weighting values that can be applied to each of the antenna elements. As can be seen from the plot of FIGURE 10, certain weights applied in the correct combination of code and spatial values result in SINR values near 1 so that optimal signal detection is achieved by calculating the code and spatial weights that converge to the "peaks" depicted in FIGURE 10. The method of altering the code and spatial domain weights so that convergence to the peak SINR is achieved is described in greater detail below with reference to the method of maximizing SINR section. The invention combines spatial and spectral spreading and despreading to optimally remove interference from the received signals.

Returning to the null steering procedure that forms a portion of the method for calculating weights in the spatial domain, the null steering method, illustrated schematically in FIGURE 13, provides for increased user capacity for each base station. As depicted in FIGURE 13, a first beam, "beam A," is directed by the antenna 120 using beam-forming techniques, over a particular spatial region (i.e., the signal strength is significant in the depicted region enclosed by solid lines). A second beam, "beam B," is directed by the antenna 120 over a different spatial region (enclosed by the dashed line in FIGURE 13). Both signals include sidebands, that normally would generate interference within the adjacent signal space, and null regions between the main beam and the sidebands. Of course, it will be appreciated that more complicated beam patterns may be employed having several sidebands and null regions.

In accordance with one embodiment of the invention, the null regions of beams A and B are positioned in the direction of each of the interfering transceivers (e.g., transceivers operating on the same tone set and/or code as the intended transceiver). Thus, as depicted in FIGURE 13, while beam A is directed towards remote A (since remote A is the intended receiver) the null of beam A is directed towards remote B (since remote B is an interferer). Similarly, beam B is directed towards remote B (since remote B is the intended receiver) while the null of beam B is directed towards remote A (since remote A is an interferer). A similar weighting scheme is observed when the remotes are transmitting and the base station is receiving. The same null-steering principle also may be applied to reduce the interference due to neighboring base stations.

It should be noted here that multi-path reflectors may also be treated as interfering signal sources so that null regions can be positioned to null out signals from these reflectors. However, in one embodiment, if the reflectors are not significantly time

varying, the reflected interferers are not nulled. Rather the reflected signals are advantageously phase shifted to provide constructive interference so that the SINR is increased.

The null resolution (i.e., the closeness in degrees of the nulls) which the antenna arrays are capable of providing is dependent upon several factors. Two main factors are the spacing of the antenna sensor elements and the S/N ratio of the incoming signal. For instance, if the aperture size is sufficiently large (e.g., if the sensor elements are sufficiently far apart) then a better null resolution will result. Also, if the S/N ratio of the received signal of interest is high enough, then the signal of interest could actually be placed partially within a null (so that some gain of the signal is lost, but the overall ratio between the gain null on the interferer and the gain null on the signal of interest allows for effective cancellation of the interferer and detection of the signal of interest). For example, if 15 dB of gain is necessary to close the link for a given channel, and the S/N ratio of the signal of interest is 30 dB, while the S/N ratio of the interferer is 60 dB, then if a null of -70 dB is placed on the interferer, while the signal of interest is in the same null at about -15 dB, then the interferer will have a net -10 dB gain and the signal of interest will have a net 15 dB gain so that the interferer is canceled and the link is closed. Thus, a higher S/N ratio allows the nulls to be placed closer to the signals of interest so that a higher null resolution is achieved. It should be noted here that, in accordance with one advantageous embodiment of the invention, the depth of a given null is proportional to the strength of the interferer that is to be canceled. In addition, due to the frequency diversity provided by the system, nulls can actually be collocated if the steering vectors (associated with the code weights) of two interfering remotes are sufficiently distinct to provide the necessary processing gain to close the communications link.

In an alternate embodiment, the remote terminals also include directional antennas in one preferred embodiment so that the remote terminals are also capable of null steering. FIGURE 16 is a graph plotting antenna gain (measured in decibels) versus direction (measured in degrees). A number of base stations are represented in FIGURE 16 by crosses, while other remotes (having non-orthogonal codes) are represented by small circles.

In the worst case scenario, the remote is located equidistant from three base stations (i.e., on a vertex of a hexagonal spatial cell). This case is represented in FIGURE 16 by the presence of three crosses that transmit with substantially equivalent signal strength. These base stations are shown at approximately 0, 90°, and -90° from the zero direction of the remote antenna.

Normally, each of the base stations would be received at the same level (i.e., at -85 dB) so that substantial interference would result between the three base stations when received at the remote. However, due to the beam forming weights applied by the directional antenna of the remote, the interfering base stations (i.e., the stations at ±90°)

5   are attenuated by approximately 50 dB (i.e., 120 dB minus 70 dB) relative to the intended base station (i.e., the base station at 0°). Thus, due to the fact that the beam from the receiving remote antenna is formed to have maximum gain at the intended base station, and to have minimum gain (nulls) at the strongest interfering base stations, the remote terminals are able to more easily discriminate between the signal of interest and interfering

10   signals. That is, by means of beam forming and null-steering employed at the remote terminals a much higher signal-to-interference plus noise ratio (SINR) can be obtained in much the same manner as with the base stations.

It should be noted here that the remote terminals may also employ code nulling. In an alternate embodiment, initial code nulling weights are calculated within the base station

15   and transmitted to the remote terminals. The remote terminals subsequently adapt the transmitted weights to maximize the SINR as required by the particular interference environment of each remote. By calculating the initial weights and sending these to the remote terminals, much of the intensive calculations need not be performed within the remotes. Thus, the remote terminals can be made more cost effectively.

20   In one aspect of the invention - referred to as "retrodirectivity" - the base stations adapt the spreading and despreading weights used within the base stations for transmitting and receiving signals in order to maximize the overall SINR within the communications network 100. In an alternate embodiment, this may be performed, for example, by monitoring the average bit error rate (BER) throughout the communication network 100

25   and modifying the spreading weights at each of the base stations, as well as each of the remote terminals under the control of their respective base stations, to decrease the BER.

Despread Weight Adaptation Algorithm

In one embodiment of the present invention, during the traffic establishment phase,

30   a series of pilot tones having known amplitudes and phases, are transmitted over the entire frequency spectrum. The pilot tones are at a known level (e.g., 0 dB), and are spaced apart by approximately 30 KHz to provide an accurate representation of the channel response (i.e., the amplitude and phase distortion introduced by the communication channel characteristics) over the entire transmission band. To compensate for the channel

35   distortion, a complex inverse (having an amplitude component and a phase component) of

the channel response is calculated and multiplied by the incoming signals. This initializes the weights during the traffic establishment phase.

In certain cases, where the channel induced fade is too deep to provide an adequate signal-to-noise ratio, the tone clusters where these deep nulls occur are excised
5   (i.e., discarded so as to not factor into the signal during despreading).

Since the channel response varies over time, the set of complex conjugate compensation weights are periodically recalculated to insure an accurate channel estimation.

Another method of channel equalization involves equalizing the channel effects
10   (due, for example, to noise and known interferers) by data directed methods. That is, rather than transmitting a known training signal (such as a set of pilot tones), weights are applied to the received signal so as to detect a selected property of the data signal. For example, if a PSK modulation technique is used on the data, a constant power modulus is expected in the received signal. Alternately, in a QAM signal, the data will be detected in
15   an amplitude-phase signal constellation plane to have substantially concentric rings. Thus, if the channel is equalized in such a manner as to obtain the desired signal characteristics, there is a high probability that the transmitted symbols will be accurately decoded at the receiver. This general techniques is referred to as a property restoral technique. In one embodiment of the invention the property that is restored is the finite alphabet of the QAM
20   or M-PSK symbol.

Of course, it will be appreciated by those skilled in the art that although the channel equalization method used in accordance with the invention is conceptually separable from other signal weighting and decoding methods of the present invention (discussed below), the channel equalization method may implicitly include multiple
25   cancellation and despreading methods. Therefore, the adaptive channel equalization method of the present invention used to maximize the SINR should not be considered as a separate method from the additional methods described below that refer to interference cancellation and signal despreading and decoding methods. Rather, the adaptive channel equalization method of the present invention should be understood to encompass a
30   plurality of the below described methods.

Reciprocity and Retrodirectivity

TDD is particularly advantageous in the practice of this invention since with the use of TDD the linear weighting coefficients used to compensate for channel interference
35   during transmission and reception of the encoded signals need not be re-calculated within a station. The short time duration between transmission and reception by the base station,

the fact that the transmission and reception occurs in the same frequency band and only slightly separated in time (TDD), and the fact that the remote access terminals are stationary with respect to the base stations assures that the channel is approximately reciprocal. That is, the properties of the air channel between the base and the remote

5   terminals (i.e., those properties that introduce distortion in the transmitted signal) are substantially the same for both reception and transmission. Thus, substantially the same weights can be used at a station for both despreading a signal at reception and for spreading a signal at transmission. In accordance with this retrodirectivity principle, the base station can perform most of the computation for transmission spreading weights

10   when it computes the despreading weights on reception. The transmission spreading weights are merely scalar multiples of the reception despreading weights. Similarly, in accordance with this retrodirectivity principle, the remote station can perform most of the computation for its transmission spreading weights when it computes its despreading weights on reception.

15   In an alternate embodiment of the invention, the base station can transmit the weights to the remote stations to be used in the next reception at the remote station. In this manner, processing is reduced within the remote stations since a large portion of the intensive calculations are performed solely within the base station. Thus, instead of being prohibitively sophisticated, the remote terminals can be made at a suitable size and at a

20   reasonable expense.

          Because each remote terminal stands in a different spatial relation to the other remotes and bases within the communications network, each remote terminal advantageously uses equalization weights that are individually set to maximize the SINR of signals transmitted to and received from the base station to which the remote is

25   assigned. This may be accomplished in different ways. For instance, the base station may pre-emphasize the signals sent to the remote by a calculated set of weights. Since the pre-emphasis approximately compensates for channel distortion, the remote need not perform weight adjustment calculations that are as intensive as those calculated by the base station. Thus, the remotes need not include prohibitively sophisticated processing circuitry to

30   implement this feature of the invention.

          In one aspect of the invention optimum transmit weights are calculated based on the signals received at the base station. This is called retrodirectivity. When retrodirective adaptive equalization is used to determine the set of weights used in both reception and transmission, network-wide retrodirective adaptive equalization is accomplished. Thus,

35   the channel characteristics throughout the entire system are accounted for in accordance with this aspect of the present invention.

Of course, as with other aspects of the invention, it will be appreciated that the reciprocity and system-wide retrodirective aspects of the present invention may also have application in a mobile environment. Specifically, if the time duration between transmission and reception in the TDD system is made sufficiently small, the channel may also be reciprocal for mobile transceivers so that the same principles set forth above apply in the mobile environment.

Zone Control

In a particularly preferred embodiment of the invention, a zone controller could be used to minimize the risk of interference between remote terminals that are near one another in adjacent spatial cells. According to this aspect of the invention, the zone controller is informed of the locations of each of the remotes and base stations within an assigned zone. Those remote terminals that are likely to interfere are assigned different codes and tone sets to minimize the risk of interference.

Bandwidth-on-Demand

In accordance with one aspect of the present invention, bi-directional communication is established between multiple remote user units and a telephone network via the high-bandwidth base station on a user-by-user basis. Each remote user unit upon activation, initiates communication with the high-bandwidth base station by indicating to one of the remote terminals, included within the remote user unit, the amount of bandwidth desired by the remote user unit. The remote terminals communicate with the base station via a control channel through the air (i.e., the airlink). The high-bandwidth base station then sends information concerning the requested bandwidth to a central bandwidth controller, shown in FIGURE 17, that determines whether or not the requested bandwidth can be allocated to the requesting remote user unit. In this manner, bandwidth is dynamically allocated based upon the type of user unit and the kind of data that is to be transmitted. As indicated above varying amounts of bandwidth may be assigned by allocating additional tone sets to the requesting user.

III A SPECIFIC EMBODIMENT OF THE INVENTION

The following description is a specific embodiment of the invention that includes many aspects of the description provided above. However, it should not be interpreted to limited the scope of the invention in any way

Frequency Definitions

        The total bandwidth allocation for the airlink of this specific embodiment of the
invention is 10 MHz in the range of 1850 to 1990 MHz. The total bandwidth is divided
into two 5 MHz bands called the lower RF band and the upper RF band. The separation
5   between the lowest frequency in the lower RF band and the lowest frequency in the upper
RF band (DF) is 80 MHz. The base frequency (f_{base}) for this embodiment is defined as the
lowest frequency of the lower RF band. Figure 18 shows the possible operational bands
for this embodiment.

        The lower and upper RF bands are further subdivided into sub-bands as shown in
10   Figure 19 . The first and last 0.5 MHz of each RF band are designated as guard bands and
are hence unused. The remaining 4 MHz in each RF band is subdivided into four sub-
bands sequentially numbered from 0 to 3. Furthermore, the suffix "A" indicates a sub-
band within the lower RF band and "B" indicates a sub-band within the upper RF band.
The sub-bands are paired with each sub-band pair containing one sub-band from the lower
15   RF band and another from the upper RF band.

        There are a total of 2560 tones (carriers) equally spaced in the 8 MHz of available
bandwidth. There are 1280 tones in each band. The spacing between the tones (Df) is
thus MHz divided by 1280, or 3.125 KHz.

        The total set of tones are numbered consecutively form 0 to 2559 starting from the
20   lowest frequency tone. T_i is the frequency of the ith tone:

$$T_i = f_{base} + f_{guard} + Df/2 + (i)(Df)$$

        for $0 \leq i \leq 1279$

25

$$T_i = f_{base} + DF + f_{guard} + Df/2 + (i)(Df)$$

        for $1280 \leq i \leq 2559$

where f_{base} is the base frequency defined in Table 2.3, f_{guard} is 0.5 MHz, Df is 3.125 KHz,
30   and DF is 80 MHz. Equivalently, the relationship may be expressed as:

$$T_i = f_{base} + 500 + (i + 1/2)(3.125 \text{ KHz})$$

        for $0 \leq i \leq 1279$

35

$$T_i = f_{base} + 80500 + (i + 1/2)(3.125 \text{ KHz})$$

46

for $1280 \leq i \leq 2559$

Each sub-band pair contains 640 tones (320 frequencies in the lower band, and 320
in the upper band). The mapping of tones to each sub-band is shown in Figure 20.
The set of 2560 tones is the tone space. The tones in the tone space are used to transmit
two types of data: traffic data and overhead data. The tones used for transmission of
traffic are the traffic tones, and the rest are the overhead tones.

Traffic Tones

The traffic tones are divided into 32 traffic partitions denoted by P_0 to P_{31}. (In this
embodiment a traffic channel requires at least one traffic partition.) Each traffic partition
contains 72 tones as shown in Figure 21 . Tone mapping into the ith traffic partition (P_i)
is shown in Table 2.5.

Overhead Tones

The overhead tones are used for the following channels

Forward channels:

The Common Link Channel (CLC) used by the base to transmit control
information to the Remote Units;

The Broadcast Channel (BRC) used to transmit broadcast information from the
Base to all Remote Units; and

The Remote Unit Synchronization Channel (RSC) used by the base, for example,
to transmit pilot signals, frame synchronization information.

Reverse channels:

The Common Access Channels (CACs) is used to transmit messages from the
Remote Unit to the Base; and

The Delay Compensation Channel (DCC) used to adjust a Remote Units TDD
timing.

For each sub-band pair, there is one grouping of tones assigned to each channel.
These groups of tones are referred to by the name of their channels and their sub-band pair
index (0, 1, 2, or 3). For instance, the CLC channel in sub-band pair 2 is denoted by
CLC_2.

There are two different CACs in each sub-band pair: $CAC_{i,0}$, and $CAC_{i,1}$, where i is the sub-band pair index. The two channels may be used as either solicited (SCAC) or unsolicited (UCAC). The allocation of tones to each of these channels for the ith sub-band pair is shown in FIGURE 23. Indices are provided for all tones within a given

5   channel. The absolute tone index within the tone space can be determined by the relationships shown in FIGURE 23. For instance:

For the forward channel, the 13th tone in the CLC channel in sub-band pair 2, is denoted by $CLC_2(13)$ and its absolute tone index is:

$$CLC_2(13) = T_{320.2 + 1460} = T_{2100}$$

10 For the reverse channel, the 13th tone in the first CAC channel in sub-band pair 2, is denoted by $CAC_{2,0}(13)$ and its absolute tone index is the same as above.

FIGURE 24   provides a pictorial representation of the division of the tone spaces into different tone groupings

15 Time Definitions

TDD is used by Base and the Remote Unit to transmit data and control information in both directions over the same frequency channel. Transmission from the Base to the Remote Unit are called forward transmissions, and from the Remote Unit to the Base are called reverse transmissions.

20   As shown in FIGURE 25, the duration of a forward transmission is $T_{forward}$, and the duration of a reverse transmission is $T_{reverse}$. The time between recurrent transmissions from either the Remote Unit or the Base is TTD, the TDD period. A guard period of duration $T_{f-guard}$ is inserted between the forward and reverse transmissions, and a guard period of duration $T_{r-guard}$ is inserted between the reverse and forward transmissions.

25   As shown in FIGURE 26 , in every TDD period, there are four consecutive transmission bursts in each direction. Data is transmitted in each burst using multiple tones. The burst duration is T_{burst}. A guard period of duration $T_{b-guard}$ is inserted between each burst. FIGURE 27 shows the values of the TDD parameters.

In addition to synchronizing and conforming to the TDD structure defined in the

30 last section, both the Base and the Remote Unit must synchronize to the framing structure. The framing structure is shown in FIGURE 28 . The smallest unit of time shown in this figure is a TDD period. Two TDD periods make a subframe, eight subframes make a frame, and 32 frames make a superframe.

Frame synchronization is performed at the superframe level. The frame and

35 subframe boundaries are determined from the superframe boundary.

In this embodiment we could potentially reuse all available frequencies in every
spatial cell. However, initially a reuse factor of 2 is used. Each Remote Unit is assigned
to a Sub-band Pair depending on its location within the spatial cell and the traffic loading
of the Sub-band Pair. As shown in FIGURE 29 each Remote Unit may be assigned two
5 of the four sub-band pairs depending on its location. For example, an Remote Unit in the
north-eastern part of the spatial cell in FIGURE 29 can be assigned Sub-band Pair 0 or
Sub-band Pair 2. Of course this reuse strategy reduces capacity to half of the maximum
potential capacity. The same Sub-band Pair assignment is used in all spatial cells as shown
in FIGURE 30.
10

Forward Channel Format

The physical layer has three possible implementations based on the desired range
(or quality) of transmission. The physical layer manages the trade-offs between bandwidth
efficiency (bits/symbol) and transmission coverage by providing three modes of operation:
15

High capacity mode (short range): 3 bits/symbol

Medium capacity mode (medium range): 2 bits/symbol

- Low capacity mode (long range): 1 bits/symbol

Each mode employs different details in the coded modulation scheme and, hence,
20 somewhat different formats. Nevertheless, there is abundant symmetry, redundancy, and
common elements for the three modes.

High Capacity Mode

In high capacity mode, one traffic partition is used in one traffic channel. In
25 medium and low capacity modes, two and three traffic partitions are used, respectively.
The Base transmits information to multiple Remote Units in its spatial cell. This section
describes the transmission formats for a 64 kbits/sec traffic channel, together with a 4 kbps
Link Control Channel (LCC) from the Base to a single Remote Unit. The block diagram
for the upper physical layer of the Base transmitter for high capacity mode is shown in
30 FIGURE 31, which shows data processing for one forward channel burst. (The boundary
between the upper and the lower physical layers is where the baseband signals are
translated into frequency tones. The lower physical layer can then be regarded as the
common element of the various modes and directions of transmission.) The large shaded
area shows the processing required for one traffic channel at the Base. The remainder of
35 the diagram shows how various traffic channels are combined. The details of each block
in the diagram are discussed throughout this section.

The binary source delivers data to the Base transmitter at 64 kbits/sec. This translates to 48 bits in one forward transmission burst.

The information bits are encrypted according to the triple data encryption standard (DES) algorithm.

5   The encrypted bits are then randomized in the data randomization block. The bit to octal conversion block converts the randomized binary sequence into a sequence of 3-bit symbols. The symbol sequence is converted into 16 symbol vectors. (In this description, the term vector generally refers to a column vector. A vector is generally complex unless otherwise stated. Generally, column vectors are denoted by bold lower-case characters, while row vectors are denoted by the same characters with a transpose

10   operation, denoted by a superscript T. Another widely used vector form used here is a conjugate transpose vector referred to here as Hermetian.) One symbol from the LCC is added to form a vector of 17 symbols.

The 17-symbol vector is trellis encoded. The trellis encoding starts with the most

15   significant symbol (first element of the vector) and is continued sequentially until the last element of the vector (the LCC symbol). This process employs convolutional encoding that converts the input symbol (an integer between 0 and 7) to another symbol (between 0 and 15) and maps the encoded symbol to its corresponding 16QAM (or 16PSK) signal constellation point. The output of the trellis encoder is therefore a vector of 17 elements

20   where each element is signal within the set of 16 QAM (or 16PSK) constellation signals. (The term signal will generally refer to a signal constellation point.)

A link maintenance pilot signal (LMP) is added to form an 18-signal vector, with the LMP as the first elements of the vector. The resulting (18 X 1) vector d_{fwd} is pre-multiplied by a (18 x 18) forward smearing matrix $C_{fwd-smear}$ to yield a (18 x 1) vector b.

25   Vector b is element-wise multiplied by the (18 x 1) gain preemphasis vector $g_{fwd}(p)$ to yield another (18 x 1) vector, c, where p denotes the traffic channel index and is an integer in the range [0, M_{base}] where M_{base} is the maximum number of traffic channels that can simultaneously be carried over one traffic partition. Vector c is post-multiplied by a (1 x 32) forward spatial and spectral spreading vector $g^{H}_{fwd}(p)$ to yield a (18 x 32) matrix

30   R(p). The number 32 results from multiplying the spectral spreading factor 4 and spatial spreading factor 8. The 18 x 32 matrices corresponding to all traffic channels carried (on the same traffic partition) are then combined (added) to produce the resulting 18 x 32 matrix S_{fwd}.

The matrix S_{fwd} is partitioned (by groups of four columns) into eight (18 x 4)

35   submatrices (A_0 to A_7). (The indices 0 to 7, corresponds to the antenna elements over which these symbols will eventually be transmitted.) Each submatrix is mapped to tones

within one traffic partition (denoted by partition A in FIGURE 31) according to the mapping discussed in FIGURE 22 and sent to the lower physical layer.

The lower physical layer places the baseband signals in discrete Fourier transfer (DFT) frequency bins where the data is converted into the time domain and sent to its
5   corresponding antenna elements (0 to 7) for transmission over the air. The details of the lower physical layer are discussed below.

This process is repeated from the start for the next 48 bits of binary data to be transmitted in the next forward transmission burst. The various steps in the transformation of binary data are shown in FIGURE 32. To keep the diagram simple, the
10   spreading and traffic channel combiner functions are shown in one step.

Medium Capacity Mode

The block diagram for the upper physical layer of the Base transmitter for the medium capacity mode is shown in FIGURE 33. The primary difference between the
15   transmission formats for high and medium capacity modes is the use of different trellis encoding schemes. In medium capacity mode, an 8QAM (or 8PSK) rate 2/3 trellis encoder (compared to a 16QAM or 16PSK rate 3/4 bits in one forward transmission burst, two traffic partitions (A and B) are used.

The binary source delivers binary data to the Base transmitter at 64 kbits/sec. For
20   one forward channel burst, this translates to 48 bits. The information bits are encrypted according to the triple DES algorithm. The encrypted bits are then randomized in the data randomization block. The bit to-bit conversion block converts the randomized binary sequence into a sequence of 2-bit symbols. The symbol sequence is converted into 24 symbol vectors. Two symbols from the LCC are added, and eight ones are inserted at the
25   end of the sequence to form a vector of 34 symbols. (The two symbols for the LCC carry only three bits of LCC information. The least significant bit, LSB, of the second LCC symbol is always set to one.)

The 34-symbol vector is trellis encoded. The trellis encoding starts with the most significant symbol (first element of the vector) and is continued sequentially until the last
30   element of the vector (the second LCC symbol). This process employs convolutional encoding that converts the input symbol (an integer between 0 and 3) to another symbol (between 0 and 7) and maps the encoded symbol to its corresponding 8 QAM (or 8PSK) signal constellation point. The output of the trellis encoder is therefore a vector of 34 elements where each element is a signal within a set of 8QAM (or 8PSK) constellation
35   signals.

The 34-element vector is divided into two 17-element vectors. An LMP is added
to each of the vectors to form two 18-element vectors d_{fwd} and d'_{fwd}, where the LMP is
the first element of these vectors. Each resulting vector is pre-multiplied by a (18 x 18)
forward smearing matrix $C_{fwd-smear}$ to yield another two (18 x 1) vector b and b'. Vectors
5   b and b' are then element-wise multiplied by two (18 x 1) gain preemphasis vectors $g_{fwd}(p)$
and $g'_{fwd}(p)$ to yield two (18 x 1) vectors c and c', where p denotes the traffic channel
index. Each vector is post-multiplied by its corresponding (1 x 32) Forward Spatial and
Spectral spreading Vector ($g^H_{fwd}(p)$ or ($g'^H_{fwd}(p)$)) to yield two (18 x 32 matrices R(p) and
R'(p).

10   The various 18 x 32 matrices corresponding to all traffic channels carried on traffic
partition A are combined to produce the 18 x 32 matrix S_{fwd}. Similarly, matrices from
those traffic channels carried on Traffic Partition B are combined to produce the 18 x 32
matrix S'_{fwd}.

           Matrix S_{fwd} is partitioned (by groups of four columns) into eight (18 x 4)
15   submatrices (A_0 to A_7). Each submatrix is mapped into tones within partition A according
to the mapping discussed in FIGURE 22 and is sent to the lower physical layer. Similarly,
matrix S'_{fwd} is partitioned into eight (18 x 4) submatrices (A'_0 to A'_7). Each submatrix is
mapped into tones with partition B according to the mapping discussed in FIGURE 22
and is sent to the lower physical layer.

20   The lower physical layer places the baseband signals in DFT frequency bins where
the data is converted into the time domain and sent to its corresponding antenna element
(0 to 7) for transmission over the air.

           This process is repeated from the start for the next 48 bits of binary data to be
transmitted in the next forward channel transmission burst. The various steps in the
25   transformation of binary data are shown in FIGURE 34. To keep the diagram simple, the
spreading and traffic channel combiner functions are shown in one step.
The block diagram for the upper physical layer of the Base transmitter for low capacity
mode is shown in FIGURE 35.

30   Low Capacity Mode
           The primary difference between the transmission formats for high and low capacity
modes is the use of different trellis encoding schemes. In low capacity mode, a rate 1/2
trellis encoder (compared to a rate 3/4 encoder for high capacity mode) is employed. To
transmit 48 bits in one forward transmission burst, three Traffic Partitions (A, B, and C)
35   are used.

The binary source delivers binary data to the Base transmitter at 64 kbits/sec. For one forward channel burst, this translates to 48 bits. The information bits are encrypted according to the Triple DES algorithm. The encrypted bits are then randomized in the data randomization block. The 48 bits are formed into a vector. Three symbols from the

5   LCC are then added to form a vector of 51 symbols. The 51-symbol vector is trellis encoded. The trellis encoding starts with the most significant symbol (first element of the vector) and is continued sequentially until the last element of the vector (the third LCC symbol). This process employs convolutional encoding that converts the binary input symbol (0 or 1) to another symbol (0, 1, 2, or 3) and maps the encoded symbol to its

10   corresponding QPSK signal constellation point. The output of the trellis encoder is therefore a vector of 51 elements where each element is a signal within the set of QPSK constellation signals.

The 51-element vector is divided into three 17-element vectors. An LMP is added to each of the vectors to form three 18-element vectors d_{fwd}, d'_{fwd}, and d''_{fwd}, where the

15   LMP is the first element of these vectors. Each resulting vector is pre-multiplied by a (18 x 18) forward smearing matrix $C_{fwd-smear}$ to yield another three (18 x 1) vectors b, b', and b". Vectors b, b', and b" are then element-wise multiplied by their respective (18 x 1) gain preemphasis vectors $g_{fwd}(p)$, $g'_{fwd}(p)$, and g" to yield three (18 x 1) vectors c, c', and c"; where p denotes the traffic channel index. Each vector is post-multiplied by its

20   corresponding (1 x 32) forward spatial and spectral spreading vector ($g^H_{fwd}(p)$, $g'^H_{fwd}(p)$, or $g''^H_{fwd}(p)$) to yield three (18 x 32) matrices R(p), R'(p), and R" (p).

The various 18 x 32 matrices corresponding to traffic channels carried on traffic partition A are combined to produce the 18 x 32 matrix S_{fwd}. Similarly, matrices from those traffic channels carried on traffic partitions B and C are combined to produce two 18

25   x 32 matrices, S'_{fwd} and S" $_{fwd}$, respectively. Matrix S_{fwd} is partitioned (by groups of four columns) into eight (18 x 4) submatrices (A_0 to A_7). Each submatrix is mapped into tones within partition A according to the mapping discussed in FIGURE 22 and is sent to the lower physical layer. Matrix S'_{fwd} is partitioned into eight (18 x 4) submatrices (A'_0 to A'_7). Each submatrix is mapped into tones within partition B and is sent to the lower

30   physical layer. Similarly, matrix S"$_{fwd}$ is partitioned into eight (18 x 4) submatrices (A''_0 to A''_7). Each submatrix is mapped into tones within partition C and is sent to the lower physical layer. The lower physical layer places the baseband signals in DFT frequency bins where the data is converted into the time domain and sent to its corresponding antenna element (0 to 7) for transmission over the air.

35   This process is repeated from the start for the next 48 bits of binary data to be transmitted in the next forward channel transmission burst. The various steps in the

transformation of binary data are shown in FIGURE 36. To keep the diagram simple, the spreading and traffic channel combiner functions are shown in one step. Similarly, the encryption and randomization functions are also shown in one step.

5 Encryption/Decryption

The 64 kbps binary source delivers bits to the encryption module 48 bits at a time. The encryption function is a three-stage cascade of the DES algorithm as shown in FIGURE 37.

10 Trellis Encoding/Decoding

The trellis encoding technique consists of convolutional encoding followed by a signal mapping. The three modes of the physical layer use different trellis codes. For high capacity mode, there are two possible signal constellations: 16PSK and 16QAM.

The rate 3/4 convolutional encoder for the 16 PSK constellation is shown in 15 FIGURE 38. The convolutional encoder employs an 8-state $(k=4)^{14}$ rate 1/2 mother encoder that encodes one bit out of a 3-bit input symbol, and passes the remaining bits uncoded.

The rate 1/2 convolutional encoder for the 16PSK constellation may be described by the generator polynomials (G_0=04, G_1=13), in octal representation. Equivalently, the 20 polynomial representation is:

$$G_0 = D$$
$$G_1 = D^3 + D^2 + 1$$

The rate 3/4 convolutional encoder for the 16QAM constellation is shown in FIGURE 39. The convolutional encoder employs an 8-state (k=4) rate 1/2 mother 25 encoder that encodes one bit out of a 3-bit input symbol, and passes the remaining bits uncoded.

The rate 1/2 convolutional encoder for the 16QAM constellation may be described by the generator polynomials (G_0=17, G_1=13), in octal representation. Equivalently, the polynomial representation is:

30

$$G_0 = D^3 + D^2 + D + 1$$
$$G_1 = D^3 + D^2 1$$

The two highest-order bits of the input symbol (x_2,x_1) are passed through uncoded to form the two highest-order bits of the output symbol (y_3,y_2). The lowest-order bits of 35 the input symbol (x_0) enters the rate 1/2 mother encoder (shown as the shaded box) to produce two lowest-order bits of the output symbol (y_1,y0).

The next step in the trellis encoding process is to map the output symbol onto a signal in the 16QAM (or 16PSK) constellation. The particular mappings for the 16QAM and 16PSK constellations are shown in FIGURE 40.

The resulting trellis encoder output is one of 16 possible complex numbers within 5 the 16QAM (or 16PSK) constellation shown in FIGURE 40. The actual value of each constellation point (signal) is shown in FIGURE 41. The points on the constellation have been chosen so that the average energy of the signal is 1.

In medium capacity mode, a rate 2/3 trellis code with either 8QAM or 8PSK signal mapping is employed. The convolutional encoder for the 8PSK constellation is shown in 10 FIGURE 42. It employs a 32 state (k=6) rate 1/2 mother encoder that encodes one bit out of a 2-bit input symbol, and passes the remaining bit uncoded. The rate 1/2 convolutional encoder may be described by the generator polynomials (G_0=10, G_1=45), in octal representation. Equivalently, the polynomial representation is:

15
$$G_0 = D^2$$
$$G_1 = D^5 + D^3 + D^2 + 1$$

The convolutional encoder for the 8QAM constellation is shown in FIGURE 43. It employs a 32-state (k=6) rate 1/2 mother encoder that encodes one bit out of a 2-bit input symbol, and passes the remaining bit uncoded. The rate 1/2 convolutional encoder 20 may be described by the generator polynomials (G_0=53, G_1=75), in octal representation. Equivalently, the polynomial representation is:

$$G_0 = D^5 + D^4 + D^2 + 1$$
$$G_1 = D^5 + D^3 + D^2 + 1$$

25 The highest-order bit of the input symbol (x_1) is passed through uncoded to form the highest-order bit of the output symbol (y_2). The lowest-order bit of the input symbol (x_0) enters the rate 1/2 mother encoder to produce the two lowest-order bits of the output symbol (y_1,y0).

The next step in the trellis encoding process is to map the output symbol onto a 30 signal in the 8QAM (or 8PSK) constellation. The particular mappings for the 8QAM and 8PSK constellations are shown in FIGURE 44. The resulting trellis encoder output is one of eight possible complex numbers within the 8QAM (or 8PSK) constellation shown in FIGURE 44. The actual value of each constellation point (signal) is shown in FIGURE 45. The points of the constellation have been chosen so that the average energy of the 35 signal is 1.

In low capacity mode, the de facto standard rate 1/2 encoder, shown in FIGURE 46, together with QPSK mapping is employed. The only bit of the input symbol (x_0) enters the rate 1/2 mother encoder to produce the two bits of the output symbol (y_1, y_0).

The next step in the trellis encoding process is to map the output symbol onto a signal in the QPSK constellation. The particular mapping for the QPSK constellation is shown in FIGURE 46 referred to by natural mapping. The resulting trellis encoder output is one of four possible complex numbers within the QPSK constellation shown in FIGURE 47. The actual value of each constellation point (signal) is shown in FIGURE 48. The points on the constellation have been chosen so that the average energy of the signal is one.

Cluster Smearing/Desmearing

This section defines the smearing matrix $C_{fwd\text{-}smear}$. The input to the smearing block is the (18 x 1) vector d_{fwd}. The output of the smearing operation (vector b) can then be described by the matrix multiplication of d_{fwd} and the (18 x 18) smearing matrix $C_{fwd\text{-}smear}$. That is

$$b = C_{fwd\text{-}smear}d_{fwd}$$

$C_{fwd\text{-}smear}$ is the constant valued matrix shown below:

```
[1 ]  0    0    ℓ    0    0    0    0    0    0    0    0     0     0     0     0     0     0
[α ]  βδ0  0    0    0    0    0    0    0    0    0    0     0     0     0     0     0     0
[α ]  0    βδ1  0    0    0    0    0    0    0    0    0     0     0     0     0     0     0
[α ]  0    0    βδ2  0    0    0    0    0    0    0    0     0     0     0     0     0     0
[α ]  0    0    0    βδ3  0    0    0    0    0    0    0     0     0     0     0     0     0
[α ]  0    0    0    0    βδ4  0    0    0    0    0    0     0     0     0     0     0     0
[α ]  0    0    0    0    0    βδ5  0    0    0    0    0     0     0     0     0     0     0
[α ]  0    0    0    0    0    0    βδ6  0    0    0    0     0     0     0     0     0     0
[α ]  0    0    0    0    0    0    0    βδ7  0    0    0     0     0     0     0     0     0
[α ]  0    0    0    0    0    0    0    0    βδ8  0    0     0     0     0     0     0     0
[α ]  0    0    0    0    0    0    0    0    0    βδ9  0     0     0     0     0     0     0
[α ]  0    0    0    0    0    0    0    0    0    0    βδ10  0     0     0     0     0     0
[α ]  0    0    0    0    0    0    0    0    0    0    0     βδ11  0     0     0     0     0
[α ]  0    0    0    0    0    0    0    0    0    0    0     0     βδ12  0     0     0     0
[α ]  0    0    0    0    0    0    0    0    0    0    0     0     0     βδ13  0     0     0
[α ]  0    0    0    0    0    0    0    0    0    0    0     0     0     0     βδ14  0     0
[α ]  0    0    0    0    0    0    0    0    0    0    0     0     0     0     0     βδ15  0
[α ]  0    0    0    0    0    0    0    0    0    0    0     0     0     0     0     0     βδ16
```

where,

$$a = (r_{LMP}/(1+r_{LMP}))^{1/2}$$
$$b = (1/(1+r_{LMP}))^{1/2}$$

and r_{LMP} is the ratio of pilot to data power that is a physical layer provisionable parameter whose value is nominally set to one.

Gain Preemphasis

This section discusses the gain preemphasis matrix $g_{fwd}(p)$ shown in FIGURE 31. The input to the gain preemphasis block is the (18 x1) vector b. The output of the gain preemphasis operation (Vector c) is the element-wise multiplication of vector b and the gain preemphasis vector $g_{fwd}(p)$:

$$c = b \cdot g_{fwd}(p)$$

where · represents element-wise vector multiplication. The elements of $g_{fwd}(p)$ are derived using information received at the Base. The derivation of these weights are implementation dependent.

Spectral and Spatial Spreading

This section defines the (1 x 32) forward spatial and spectral spreading vector $g^H_{fwd}(p)$ shown in FIGURE 31. The input to the spectral and spatial spreading block is the 18-element vector c. The output of the spectral and spatial spreading operation, (18 x 32) matrix R(p), is the matrix multiplication of c and the (1 x 32) spectral and spatial spreading vector $g^H_{fwd}(p)$:

$$R(p) = cg^H_{fwd}(p)$$

where,

$$g^H_{fwd}(p) = [g_0\, g_1\, g_2 \cdots g_{30}\, g_{31}]$$

The elements of vector $g^H_{fwd}(p)$ are transmit spreading weights calculated throughout the transmission. The algorithm for the derivation of these weights is implementation dependent. However, to clarify the procedure, a specific algorithm for the derivation of these weights is described below.

The Base derives its new weights based on the most recent data received on the reverse channel. The transmit weights are a scaled version of the received weights using eight antenna inputs with four receive frequencies per antenna. The receive weight vector $w^H_{rev}(p)$ has 32 elements (w_0 - w_{31}) that are mapped to spatial and spectral components as shown in FIGURE 49.

For the Base traffic establishment procedure, the transmit weights (g_0 - g_{31}) are calculated according to the following equation:

$$g^H_{fwd}(p) = a_{fwd}(n) \, h(k_{fwd} w^H_{rev}(p))$$

5   where k_{fwd} is the Base transmission constant, $a_{fwd}(n)$ is the Base gain ramp-up factor for the nth packet, and h(.) is a function that limits the norm of its argument to 23 dBm

$$h(v) = v$$
$$\text{for } \| v \|^2 < 23 \text{ dBm}$$
10    $$h(v) = 23 \text{ dBm (scale factor)} (v/ \| v \|^2)$$
$$\text{otherwise}$$

For the Base steady-state procedure, receive weights are adaptively calculated using the following equation:

15    $$w_{rev}(p) = R^{-1}_{xx} r_{xy}$$
where

$w_{rev}(p)$ is the (32 x 1) weight vector;

20   r_{xy} is an estimate of the (32 x 1) cross-correlation vector of the received (32 x 1) vector x and the despread data y, multiplied by an estimate of the channel equalization weights; and

R^{-1}_{xx} is an estimate of (32 x 32) inverted auto-correlation matrix of the received
25   vector x. (R^{-1}_{xx} may be computed using the Recursive Modified Gramm-Schmidt (RMGS) algorithm.)

r_{xy} is cross-correlated against the despread data after a resmearing step and a gain pre-emphasis reapplication step.

The receive weights (w_0 - w_{31}) are mapped to spatial and spectral components
30   according to the mapping shown in FIGURE 49. The transmit weights (g_0 - g_{31}) are a scaled version of the receive weights. The scaling is made according to the following equation:

$$g^H_{fwd}(p) = k_{fwd} w^H_{rev}(p)$$

35   where k_{fwd} is the Base steady-state transmission constant.

Correlation estimates are computed over eight reverse-channel bursts. The new despreading weights are applied to eight reverse channel burst with no delay. The spreading weights are applied to eight forward channel bursts after a 4-burst delay. Correlation estimates are made using an exponentially averaged block summation. The exponential decay constant is provisionable with a nominal value of 0.7.

An illustrative flowchart of an embodiment of the adaptive solution of spectral and spatial weights is shown in FIGURE 85.

Forward Control Channel Transmission Format

The block diagram for the physical layer of the Common Link Channel (CLC) channel transmissions is shown in FIGURE 50. A CLC message is a 64-bit binary sequence. The bit to di-bit conversion block converts the binary sequence into a sequence of 2-bit symbols of length 32. The vector formation block converts the symbol sequence into a (32 x 1) vector. Each element of the resulting vector is mapped into its corresponding signal in the QPSK signal constellation to form another (32 x 1) vector, s. The mapping for the QPSK signal is shown in FIGURE 51.

The resulting vector is passed through two parallel paths. In the first path, the vector s is sent directly for spectral and spatial spreading that involves post-multiplying it by the (1 x 32) spreading vector g_{clc}^{H}:

$$g_{c}^{H} = [g0\ g1\ g2...g30\ g31]$$

(g_{clc}^{H} is discussed further below.) The resulting (32 x 32) matrix is D_{clc}. Matrix D_{clc} is then sent to the antenna demultiplexer where it is partitioned (by groups of 4 columns)into eight (32 x 4) submatrices A_0 to A_7. The elements of these matrices will ultimately be transmitted on antennas 0 to 7, respectively.

In the second path, the vector s is code-gated. The code-gating operation is described by the element-wise multiplication of the (32 x 1) vector s with a (32 x 1) code-gating vector Y_{clc}. The resulting (32 x 1) vector is S':

$$s' = s \cdot i_{clc}$$

The vector i_{clc} is described below.

The resulting (32 x 1) vector s' is sent for spectral and spatial spreading that involves post-multiplying it by the (1 x 32) spectral and spatial spreading vector g_{clc}^{H}. The resulting (32 x 32) matrix is D'_{clc} Matrix D'_{clc} is then sent to the antenna demultiplexer where it is partitioned (by groups of 4 columns) into eight (32 x 4) submatrices A'_0 to A'_7. Each of these matrices (A_0 to A_7) and (A'_0 to A'_7) is then sent to a time demultiplexer

where it is further partitioned (by groups of 4 rows) into eight (4 x 4) submatrices. This yields 128 (4 x 4) matrices (D_0 to D_{63}) and (D'_0 to D'_{63}).

The transmission of one 64 bit CLC message requires 16 forward channel bursts or 4 TDD periods. In each of these bursts, eight (one for each antenna) of the (4 x 4) matrices are mapped onto tones and sent to the lower physical layer for transmission over the air. The interleaving and tone mapping functions are described herein.

The vector g_{clc} is defined as the Kronecker product of a (8 x 1) spatial spreading vector d and a (4 x 1) spectral spreading vector f:

$$g_{clc} = kron(d,f)$$

where d, is given by

$$\begin{vmatrix} d_0 \\ d_1 \\ d_2 \\ d_3 \\ d_4 \\ d_5 \\ d_6 \\ d_7 \end{vmatrix}$$

and f is given by

$$\begin{vmatrix} f_0 \\ f_1 \\ f_2 \\ f_3 \end{vmatrix}$$

The resulting vector g_{clc} is given by:

$$\begin{vmatrix} d_0 f_0 \\ d_0 f_1 \\ d_0 f_2 \\ d_0 f_3 \\ d_1 f_0 \\ \cdot \\ \cdot \\ \cdot \\ d_7 f_2 \\ d_7 f_3 \end{vmatrix}$$

60

The $g_{clc}{}^H$ is the conjugate transpose of g_{clc}.

The spreading vector f is a column of the (4 x 4) Hadamard matrix H_4, that may be chosen randomly by the Base.

The spreading vector d is the kth column of the (8 x 72) CLC Spatial Spreading Weights Table. The column index k is provided by the MAC layer through the parameter CLC beam.

A (N x N) Hadamard matrix denoted by H_N is obtained by the following recursion: H_{2n} equals

$$\begin{vmatrix} Hn & Hn \\ Hn & Hn \end{vmatrix}$$

where H_0 is initialized at 1. For instance, the 4 x 4 Hadamard matrix (H_4) is:

$$\begin{vmatrix} 1 & 1 & 1 & 1 \\ 1 & -1 & 1 & -1 \\ 1 & 1 & -1 & -1 \\ 1 & -1 & -1 & 1 \end{vmatrix}$$

The code-gating vector i_{clc} is:

$$i_{clc} = b_{clc} \cdot h_{clc}$$

where the vector h_{clc} is the 0th column of the (32 x 32) Hadamard matrix (H_{32}), that is the all ones vector and the ith element of the (32 x 1) vector b_{clc} is given by:

$$b_{clc} = e^{j2\pi i k_{offset}/32}$$

The k_{offset} (an integer between 0 and 31) is the Base station offset code (BSOC) for the transmitting Base.

Interleaving

There are 16 burst in every CLC transmission (burst 0 to burst 15). For each antenna, the interleaver outputs one of the 16 possible (4 x 4) matrices in each burst. FIGURE 52 shows the order of the transmission used by the interleaver.

Tone Mapping

There are 128 (4 x 4) matrices to be mapped onto tones for transmission over the air. FIGURE 53 shows the mapping of a (4 x 4) matrix at the output of the interleaver into tones. The absolute tone indices can be obtained using FIGURE 23.

5   The Broadcast Channel

The block diagram for the physical layer of BRC channel transmissions is shown in FIGURE 54. The block diagram is very similar to that for the CLC shown in FIGURE 50. However, for the sake of completeness, and to point out the small differences, the details of the BRC transmission format are included in this section.

10   The primary differences between the CLC and the BRC transmissions on the forward channel are:

The Base uses all our BRC channels (in the four sub-band pairs) while for the CLC, channel selection is based on its operating sub-band pair

The Base forms 10 spatial beams (activated sequentially) to cover all the RUs in

15   one hemisphere, that means that the time to broadcast a BRC message is ten times as long as transmission of a CLC message

A BRC message is a 64-bit binary sequence. The bit to di-bit conversion block converts the binary sequence into a sequence of 2-bit symbols of length 32. The vector formation block converts the symbol sequence into a (32 x 1) vector. Each element of the

20   resulting vector is mapped into its corresponding signal in the QPSK signal constellation to form another (32 x 1) vector s. The mapping for the QPSK signal is identical to that for the CLC shown in FIGURE 51.

The resulting vector is passed through two parallel paths. In the first, path, the vector s is sent directly for spectral and spatial spreading that involves post-multiplying it

25   by the (1 x 32) spectral and spatial spreading vector g_{brc}^{H}.

$$g_{brc}^{H} = [g0 \ g1 \ g2...g30 \ g31]$$

The g_{brc}^{H} is discussed below.

30   The resulting (32 x 32) matrix is D_{brc}. Matrix D_{brc} is then sent to the antenna demultiplexer where it is partitioned (by groups of four columns) into eight (32 x 4) submatrices A_0 to A_7. The elements of these matrices will ultimately be transmitted on antennas 0 to 7, respectively.

In the second path, the vector s is code-gated. Code-gating is described by the

35   element-wise multiplication of the (32 x 1) vector s with a (32 x 1) code-gating vector i_{brc}. The resulting (32 x 1) vector is s':

$$s' = s \cdot Y_{brc}$$

The vector Y_{brc} is described below.

The resulting (32 x 1) vector s' is sent for spectral and spatial spreading, that involves post-multiplying it by the (1 x 32) spreading vector g_{brc}^H. The resulting (32 x 32) matrix is D'_{brc}. Matrix D'_{brc} is then sent to the antenna demultiplexer where it is partitioned (by groups of four columns) into eight (32 x 4) submatrices A'_0 to A'_7. Each of these matrices (A_0 to A_7) and (A'_0 to A'_7) is then sent to a time demultiplexer where they are further partitioned (by groups of four rows) into eight (4 x 4) submatrices. This yields 128 (4 x 4) matrices (D_0 to D_{63}) and (D'_0 to D'_{63}).

For one spatial beam, the transmission of one 64-bit BRC message requires 16 forward channel bursts or four TDD periods. In each of these bursts, eight (one for each antenna) of the (4 x 4) matrices are mapped onto tones and sent to the lower physical layer for transmission over the air. The interleaving and tone mapping functions are described herein.

This process is repeated 10 times to provide 10 spatial beams with different directions so that all the RUs in a spatial cell can detect the broadcast message. The details of the beam sweeping are described below. The duration of a BRC transmission is therefore 160 bursts or 40 TDD periods.

The vector g_{brc} is defined as the Kronecker product of a (8 x 1) spatial spreading vector d and a (4 x 1) spectral spreading vector f:

$$g_{brc} = kron(d,f)$$

where d, is given by

$$
\begin{vmatrix}
d_0 \\
d_1 \\
d_2 \\
d_3 \\
d_4 \\
d_5 \\
d_6 \\
d_7
\end{vmatrix}
$$

and f is given by

$$
\begin{vmatrix}
f0 \\
f1 \\
f2 \\
f3
\end{vmatrix}
$$

The resulting vector g_{brc} is given by:

$$
\begin{vmatrix}
\delta 0 f 0 \\
\delta 0 f 1 \\
\delta 0 f 2 \\
\delta 0 f 3 \\
\delta 1 f 0 \\
\cdot \\
\cdot \\
\cdot \\
\cdot \\
\delta 7 f 2 \\
\delta 7 f 3
\end{vmatrix}
$$

The g_{brc}^H is the conjugate transpose of g_{brc}. The spreading vector f is a column of the (4 x 4) Hadamard matrix H_4, that may be chosen randomly by the Base. The spreading vector d is a column of the BRC Spatial Spreading Weights Table that will be described in the next release of this document. The Base transmits simultaneously on all the sub-band pairs; for each sub-band pair, 10 different spatial beams are formed and activated sequentially to cover al the RUs in the spatial cell.

The code-gating vector i_{brc} is:

$$i_{brc} = b_{brc} \, h_{brc}$$

where the vector h_{brc} is the 0th column of the (32 x 32) Hadamard matrix (H_{32}), that is the all ones vector and the ith element of the (32 x 1) vector b_{clc} is given by:

$$b_{brc} = e^{j2pik} \text{offset}^{32}$$

The k$_{offset}$ (an integer between 0 and 31) is the BSOC for the transmitting Base.

For every spatial beam, there are 16 bursts in every BRC transmission (burst 0 to burst 15). For each antenna, the interleaver outputs one of the 16 possible (4 x 4) matrices in each burst. The interleaving rule is identical to the CLC interleaving rule shown in FIGURE 52. There are a total of spatial beams. This process is therefore repeated sequentially ten times, once for every spatial beam.

For every spatial beam, there are 128 (4 x 4) matrices to be mapped onto tones for transmission over the air. FIGURE 55 shows the mapping of a (4 x 4) matrix at the output of the interleaver into tones. The absolute tone indices can be obtained using FIGURE 23.

Broadcast channel signals are spatially beamformed and transmitted sequentially via ten predetermined team patterns per sub-band pair. This results in four broadcast channel signals (one per sub-band pair) that are simultaneously swept through each spatial cell. This is shown in FIGURE 56.

Each BRC message requires 40 TDD intervals or 120 ms to transmit. New BRC message may only be started on even frame boundaries. Each of the four sub-band pairs transmits the same BRC message at the same time and the BRC beam sweeps are synchronous within a spatial cell and for all Bases within a this embodiment system. BRC beams are swept in a clockwise pattern.

Reverse Channel Format

As for the forward channel transmissions, there are three different possible implementations of the physical layer. We refer to these modes as:

High capacity mode (short range): 3 bits/symbol

Medium capacity mode (medium range): 2 bits/symbol

Low capacity mode (long range): 1 bit/symbol.

High Capacity Mode

The block diagram for the upper physical layer of the Remote Unit transmitter for high capacity mode is shown in FIGURE 57.

The binary source delivers binary data to the Remote Unit transmitter at 64 kbits sec. For one reverse channel burst, this translates to 48 bits. The information bits are

encrypted according to the triple DES algorithm. The encrypted bits are then randomized in the data randomization block.

The bit to octal conversion block converts the randomized binary sequence into a sequence of 3-bit symbols. The symbol sequence is converted into 16-symbol vectors.

5   One symbol from the LCC is added to form a vector of 17 symbols.

The 17-symbol vector is trellis encoded. The trellis encoding starts with the most significant symbol (first element of the vector) and is continued sequentially until the last element of the vector (the LCC symbol). This process employs convolutional encoding

10   that converts the input symbol (an integer between 0 and 7) to another symbol (between 0 and 15) and maps the encoded symbol to its corresponding 16QAM (or 16PSK) signal constellation point. The output of the trellis encoder is therefore a vector of 17 elements where each element is a signal within the set of 16QAM (or 16PSK) constellation signals.

A LMP signal is added to form an 18-signal vector, with the LMP as the first

15   element of this vector. The resulting vector d_{rev} is pre-multiplied by a (18 x 18) reverse smearing matrix $C_{rev-smear}$ to yield a (18 x 1) vector b. Vector b is post-multiplied by a (1 x 4) reverse spreading vector g^H_{rev} to yield a (18 x 4) matrix S_{rev}. Elements of matrix S_{rev} are mapped to tones within traffic partition A according to the mapping discussed in FIGURE 22 and are sent to the lower physical layer. The lower physical layer places the

20   baseband signals in their corresponding DFT frequency bins where the data is converted into the time domain and sent for transmission over the air.

This process is repeated from the start for the next 48 bits of binary data to be transmitted in the next reverse channel transmission burst. The various steps in the transformation of binary data are shown in FIGURE 58.

25

Medium Capacity Mode

The block diagram for the upper physical layer of the Remote Unit transmitter for medium capacity mode is shown in FIGURE 59.

The binary source delivers binary data to the Remote Unit transmitter at 64

30   kbits/sec. For one reverse channel burst, this translates to 48 bits. The information bits are encrypted according to the triple DES algorithm. The encrypted bits are then randomized in the data randomization block. The bit to di-bit conversion block converts the randomized binary sequence into a sequence of 2-bit symbols. The symbol sequence is converted into 24 symbol vectors. Two symbols from the LCC are added, and eight ones

35   are inserted at the end of the sequence to form a vector of 34 symbols.

The 34-symbol vector is trellis encoded. The trellis encoding starts with the most significant symbol (first element of the vector) and is continued sequentially until the last element of the vector (the second LCC symbol). This process employs convolutional encoding that converts the input symbol (an integer between 0 and 3) to another symbol (between 0 and 7) and maps the encoded symbol to its corresponding 8 QAM (or 8PSK) signal constellation point. The output of the trellis encoder is therefore a vector of 34 elements where each element is a signal within the set of 8QAM (or 8PSK) constellation signals.

The 34-element vector is divided into two 17-element vectors. An LMP is added to each of the vectors to form two 18-signal vectors d_{rev} and d'_{rev}, with the LMP as the first element of these vectors. Each resulting vector is pre-multiplied by a (18 x 18) reverse smearing matrix $C_{rev-smear}$ to yield another two (18 x 1) vectors b and b'. Each vector is post-multiplied by its corresponding (1 x 4) reverse spreading vector (g^H_{rev} or g'^H_{rev}) to yield two (18 x 4) matrices S_{rev} and S'_{rev}. Elements of matrix S_{rev} are mapped to tones within traffic partition A according to the mapping discussed in FIGURE 22 and are sent to the lower physical layer. Similarly, elements of matrix S'_{rev} are mapped to tones within traffic partition B and are sent to the lower physical layer. The lower physical layer places the baseband signals in DFT frequency bins where the data is converted into the time domain and sent for transmission over the air.

This process is repeated from the start for the next 48 bits of binary data to be transmitted in the next reverse channel transmission burst. The various steps in the transformation of binary data are shown in FIGURE 60.

Low Capacity Mode

The block diagram for the upper physical layer of the Remote Unit transmitter for low capacity mode is shown in FIGURE 61. The binary source delivers binary data to the Remote Unit transmitter at 64 kbits/sec. For one reverse channel burst, this translates to 48 bits. The information bits are encrypted according to the triple DES algorithm. The encrypted bits are then randomized in the data randomization block. The 48 bits are formed into a vector, and three bits from the LCC are added to form a vector of 51 bits.

The 51-bit vector is trellis encoded. The trellis encoding starts with the most significant bit (first element of the vector) and is continued sequentially until the last element of the vector (the third LCC bit). This process employs convolutional encoding that converts the binary input symbol (0 or 1) to another symbol (0, 1, 2, or 3) and maps the encoded symbol to its corresponding QPSK signal constellation point. The output of the trellis encoder is therefore a vector of 51 elements where each element is a signal

67

within a set of QPSK constellation signals. The 51-element vector is divided into three 17-element vectors. An LMP is added to each of the vectors to form three (18 x 1) vectors d_{rev}, d'_{rev}, and d''_{rev}, with the LMP as the first element of these vectors. Each resulting vector is pre-multiplied by a (18 x 18) reverse smearing matrix $C_{rev-smear}$ to yield

5   another three (18 x 1) vectors b, b', and b". Each vector is post-multiplied by its corresponding (1 x 4) reverse spreading vector (g^H_{rev}, g'^H_{rev}, or g''^H_{rev}) to yield three (18 x 4 matrices S_{rev}, S'_{rev}, and S''_{rev}. Elements of matrix S_{rev} are mapped to tones within traffic partition A according to the mapping discussed in FIGURE 22 and are sent to the lower physical layer. Similarly, elements of matrices S'_{rev}, and S''_{rev} are mapped to tones within

10   traffic partition B and C, respectively, and are sent to the lower physical. The lower physical layer places the baseband signals in their corresponding DFT frequency bins where the data is converted into the time domain and sent for transmission over the air.

         This process is repeated from the start for the next 48 bits of binary data to be transmitted in the next reverse channel transmission burst. The various steps in the

15   transformation of binary data are shown in FIGURE 62.

         The encryption function is identical to that for the forward channel described herein.

         The trellis encoding schemes for all three capacity modes are identical to those for the forward channel described herein.

This section specifies the smearing matrix $C_{rev\text{-}smear}$. The input to the smearing block is the (18 x 1) vector D_{rev}. The output of the smearing operation (vector b) can then be described by the matrix multiplication of d_{rev} and the (18 x 18) smearing matrix $C_{rev\text{-}smear}$. That is

$$b = C_{rev\text{-}smear} d_{rev}$$

$C_{fwd\text{-}smear}$ is the constant valued matrix shown below:

$$
\begin{bmatrix}
0 & 0 & 0 & 0 & 0 & 0 & 0 & 0 & 0 & 0 & 0 & 0 & 0 & 0 & 0 & 0 & 0 & 0 \\
\alpha & \beta_{50} & 0 & 0 & 0 & 0 & 0 & 0 & 0 & 0 & 0 & 0 & 0 & 0 & 0 & 0 & 0 & 0 \\
\alpha & 0 & \beta_{51} & 0 & 0 & 0 & 0 & 0 & 0 & 0 & 0 & 0 & 0 & 0 & 0 & 0 & 0 & 0 \\
\alpha & 0 & 0 & \beta_{52} & 0 & 0 & 0 & 0 & 0 & 0 & 0 & 0 & 0 & 0 & 0 & 0 & 0 & 0 \\
\alpha & 0 & 0 & 0 & \beta_{53} & 0 & 0 & 0 & 0 & 0 & 0 & 0 & 0 & 0 & 0 & 0 & 0 & 0 \\
\alpha & 0 & 0 & 0 & 0 & \beta_{54} & 0 & 0 & 0 & 0 & 0 & 0 & 0 & 0 & 0 & 0 & 0 & 0 \\
\alpha & 0 & 0 & 0 & 0 & 0 & \beta_{55} & 0 & 0 & 0 & 0 & 0 & 0 & 0 & 0 & 0 & 0 & 0 \\
\alpha & 0 & 0 & 0 & 0 & 0 & 0 & \beta_{56} & 0 & 0 & 0 & 0 & 0 & 0 & 0 & 0 & 0 & 0 \\
\alpha & 0 & 0 & 0 & 0 & 0 & 0 & 0 & \beta_{57} & 0 & 0 & 0 & 0 & 0 & 0 & 0 & 0 & 0 \\
\alpha & 0 & 0 & 0 & 0 & 0 & 0 & 0 & 0 & \beta_{58} & 0 & 0 & 0 & 0 & 0 & 0 & 0 & 0 \\
\alpha & 0 & 0 & 0 & 0 & 0 & 0 & 0 & 0 & 0 & \beta_{59} & 0 & 0 & 0 & 0 & 0 & 0 & 0 \\
\alpha & 0 & 0 & 0 & 0 & 0 & 0 & 0 & 0 & 0 & 0 & \beta_{510} & 0 & 0 & 0 & 0 & 0 & 0 \\
\alpha & 0 & 0 & 0 & 0 & 0 & 0 & 0 & 0 & 0 & 0 & 0 & \beta_{511} & 0 & 0 & 0 & 0 & 0 \\
\alpha & 0 & 0 & 0 & 0 & 0 & 0 & 0 & 0 & 0 & 0 & 0 & 0 & \beta_{512} & 0 & 0 & 0 & 0 \\
\alpha & 0 & 0 & 0 & 0 & 0 & 0 & 0 & 0 & 0 & 0 & 0 & 0 & 0 & \beta_{513} & 0 & 0 & 0 \\
\alpha & 0 & 0 & 0 & 0 & 0 & 0 & 0 & 0 & 0 & 0 & 0 & 0 & 0 & 0 & \beta_{514} & 0 & 0 \\
\alpha & 0 & 0 & 0 & 0 & 0 & 0 & 0 & 0 & 0 & 0 & 0 & 0 & 0 & 0 & 0 & \beta_{515} & 0 \\
\alpha & 0 & 0 & 0 & 0 & 0 & 0 & 0 & 0 & 0 & 0 & 0 & 0 & 0 & 0 & 0 & 0 & \beta_{516}
\end{bmatrix}
$$

where,

$$a = (r_{LMP}/(1+r_{LMP}))^{1/2}$$
$$b = (1/(1+r_{LMP}))^{1/2}$$

r_{LMP} is the ratio of pilot to data power that is a physical layer provisionable parameter whose value is nominally set to one.

The d_is are elements of the cluster scrambling vector d_{smear} that is unique to the Remote Unit. d_{smear} is a 17-element vector that is used to ensure that the smeared data from one user received in a particular traffic partition at the Base is uncorrelated with

other users within the same traffic partition in the local spatial cell and adjacent spatial cells. d_{smear} is given by:

$$\begin{vmatrix} d_0 \\ d_1 \\ \cdot \\ \cdot \\ \cdot \\ d_{15} \\ d_{16} \end{vmatrix}$$

or

$$\begin{vmatrix} e^{j\phi(0)} \\ e^{j\phi(1)} \\ \cdot \\ \cdot \\ \cdot \\ e^{j\phi(15)} \\ e^{j\phi(16)} \end{vmatrix}$$

The ith element of d_{smear} has the form $e^{jf_{smear}(i)}$ where $f_{smear}(i)$ is a real number between 0 and 2p generated by a pseudo-random number generator creating unique sequences for each Remote Unit. The details of the pseudo-random number generator are implementation dependent and need not be known at the Base.

Spectral Spreading

This section defines the (1 x 4) reverse spectral spreading vector g^H_{rev} shown in FIGURE 57. The input to the spectral spreading block is the (18 x 1) vector b. The output of the spectral and spatial spreading operation, (18 x 4) matrix S_{rev}, is the matrix multiplication of b and the (1 x 4) Spectral spreading vector g^H_{rev}:

$$S_{rev} = bg^H_{rev}$$

where,

$$g^H_{rev} = [g0\ g1\ g2...g30\ g31]$$

The elements of vector g^H_{rev} are transmit spreading weights calculated throughout the transmission. The algorithm for the derivation of these weights is implementation dependent. However, to clarify the procedure a specific algorithm for the derivation of these weights is described below.

The Remote Unit derives its new transmit weights based on the most recent data received on the forward channel. The transmit weights are a scaled version of the received weights using four receive frequencies for a single antenna.

The receive weight vector w^H_{fwd} has four elements (w_0 - w_3) that are mapped to spectral components as shown in FIGURE 63.

For the Remote Unit traffic establishment procedure, the transmit weights (g_0 - g_3) are calculated according to the following equation:

$$g^H_{rev}(p) = a_{rev}(n)\, p_{rev}\, w^H_{fwd}$$

where $a_{fwd}(n)$ is the Base gain ramp-up factor for the nth packet and where p_{rev} is the Remote Unit power management factor defined by the equation below:

$$p_{rev} = l_p k_{fwd} + (1-l_p)\, k_{rev}\, (p_{loss}(n,p)/\, \|(w_{fwd}(p))\|)$$

where,

l_p is the exponential decay or "forget factor" nominally set to 0.97

p_{loss} is the reciprocal of the Base-Remote Unit channel gain measured using the Remote Unit Synchronization Pilot (RSP) tones

k_{rev} is the target Base receive power (nominally -103 dBm)

n is the burst index

p is the link index

For the Remote Unit traffic establishment procedure, the receive weights are adaptively calculated using the following equation:

$$w_{fwd} = R^{-1}_{xx}\, r_{xd}$$

where

w_{fwd} is the (4 x 1) receive weight vector

r_{xd} is an estimate of the (4 x 1) cross-correlation vector of the received (4 x 1) vector x and the LMP (or the desired data) d

R^{-1}_{xx} is an estimate of the (4 x 4) inverted auto-correlation matrix of the received vector x

For the Remote Unit steady-state procedure, receive weights are adaptively calculated using the following equation:

$$w_{fwd} = R^{-1}_{xx} \, r_{xy}$$

where

5   w_{fwd} is the (4 x 1) weight vector

r_{xy} is an estimate of the (4 x 1) cross-correlation vector of the received (4 x 1) vector x and the despread data y

R^{-1}_{xx} is an estimate of the (4 x 4) inverted auto-correlation matrix of the received vector x

10   The receive weights (w_0 - w_3) are mapped to spectral components according to the mapping shown in FIGURE 63. The transmit weights (g_0 - g_3) are a scaled version of the receive weights. The scaling is made according to the following equation:

$$g^{H}_{rev}(p) = p_{rev} \, w^{H}_{fwd}$$

where p_{rev} is the Remote Unit power management factor defined earlier.

15   Correlation estimates are computed over four forward-channel burst. The new despreading weights are applied to four forward channel bursts with no delay. The spreading weights are applied to eight reverse channel bursts after an 8-burst delay. Correlation estimates are made using an exponentially average block summation. The exponential decay constant is provisional with a nominal value of 0.7.

20

Reverse Control Channel Transmission Format

The block diagram for the physical layer of the solicited and unsolicited Common Access Channel (CAC) channel transmissions is shown in FIGURE 64.

A CAC message is a 56-bit binary sequence composed of a training sequence,
25   information bits, and CRC parity bits. The vector formation block converts the binary sequence into a (56 x 1) vector. Each element of the resulting vector is mapped into its corresponding signal in the BPSK signal constellation to form another (56 x 1) vector s. The mapping for the BPSK signal is shown in FIGURE 65.

The resulting vector is passed through two parallel paths. In the first path, the
30   vector s is sent directly for spectral spreading that involves post-multiplying it by the (1 x 2) spectral spreading vector g_{cac}^{H}:

$$g^{H}_{cac} = [1\ 1]$$

35

The resulting (56 x 2) matrix is D_{cac} given by:

$$\begin{vmatrix} s(0) & s(0) \\ s(1) & s(1) \\ ... & ... \\ s(54) & s(54) \\ s(55) & s(55) \end{vmatrix}$$

where s(k) is the kth element of vector s. Matrix D_{cac} is then sent to the demultiplexer where it is partitioned (by group of eight rows) into seven (8 x 2) submatrices D_0 to D_6.

In the second path, the vector s is code-gated. The code-gating operation is described by the element-wise multiplication of the (56 x 1) vector s with a (56 x 1) code-gating vector Y_{cac}. The resulting (56 x 1) vector is s':

$$s' = s \cdot i_{cac}$$

The vector i_{cac} is described below.

The resulting (56 x 1) vector s' is sent for spectral spreading that involves post-multiplying it by the (1 x 2) spectral spreading vector g_{cac}^H. The resulting (56 x 2) matrix is D'_{cac}:

$$\begin{vmatrix} s'(0) & s'(0) \\ s'(1) & s'(1) \\ ... & ... \\ s'(5 & s'(5 \\ s'(5 & s'(5 \end{vmatrix}$$

where s'(k) is the kth element of vector s'. Matrix D'_{cac} is then sent to the demultiplexer where it is partitioned (by groups of eight rows) into seven (8 x 2) submatrices D'_0 to D'_6.

The transmission of one 56 bit CAC message requires 14 reverse channel bursts. In each of these burst, one of the 14 (8x2) matrices is mapped onto tones and sent to the lower physical layer for transmission over the air. The interleaving and tone mapping functions are described below.

The code-gating vector i_{cac} is :

$$i_{cac} = b_{cac} \cdot h_{cac}$$

and

$$b_{cac}(I) = e^{j2\pi k_{offset}/56}$$

where $b_{cac}(i)$ is the ith element of the (56 x 1) vector b_{cac}. The k_{offset} is the BSOC for the receiving Base, that ranges between 0 and 31. Every Remote Unit is assigned a pair of

code keys: the solicited CAC code key and the unsolicited CAC code key. The code keys are integer numbers between 0 and 63.

The 56 elements of the vector h_{cac} are the first 56 elements of the kth column of the (64 x 64) Hadamard matrix (H_{64}), where k is the value of the solicited or the unsolicited code key for the transmitting Remote Unit depending on the type of CAC transmission. For instance, if, for a given Remote Unit, the solicited code key is the number 13, and the unsolicited code key is the number 15:

In SCAC transmissions, elements of the vector h_{cac} are the first 56 elements of the 13th column of the (64 x 64) Hadamard matrix

In UCAC transmissions, elements of the vector h_{cac} are the first 56 elements of the 15th column of the (64 x 64) Hadamard matrix

There are 14 burst in every CAC transmission (burst 0 to burst 13). The interleaver outputs one of the 14 possible (8 x 2) matrices (D_0 to D_6) or (D'_0 to D'_6), in each burst. FIGURE 66 shows the order of the transmission used by the interleaver. There are two CACs in each sub-band pair. The Remote Unit will use one of these channels depending on the CAC ID parameter received from its MAC layer. If the CAC ID is 0, the $CAC_{i,0}$ is selected; if the CAC ID is 1, the $CAC_{i,1}$ is selected. FIGURE 67 shows the mapping of the (8 x 2) matrix at the output of the interleaver into tones.

Lower Physical Layer Format

The transmitter for the lower physical layer of this embodiment is functionally described by the block diagram in FIGURE 68. The lower physical layer functionality is identical in forward and reverse channels.

In the forward channel, for traffic channel transmissions, the process shown in FIGURE 68 is performed in parallel eight times for eight different antenna elements. Furthermore, the Base may combine data intended for various users into the same DFT bin to reduce processing requirements. It is possible to further reduce the processing by simultaneously transmitting traffic and control information (at the Base or the Remote Unit) as they are carried on non-overlapping frequency tones. These techniques, however, are implementation dependent and do not change the functional characteristics of the DFT operation. As shown in FIGURE 68, complex baseband signals enter the tone mapping

block, where they are assigned into tones according to a unique mapping to either a traffic or a control channel.

The tone-mapped complex signals are complex signals are demultiplexed into lower sub-band and upper sub-band tones, and are placed into their corresponding DFT
5 bins. The remaining DFT bins are filled with zeros and the inverse DFT operation is performed, thereby transforming the data into the time domain. The discrete time-domain samples are then converted into an analog signal, converted to the appropriate RF frequency, and transmitted over the antenna.

As there are four sub-band pairs, there are four pairs of DFT blocks, where each
10 DFT block spans one MHz of usable bandwidth. The spacing between the adjacent bins in one DFT block is 3.125 kHz. Each DFT block has 512 bins of which only 320 bins are used. Tone mapping into corresponding DFT bins in each DFT block are shown in FIGURE 69. FIGURE 70 depicts tone mapping pictorially. As shown, the frequency span of one DFT block is 1.6MHz where only 1 MHz is used for data transmission. The
15 relationship between tones and the actual frequency for each bin is explained herein.

The inverse DFT operation is carried out to convert the baseband signals into time domain. The mathematical representation of the operation is:

$$x(n) = S \ X(k)^{ej2pnk/512}$$

20

where X(k) is the complex baseband signals in the frequency domain (the contents of the kth bin of a DFT block), and x(n) is the nth real-valued component of the time-domain sample. The inverse DFT operation may be carried out using Inverse Fast Fourier Transform (IFFT) techniques.

25 The baseband transmit signals obtained after the IDFT operation must be real. The real-valued time-domain sample outputs are then converted to the proper RF frequency and the appropriate analog waveform for transmission.

Airlink Physical Layer Power Output Characteristics

30 The power output characteristics of Base transmissions on the forward channel are different from that of the Remote Unit transmissions on the reverse channel.

The forward channel transmission from a Base to a given Remote Unit is maintained at a fixed power level during the duration of a connection. The power level is determined by the Base radio management entity (RME) prior to the start of the
35 connection using a power management algorithm.

A forward RF channel transmission is initiated by a 180 ms ramp-up period (240 forward channel bursts) during the traffic establishment period. The ramp-up starts after a connection is established between the Base and a given Remote Unit. The data transmitted during this period are known link maintenance pilots. The maximum (steady state) power is reached after 240 channel bursts (180 msec) and maintained throughout the connection.

The following equation shows the forward channel ramp-up schedule relative to the steady state power,

$$a_{fwd}(n) = (1-e^{-5(8[n/8])}/(1-e^{-5}))^2$$

for n<240

$$a_{fwd}(n) = 1$$

otherwise

where n is the forward channel burst number relative to the start of the transmission.

The reverse channel transmissions from a Remote Unit to its Base is adaptively varied to ensure that the received power from all RUs at their Base is maintained at a relatively constant level. The Remote Unit power management algorithm is implementation dependent. One example of the algorithm is discussed in the Section on the Reverse Channel Format

A reverse RF channel transmission is initiated by a 180 ms ramp-up period (240 reverse channel bursts) during the traffic establishment period. The ramp-up starts after a connection is established between the Remote Unit and its Base. The data transmitted during this period are known LMPs. The maximum (steady state) power is reached after 240 reverse channel bursts (180 msec).

The following equation shows the reverse channel ramp-up schedule relative to the steady state power,

$$a_{rev}(n) = (1-e^{-5(8[n/8])}/(1-e^{-5}))^2$$

for n<240

$$a_{rev}(n) = 1$$

otherwise

where n is the reverse channel burst number relative to the start of the transmission.

A "PROOF-OF-CONCEPT" EMBODIMENT

The signal processing procedure described generally above can be implemented in a "proof-of-concept" embodiment by circuitry within the high-bandwidth base station 110 and the radio access stations 187, 192. In addition, the dynamic bandwidth allocation method of the present invention is implemented in a "proof-of-concept" embodiment within the circuitry of the communications network 100 depicted below.

FIGURE 71 is a schematic block diagram showing the main structural elements of one implementation of the high bandwidth efficiency, bandwidth-on-demand communications network 100. Specifically, the communications network 100 is shown to include a plurality of full-rate, high-bandwidth, radio access stations 192 as well as a low-rate, high-bandwidth radio access station 187. Typically, a full-rate, high-bandwidth radio access station 192 is able to provide for communication between a base station 110 and a large number of subscribers 130, while the low-rate, high-bandwidth radio access station 187 is able to provide for communication with the base station 110 only one or a few subscribers 130 at a time.

The subscribers 130 communicate with the full-rate or low-rate, high-bandwidth radio access stations 192, 187 via a cable or other communication link. The high-bandwidth radio access stations 192, 187, in turn, communicate bidirectionally with the base station 110 via wireless communications channels to form an air-link. The structure and operation of the base station 110 as well as the structure and operation of the full and low-rate, high-bandwidth radio access stations 192, 187, will be discussed in greater detail below with reference to FIGURE 72 and 73.

The base station 110 together with the full and low-rate, high-bandwidth radio access stations 192, 187 together comprise a subsystem 150. The subsystem 150 communicates bidirectionally with a telecommunications network 160 via a land line 170 that may, for example, comprise a copper cable or a fiber-optic connection. Alternatively, the link 170 may comprise a microwave link. The telecommunications network 160 may include for example, the public switched telephone network, a mobile telephone switching office (MTSO), a private data network, a modem bank or a private branch exchange, as is well known in the art.

FIGURE 74 is a simplified schematic block diagram that shows the main functional and structural elements of the bandwidth-on-demand communications network 100 in greater detail. The communications network 100 is shown in FIGURE 74 to connect a plurality of the subscriber units (e.g., the computer 131, the telephone 132, a plurality of

5   telephones 140 in communication with a public switching network, or a plurality of computer terminals 145 within a local area network) to public or private data or telephone networks 150-156. Public data network 150, the private data network 152, the private telephone network 154, and the public telephone network 156 communicate with an asynchronous telecommunications multiplexer (ATM) 162 over lines 163, 164, 165, and

10   166, respectively, via a plurality of network interfaces, designated generally by a block 160. The asynchronous telecommunications multiplexer 162 acts as a multiplexing switch and connects with the high-bandwidth base station 192 via the communications link 170, that advantageously comprises a fiberoptic link, a copper wire, or a microwave transmission link. The high-bandwidth base station 110 provides radio frequency output

15   signals to the receiving stations via the antenna 120.

A bandwidth demand controller 175 communicates with the high-bandwidth base station 110, asynchronous telecommunications manager switch 162, and the network interfaces 160 via lines 176, 177 and 178, respectively. The bandwidth demand controller 175 also communicates with an intelligent service node 180 via a line 179. The intelligent

20   service node 180 communicates with the ATM switch 162 via a line 182. The above-described elements of the bandwidth on demand communications network 100 comprise the telecommunications network side 183 of the bandwidth-on-demand communication system 100. The telecommunications network side 183 communicates with the low rate high-bandwidth radio access station 187 via an antenna 185 or the full

25   rate high band width radio access station 192 via an antenna 190. The radio access station 187 connects to a plurality of the subscriber units including the telephone 132 and the computer 131. The radio access station 192 is configured to communicate with multiple subscribers 140 via a public switching network 195 that connects to the radio access station 192 via a communications link 194. The full rate radio access station 192 further

30   connects to the computer terminals 145 via a local network 197 that connects to the radio access station 192 via communication link 196. Each of the subscriber units 131, 132, 140 and 145, together with the elements 185-197 of the communications system 100, comprise a subscriber network side 199 of the bandwidth-on-demand communications system 100.

The high-bandwidth base station 110 in association with the bandwidth demand

35   controller 175, and the high-bandwidth radio access stations 187, 192 that communicate with the high-bandwidth base station 110 via an air link, are the heart of the bandwidth on

demand communication system 100. Although only a single high-bandwidth base station
100 is depicted in FIGURE 74, it will be understood that a plurality of high-bandwidth
base stations are advantageously included within the high-bandwidth communication
system 100. Each of the high-bandwidth base stations 110 is capable of supporting from
5   one to hundreds of simultaneous bi-directional users. Each user may request in advance,
or optionally, during the course of communications, an amount of bandwidth from 8
kilobits to 1.544 megabits per second. Furthermore, each high-bandwidth base station
110 may have one or multiple transmitting and receiving antennas 120. The
high-bandwidth base stations 110 are high-bandwidth radio transceivers, that, with their
10   associated antennas 120, may be located on towers, on top of buildings, inside buildings,
or in other convenient locations.

           A bandwidth controller 175 is associated with the high-bandwidth base stations
110. The bandwidth demand controller 175 provides intelligence to monitor information
transmitted to the base stations 110 from the radio access stations 187, 192. Specifically,
15   the information transmitted from the high-bandwidth radio access stations 187, 192 are
converted to intelligence within the bandwidth demand controller 175 in order to instruct
the base stations 110 how much bandwidth to provide a given radio access station 187,
192. Although shown in FIGURE 74 as a separate element from the high-bandwidth base
station 110, the bandwidth demand controller 175 may be integral to a base station 110,
20   may be attached locally to a base station 110, or may be remote and connected to a base
station 110 via the communication link 176. The bandwidth demand controller 175
further acts as a central bandwidth controller that insures that the bandwidth appropriated
at each communication link throughout the communications network 183 is consistent
with the bandwidth assigned to a particular channel on the high-bandwidth base station
25   110. Thus, the bandwidth demand controller 175 controls bandwidth allocated within the
asynchronous telecommunications multiplexer switch 162, and the network interfaces 160.
Additionally, the bandwidth demand controller 175 communicates bandwidth information
to the intelligent service node 180 that is used to manage the delivery of the user data to
the appropriate network 150-156. The intelligent service node 180 can control the ATM
30   switch 162 to manage bandwidth changes and the network interfaces 160.

           The high-bandwidth radio access stations 187, 192, as shown in FIGURE 74, are
exemplary of a plurality of high-bandwidth radio access stations that are included within
the bandwidth on demand communication system 100. One or more of the
high-bandwidth radio access stations 187, 192 are capable of communicating with one or
35   more high-bandwidth base stations 110 utilizing the air interface. In addition, each of the
radio access stations 187, 192 is capable of supporting one or more interfaces such as the

connections between the telephone 132 and the standard computer 131, as well as the telephone network interface (PBX) 195 and the computer network comprising the terminals 145 and the LAN 197. The high-bandwidth radio access stations 187, 192 have the capability to interpret bandwidth needs of the devices connected to the radio access

5   stations 187, 192, and communicate these bandwidth needs via the air interface and the base station 110, to the bandwidth demand controller 175. Advantageously, the bandwidth demand controller 175 can further communicate these bandwidth demands to the ATM switch 162 or the intelligent service node 180, and the network interfaces 160.

In operation, one of the connected subscriber units (e.g., the computer 131, the

10 telephone 132, the PBX 195, or the LAN 197) requests bandwidths via a connection to one of the high-bandwidth radio access stations 187, 192. The radio access station 187, 192 transmits a request for access and bandwidth to the high-bandwidth base station 110 via the antenna 185, 190, the air interface, and the antenna 120. The request for access is made via a communications control channel available to all subscribers within the area of

15 use. If two subscribers simultaneously request connection, then a random accessing protocol is employed to determine which unit is first granted control of the communications control channel.

The high-bandwidth base station 110 communicates all bandwidth requests to the bandwidth demand controller 175. The bandwidth demand controller performs an

20 allocation of the requested bandwidth and advantageously arranges system resources within the telecommunications network side 183 (including the intelligent service node 180, the ATM switch 162, and the network interfaces 160). Once the bandwidth demand controller 175 determines the amount of bandwidth available for allocation, and compares this with the requested bandwidths, the bandwidth demand controller 175 either

25 immediately allocates the requested bandwidth, or begins a negotiation process using the available amount of bandwidth. This bandwidth negotiation occurs between the bandwidth demand controller and the radio access station 187, 192 through the base station 110 and the air interface.

Thus, the radio access station 187, 192 either receives an acknowledgment that the

30 bandwidth requested is available, and subsequently begins transmitting data, or the radio access station 187, 192 receives an offer of less bandwidth from the bandwidth demand controller 175. If an offer of less bandwidth is transmitted to the high-bandwidth radio access station 187, 192, the radio access station 187, 192 determines whether the connected device or network can effectively operate with the offered bandwidth. If the

35 connected device or network can effectively operate with the offered bandwidth, the radio access station 187, 192 begins transmitting data at the offered bandwidth. However, if the

radio access station 187, 192 determines that the offered bandwidth is not adequate for operation of the connected device or network, the radio access station 187, 192 notifies the connected device or network that access is not available, and further notifies the bandwidth demand controller 175 (via the base station 110 and the air interface) that the offered bandwidth will not be used by the radio access station 187, 192.

If a suitable bandwidth is available, the bandwidth controller allocates this bandwidth to establish a communications channel with the requesting subscriber. Thus, for example, the telephone subscriber unit 132 may indicate that a data rate of 8 Kb per second is required (that corresponds to a particular bandwidth) while the computer subscriber unit 131 may indicate that a total transmission rate of 128 Kb per second (corresponding to another given bandwidth) in order to establish effective communications with the high-bandwidth base station 110. If the communications network 100 is unable to provide the requested amount of bandwidth, a negotiations process commences wherein the high-bandwidth base station 110 transmits an alternative bandwidth, that is less than the requested bandwidth, to the requesting subscriber unit via the radio access station 187. The requested subscriber unit then indicates to the high-bandwidth base station 110 whether or not the allocated bandwidth is suitable for the communications needs of the subscriber unit.

As will be described in greater detail below, the bandwidth demand controller 175 allocates bandwidth by assigning one or more frequency tone set and one or more spreading code to the subscriber unit in accordance with a pre-defined bandwidth allocation procedure. Each tone set and spreading code increases bandwidth by an additional factor. In one advantageous embodiment, bandwidth can be allocated in amounts as small as 8 Kbits/sec to as large as 1.544 Mbits/sec to define the communications channel.

Once a communications channel is established for the requesting subscriber 130, data representing either human voice communications or computer-to-computer communications in digital form, is transmitted between the high-bandwidth base station 110 and the high-bandwidth radio access station 187, 192. As will be described in greater detail below, the digitally encoded signal contains forward error correction together with signal spreading and other modulation techniques.

All data received by the high-bandwidth base station 110 from all communicating radio access stations 187, 192 are multiplexed into an asynchronous telecommunications multiplexed data stream and transmitted, via the communication link 170, to the ATM switch 162. At the ATM switch 162, the data stream is switched (i.e., demultiplexed)

with the optional assistance of the intelligent service node 180 to the appropriate network interfaces 160, and from there onto the appropriate network 150-156.

As will be discussed in further detail below, the bandwidth demand controller 175 also controls bandwidth allocation for the network interfaces 160 and the ATM switch

5   162. In this manner, the bandwidth allocated throughout an entire communications link (i.e., from a subscriber to a data or telephone network) can be flexibly assigned according to the needs of each subscriber unit. Furthermore, the preferred embodiment assures that the bandwidth through the air interface and the bandwidth through the land line connections are appropriately matched.

10   When a device or network connected to a high-bandwidth radio access station 187, 192 no longer requires bandwidth, the radio access station 187, 192 ceases transmission to the base station 110, and notifies the bandwidth demand controller that the bandwidth is now released for reallocation.

15   The "Proof-of-Concept Embodiment" - Remote Terminal Hardware

FIGURE 72 is a functional block diagram that shows the main functional elements of the full-rate, high-bandwidth radio access station 192. It should be understood, for purposes of the present description, that the full-rate, high-bandwidth radio access station 192 described herein is substantially identical in structure and operation to the low-rate,

20   high-bandwidth radio access station 187, with the exception that the low-rate, high-bandwidth radio access statior 187 provides communication access for only a single subscriber 130. As shown in FIGURE 72, the full-rate, high-bandwidth radio access station 192 comprises a transmit receive switch 300 that connects bidirectionally with the antenna 120. The structure and operation of the antenna 120 will be described in greater

25   detail below with reference to FIGUREs 6 and 7. The transmit and receive switch 300 connects to a down converter 305 when in the receive mode and an up converter 307 while in a transmit mode. The transmit/ receive switch 300 further receives synchronization and packet timing data from a synchronization circuit 312.

The down converter 305 receives the radio signals from the antenna 120 via the

30   switch 300. In addition, the down converter 305 receives a local oscillator reference as well as an analog-to-digital converter clock from the synchronization circuit 312. The down converter 305 communicates with a demodulator 310 that, in turn, provides a feedback of automatic gain control level to the down converter 305. The demodulator 310 communicates bidirectionally with the synchronization circuit 312 and also provides

35   an output to a code-nulling circuit 315. The code-nulling circuit 315 provides a frequency error signal to the synchronization circuit 312, and also communicates with a

multidimensional trellis decoder 320. The multidimensional trellis decoder 320 connects to a digital data interface 325. The digital data interface 325 communicates bidirectionally with a remote control circuit 330. The remote control circuit 330 receives inputs from the demodulator circuit 310, the code-nulling circuit 315, and the multidimensional trellis
5   decoder 320. The control circuit 330 further transmits status signals and receives command signals from the base station 110 (see FIGURE 74). Finally, the remote control circuit 330 outputs axis parameters to a multidimensional trellis encoder 335, that also communicates with the digital interface 325. The multidimensional trellis encoder 335 communicates with a SCMA coding circuit 340. The SCMA coding circuit 340 further
10   receives an input from the code-nulling circuit 315. The SCMA coding circuit 340 outputs signals to a modulator circuit 345 that also receives an input from the synchronization circuit 312. Finally, the modulation circuit 345 together with the synchronization circuit 312 provide inputs to the up converter 307. The up converter 307 outputs the data signal to the transmit receive switch 300 while the transmit receive switch
15   is in the transmit mode. This signal is output over an error interface to the multiple subscribers 130 via the antenna 120.

In operation, once it is the proper time to receive a data packet, the transmit/receive switch 300 switches the antenna 190 into the down converter 305. The down converter 305 takes the signal at the transmission frequency (see, e.g., about 2
20   gigaHertz), and translates this to the proper frequency for digitization. The DMT-SS demodulator then performs a fast Fourier transform (FFT) and presents the individual frequency bins to the code-nulling network 315. As discussed briefly above, the code-nulling network 315 applies code-nulling weights to the despreading codes in order to cancel interference due to transmissions having non-orthogonal spreading codes. The
25   code-nulling network 315 also despreads the demodulated signal provided by the DMT-SS demodulator 310 and produces output demodulated symbols.

The demodulated symbols are provided as an input to the multi-dimensional trellis decoder 320 in order to decode the symbols in accordance with pragmatic Viterbi decoding methods. Receive bits are provided at the output of the multidimensional trellis
30   decoder 320. The receive bits pass through a digital data interface 325 that, in one embodiment, serves as a data interface for a T1 link.

On the transmit side, data to be transmitted enters the digital data interface 325 via the T1 link and enters the multidimensional trellis encoder 335 for trellis encoding. It will be understood, of course, that other kinds of error encoding and symbol encoding such as
35   Reed-Solomon error coding, and QAM or BPSK symbol encoding are performed within the encoder 335. The encoded symbols enter the spreading circuit 340 wherein the

spreading code together with the appropriate code weights are applied to the input symbols. The spread symbols are DMT-SS modulated as represented within the block 345 and the resulting signal is translated to the high frequency band via the up-converter 307. The transmit/receive switch 300 is then switched to connect the up converter 307 to the antenna 190 so that the modulated and encoded data signal is transmitted via the antenna 190.

Immediately after one of the radio access terminals 187, 192 has been installed and is just coming on-line for the first time, the radio access station 187, 192 does not have information regarding the location of the assigned base station 110. Furthermore, the remote access station 187, 192 does not have information concerning the interference resulting from other transmitters and reflectors within the environment of the remote station 187, 192. Thus, each remote, upon initialization, must "learn" the location of the base station as well as the location of different interferes and reflectors within the immediate environment of the remote. Because the remote installer points the remote antenna array in the direction of the nearest base station 110, the strongest signal received by the remote is generally from around the 0° direction. The remote subsequently fine tunes, or adaptively adjusts the beam forming so as to obtain the maximum SINR for the signal received from the nearest base station 110.

When the radio access station 192 transmits to the base 110, the base station 110 expects to receive each of the signals transmitted from the remotes at the same power level. Thus, a gain control level is reported to the remote control 330 within the radio access station 192 from the DMT-SS demodulator 310. This automatic gain control level (AGCL) is also transmitted from the DMT-SS modulator 310 to the up-converter 307 so that the gain of the power amplifier (not shown within the up-converter 307) can be adjusted. In this manner, the base stations 110 can assure that the signal transmitted from the remote access terminals 187, 192 arrive at the base station 110 at the proper level.

The radio access stations 187, 192 also have to perform synchronization. That is, although the remote access terminals 187, 192 are preprogrammed to operate within a TDD system, the specific information concerning the distinction between the transmit and receive packages as well as the exact timing of the packet transfer still must be determined by the radio access stations 187, 192 when a radio access station first comes on line. Subsequently, the remote terminals 187, 192 must acquire frequency synchronization for the DMT-SS signals so that the remotes are operating at the same frequency and phase as the base station 110. For this reason, the DMT-SS demodulator 310 generates a packet reference that is utilized by the synchronization circuitry 312 to establish the basic transmit/receive timing (i.e., the packet timing for the T/R switch 300). In addition, the

packet timing is provided as a receive gate to the demodulator 310 and as a transmit gate to the modulator 345 so that the remote access station 187, 192 transmits and receives at the appropriate intervals.

Within the code-nulling network 315, measurements are taken on the waveform to
5   determine the frequency error.   The measured frequency error is provided to the synchronization circuitry 312 so that the radio access station 187, 192 can come into frequency and phase lock with the base station 110. This synchronization information is transmitted from the synchronization circuitry 312 to the up-converter 307 and the down-converter 305 as a local oscillator reference and also as a digital-to-analog
10 converter clock (or conversely, an analog-to-digital converter clock).

The code-nulling network 315 also estimates the characteristics of the multitask channel (i.e., the frequency response of the multipath channel). The channel estimates are provided to the spreading circuitry 340 so that the preemphasis function can be performed to adaptively equalize the multipath channel. Furthermore, the code-nulling network 315
15 provides an estimate of the received power and the SINR to the remote control circuitry 330.   In addition, an estimate of the bit error rate (BER) is provided from the multidimensional trellis decoder 320 to the remote control circuitry 330.   These parameters are used by the remote control circuitry 330 to control the flow of data via the digital data interface 325 with the subscriber (e.g., a PBX or a LAN). Furthermore, status
20 signals based upon these input parameters to the remote control circuitry 330 are also transferred to the subscriber. Tne status signals indicate to the subscribers whether or not the radio access terminal is operating properly.

When the radio access terminals 187, 192 first dials onto the network 100 (i.e., the remote is trying to establish connection with the base) the base provides the remote 187,
25 192 with a set of access parameters that includes, for example, the appropriate starting codes to use, which tone sets to receive and transmit on, etc., so that a communication channel is set up between the base station 110 and the remote station 187, 192.

FIGUREs 21A and 21B depicts the digital architecture within the remote access terminals 187, 192. The remote digital architecture includes an interface card 2100 that
30 communicates bidirectionally with a layer processing accelerator (LPA) card 2110 as well as a transmitting LPA card 2120.

The interface card 2100 (shown in greater detail in FIGURE 76 below) includes an ETHERNET interface card, a global positioning system (GPS) interface and other control interfaces. The ETHERNET interface communicates bidirectionally with a monitoring
35 computer such as an Apple MacIntosh, while the GPS interface derives timing data for synchronization purposes from the base station transmission, while the control interface

outputs printer control bits for controlling the tuner. The interface card 2100 further includes three digital signal processing chips that, advantageously comprise PMS320C40 digital signal processing chips ("C40s") available from Texas Instruments. In addition, a Viterbi decoder as well as a T1 and an integrated services digital network (ISDN) interface are included on the interface card 2100 to provide an interface between the T1 communication link as well as the ISDN communication link with the subscribers.

As shown in FIGURE 75A, the interface card 2100 further includes an additional PMS320C40 digital signal processing chip as well as an additional Viterbi, T1, ISDN interface that are crossed out. This is to indicate that these chips, although physically present on the interface card 2100, are not used within the remote digital subsystem although the same interface card is typically used in the base station 110. This is done because it is less expensive to manufacture a single interface card for both the base station 110 and the remotes 187, 192 rather than providing a specific card for the remotes and bases.

Finally, the interface card 2100 includes a G-link receiver that receives sampled data from the receiver digital-to-analog converter and a G-link transmitter that transmits sample data to the transmitter analog-to-digital converter.

The sample data received from the digital-to-analog converter passes through the G-link receiver within the interface card 2100. The G-link receiver provides the received waveform data to a receiving LPA card 2110 (FIGURE 75B). The LPA card 2110 will be described in greater detail below with reference to FIGUREs 77A-77D. Briefly, the receiving LPA card 2110 includes a pair of SHARP LH9124 ("9124s") digital signal processing chips 2112, 2114, as well as a pair of Texas Instruments TMS320C40 digital signal processing chips 2116, 2118.

The receiving LPA card 2110 demodulates the received data and provides the demodulated data to one of the TMS320C40 DSP chips within the interface card 2100. After further digital signal processing, the data is decoded and then transmitted to the subscriber via the T1 interface. Of course, it will be understood that if the radio access terminal comprises one of the low-rate radio access terminals 187, then a suitable communications link other than a T1 link will connect to the interface card 2100.

When data is to be transmitted, information supplied by the T1 interface, or other communication link, enters the interface card 2100, as shown in FIGURE 75A, and passes through a series of digital signal processing chips within the interface card 2100. The transmit data output from the interface card 2100 enters a transmit LPA card 2120, that has a substantially similar architecture to the received LPA card 2110. The transmit LPA card 2120 converts the transmit data into transmit waveform data suitable to be sent to the

transmitter analog-to-digital converter via the G-link transmitter within the interface card 2100.

FIGURE 76 is a software block diagram that indicates the general processing steps performed by each of the digital signal processing chips within the digital signal processing
5   architecture of the radio access terminals 187, 192. Specifically, control signals are generated by the TMS320C40 digital signal processing chips 2102, 2106, while the symbol modulation (e.g., including trellis coded, Reed-Solomon, and QAM, BPSK, or M-ARY modulation) is performed by the digital signal processing chips 2104, 2106.

Within the receiving LPA, the 9124 digital signal processor 2112 in conjunction
10 with the C40 digital signal processor 2116 perform the operations relating to the fast Fourier transform. The 9124 digital signal processor 2114 in conjunction with the C40 digital signal processor chip 2118 perform the processing steps relating to the code-nulling and adaptive equalization aspects of the present invention. In like manner, within the transmitting LPA 2120, the C40 digital signal processing chip 2124, together with the
15 9124 digital signal processing chip 2128, perform the digital signal processing steps relating to the inverse fast Fourier transform (IFFT), while DSP chips 2122 and 2126 perform the signal spreading operations used to provide modulation in accordance with the present invention.

FIGUREs 78A-78C are more detailed block diagrams showing the digital
20 architecture used to support the main digital signal processing C40 chips on the interface card 2100 of the remote terminals 187, 192. Several interface support circuits are employed to precondition data received by the digital signal processing chip 2102. In particular, a receive/transmit control interface circuit, an ETHERNET interface circuit, an erasable programmable logic device (EPLD) synchronization circuit, and a universal
25 asynchronous receiver/transmitter (UART) serve as an interface between the DSP chip 2102 and circuitry external to the interface card 2100. In addition, a programmable read-only memory (PROM)/random access memory (RAM), an electrically erasable PROM, a received signal strength indicator (RSSI) input circuit and a plurality of light-emitting diode (LED) switch drivers all communicate with the DSP chip 2102 via a
30 common bus.

The C40 DSP chip 2104 is also supported by interface circuitry. Specifically, an integrated services digital network (ISDN) interface and a T1 interface provide a connection to ISDN and T1 equipment, while a supporting Viterbi encoder/decoder, as well as a PROM/RAM, provide digital signal processing support for the DSP chip 2104
35 via a common bidirectional bus.

In addition to receiving signals from the DSP chip 2104 and orderwire FFT data, the C40 DSP chip 2106 communicates bidirectionally with a PROM/RAM and a codec via a bidirectional common bus. The codec in communication with the DSP 2106 communicates bidirectionally with an orderwire headset.

The G-link receiver provides a clock synchronization signal to the G-link transmitter, as well as to an EPLD. In addition, the receiving G-link transmits RSSI data to the RSSI input in communication with the C40 DSP chip 2102. The EPLD that receives the synchronization signal from the receiving G-link circuit provides a receive address, a frame sync signal, and a transmit address as control outputs.

In operation, each of the DSP chips 2102, 2104, 2106 uses the local PROM/RAM for storage and retrieval of data and for use as a look-up table. The C40 DSP chip 2102 receives the RSSI input data to implement automatic game control (AGC). That is, an indication of the signal intensity is provided via the RSSI input to the DSP chip 2102 so that the remote terminal 187, 192 can automatically adjust the receive gain so that the signal is received at the appropriate level. The ETHERNET interface allows the remote terminal 187, 192 to transmit data out to a local computer or operator. The receive/transmit control interface circuit sends control bits to the radio frequency electronics of the remote terminal 187, 192 in order to control the RF electronics. The EPLD synchronization circuit receives an envelope detector output from the RF circuit within the receiver of the remote terminal 187, 192 in order to achieve TDD synchronization. The UART circuit provides for the input of a universal global positioning system (GPS) time clock for use by the remote terminals 187, 192. Finally, the electrically erasable PROM allows the radio access terminals 187, 192 to store information from test to test as a kind of statistical record.

The operations of the other support circuitry depicted in FIGUREs 78A-78C are well known to those of ordinary skill in the art and need not be described in detail for a complete understanding of the present invention.

FIGUREs 77A-77D are a more detailed block diagram of the LPA cards 2110, 2120 of the remote terminals 187, 192 that shows the support circuitry used to support the operation of the SHARP LH9124 DSP chips, as well as the TMS320C4 DSP chips from Texas Instruments. It should be understood that although FIGUREs 77A-77D depict only the receiving LPA card 2110 that the architecture of the LPA card 2110 is substantially similar to that of the transmitting LPA card 2120 so that essentially the same description applies to both LPA cards. Input data in quadrature form (e.g., 24 In-phase bits and 24 Quadrature bits) are provided as an input to a double buffer 2402 via a 48-bit input bus. A first portion of the double buffer 2402 is controlled via input address and

control bits, while a second portion of the double buffer 2402 is controlled via an address generator 2404. The address generator 2404 communicates with the TMS 320C40 DSP chip 2116 via a bus 2406.

The double buffer 2402 communicates with the SHARP LH9124 digital signal
5 processing chip 2112 via a bidirectional bus and also supplies data as an input to a first in/first out (FIFO) buffer 2408. In one preferred embodiment, the FIFO comprises a 5K x 48-bit buffer. The FIFO 2408 communicates with the DSP chip 2112, as well as with a double buffer 2410. Like the double buffer 2402, the double buffer 2410 advantageously comprises a pair of 32K x 48-bit RAMs. Furthermore, the double buffer 2410 is under the
10 control of the address generator 2412 that communicates with the buffer 2406. The double buffer 2410 communicates bidirectionally with the DSP chip 2116 via the bus 2406.

The SHARP DSP chip 2112 further receives input from a sine/cosine look-up table 2414. The sine/cosine look-up table 2414 receives input from a rectangular-to-polar
15 converter 2416 that in one embodiment comprises a signal processing chip sold under Model Number PDSP16330 and available from GEC Plessey. Finally, the DSP chip 2112 receives sequencing data from a sequencer 2418, that also communicates with the bus 2406. The output of the digital signal processor chip 2112 is provided as an input to a double buffer 2420, that is substantially similar in structure to the double buffers 2402 and
20 2410. A first portion of the double buffer 2420 is under the control of an address generator 2422 that receives signals from the DSP chip 2116 via the bus 2406.

The second half of the LPA card 2110 is substantially similar in architecture to the first half described above. Specifically, input data in quadrature form (e.g., 24 In-phase bits and 24 Quadrature bits) are provided as an input to a second half of the double buffer
25 2420 from the first half of the buffer 2420. The second half of the double buffer 2420 is controlled via an address generator 2424. The address generator 2404 communicates with the TMS 320C40 DSP chip 2118 via a bus 2426.

The double buffer 2420 communicates with the SHARP LH9124 digital signal processing chip 2114 via a bidirectional bus and also supplies data as an input to a first
30 in/first out (FIFO) buffer 2428. In one preferred embodiment, the FIFO 2428 comprises a 5K x 48-bit buffer. The FIFO 2428 communicates with the DSP chip 2112, as well as with a double buffer 2430. Like the double buffer 2420, the double buffer 2430 advantageously comprises a pair of 32K x 48-bit RAMs. Furthermore, the double buffer 2430 is under the control of the address generator 2432 that communicates with the buffer
35 2426. The double buffer 2430 communicates bidirectionally with the DSP chip 2118 via the bus 2426.

The SHARP DSP chip 2114 further receives input from a sine/cosine look-up table 2434. The sine/cosine look-up table 2434 receives input from a rectangular-to-polar converter 2436 that in one embodiment comprises a signal processing chip sold under Model Number PDSP16330 available from GEC Plessey. Finally, the DSP chip 2114 receives sequencing data from a sequencer 2438, that also communicates with the bus 2426. The output of the digital signal processor chip 2114 is provided as an input to a buffer 2440, that advantageously comprises a 32K x 48 RAM. The buffer 2440 is under the control of an address generator 2442 that receives signals from the DSP chip 2118 via the bus 2426.

The C40 DSP chips 2116 and 2118, respectively, receive GPS timing via UART circuits 2450, 2452. Furthermore, each of the DSP chips 2116, 2118 communicates with respective RAM chips 2454, 2456, that advantageously comprise 128K x 32 random access memories.

The DSP chips 2116, 2118 further communicate with EPROMs 2460, 2470, respectively, and RAMs 2462, 2472, respectively, via local buses 2464, 2474, respectively. In one advantageous embodiment the EPROMs 2460, 2470 comprise a 512K x 8 memory, while the RAMs 2462, 2472 comprise a 128K x 32 RAM. A pair of internal communication ports provide for communication between the DSP circuits 2116, 2118, while two pair of input/output external communication ports connect to each of the DSP chips 2116, 2118.

In operation, the DSP chips 2116, 2118 employ the respective memories 2460, 2462, 2470, 2472 to perform processing associated with the fast Fourier transform and code spreading or code-nulling processing operations. Meanwhile, the double buffer 2402 collects input data symbols in quadrature. The double buffer 2402 is provided so that while data is being collected from one packet, data from the previous packet can be processed.

As can be seen from FIGUREs 77A-77D, two substantially identical processing engines are provided separated by the double buffer 2420. In one advantageous embodiment each of the 9124 DSPs 2112, 2114 operate at a 40-mHz sample rate and include six multipliers so that data can be streamed through in substantially real time.

The "Proof-of-Concept Embodiment" - Base Station Hardware

FIGURE 73 is a functional block diagram showing the main functional elements of the base station 110 shown in FIGURE 74. As shown in FIGURE 73, the base station 110 includes a transmit/receive switch 400 that communicates bidirectionally with a plurality of the antennas 120. While in the receive mode, the switch 400 communicates

90

with a down converter 405, and in the transmit mode, the transmit receive switch 400 communicates with an up converter 407. The down converter 405 also receives inputs from a frequency reference circuit 409 and provides outputs to a demodulator 410. The demodulator 410 feeds back an automatic gain control level to the down converter 405

5   and also receives inputs from a packet timing generator 412. The packet timing generator 412 receives analog-to-digital converter clock inputs from the frequency reference circuit 409.

The demodulator 410 provides inputs to a beam forming and code-nulling circuit 415. The beam forming and code-nulling circuit 415 communicates with a

10 multidimensional trellis decoder 420 that, in turn, communicates bidirectionally with a network/data interface circuit 425.

The network/data interface circuit 425 provides outputs to and receives inputs from the telecommunications network 160 (see FIGURE 74). Furthermore, the network/data interface circuit 425 provides an output signal to the packet timing generator

15 412 and also communicates bidirectionally with a base control circuit 430. The base control circuit 430 receives inputs from the demodulator 410, the beam forming/code-nulling circuit 415, and the multidimensional trellis decoder 420. The base control circuit 430 also communicates bidirectionally with an operator station (not shown) within the telecommunications network 160.

20 The network/data interface circuit 425 communicates with a multidimensional trellis encoder 435. The multidimensional trellis encoder 435 provides an output to a retroactive beam forming network and SCMA circuit 440. The network 440 also receives inputs from the beam forming/code-nulling circuit 415 as well as the base control circuit 430. The retroactive beam forming and SCMA network 440 provides an output to a

25 modulator 445 that also receives inputs from the packet timing generator 412. Finally, the modulator 445 together with the frequency reference circuit 409 provide inputs to the up converter 407, that in turn provides an output to the transmit/receive switch 400 while in the transmit mode. Signals provided by the up converter are transmitted to the various high-bandwidth radio access stations 192, 187 by means of the antennas 120.

30 The operation of a base station is substantially similar to the operation of the radio access station 187, 192. Specifically, the transmit/receive switch 400 switches the antenna array 120 into the down-converter 405. The down-converter 405 takes the signal at the transmission frequency (see, e.g., about 2 gigaHertz), and translates this to the proper frequency for digitization. The multi-sensor DMT-SS demodulator 410 then performs a

35 fast Fourier transform (FFT) and presents the individual frequency bins to the beam forming/code-nulling network 415. As discussed briefly above, the code-nulling network

415 applies code-nulling and beam forming weights to the despreading codes in order to cancel interference due to transmissions having non-orthogonal spreading codes. The code-nulling network 415 also despreads the demodulated signal provided by the multi-sensor DMT-SS demodulator 410 and produces output demodulated symbols.

5   The demodulated symbols are provided as an input to the multi-dimensional trellis decoder 420 in order to decode the symbols in accordance with pragmatic Viterbi decoding methods. Receive bits are provided at the output of the multidimensional trellis decoder 420. The receive bits pass through a digital data interface 425 that, in one embodiment, serves as a data interface for a T3/SONET interface link.

10   On the transmit side, data to be transmitted enters the digital data interface 425 via the T3/SONET link and enters the multidimensional trellis encoder 435 for trellis encoding. It will be understood, of course, that other kinds of error encoding and symbol encoding such as Reed-Solomon error coding, and QAM or BPSK symbol encoding are performed within the encoder 435. The encoded symbols enter the

15   beam-forming/code-spreading circuit 440 wherein the spreading code together with the appropriate beam forming and null-steering code weights are applied to the input symbols. The spread symbols are DMT-SS modulated as represented within the block 445 and the resulting signal is translated to the high frequency band via the up-converter 407. The transmit/receive switch 400 is then switched to connect the up converter 407 to the

20   antenna array 120 so that the modulated and encoded data signal is transmitted via the antenna 120.

           For synchronization of the base stations 110 all of the bases 110 are locked onto GPS time. In this manner, no matter how big the communications network 100 becomes, all of the base stations 110 always have the proper TDD synchronization. Thus, the base

25   stations 110 always start transmitting at the same time and receiving at the same time. At the packet timing generator 409, the frequency reference is GPS derived and this is used to control the T/R switch 400. This is particularly advantageous because the timing does not have to be derived from the waveforms transmitted by several remotes. Since the remote terminals 187, 192 derive their synchronization timing from the base stations 110,

30   the remotes will be synchronized to GPS time.

           The packet timing generator 412 receives a clock signal from the timing generator 409 so that the packet timing generator 412 can supply transmit and receive gating signals to the modulator 445 and the demodulator 410, respectively.

           In an alternative embodiment, it would be possible to establish a universal timing

35   mechanism for all of the base stations 110 and the remote terminals 187, 192 provided from the network via the network interface 425. In such an embodiment. an specially

defined ATM adaptation layer could be used to provide a clock to the interface 425. Management information and connection power control information could also be supplied over the T3 or SONET link. Such information could be provided to the base controller 430 that will send the proper signals out to the remotes 187, 192 through the
5   wireless signaling network for connection set up and carry out other management functions.

      It should further be noted that the down-converter 405 and up-converter 407 contain separate RF electronics that include slight imperfections so that they may not be perfectly matched. For this reason, a transmit/receive compensation is performed using
10   additional compensation weights. The purpose of this compensation is to compensate for the differences in phase and amplitude introduced into the signals by the transmit and receive RF electronics. By applying the compensation weights. the same beam pattern is produced on the transmit side as on the receive side.

      FIGUREs 79A-79D are a schematic block diagram that depicts the overall digital
15   signal processing architecture layout within the base stations 110. The base station 110 is laid out into a radio frequency chassis portion 2500 and a digital chassis portion 2510. The multiple element antenna array 120, that for ease of illustration is depicted in FIGUREs 79A-79D as comprising four antennas, connects to corresponding transmit/receive modules 2512. Each transmit/receive module 2512 includes the
20   transmit/receive switch 400, as well as a receiver, a transmitter, and an amplifier. It should be noted that in accordance with one advantageous aspect of the present invention, each antenna element is provided with an individual amplifier. By using this distributed amplifier configuration instead of one large amplifier to power the entire antenna array, power is saved. In addition, in the event of amplifier failure, only one of multiple antenna
25   elements fails rather than the entire antenna array. Thus, the present invention provides for graceful degradation of signal quality in the event of an amplifier failure.

      An analog-to-digital converter/digital-to-analog converter pair 2515 provides for analog-to-digital and digital-to-analog conversion of the received and transmitted signals. The digitized received signals enter the digital chassis 2510, while the digital transmit
30   signals are provided as an output of the digital chassis 2510.

      The digital chassis 2510 includes a G-link interface circuit that provides outputs to a plurality of receiver LPAs 2520 via a plurality of 32-bit busses. The LPAs 2520 perform the FFTs and channel estimation in parallel (e.g., one of the LPAs performs signal processing on each of the even symbols, while the other performs equivalent signal
35   processing steps on the odd receive symbols).

The LPAs 2520 provide the processed signals to LPAs 2530, that are substantially similar in construction to the LPAs 2520 and the LPAs 2110 and 2120. The LPAs 2530 perform QR decomposition and output the decomposed signals to LPA cards 2540.

The LPA cards 2540 perform matrix operations involved in the null-steering and code-nulling procedures. The retrodirective weights calculated within the LPA cards 2540 are provided as inputs to LPA cards 2550 in the transmitter path for use during data spreading, beam forming, and generating IFFTs.

An additional LPA card 2560 is provided as a digital signal processing engine for the transmitter/receiver calibration (i.e., T/R compensation). The T/R calibration LPA card 2560 communicates with a probe antenna 2565 via a G-link interface, an analog-to-digital/digital-to-analog converter, and a transmit/receive calibration module 2570. The transmit/receive calibration module 2570 includes a receiver, a transmitter, a transmitting amplifier, and a transmit/receive switch. As described briefly above, the purpose of the probe antenna is to compensate for distortion due to the transmitter and receiver paths through the base station 110. That is, the transmit/receive modules 2512 introduce a certain amount of distortion and phase delay into the transmitted and received signal so that it is necessary to compensate for these distortions to provide an accurate production of the transmit and receive signals. The probe antenna path acts like a remote station so that when the base station 110 is transmitting from the antenna array 120, this information is received on the probe 2565. Conversely, when the probe antenna 2565 is transmitting, the antenna array 120 of the base station 110 is receiving the known signal transmitted by the probe antenna 2565. By signal processing performed within the transmit/receive calibration LPA card 2560, the differential amplitude and phase across the phase transmitter and receiver paths can be determined. Thus, the base station 110 can compensate for these distortions by means of the signals transmitted and received by the probe antenna 2565.

A global positioning system antenna 2580 receives GPS timing to provide a reference clock for each of the local oscillators within the base station 110. This ensures that accurate synchronization can be obtained throughout the entire wireless communication system 100.

FIGUREs 6 and 7 show alternative embodiments of the directional antenna arrays 120 that may be used in the system of the present invention. A first embodiment of the base station antenna implementation is designated generally as 120a. The antenna 120a is a circular patch slot array antenna including a protective RADOME 505 available from RADIX Technologies, Inc. of Mountain View, California, a generally cylindrical housing 507, and a support pole 510. A plurality of multi-element vertical patch arrays 515 are

94

depicted in cutaway in Figure 6. Each of the patch arrays 515 are capable of directionally emitting radio frequency signals so as to provide beam forming capabilities necessary for the proper implementation of the present invention. In one embodiment, the height of the cylindrical portion 507 is approximately 18", while the diameter of the RADOME 505 is

5 approximately 5-16".

In one advantageous embodiment, the antenna 120a includes a vertical stack of 4 microstrip patch antennas. Four of these stacks will respectively be oriented to cover four 90° quadrants. Thus, a total of 16 circumferential stacks of microstrip flared-notch antennas (where each vertical stack comprises eight notches) will be included on the base

10 antenna 120a. For both the remote and base antennas, the preferred sensor element spacing is one-half wavelength.

Figure 7 depicts a second implementation of the base station antenna of the present invention that is generally designated as 120b. The antenna 120b includes a RADOME 520, a generally cylindrical portion 525, and a support pole 530. The RADOME 520 is

15 approximately 18-24" in diameter while the cylindrical portion 525 is approximately 14" in height. As shown in cutaway, the antenna 120b includes a flared circular horn configuration 535 as well as a plurality of monopole transmission elements 540. The monopole elements 540 may be used for beam forming purposes such as that that is necessary for the optimum operation of the present invention.

20 FIGURE 80 is a transceiver block diagram showing the main structural elements of the down converter 305 depicted in FIGURE 72. As shown in FIGURE 80, the antenna 190 and the transmit/receive switch 300 connect to bandpass filters 702, 704 that, in turn, connect to amplifier 706, 708, respectively. The path through the filter 702 and the amplifier 706 constitutes the receive path that is part of the down converter 305, while the

25 path that is through the amplifier 708 and the bandpass filter 704 constitutes part of the transmission pass that is a part of the up converter circuit 307. The output of the amplifier 706 and the input of the amplifier 708 connect to a switch 710. The switch 710 is used to switch between the transmission and receiving paths associated with the down and up converters 305, 307, respectively.

30 Although the up converter 307 and the down converter 305 are represented in FIGURE 72 as functionally distinct blocks, it will be appreciated by one of ordinary skill in the art that the same structural elements may be used to perform the functions of both the up converter and the down converter in an architecture that reuses amplifiers and saw filters within the transmitter and receiver path. The switch 710 connects to a bandpass

35 filter 712. In one advantageous embodiment, the bandpass filter 712 has a bandpass frequency between 1,865 MHz and 1,950 MHz. The bandpass filter 712 connects to a

multiplier 715 that receives an input from a first local oscillator having an oscillation frequency of 1667.5 MHz. The multiplier 715 connects to a digital attenuator circuit 720 that receives a gain control input from the demodulator 310 (see FIGURE 72). The digital attenuator 720 connects to an amplifier 724 via a switching circuit 722. The

5   switching circuit 722 allows the amplifier 724 to be used bidirectionally in both the transmitter and receive paths. That is, when switched in a first direction, the output of the amplifier 724 connects to the digital attenuator circuit 720 while when switched in a second mode, the input of the amplifier 724 connects to the digital attenuation circuit 720. By using the same amplifier (i.e., the amplifier 724) in both the transmitter and receiver

10   paths the same amplifier characteristics are observed in both paths so that transmission and reception compensation is greatly simplified. The switching network 722 further connects to a summing circuit 725.

When operating in a receiving mode, the summing circuit 725 acts as a signal splitter while, when in the transmitting mode, the summing circuit 725 acts to linearly add

15   a pair of input signals. The summing circuit 725 connects to parallel amplification and filtering paths having corresponding elements. Specifically, one input to the summing circuit 725 comprises a saw bandpass filter 730 having a center frequency of 270 MHz and a bandwidth of 1.5 MHz. A corresponding saw bandpass filter 732 has a center frequency of 200 MHz and a bandwidth of 1.5 Mhz. The bandpass filters 730, 732 connect,

20   respectively, to amplifiers 738, 740 via switching networks 734, 736. Again, the switching networks 734, 736 insure that identical amplifier characteristics are observed in both the transmit and receive paths. The amplifiers 738, 740 advantageously provide an amplification factor. The switching circuits 734, 736 connect to corresponding saw bandpass filters 742, 744. The bandpass filter 742 has a center frequency of

25   approximately 280 Mhz and a bandwidth of 1.5 Mhz, while the bandpass filter 744 has a center frequency of 200 Mhz and a bandwidth of 1.5 Mhz. The bandpass filters 742, 744 connect, respectively, to corresponding amplifiers 750, 752 via switching networks 746, 748. The amplifiers 750, 752 advantageously provide an amplification factor. The switching networks 746, 748 connect to corresponding multipliers 754, 756. The

30   multiplier 754 receives a local oscillator input signal oscillating at 281.25 Mhz, while the multiplier 756 receives a local oscillator input signal oscillating at approximately 201.25 Mhz.

The multipliers 754, 756 connect to corresponding low pass filters 758, 760, that in turn connect to switches 762, 764, respectively. The switch 762 receives an input

35   signal from an amplifier 766 and provides an output signal to an amplifier 768, while the switch 764 receives an input signal from an amplifier 770 and provides an output signal to

an amplifier 772. The amplifiers 766 through 772 advantageously have an amplification factor. Amplifiers 766, 770 form a part of the transmission path, and therefore properly belong to the up converter 307, while the amplifiers 768, 772 belong to the reception path and therefore, properly belong to the down converter 305 of FIGURE 72. The amplifiers
5   766, 770 connect to digital-to-analog converters 774, 778, respectively. The digital-to-analog converters 774, 778 also comprise a portion of the up converter 307 and receive a digital-to-analog clock pulse from the synchronization circuit 312. The amplifiers 768, 772 connect to analog-to-digital converters 776, 780, also comprise a portion of the down converter 305 that receive analog-to-digital converter clock inputs
10 from the synchronization circuit 312 (see FIGURE 72).

.   The inputs to the digital-to-analog converters 774, 778 are received from the modulation circuit 345, while the outputs of the analog-to-digital converters 776, 780 are provided as inputs to the demodulation circuit 310.

The operation of the up/down converter circuit depicted in FIGURE 80 will first
15 be described with reference to the received path and will next be described with reference to the transmission path. Within the received mode, signals picked up by the antenna 120 are transmitted to the switch 300 and passed through the bandpass filter 702 so as to attenuate any signals that are not within the frequency band of interest (i.e., frequencies between 1,865 Mhz and 1,950 Mhz). The filtered signals are then amplified by an
20 amplification factor within the amplifier 706. The output of the amplifier 706 is provided as an input to the switch 710 that allows the amplified signal to be passed through the bandpass filter 712 that further filters out any undesired signals outside of the designated bandpass range.

Signals that are allowed to pass through the filter 712 are multiplied by the local
25 oscillator frequency at 1,667.5 Mhz within the multiplier 715. Thus, the multiplier 715 acts as a synchronous detector that may be used to cause a first down conversion of the signal from approximately the 2 GHz range down to the 200 to 300 Mhz range. This down-converted signal is then attenuated by means of the digital attenuation circuit 720 and amplified with an amplification factor by means of the amplifier 724. The
30 down-converted signal is then split within the signal splitter 725 so that one portion of the signal enters the saw bandpass filter 730 while an identical portion of the signal enters the saw bandpass filter 732.

The portion of the signal that enters the bandpass filter 730 is filtered to attenuate signals outside of the frequency range of 279.25 Mhz and 280.75 Mhz. This filtered signal
35 is then amplified by a factor via the amplifier 738 and is then filtered again through the filter 742 having substantially identical characteristics to the filter 730. Once again, the

filtered signal is amplified by the amplifier 750 with an amplification factor and this signal is input to the multiplier 754. The multiplier 754 acts as a synchronous detector that converts the signal output by the amplifier 750 to substantially a base band signal by multiplying the oscillator signal at 281.25 Mhz. The base band signal is then passes through the low pass filter 758 and from there is supplied as an input to the amplifier 768 via the switch 762. The amplifier 768 amplifies the base band signal by a factor and this signal is then converted to digital data by means of the analog-to-digital converter 776.

The second portion of the signal output by the splitter 725 follows a substantially similar path to that followed by the first portion of the signal output by the splitter 725, with the exception that the second portion of the signal is filtered to pass bandwidths between 199.25 Mhz and 200.75 Mhz. Furthermore, this portion of the signal is synchronously detected within the multiplier 756 by means of a local oscillator signal at 201.25 Mhz. In this manner, signals received by the antenna 120 are asynchronously detected, down-converted to the base band level, and digitized so as to provide digital information to be demodulated by the demodulator 310.

The transmission path for signals that are to be transmitted by the high-bandwidth base station 110 is substantially the same through the up converter as through the down converter with the exception that the order of the signal processing steps is reversed. Specifically, modulated digital signals serve as the inputs to digital-to-analog converters 774 and 778, so as to produce analog signals that are amplified by the amplifiers 766 and 770, respectively. The amplified analog signals pass through the switching circuits 762, 764 and are filtered by respective low pass filters 758, 760. Along the first path the analog signal is up-converted by modulation (i.e., multiplication) with the local oscillator signal at 281.25 Mhz while the second signal is up-converted by modulation with an oscillator at 201.25 Mhz. The first modulated signal is then amplified and filtered via the amplifiers 750, 738 and the filters 742, 730 so as to provide a well defined signal between 200 and 79.25 Mhz and 280.75 Mhz. The second signal is likewise amplified and filtered via the amplifiers 752, 740 and the filters 744, 732, so as to provide a well defined signal within the frequency range of 199.25 Mhz and 200.75 Mhz. The two signals that are output from the bandpass filters 730 and 732 are provided as inputs to the summing circuit 725. The summing circuit 725 linearly adds the two input signals, and these signals are amplified by the amplifier 724. The digital attenuation circuit 720 then attenuates the amplified output signal and the multiplier 715 further up converts this signal by multiplication with the oscillator frequency at 1,667.5 Mhz. In this manner, the original input signals containing the communication information are up-converted to the transmission frequency range. The signal to be transmitted is then filtered between 1,865

and 1,950 Mhz within the filter 712 and the signals amplified in the amplifier 708 after passing through the switch 710. The amplified transmission signal is further filtered within the bandpass filter 704 and this filtered and amplified signal is provided as an output to the antenna 120 via the transmission/receive switch 300.

5   FIGURE 80A is a schematic block diagram showing the main internal functional elements of the synchronization circuitry 312. As shown in FIGURE 80A, the synchronization circuit 312 includes a frequency controller 785 that connects to a 40 Mhz reference oscillator 787 having a 2-bit input from a data clock (not shown). The 40 Mhz reference oscillator 787 outputs a signal to a divide-by-eight binary counter 789 that, in
10   turn, supplies the output signal references for local oscillators 791, 793 and 795. The local oscillator 791 provides the oscillation frequency at 1,667.5 Mhz, while the oscillators 793, 795, respectively, provide the oscillation frequencies of 281.25 Mhz and 201.25 Mhz. Finally, the divide-by-eight binary counter 789 further provides a clock input pulse for each of the analog-to-digital and digital-to-analog converters 774 through 780.

15   FIGURE 81 depicts a schematic block diagram of the main elements of the down converter 405 within the base station 110 depicted in FIGURE 73. Specifically, the antenna 120 connects to a bandpass filter 802 via the transmit/receive switch 400 while the switch 400 is in the receive mode. The filter 802 passes frequencies about 1,865 Mhz and below 1,950 Mhz. The filter 802 connects to the input of an amplifier 804 that, in turn,
20   connects to a second bandpass filter 806 that has substantially the same characteristics as a filter 802. The filter 806 provides an input to a multiplier 809 that also receives inputs from a local oscillator (not shown in FIGURE 81) at an oscillation frequency of 1,667.5 Mhz. The output of the multiplier 809 connects to a digital attenuator 811 that receives a gain control input fee as the demodulator circuit 410 (see FIGURE 73). The output of the
25   digital attenuator 811 serves as the input to an amplifier 813 having an amplification factor.

The amplified signal output from the amplifier 813 enters a signal splitter 815 that divides the signal into, for example, six substantially identical portions. Each of the six signals output by the splitter 815 are filtered, amplified, down-converted and digitized in
30   substantially the same way.

The first signal enters a bandpass filter 817 having a center frequency of 281.5 Mhz with a bandwidth of 1.5 Mhz. The output of the bandpass filter 817 serves as an input to an amplifier 819 having an amplification factor. The output of the amplifier 819 serves as the input to a bandpass filter 821 having substantially the same characteristics as
35   a bandpass filter 817. The output of the bandpass filter 821 connects to an amplifier 823 having an amplification factor, while the output of the amplifier 823 serves as the input to

a multiplier 825. The multiplier 825 also receives a local oscillator input at 282.5 Mhz so as to act as a synchronous detection circuit that has an output connected to a low pass filter 827. The output of the low pass filter 827 serves as the input to an amplifier 829, while the output of the amplifier 829 serves as the input to an analog-to-digital converter
5   831. The analog-to-digital converter 831 further receives a 10 Mhz clock input from the frequency reference circuit 409 (see FIGURE 73). The output of the analog-to-digital converter 831 serves as the input to the demodulator circuit 410 in FIGURE 73.

The second portion of the signal output from the signal splitter 815 is input to a saw bandpass filter 833 having a center pass frequency of 280 Mhz and a bandwidth of 1.5
10 Mhz. The bandpass filter 833 connects to the input of an amplifier 835 that, in turn, outputs a signal to a bandpass filter 837 having substantially the same characteristics as the bandpass filter 833. The output of the filter 837 serves as the input to an amplifier 839 having an amplification factor. The output of the amplifier 839 connects as an input to a multiplier circuit 841 which also receives a local oscillator signal at 282.5 Mhz. The
15 output of the multiplier circuit 841 serves as the input to a low pass filter 843 that, in turn, connects to the input of an amplifier 845 having an amplification factor. The output of the amplifier 845 is input to an analog-to-digital converter 847 that operates off of an analog-to-digital clock of 10 Mhz. The 10 Mhz clock is received from the frequency reference circuit 409 of FIGURE 73. The output of the analog-to-digital converter 847
20 serves as an input to the demodulating circuit 410 (see FIGURE 73).

The third portion of the signal output by the signal splitter 815 enters a bandpass filter 849 that has a center pass frequency of 278.5 Mhz and a bandwidth of 1.5 Mhz. The output of the bandpass filter 849 enters the input of an amplifier 851 having an amplification factor, while the output of the amplifier 851 connects to the input of a
25 bandpass filter 853 having substantially the same bandpass characteristics as the filter 849. The output of the filter 853 connects to the input of an amplifier 855 that, in turn, connects to a multiplier 857 that connects to an analog-to-digital converter 863 via a low pass filter 859 and an amplifier 861. The amplifier 855, the multiplier 857, the low pass filter 859, the amplifier 861, and the analog-to-digital converter 863 are substantially
30 identical to the corresponding elements 823, 825, 827, 829 and 831, and function in substantially the same manner.

The fourth portion of the signal output from the signal splitter 815 enters a bandpass filter 865 having a center bandpass frequency of 201.5 Mhz and a bandwidth of 1.5 Mhz. The output of the bandpass filter 865 serves as the input to an amplifier 866
35 having an output connected to a bandpass filter 867 that has substantially identical filtering characteristics as the bandpass filter 865. The output of the bandpass filter 867 connects

100

to the input of an amplifier 868 having an amplification factor. The output of the amplifier 868 connects to a multiplier 869 that also receives a local oscillator frequency of 202.5 Mhz. Thus, the multiplier 869 acts as a synchronous detector that outputs a down-converted base band signal to a low pass filter 870. The low pass filter 870 provides an input to an amplifier 871 having an amplification factor and the output of the amplifier 871 serves as the input to an analog-to-digital converter 872 that receives a 10 Mhz analog-to-digital converter clock from the frequency reference circuit 409. The output of the analog-to-digital converter 872 serves as an input to the demodulating circuit 410 (see FIGURE 73).

The fifth and sixth portions of the signals output by the signal splitter 815 are provided as inputs to analog-to-digital converters 880, 888, respectively, via bandpass filters 873, 881, amplifiers 874, 882, bandpass filters 875, 883, amplifiers 876, 884, multipliers 877, 885, low pass filters 878, 886, and amplifiers 879, 887, respectively. Each of the circuit elements between the splitter 815 and the analog-to-digital converters 880, 888 are substantially identical to their corresponding elements between the signal splitter 815 and the analog-to-digital converter 872, with the exception that the bandpass filters 873 and 875 have a center frequency of 200 Mhz and the bandpass filters 881, 883 have a center pass frequency of 198.5 Mhz.

The operation of the down converter portion of the base station 110 is substantially similar to that of the down converter portion of the high-bandwidth base station 110. Specifically, signals received by the antenna 120 and switched to the receiving path by the switch 400 are filtered and amplified by means of the filters 802, 806 and the amplifier 804. Subsequently, the signal is down-converted to a lower frequency band by synchronous detection within the multiplier 809. After the first down conversion step, the signal is digitally attenuated by means of the attenuator 811 and then amplified by means of the amplifier 813. The signal is then split into a plurality of substantially identical signals that each follow a different detection path. Each of the detection paths is substantially identical, with the exception that each path down converts the detected signal into a different base band frequency range. Thus, for example, the first portion of the split signal is filtered about a center frequency of 281.5 Mhz by the bandpass filters 817, 821, and is amplified by the amplifiers 819, 823. This filtered signal then is synchronously detected by the multiplier 825 and converted to base band. This base band signal is subsequently filtered, amplified and digitized within the low pass filter 827, the amplifier 829, and the analog-to-digital converter 831. This sequence of detection is substantially the same for each of the six signal portions output by the signal splitter 815, with the exception that the bandpass filters operate at different centering frequencies and the local

oscillator signals that serve as inputs to the various multipliers are different for the bottom three signal portions than for the top three signal portions.

FIGURE 81A is a simplified schematic block diagram showing the main internal components of the frequency reference circuit 409. As shown in FIGURE 81A, the frequency reference circuit 409 includes a frequency control circuit 890, a 40 Mhz reference oscillator 891, and a divide-by-four circuit 892. The divide-by-four circuit 892 provides outputs to local oscillators 893, 894 and 895, as well as to each of the analog-to-digital converter circuits and the digital-to-analog converter circuits (see FIGURE 82). The local oscillator 893 provides the 1,667.5 Mhz output signal, while the local oscillators 894 and 895, respectively, provide the 281.25 and the 201.25 Mhz oscillator signals.

FIGURE 82 is a schematic block diagram that shows the main internal components of the up converter 407 along the transmission path of the base station 110 (see FIGURE 73). The antenna 120 connects to a bandpass filter 902 via the switch 400 when the switch 400 is in the transmission mode. The bandpass filter 902 allows frequencies between 1,865 Mhz and 1,950 Mhz to pass. The bandpass filter 902 connects to the output of a power amplifier 904 having an amplification factor. The input of the power amplifier 904 connects to a bandpass filter 906 having frequency pass characteristics that are substantially the same as the bandpass filter 902. The input of the bandpass filter 906 connects to the output of a multiplier 908 that receives a first input from a local oscillator having an oscillation frequency of 1,667.5 Mhz and a second input from a digital attenuator circuit 910. The digital attenuator circuit 910 receives gain control inputs from the modulation circuit 445 (FIGURE 73). The input of the digital attenuator circuit 910 connects to the output of a power amplifier 912 that, in turn, receives inputs from a summing circuit 914. The summing circuit 914 receives, in one embodiment, six separate inputs that are linearly added within the summing circuit 914 to provide an output to the amplifier 912. Each of the six inputs to the summing circuit 914 connects to a bandpass filter having a 1.5 Mhz bandwidth. Specifically, the bandpass filters 920, 930, 940, 950, 960 and 970 serve as inputs to the summing circuit 914. The bandpass filters 920, 930, 940, 950, 960 and 970, respectively, have center pass frequencies of 281.5 Mhz, 280 Mhz, 278.5 Mhz, 201.5 Mhz, 200 Mhz and 198.5 Mhz. Each of the bandpass filters 920-970, respectively, connect to the outputs of amplifiers 921-971. The amplifiers 921-971, respectively, receive inputs from bandpass filters 922-972. The bandpass filters 922-972 have substantially the same frequency path characteristics as the bandpass filters 920-970. The bandpass filters 922-972 each connect to outputs of amplifier circuits 923-973.

The amplifier circuits 923-973 connect to the outputs of respective multipliers 924-974. The multipliers 924, 934, 944 receive local oscillator input signals at an oscillation frequency of 282.5 Mhz, while the multipliers 954, 964, 974 receive local oscillator inputs at 202.5 Mhz. Each of the multipliers 924-974 connect to corresponding low pass filters 925-975. The low pass filters, in turn, receive inputs from the output of respective amplifiers 926-976. Finally, each of the amplifiers 926-976, respectively, receive inputs from digital-to-analog converters 927-977. Each of the digital-to-analog converters 927-977 receive digital-to-analog converter clock input signals at 10 Mhz from the output of the divide-by-four binary counter 892 (see FIGURE 81A) and also receive inputs from the modulator circuit 445 shown in FIGURE 73.

In operation, modulated data signals serve as inputs to the digital-to-analog converters 927-977. The digital-to-analog converters 927-977 convert the modulated digital data signals into analog signals that are subsequently amplified by the amplifiers 926-976, and filtered by the low pass filters 925-975. The outputs of the low pass filters 925-975 enter as one input of the multipliers 924-974, respectively. The second inputs of the multipliers 924-974 receive local oscillator inputs at either 282.5 Mhz or 202.5 Mhz. Thus, the signals output from the low pass filters 925-975 are up-converted to a first high frequency level. The up-converted signals output by the multipliers 924-974 are subsequently amplified and filtered by means of the amplifiers 923-973 and 921-971, and the filters 922-972 and 920-970. The outputs to the filters 920-970 serve as inputs to the summing circuit 914, that linearly sums each of the signals applied at the six input terminals.

The summed output of the summing circuit 914 serves as an input to the power amplifier 912. The output of the power amplifier 912 enters the digital attenuator circuit 910 so as to fine tune the gain control applied to the signal output from the signal amplifier 912, and the output of the digital attenuator 910 serves as the first input to the multiplier 908. The second input of the multiplier 908 is the local oscillator signal at 1,667.5 Mhz. Thus, the multiplier 908 serves to up convert the signal output from the digital attenuator 910 to the transmission frequency of the base station 110. The output of the multiplier 908 is subsequently filtered and amplified by means of the filters 902, 906 and the amplifier 904. Finally, the output of the filter 902 serves as the input of the switch 400 in the transmit mode, that relays this up-converted and amplified signal to the antenna 120.

METHOD OF DYNAMICALLY ALLOCATING BANDWIDTH

The bandwidth allocation method performed by the bandwidth demand controller (see FIGURE 74) is depicted in FIGURE 83. The method begins in a start block 3300. Once the bandwidth allocation method begins, initialization functions are performed including, as shown in FIGURE 83, determining if the number of antenna sensor elements has been changed since the last use of the base station 110 or remote terminal 187, 192. For example, it may be desirable to provide a base station 110 or remote access terminal 187, 192 with increased spatial resolution capability so that the base or remote station can more accurately discriminate between incoming signals. In such a case, the base station 110 or remote terminal 187, 192 would be deactivated while a new antenna is installed having a greater number of sensor elements that, as well known in the art, would provide a greater degree of directional discrimination or spatial division for that base station or remote. Once the installation of a new antenna is complete, then the installer reactivates the base 110 or remote 187, 192 and, as indicated within a decision block 3305 a test is performed to determine if a number of antenna elements is changed. If a number of antenna elements has changed, control passes to an activity block 3310 wherein the number of tones within a tone set is redefined (e.g., to a smaller number if the number of antenna elements increases) so that the matrices used to calculate the complex weights applied to the sensors and tones within a tone set maintain the same dimensionality. Thus, as discussed above, essentially the same SINR is preserved while processing costs are not increased. After the initialization such as performed within the activity block 3310, control passes to a decision block 3315 wherein a determination is made if a new user is requesting bandwidth. If it was determined, however, within the decision block 3305 that the number of antenna elements has not been changed, then the method passes immediately to the decision block 3315 to the decision block 3305.

If it is determined within the decision block 3315, that a new user has not requested bandwidth through the access channel, then control passes to a subroutine block 3320 wherein the bandwidth assignments already allocated within the communications link are modified, if necessary, to maximize the SINR. Control returns from the subroutine block 3320 to the decision block 3315 until it is determined that a new user is requesting bandwidth over the control access channel.

When a new user requests bandwidth, control passes to an activity block 3325 to determine how much bandwidth is requested. As discussed above, the requested bandwidth is predicated upon the type of data that is transmitted (e.g., voice, video, data, etc.) as well as the transmitting device. For example, if an individual telephone unit is transmitted, then as few as 8 kilobits per second of bandwidth may be requested, while if a P-1 link connected to a PBX is requesting bandwidth, as much as 1.544 Mhz will be

requested. In one embodiment, the requesting device transmits an initialization or identification signal that indicates to the remote station 187, 192 the bandwidth requirements of the requested device.

Once the quantity of bandwidth requested is determined within the activity block

5   3325, control passes to a decision block 3330 or a determination is made if the communications channel has sufficient free bandwidth to accommodate the requesting unit. If it is determined that the channel does not have sufficient free bandwidth to accommodate the optimum bandwidth requested by the new user, then control of the method passes to an arbitration phase wherein a determination is first made within a

10   decision block 3335 if the user can use less bandwidth. If a user cannot operate with less bandwidth than requested, then the user is disconnected and access is denied to the communications channel as indicated within activity block 3340. However, if it is determined that the user can operate with less bandwidth, then the base station 110 asks the user, via the remote station 187, 192, for a lower bandwidth requirement as indicated

15   within an activity block 3345. Control then returns to the activity block 3325 wherein the quantity of requested bandwidth is again determined. Of course, it will be understood, that the base station may present a suggested bandwidth that is allowable to the user via the remote station 187, 192 if the user is sophisticated enough to determine if such a suggested bandwidth would be sufficient to provide normal operation of the user

20   communication device.

However, if it is determined that the communication channel has sufficient free bandwidth to accommodate the requesting user, then control passes from the decision block 3330 to a decision block 3350 wherein a test is performed to determine if there are any free tone sets. That is, if there are any tone sets that have not yet been allocated to

25   other users within the region of the requesting remote terminal 187, 192. If there are free tone sets within the region of the requesting room or terminal 187, 192, then control passes to an activity block 3355 wherein one or more of the free tone sets is allocated to the user for use in transmitting data from the remote associated with the user to the base within the remote spatial cell. Control then passes from the activity block 3355 to an

30   activity block 3360. If there is determined, however, within the decision block 3350 that there are no free tone sets, then control passes instead to an activity block 3365 wherein one or more currently used tone sets are allocated to the user for the transmission of data between the remote 187, 192 and base station 110. It is possible that multiple tone sets will be allocated to a requesting user if a very high bandwidth is requested by the user. It

35   should also be noted here, that because the tone sets are grouped into four approximate 1 Mhz bands that when multiple tone sets are allocated to a single user to establish a

separate communications channel, these tone sets are typically within the same 1 Mhz band.

Once control passes from either the activity block 3355 or the activity block 3365 to the activity block 3360, one or more codes (i.e., spreading codes used to modulate the various tones within the allocated tone set or tone sets) are allocated to the user making sure that the same code (i.e., on the same tone set) is not used by a proximate remote to the remote connected to the new user. In this manner, maximum frequency and code reuse is achieved by spatially separating users having the same tone sets and code assignments. Of course, it will be understood, that due to the adapted channel equalization method described above, that the spreading codes initially assigned to the remote terminals that, on line, are typically not are well-defined codes, but rather constitute linear adapted spreading weights to maximize the SINR. Therefore, it is highly unlikely that a newly allocated code will be identical to any of the spreading weights assigned to remote terminals within the same proximity as the remote terminal assigned to the new user. As discussed in greater detail above, the criteria for modifying spreading codes assigned to each new user requires that the spreading weights be linearly independent to provide at least one degree of freedom for each user within a given spatial cell site.

Control passes from the activity block 3360 to a decision block 3370 wherein a determination is made if the maximum constellation size (i.e., for any arbitrary M-ary modulation format) is sufficient to maintain the requested bandwidth given the number of tone sets and codes allocated to the user. That is, if the newly defined communication channel tolerates a sufficiently high constellation size then the required bandwidth will be satisfied for the requesting user. However, if the channel is not always resistant enough to handle the necessary constellation size to maintain the bandwidth required for operation of the new user, then additional codes or tone sets must be allocated to the user in accordance with the method described. Once the tone sets, codes, and modulation format are defined for the newly requested communication channel, control passes to the subroutine block 3320 wherein the bandwidth assignments are modified, as necessary, to maximize the SINR. Control then returns to the decision block 3315 and the process repeats as described.

ALTERNATIVE EMBODIMENT OF THE INVENTION: ADAPTIVE BEAMFORMING FOR PLURAL DISCRETE TONES FOLLOWED BY COMBINING RESULTANT SIGNALS

Figure 84A and Figure 84B show an alternate embodiment of the invention, where the spectral processing and the spatial processing are separated. The spatial weights are computed independently for each carrier frequency. The spatial weights are then multiplied by spectral weights which are again calculated separately to produce a composite weight. In other words, the combined spectral/spatial beamformer is broken into a separate spectral beamformer and a separate spatial beamformer which operate independently. Figure 84A shows how the received signals on the antennas through M-1 are processed by the spatial beamformer to produce the coefficients A0 through AN-1. Figure 84A also shows how the received signals on the antennas 0 through M-1 are processed by the spectral beamformer to produce the coefficients B0 through BN-1. Figure 84B shows how the spatial coefficients A0 are applied to tone frequency 0 and how the result thereof is then independently operated on by the spectral coefficients B0, with the resultant signals then being transmitted on the antennas through M-1.

Similarly, Figure 84B shows how the spatial coefficients AN-1 are applied to tone frequency n-1 and how the result thereof is then independently operated on by the spectral coefficients BN-1, with the resultant signals then being transmitted on the antennas 0 through M-1. Thus, it is seen how the spatial weights are computed independently for each carrier frequency and then the spatial weights are multiplied by spectral weights which are calculated separately to produce a composite weight.

In one form of this alternate embodiment, the base station and the remote unit can exchange as few as two tones, one in each of the two sub-bands. The separation of 80 Mhz between the two sub-bands spreads the tones far enough apart so that noise bursts and interfering signals in one sub-band do not degrade the other in the other sub-band. The two tones can be separately processed by spatial spreading and despreading and thereafter combined to form the resultant signal. This alternate embodiment has the advantage of a simplified computation, while retaining a reasonable immunity to noise and interference.

At the receiving station, each tone received by the multielement antenna array is spatially despread in a process analogous to receive beamforming. The resultant signals are then combined. A first method of signal-combining is equal gain combining, where the signals are added together. An alternate method of signal combining is maximal ration combining, where the output signal is chosen from the two tones having the better SINR.

At the transmitting station, the alternate embodiment spatially spreads a data signal modulated with the first tone. The spatial spreading uses spatial spreading codes in a process analogous to transmit beamforming. Separately, the alternate embodiment spatially spreads the data signal modulated with the second tone. Then, the two spatially

spread signals are combined and transmitted from the multi-element antenna array, forming a transmitted spread signal that is spectrally and spatially spread.

The alternate embodiment of the invention can have the spatial despreading steps adaptively position spatial directions of the receiver sensitivity towards a desired signal source and/or diminish the receiver sensitivity from interfering sources. The alternate embodiment can also have et spreading steps adaptively position transmitted signal energy of the transmitted despread signal towards a source of the received spread signal and/or adaptively diminish the transmitted signal energy towards interferers. The alternate embodiment works well within the TDD protocol.

Figure 85A is a flow diagram of the computational steps performed in the base station. In the transmission portion of the base station, traffic symbols are input on line 5 to the smear matrix step 10. Link maintenance pilot signals are input on line 7 to the digital signal processor (DSP) data processing RAM 12. Stored pilot signals are output from the RAM 12 to the link maintenance pilot (*LMP) register 14 and are then applied as one input to the smear step 10. The smear matrix 16 is also applied to the smear step 10. The output of the smear matrix 16 is also applied to the smear step 10. The output of the smear step 10 is applied to the gain emphasis step 20. The values from the gain RAM 25 are applied to the gain emphasis step 20 to provide output values which are then applied to the beam form spreading step 30. Spreading weights in a spread weight RAM 32 are applied to the beam form spread step. The X vector is output on line 40 from the beam form spread step and is sent to the transmitt..r for transmission to the remote stations.

On the receive side of the signal processing in the base station, the X vector from the receivers is input on line 50 to the beam form despread step 60. The despreading weight RAM 62 applies the despreading weights to the beam form despread step 60. The signal output from the beam form despread 60 is then applied to the gain emphasis step 70. Values from the gain RAM 25 are applied to the gain emphasis step 70. Values form the gain RAM 25 are applied to the gain emphasis step 70. Values output from the gain emphasis step 70 are applied to the desmear step 80. Values for pilot signals from the gain emphasis step 70 are stored in the LMP register 72 and are applied to the desmear step 80. The desmear matrix is also applied form step 74 to the desmear step 80. Traffic symbols output from the desmear step 80 on line 82 are then available to be utilized and further distributed in the base station. The pilot signals output form the LMP register 72 are stored in the LMP digital signal processing DP RAM 76 and are then output on line 78.

Various values used in the spreading and despreading computations are updated as is shown in Figure 85A. The X vector input on line 50 is applied to the updated weight

step 54. The X vector input online 50 is also applied to the data correction step 93 whose output is applied to the update weight step 54. The updated weight values output from the updated weight step 54 are sent to the valid weights step 56 and are then output to the despread RAM 62. The traffic establishment support 86 provides values to the property

5   map 84 which processes traffic signals from line 82 and applies the output to the smear step 89. Maintenance pilot signals online 81 are applied to the digital signal processing DP RAM 83 whose output is applied to the LMP register 85 whose output is applied to the smear step 89. The smear matrix 87 is also applied to the smear step 89. The output of the smear step 89 is applied to the gain deemphasis step 91 whose output is applied to

10 the data correlation step 93 whose output is applied to the updated weight step 54 as previously described. In addition, the output from the smear step 89 is applied to the element-wise gain covariance step 64. Another input to the element-wise gain covariance step 64 is applied from the output of the beam form despread step 60. The output of the element-wise gain covariance step 64 is applied to the block normalization of elements

15 step 66 which is in turn applied to the element-wise conjugation step 68 which outputs the values to the gain RAM 25. In this manner, the base station can perform both despreading operations for received signal vectors online 50 and spreading operations to transmit traffic symbols input on line 5, in accordance with the invention.

           Figure 85B shows the processing of the common access channel signals. Two

20 common access channels (CAC) signals from the transmitter are processed. A first signal is processed being received on the input line 102 and is applied to the RMGS auto-correlation step 104, whose output goes to the digital signal matrix step 106 whose output goes to the digital signal processor. The common access channel signal online 102 is also applied to the select ungated packets step 108 and to the select gated packets step 110.

25 The output of the select ungated packets 108 is applied to the subtract even/odd packets step 112. The output of the selected gate packets 110 is applied to the apply code key step 114. The CAC code key step 116 applies it's value to the apply code key step 114. The output of the apply code key step 114 is also applied to the subtract even/odd packets step 112. The output of the subtract even/odd packets step 112 ids applied to the RMGS

30 autocorrelation step 118, whose output is also applied to the compute T matrix step 106. The output of the compute T matrix step 106 is then applied to the digital signal processor.

           A second one of the two CAC signals input from the receiver on line 120 is applied to the select ungated packets step 122 and the select gated packets step 124. The output

35 of the select ungated packets step 122 is applied as one input to the combined gated/ungated packets step 126. The output of the selected gated packet steep 124 is

applied to the apply code key step 128 which also receives a signal from the CAC code key step 130. The output of the applied code key step 128 is the second input to the combined gated/ungated packets step 126. The output of the combined gated/ungated packets step 126 is applied to the apply despread weight step 132. A signal from the

5   digital signal processor is applied to the rotated weight RAM 134 whose output is applied to the compute despread weight step 136. The output of the compute despread weight step 136 is applied to the apply despread weight 132, whose output is sent to the digital signal processor. In this manner, the steps shown in Figure 85B carry out processing of the common access channel signals.

10   Although the preferred embodiments of the invention have been described in detail above, it will be apparent to those of ordinary skill in the art that obvious modifications may be made to the invention without departing from its spirit or essence. For example, signal constellation formats other than PSK, BPSK and QAM could be used in accordance with the system of the present invention. Furthermore, the system could optimize for bit

15   error rate (BER) rather than SINR. Also, the number of tones in a tone set, and the number of tone sets and cluster sets in a band could be selected based upon the specific application. The selected frequency bands could also be varied as called for by specific conditions. The TDD format could be altered based upon the multipath environment to insure that an effectively static channel is observed in successive TDD frames. The

20   maximization of the SINR could be performed based upon some signal property other than constant modulus, etc. Consequently, the preceding description should be taken as illustrative and not restrictive, and the scope of the invention should be determined in view of the following claims

CLAIMS

What is claimed is:

1. A highly bandwidth-efficient communications method, comprising:

receiving a received spread signal at a base station having a multi-element antenna array with a first plurality of antenna elements arranged in a spaced vertical direction and a second plurality of antenna elements arranged in a spaced horizontal direction;

said received spread signal comprising a first data signal spread over a plurality of discrete tones in accordance with a remote spreading code assigned to a remote unit for a first time period;

adaptively despreading the signal received at the base station by using first despreading codes that are based on the characteristics of the received signals at the first plurality of antenna elements of said array and perform vertical beam steering; and

adaptively despreading the signal received at the base station by using second despreading codes that are based on the characteristics of the received signals at the second plurality of antenna elements of said array to perform horizontal beam steering.

2. The highly bandwidth-efficient communications method of claim 1, further comprising:

spreading a second data signal at the base station with first spreading codes derived from said first despreading codes, that distributes the second data signal over a plurality of discrete tones and the first plurality antenna elements of said array, forming a first spectrally spread signal that is spectrally and spatially spread vertically;

spreading the second data signal at the base station with second spreading codes derived from said second despreading codes, that distributes the second data signal over the plurality of discrete tones and the second plurality antenna elements of said array, forming a second spectrally spread signal that is spectrally and spatially spread horizontally; and

transmitting said first and second spread signals during a second time period.

3. The highly bandwidth-efficient communications method of claim 1, further comprising:

receiving at the base station during an initialization period, a pilot spread signal comprising a known data signal spread over a plurality of discrete tones;

correlating the known data signal from the pilot spread signal with a reference known data signal and forming said first despreading code that is based on the characteristics of the received signals at the first plurality of antenna elements arranged in the spaced vertical direction, where a given element of the first despreading code corresponds to a given one of the first antenna elements and a given one of the discrete tones; and

correlating a known data signal from the pilot spread signal with a reference known data signal and forming said second despreading code that is based on the characteristics of the received signals at the second plurality of antenna elements arranged in the spaced horizontal direction, where a given element of the second despreading code corresponds to a given one of the second antenna elements and a given one of the discrete tones.

4. The highly bandwidth-efficient communications method of claim 2, wherein both the first and the second spread signals have a spectral form of a discrete multitone signal transmitted on multiple elements in the array.

5. The highly bandwidth-efficient communications method of claim 1, wherein the despreading step is a multiplication of a complex number representation of the despreading codes times a complex number representation of the received spread signal.

6. The highly bandwidth-efficient communications method of claim 2, wherein the spreading step is a multiplication of a complex number representation of the second spreading codes times a complex number representation of the data signal to be transmitted.

7.   The highly bandwidth-efficient communications method of claim 1, wherein the despreading steps determine values of complex despreading codes which are then multiplied with a complex number representation of the received signals, resulting in an estimate of the first data signal.

8.   The highly bandwidth-efficient communications method of claim 1, wherein the despreading steps adaptively position the spatial direction of receive sensitivity towards a desired signal source and diminish receive sensitivity from interfering sources.

9.   The highly bandwidth-efficient communications method of claim 2, wherein the spreading steps adaptively position transmitted signal energy of the spread signals towards a source of the received spread signal and adaptively diminishes transmitted signal energy towards interferers.

10. The highly bandwidth-efficient communications method of claim 2, wherein the first period and the second period are parts of a time division duplex period.

11. The highly bandwidth-efficient communications method of claim 1, wherein the antenna array has a planar symmetry.

12. The highly bandwidth-efficient communications method of claim 1, wherein the antenna array has a cylindrical symmetry.

13. A highly bandwidth-efficient communications system, comprising:

means for receiving a received spread signal at a base station having a multi-element antenna array with a first plurality of antenna elements arranged in a spaced vertical direction and a second plurality of antenna elements arranged in a spaced horizontal direction;

said received spread signal comprising a first data signal spread over a plurality of discrete tones in accordance with a remote spreading code assigned to a remote unit for a first time period;

means for adaptively despreading the signal received at the base station by using first despreading codes that are based on the characteristics of the received signals at the first plurality of antenna elements of said array and perform vertical beam steering; and

said despreading means adaptively despreading the signal received at the base station by using second despreading codes that are based on the characteristics of the received signals at the second plurality of antenna elements of said array to perform horizontal beam steering.

14.   The highly bandwidth-efficient communications system of claim 13, further comprising:

means for spreading a second data signal at the base station with first spreading codes derived from said first despreading codes, that distributes the second data signal over a plurality of discrete tones and the first plurality antenna elements of said array, forming a first spectrally spread signal that is spectrally and spatially spread vertically;

said means for spreading also spreading the second data signal at the base station with second spreading codes derived from said second despreading codes, that distributes the second data signal over the plurality of discrete tones and the second plurality antenna elements of said array, forming a second spectrally spread signal that is spectrally and spatially spread horizontally; and

means for transmitting said first and second spread signals during a second time period.

15.   The highly bandwidth-efficient communications system of claim 13, further comprising:

means for receiving at the base station during an initialization period, a pilot spread signal comprising a known data signal spread over a plurality of discrete tones;

means for correlating the known data signal from the pilot spread signal with a reference known data signal and forming said first despreading code that is based on the characteristics of the received signals at the first plurality of antenna elements arranged in the spaced vertical direction, where a given element of the first despreading code corresponds to a given one of the first antenna elements and a given one of the discrete tones; and

said correlating means also correlating a known data signal from the pilot spread signal with a reference known data signal and forming said second despreading code that is based on the characteristics of the received signals at the second plurality of antenna elements arranged in the spaced horizontal direction, where a given element of the second despreading code corresponds to a given one of the second antenna elements and a given one of the discrete tones.

16. The highly bandwidth-efficient communications system of claim 14, wherein both the first and the second spread signals have a spectral form of a discrete multitone signal transmitted on multiple elements in the array.

17. The highly bandwidth-efficient communications system of claim 13, wherein the despreading is a multiplication of a complex number representation of the despreading codes times a complex number representation of the received spread signal.

18. The highly bandwidth-efficient communications system of claim 14, wherein the spreading is a multiplication of a complex number representation of the second spreading codes times a complex number representation of the data signal to be transmitted.

19. The highly bandwidth-efficient communications system of claim 13, wherein the despreading determines values of complex despreading codes which are then multiplied with a complex number representation of the received signals, resulting in an estimate of the first data signal.

20. The highly bandwidth-efficient communications system of claim 13, wherein the despreading adaptively positions the spatial direction of receive sensitivity towards a desired signal source and diminishes receive sensitivity from interfering sources.

21. The highly bandwidth-efficient communications system of claim 14, wherein the spreading adaptively positions transmitted signal energy of the spread signals towards a source of the received spread signal and adaptively diminishes transmitted signal energy towards interferers.

22. The highly bandwidth-efficient communications system of claim 14, wherein the first period and the second period are parts of a time division duplex period.

23. The highly bandwidth-efficient communications system of claim 13, wherein the antenna array has a planar symmetry.

24. The highly bandwidth-efficient communications system of claim 13, wherein the antenna array has a cylindrical symmetry.

FIG. 1A

FIG. 1B

FIG. 1C

FIG. 1D

BASE STATION Z

MEMORY

SIGNAL PROCESSOR

HIGH ELEVATION REMOTE UNIT X

LOW ELEVATION REMOTE UNIT Y

FIG. 2

BASE STATION Z

T1 T2 T3 T4

A 1
A 2
A 3
A 4
B 1
B 2
B 3
B 4
C 1
C 2
C 3
C 4
D 1
D 2
D 3
D 4
A T O N E N T

MEMORY

TRANS

TRANS

TRANS

TRANS

SIGNAL PROCESSOR

VERT.

HORIZ.

A

B

C

D

FIG. 3A

FIG. 3B

FIG. 3C

FIG. 3D

SUBSCRIBER #4 TONE SET

SUBSCRIBER #3 TONE SET

SUBSCRIBER #2 TONE SET

SUBSCRIBER #1 TONE SET

TONE FREQUENCIES
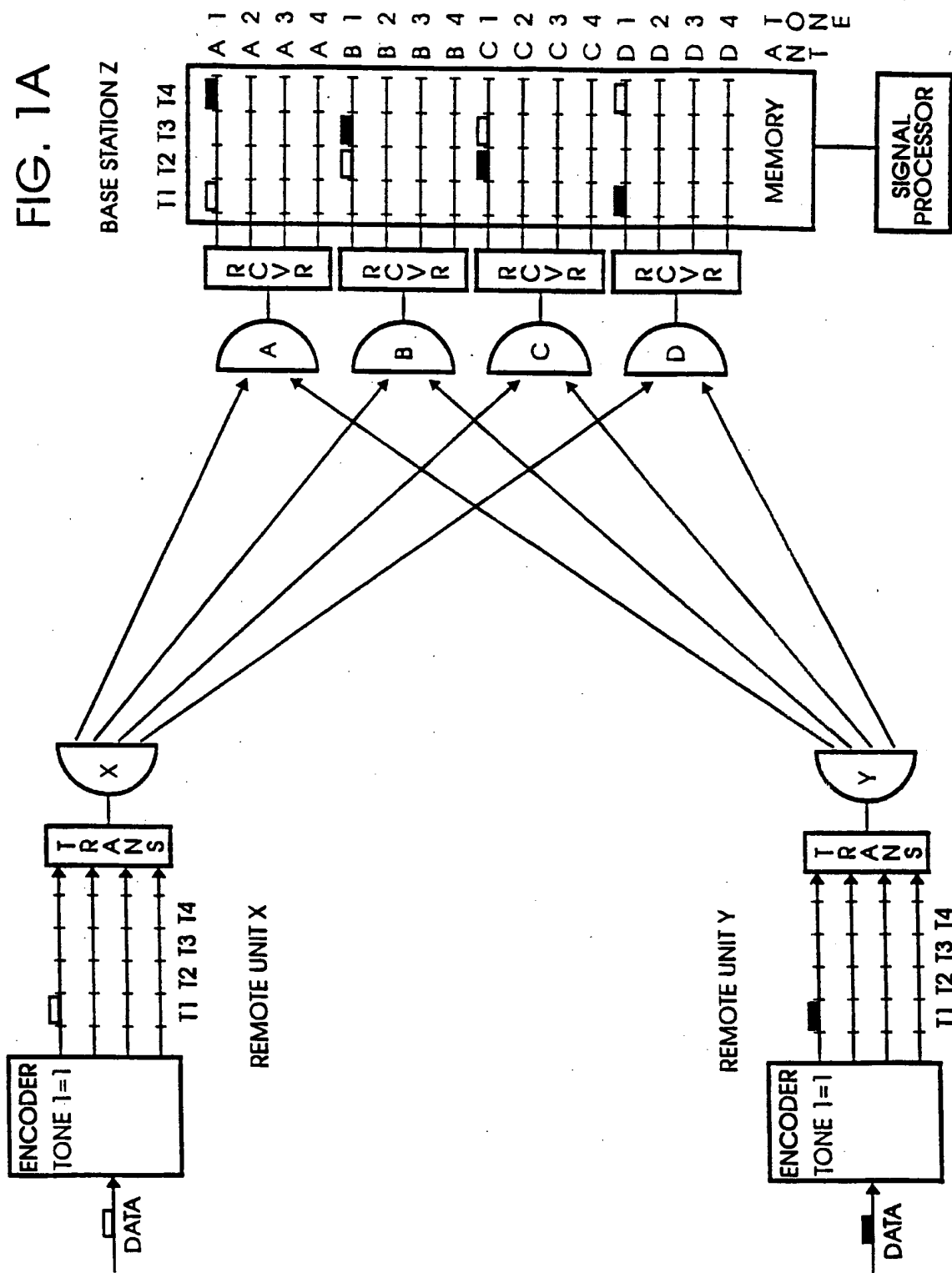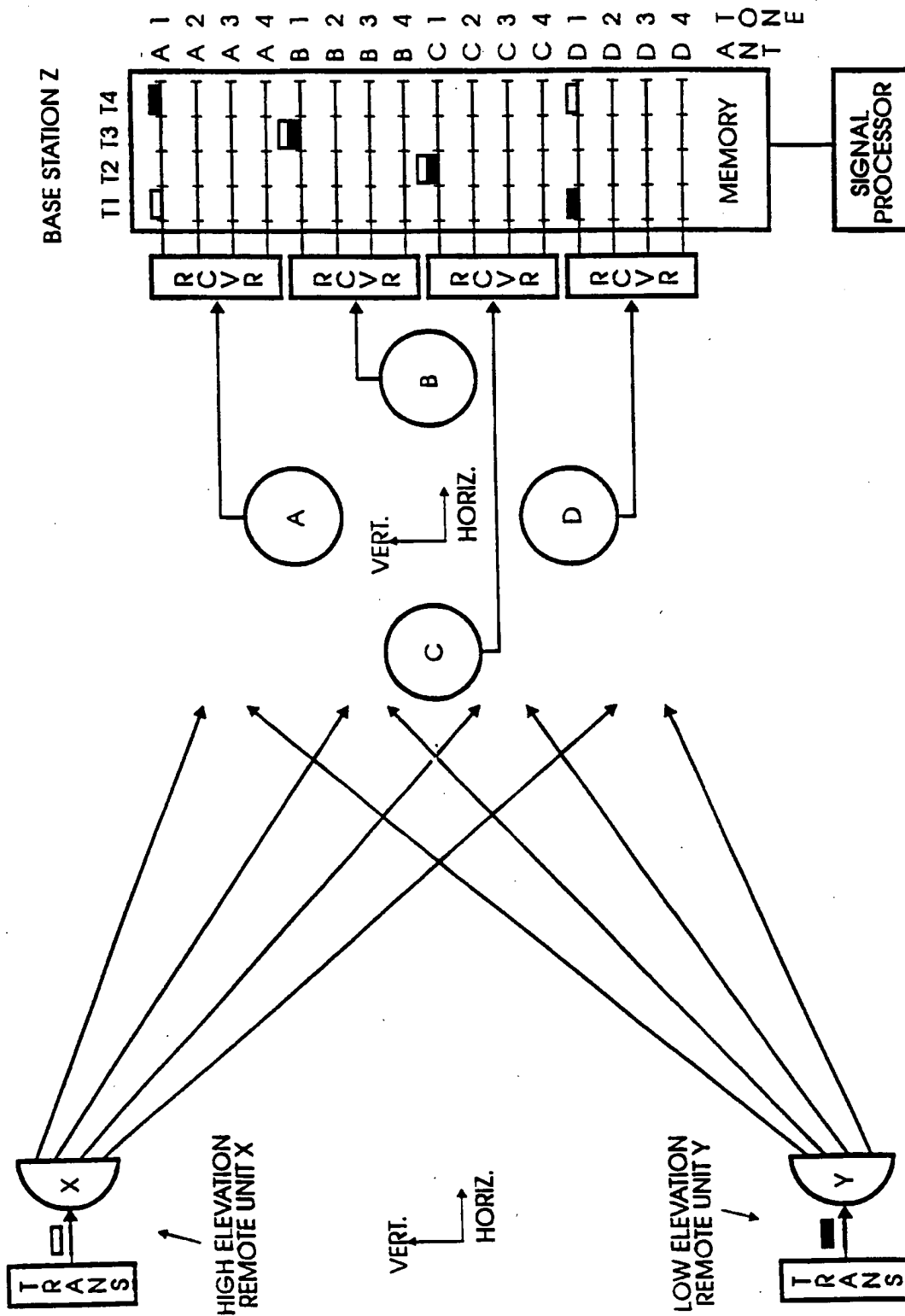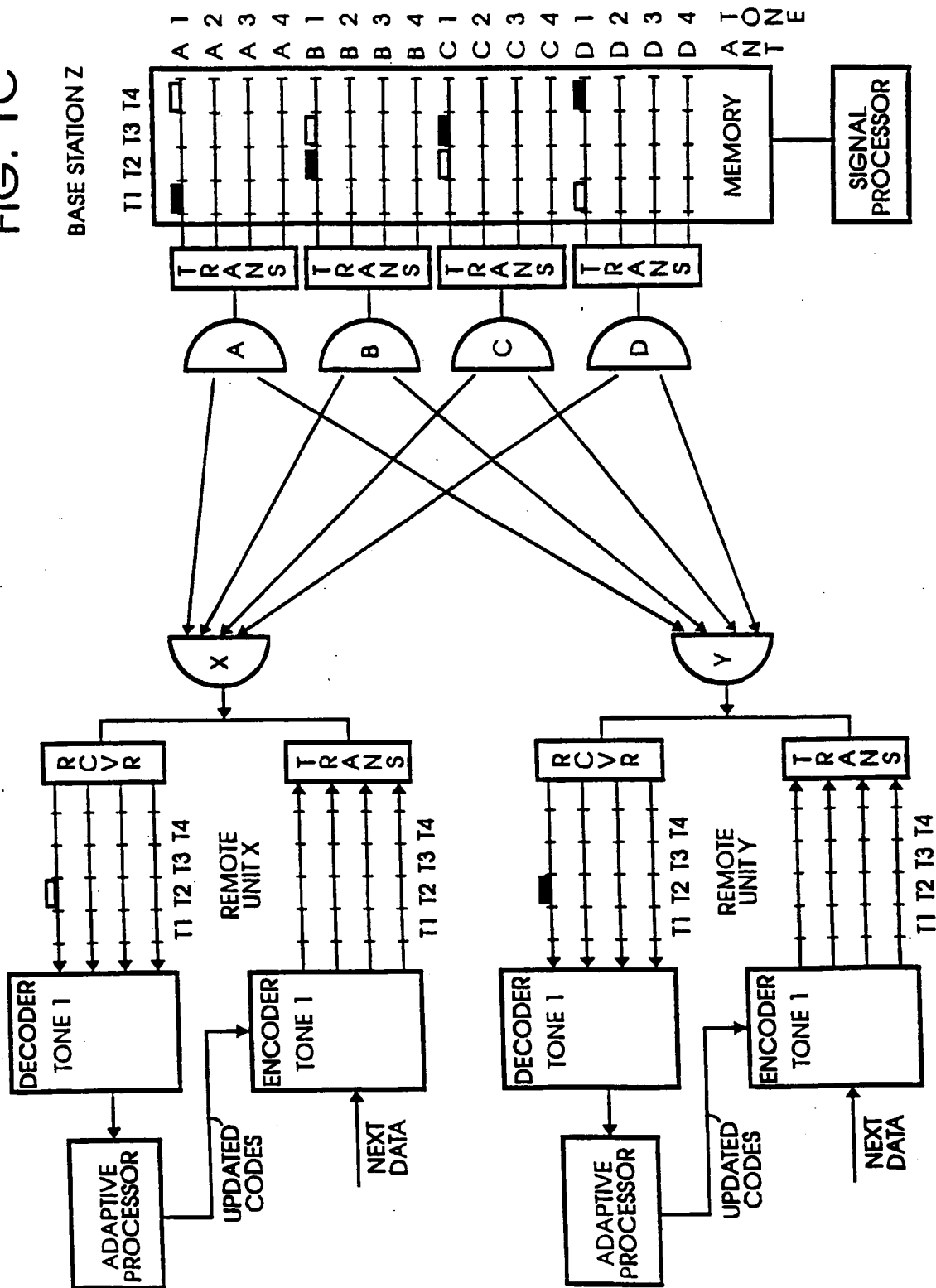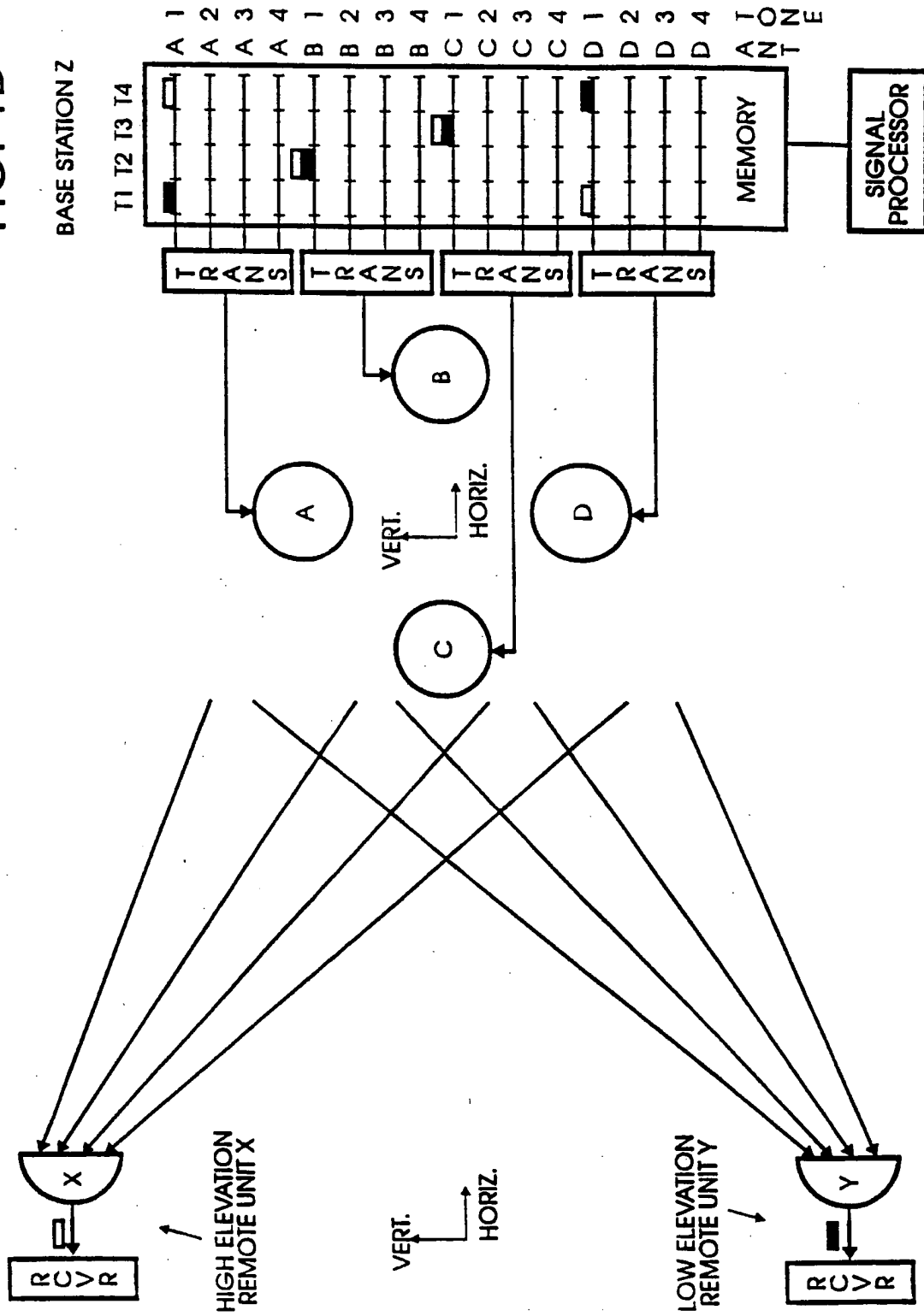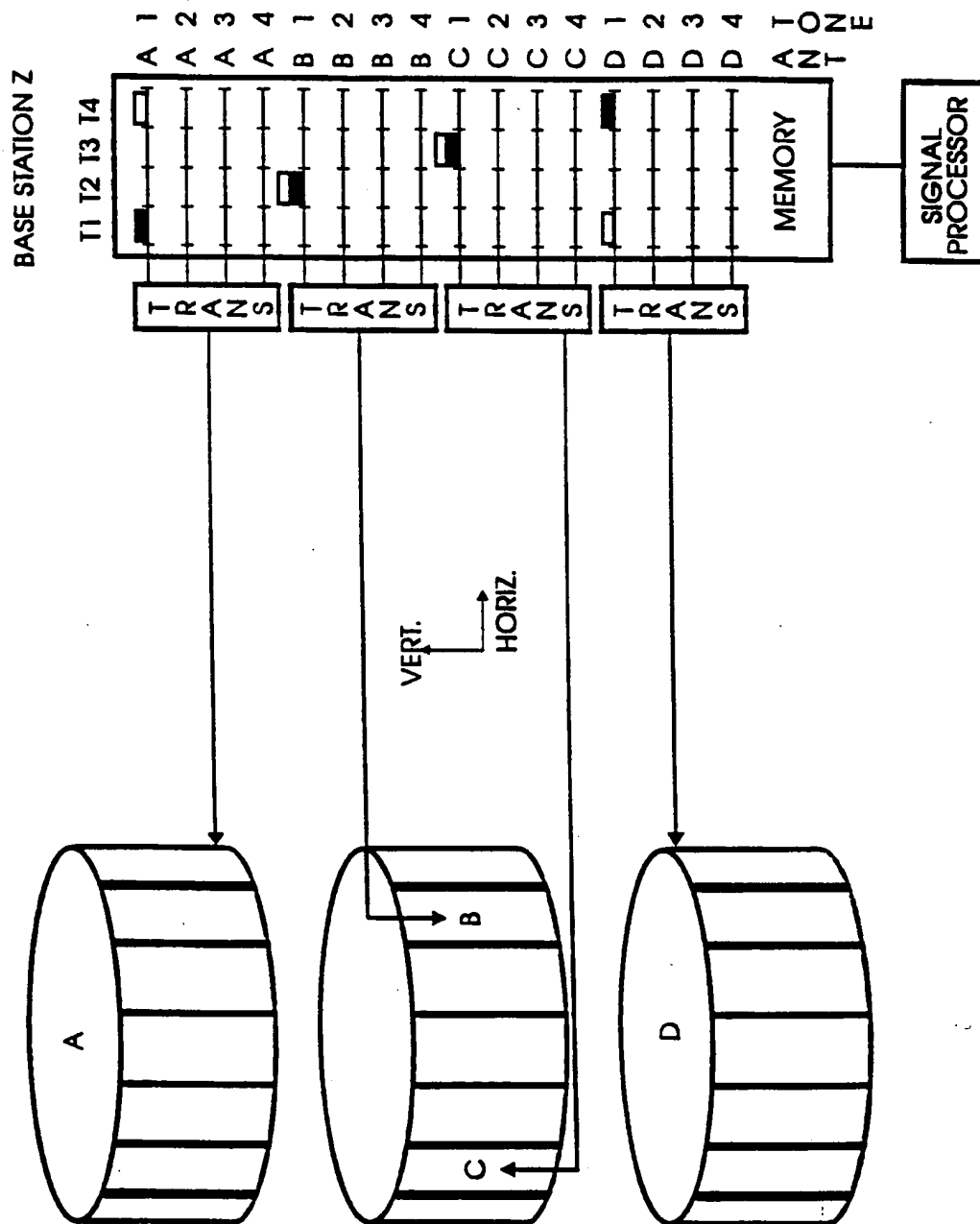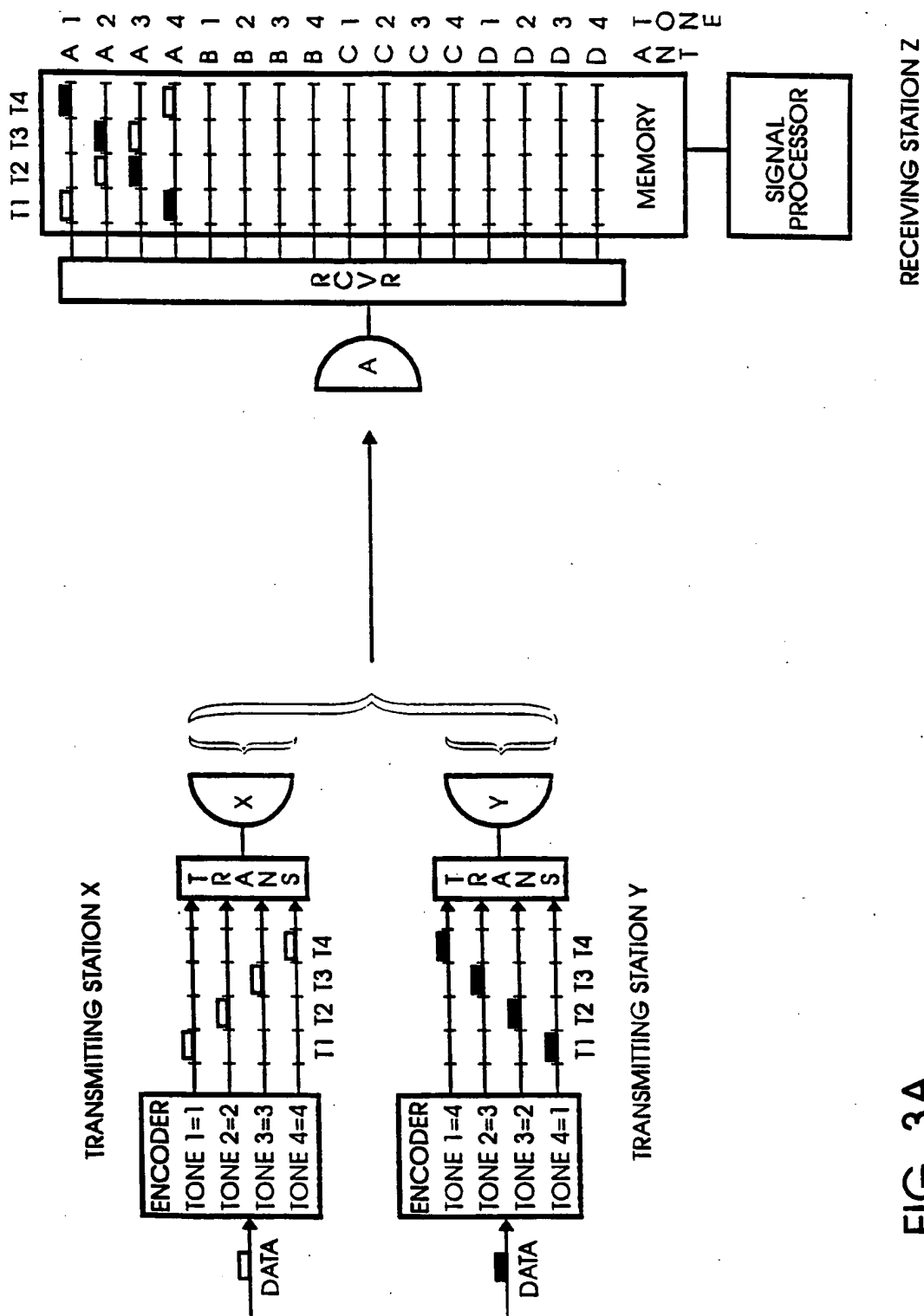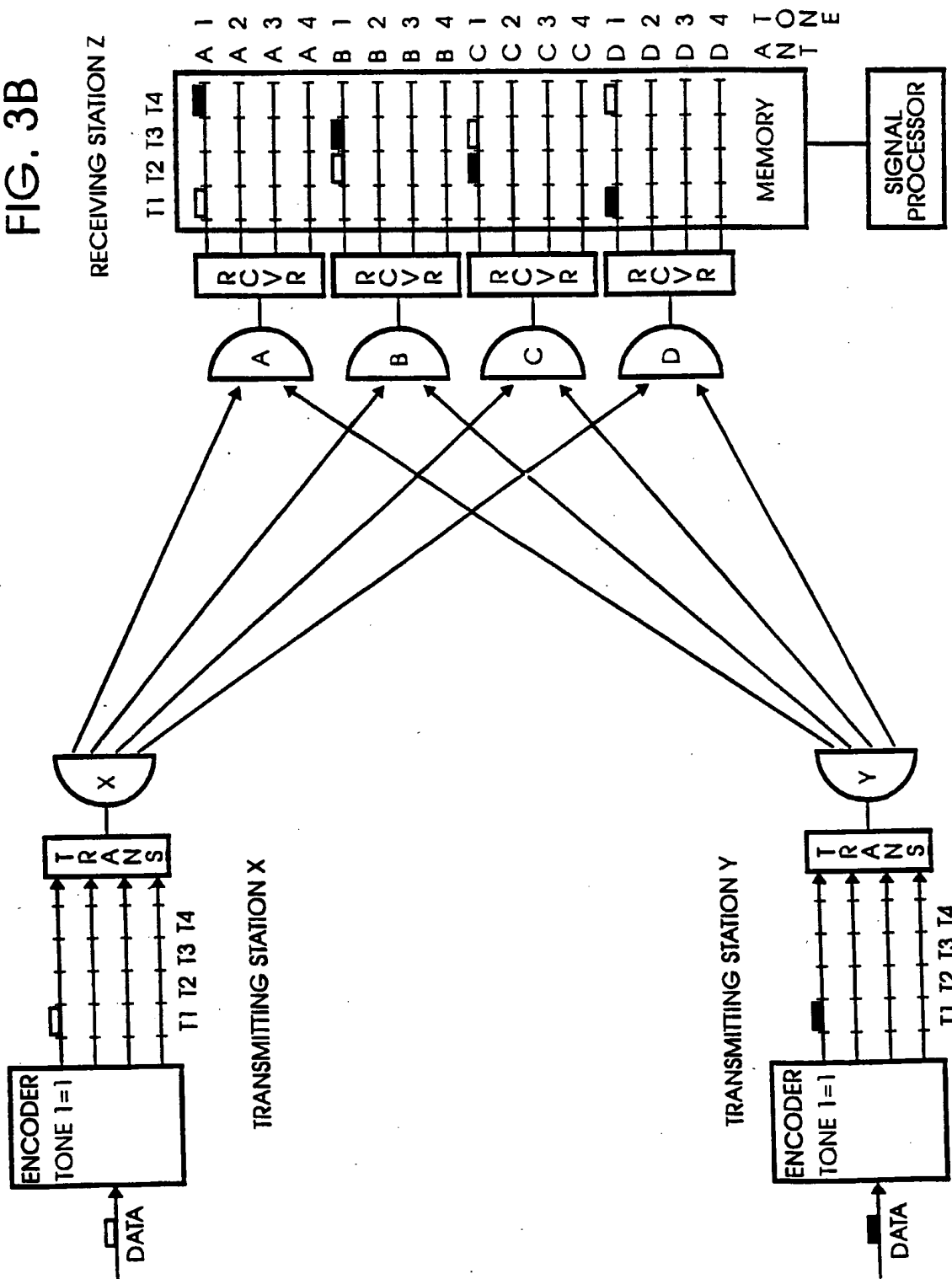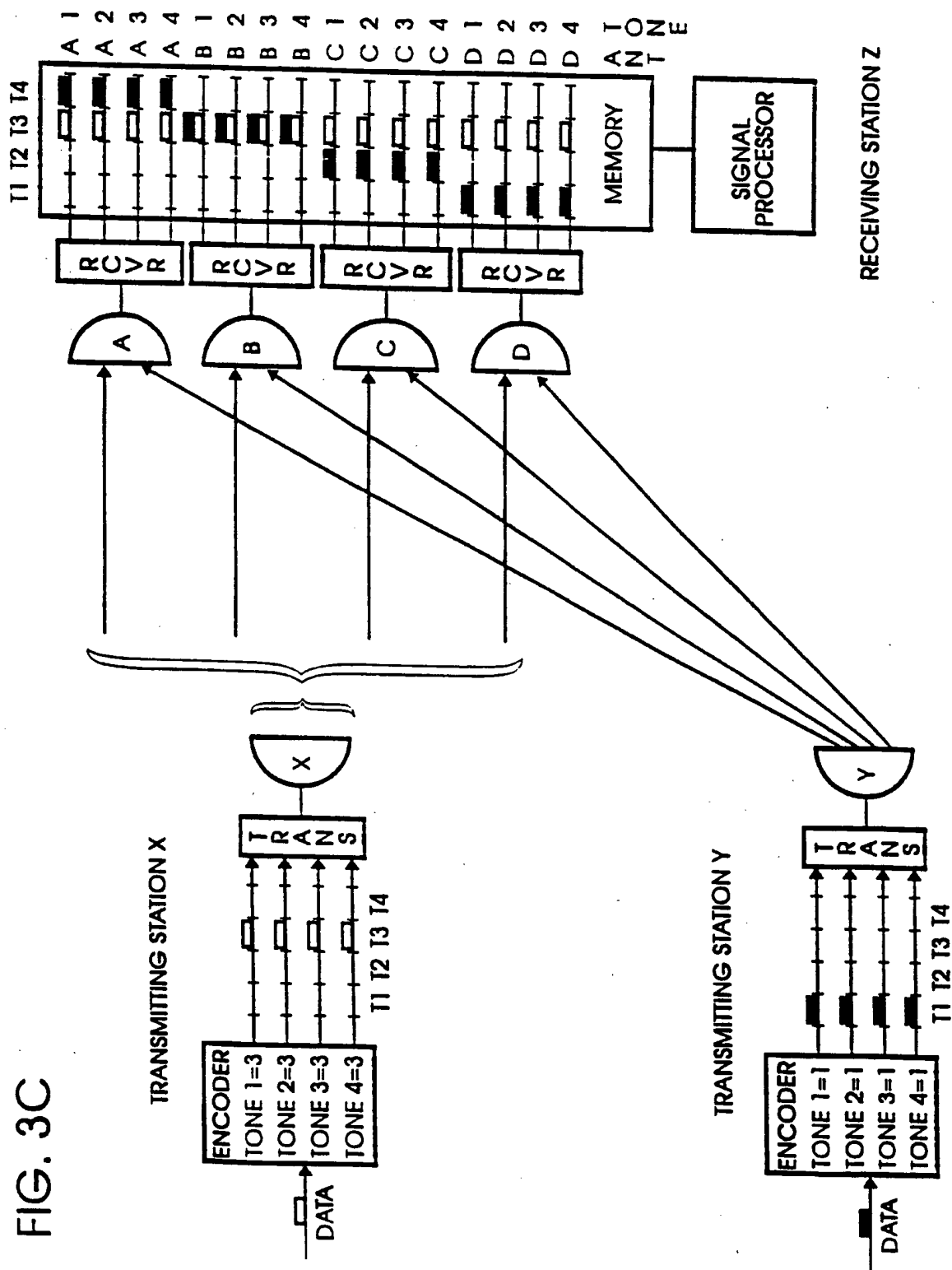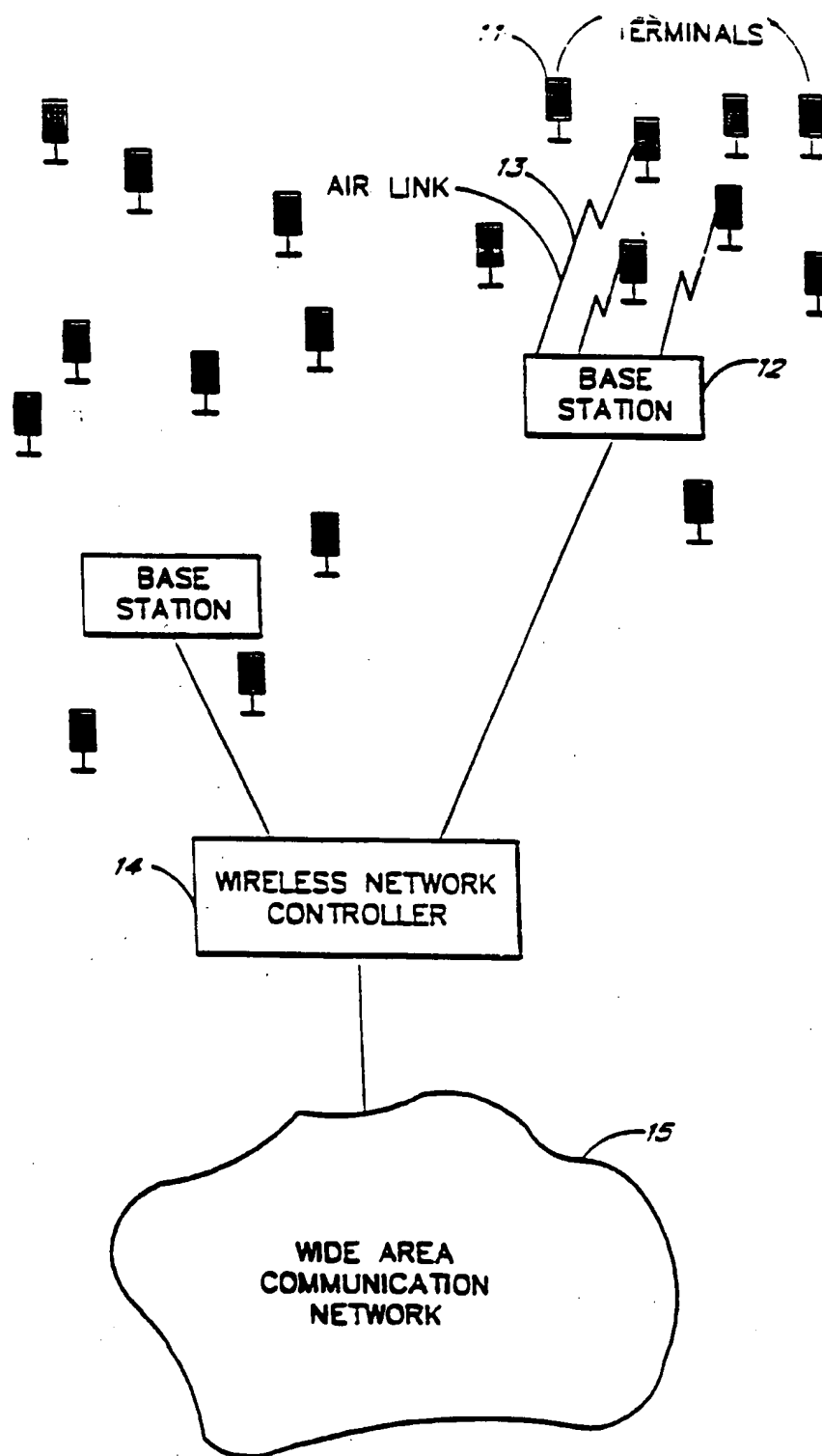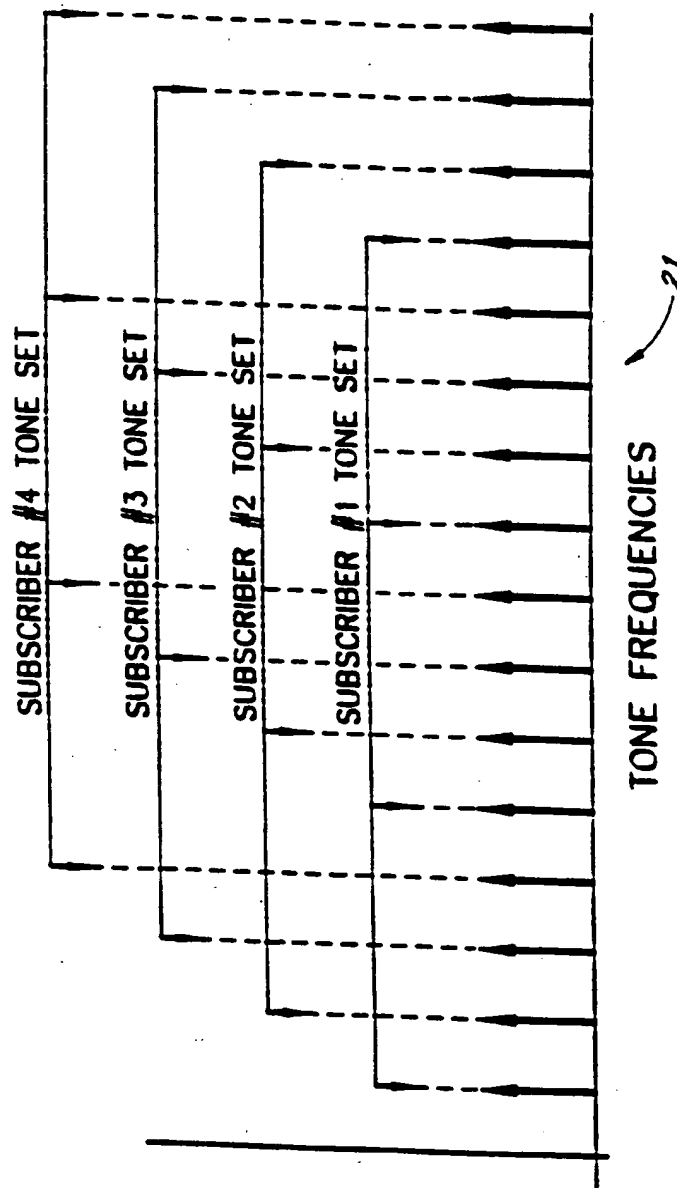
FIG. 3E
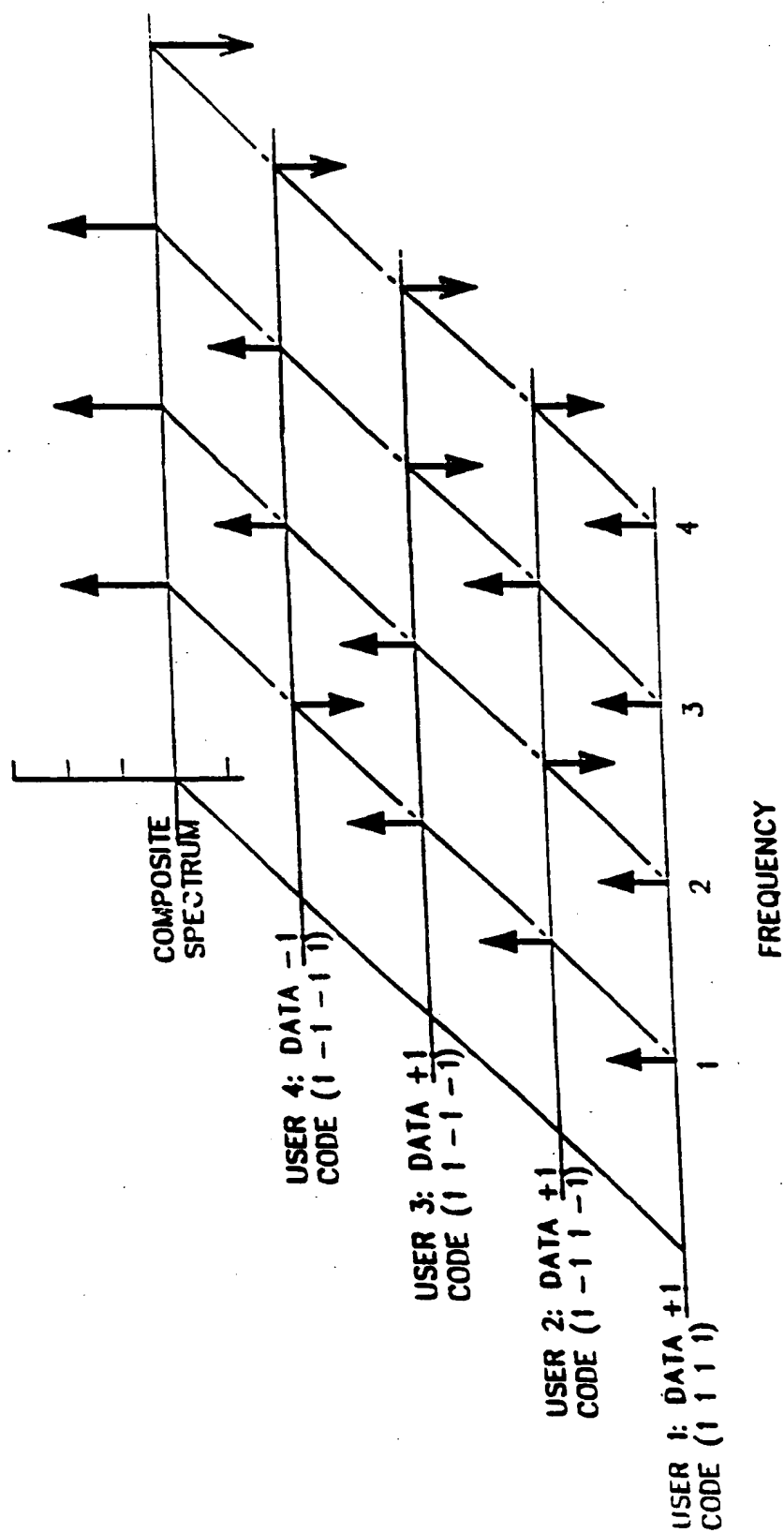
FIG. 3F
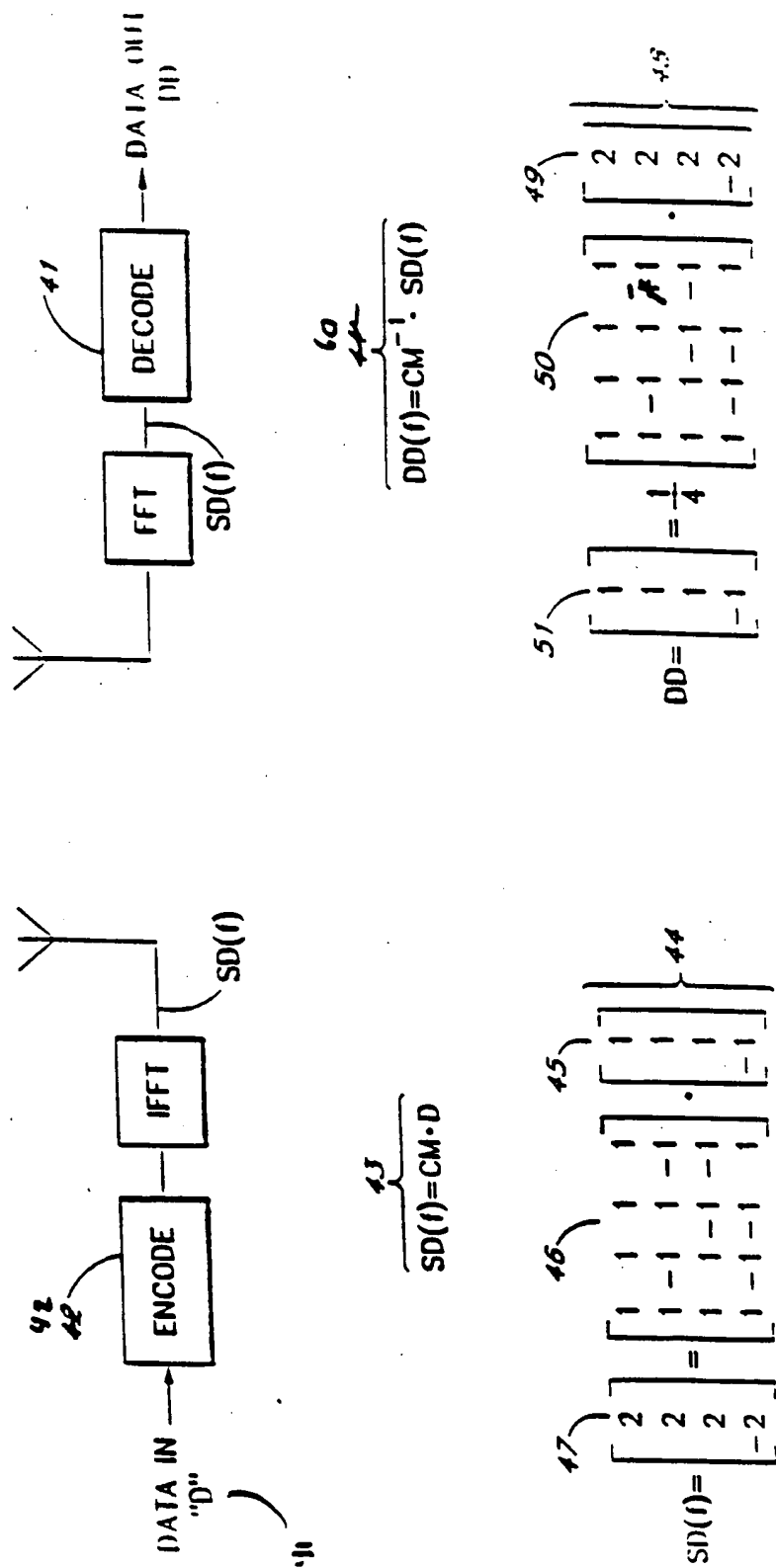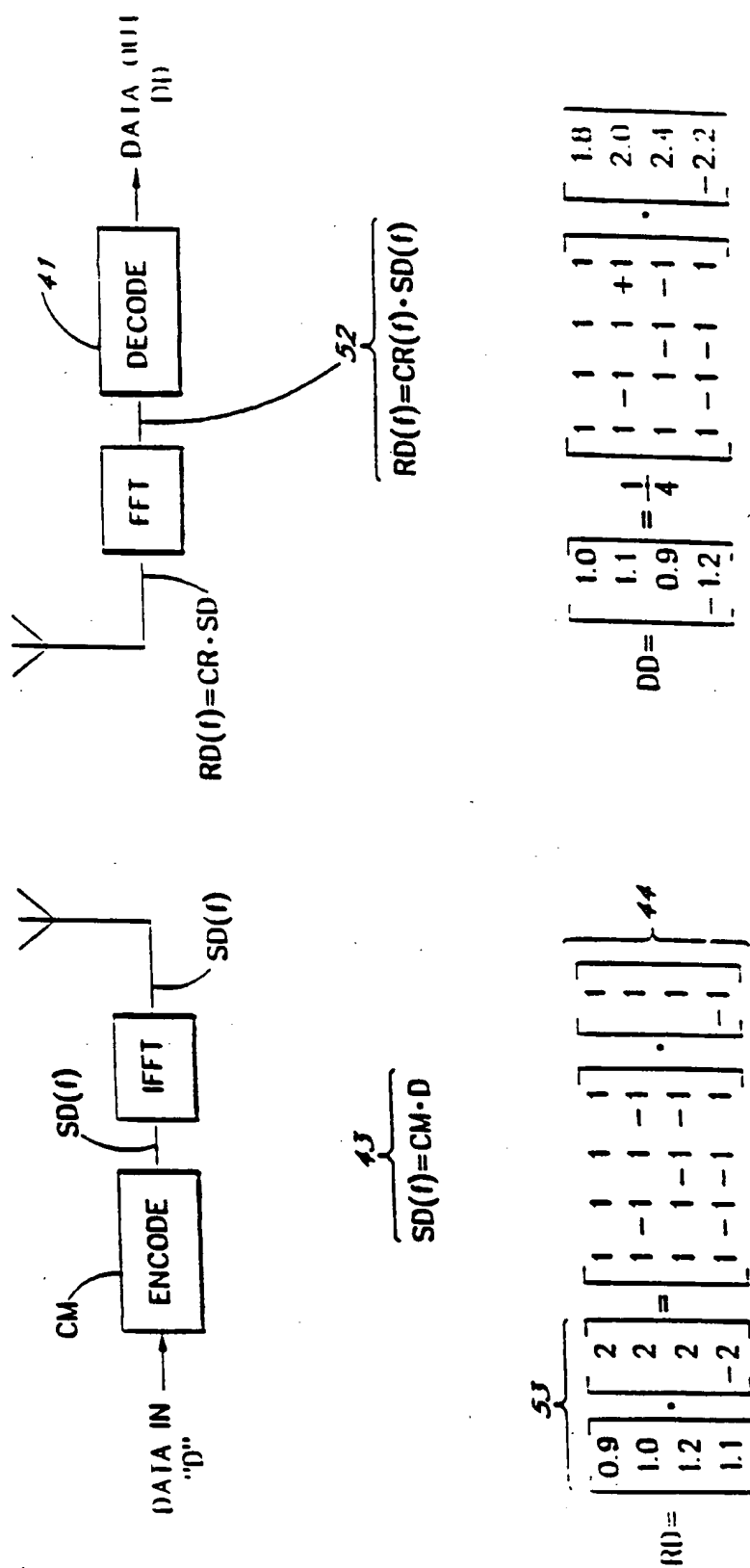
FIGURE 4

FIGURE 5
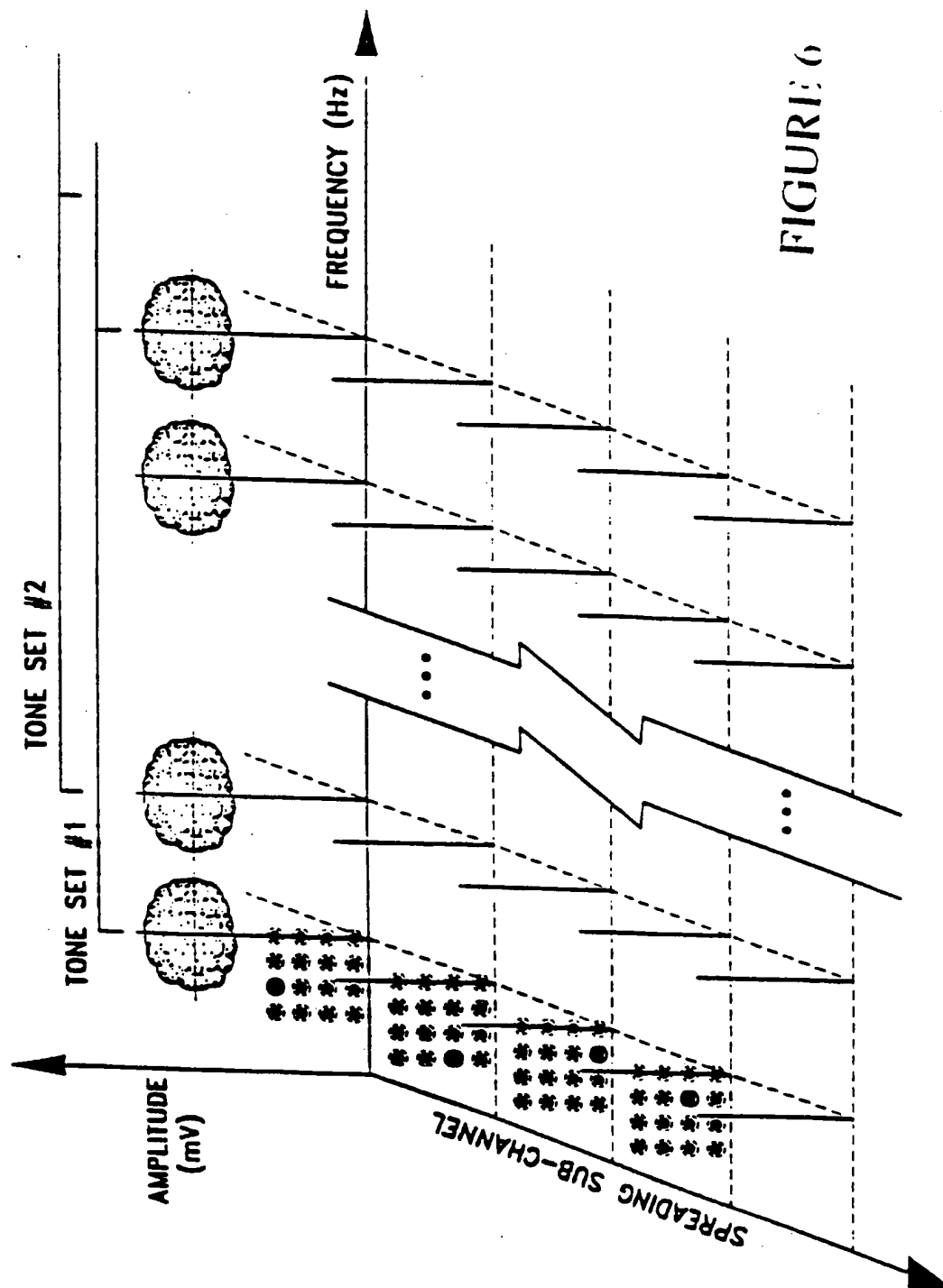
FIGURE 6
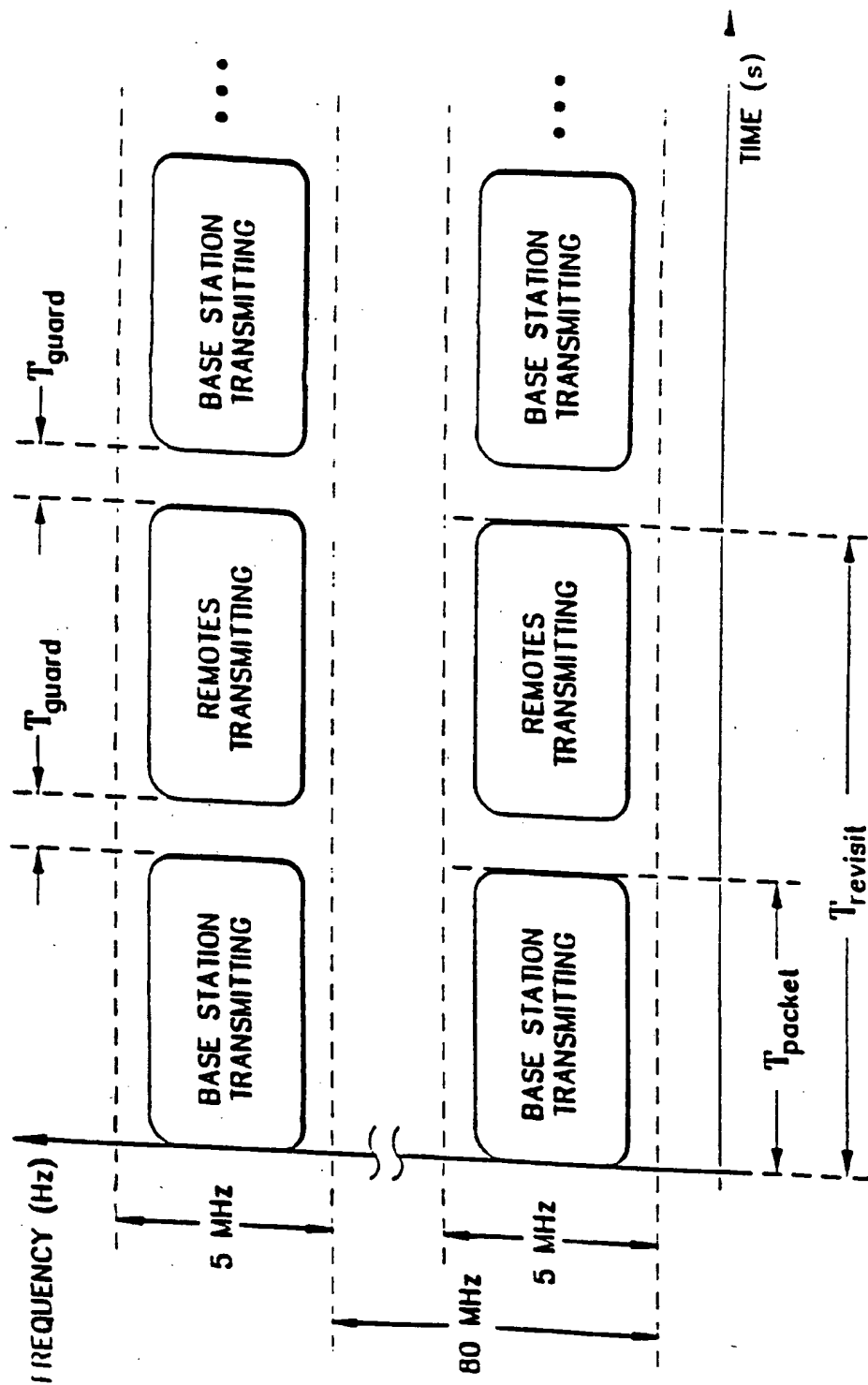
FIGURE 7
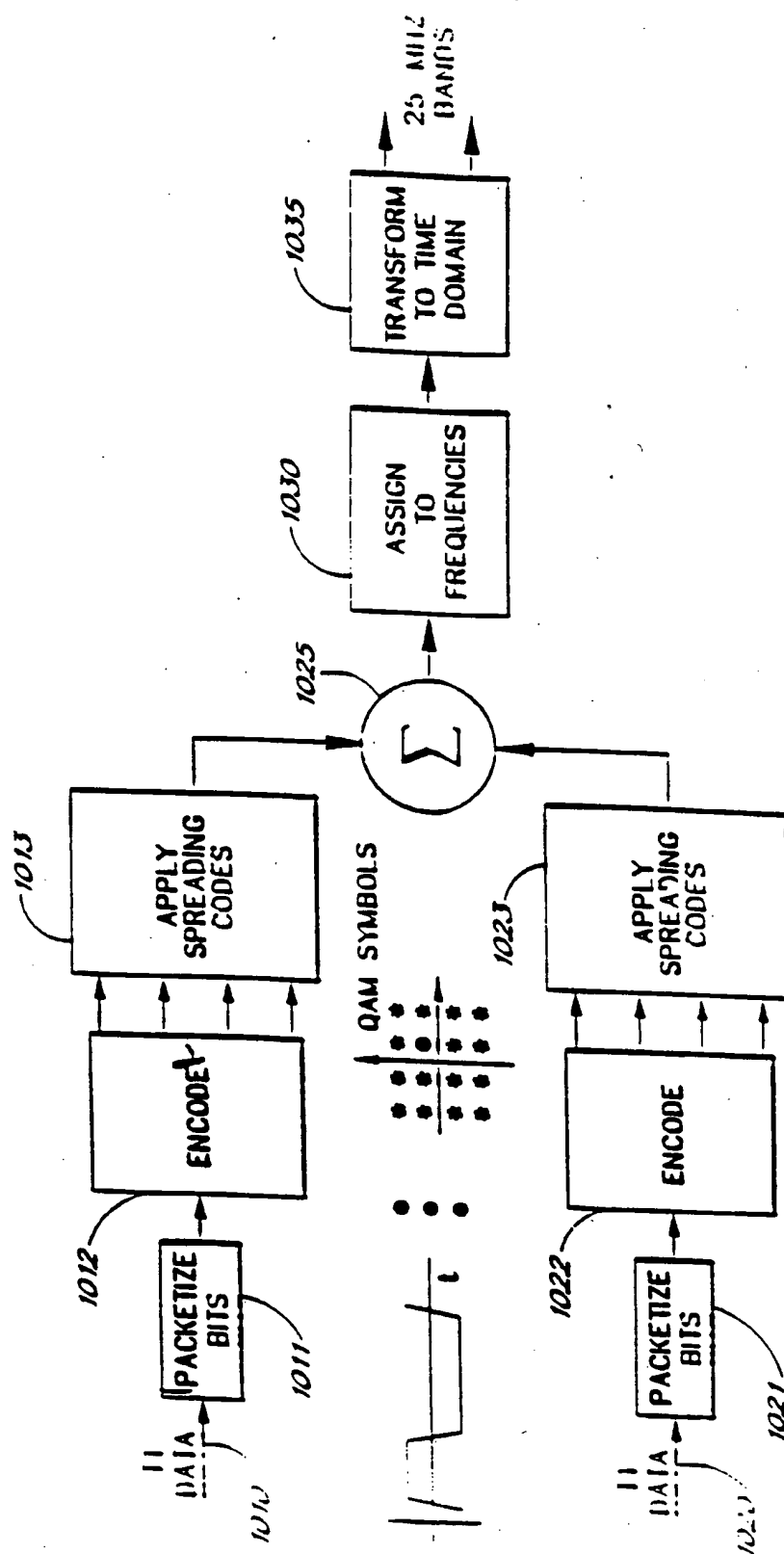
FIGURE 8

FIGURE 9

FIGURE 10

120b

520

525

515

530

FIGURE 12

540

507

120a

515

510

525
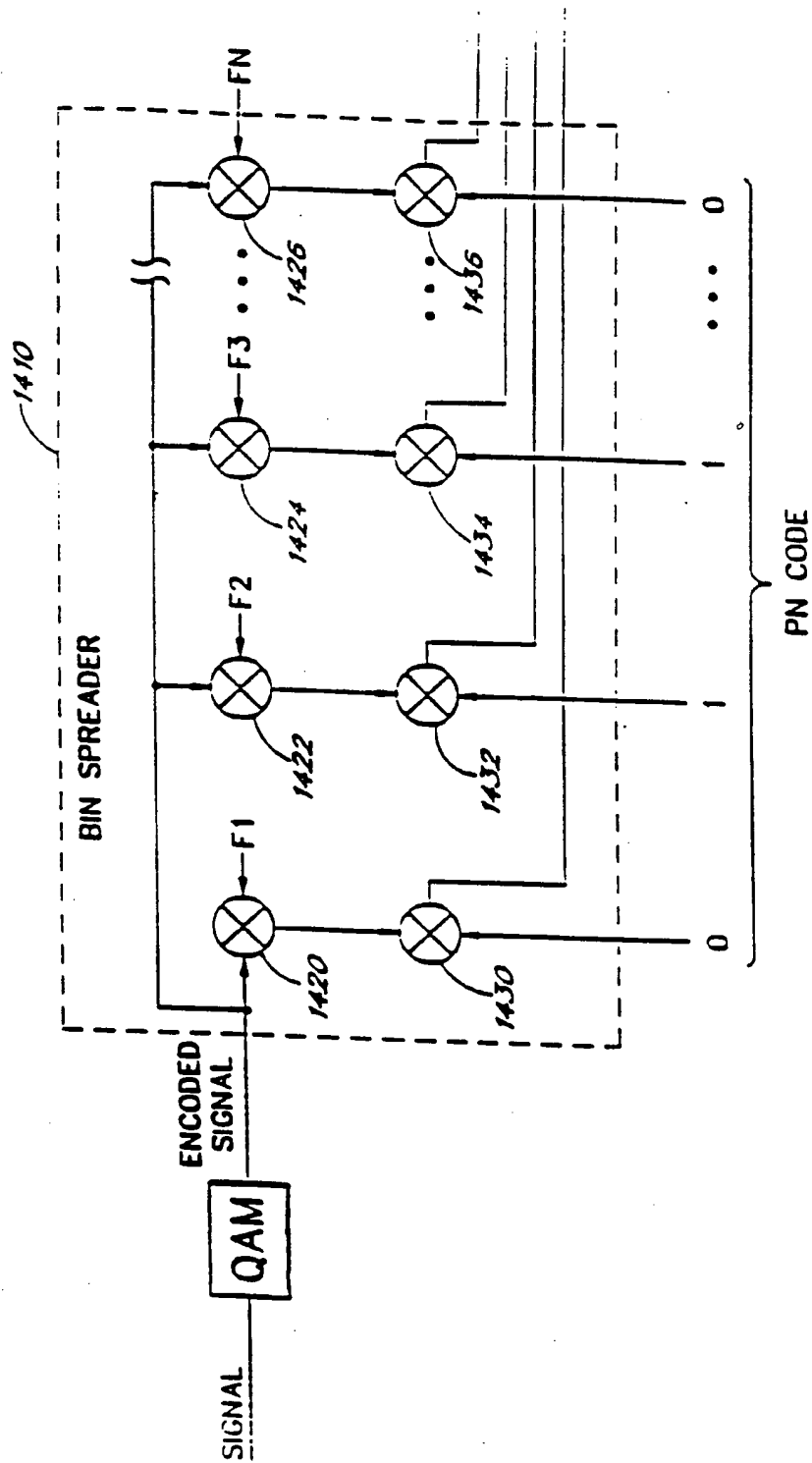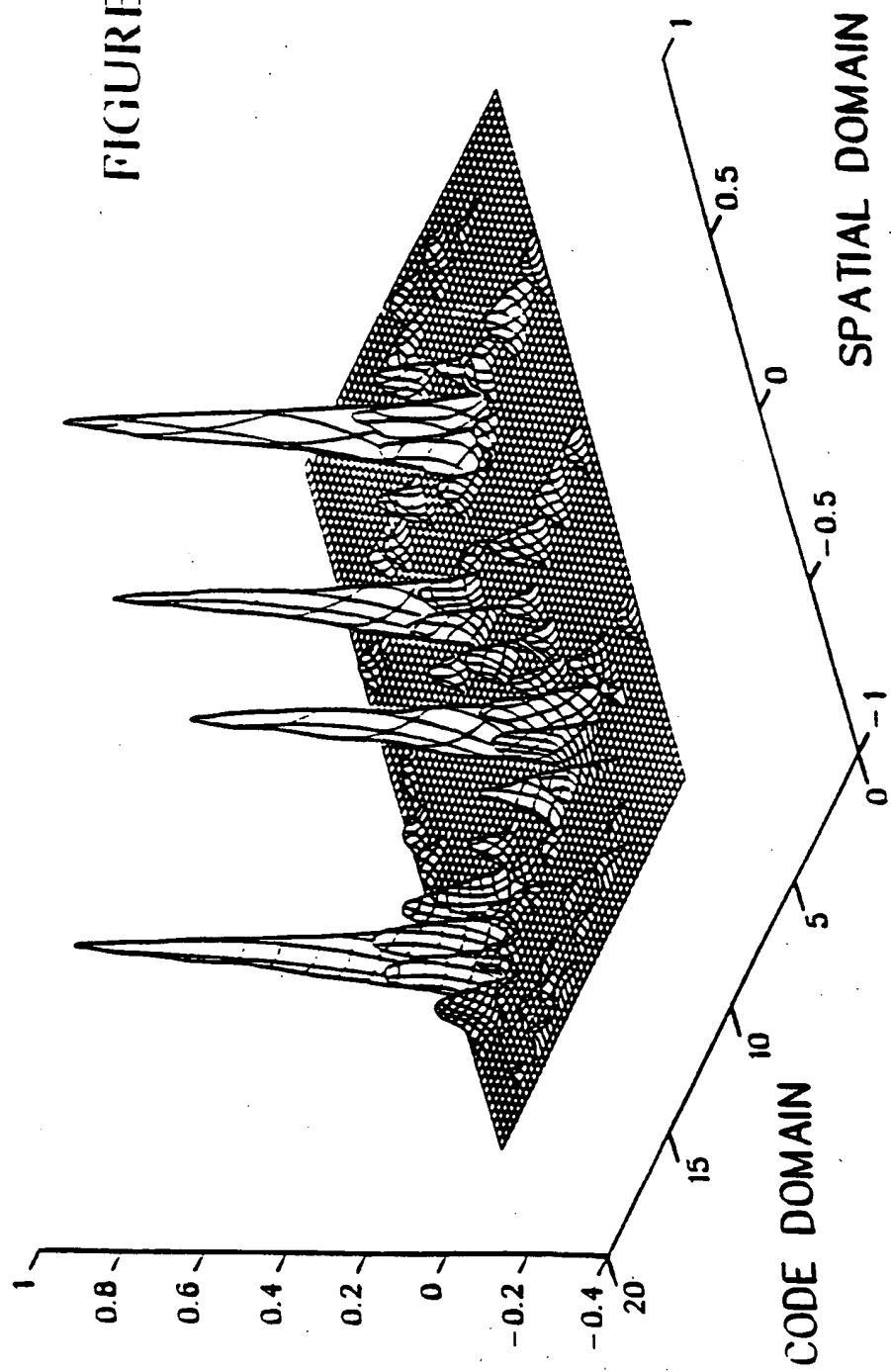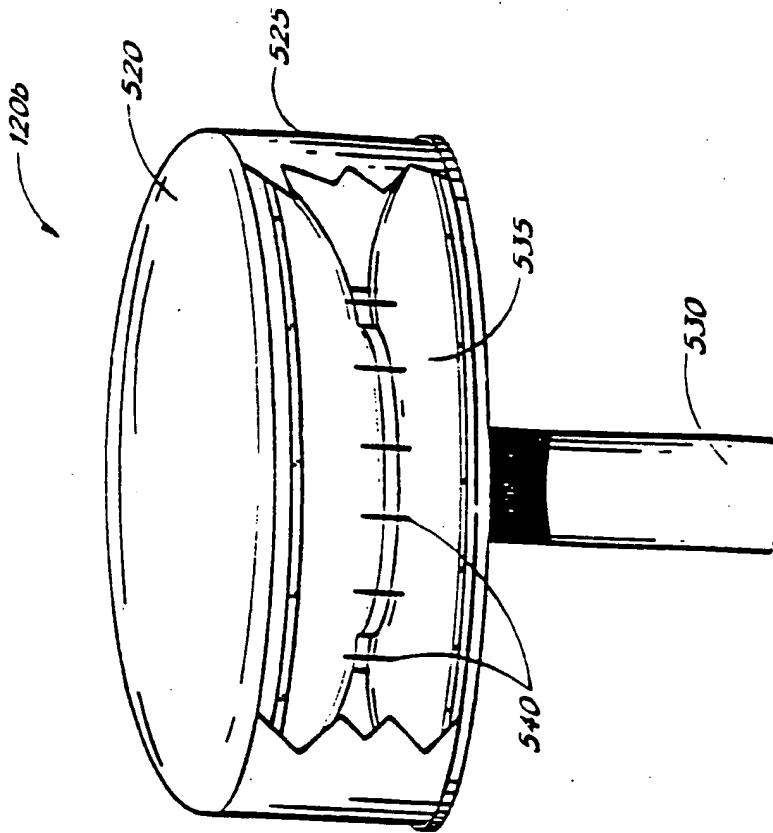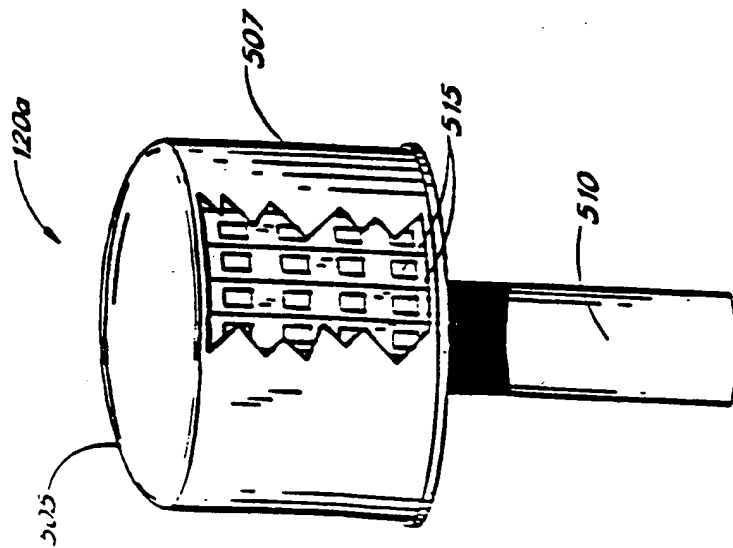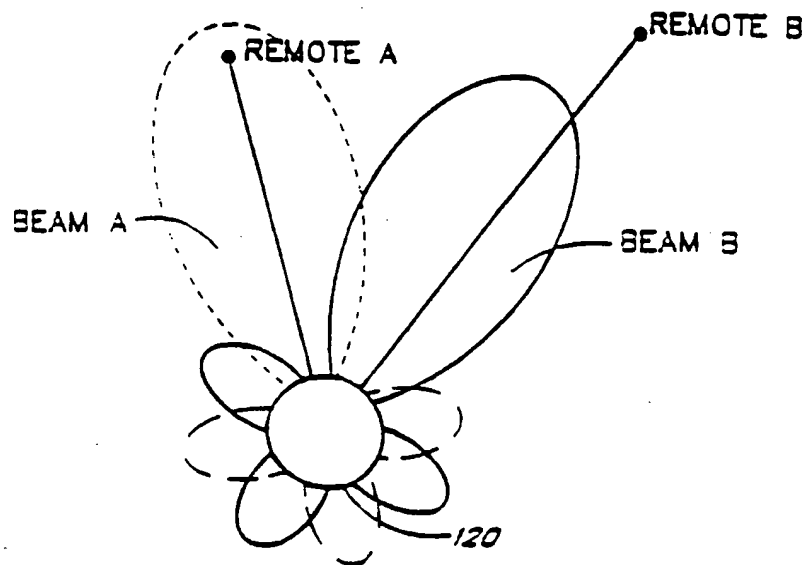
FIGURE 11

FIGURE 13

FIGURE 14

Inverse Frequency-Channelized
Spreader Implementation
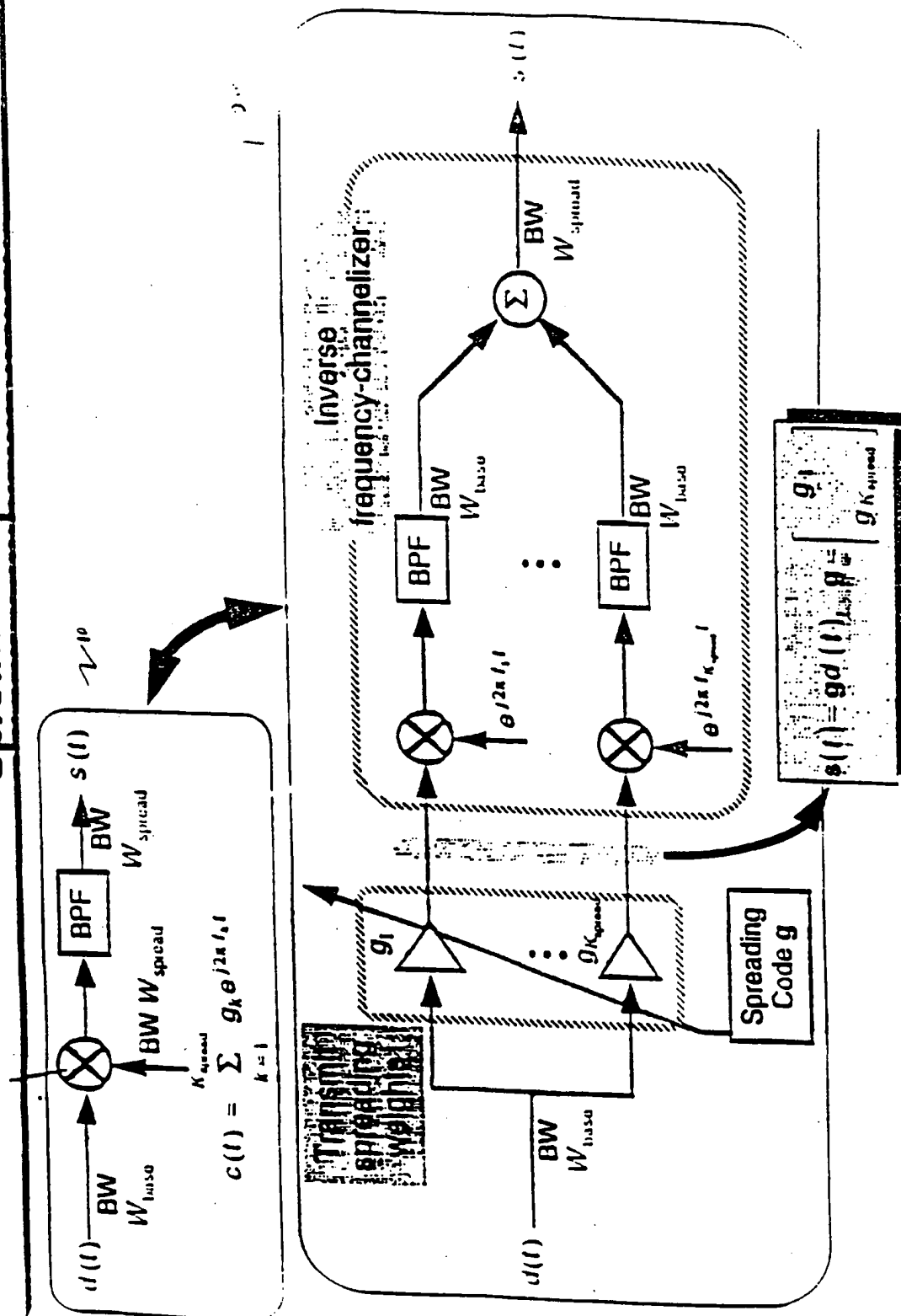
FIGURE 15

Frequency-Channelized
Despreader Implementation

FIGURE 16

TELEPHONE NETWORK

160

SWITCHING INTERFACE

BANDWDTH CONTROLLER

REMOTE SUBSCRIBER

165

120

BASE

110

REMOTE SUBSCRIBER

165
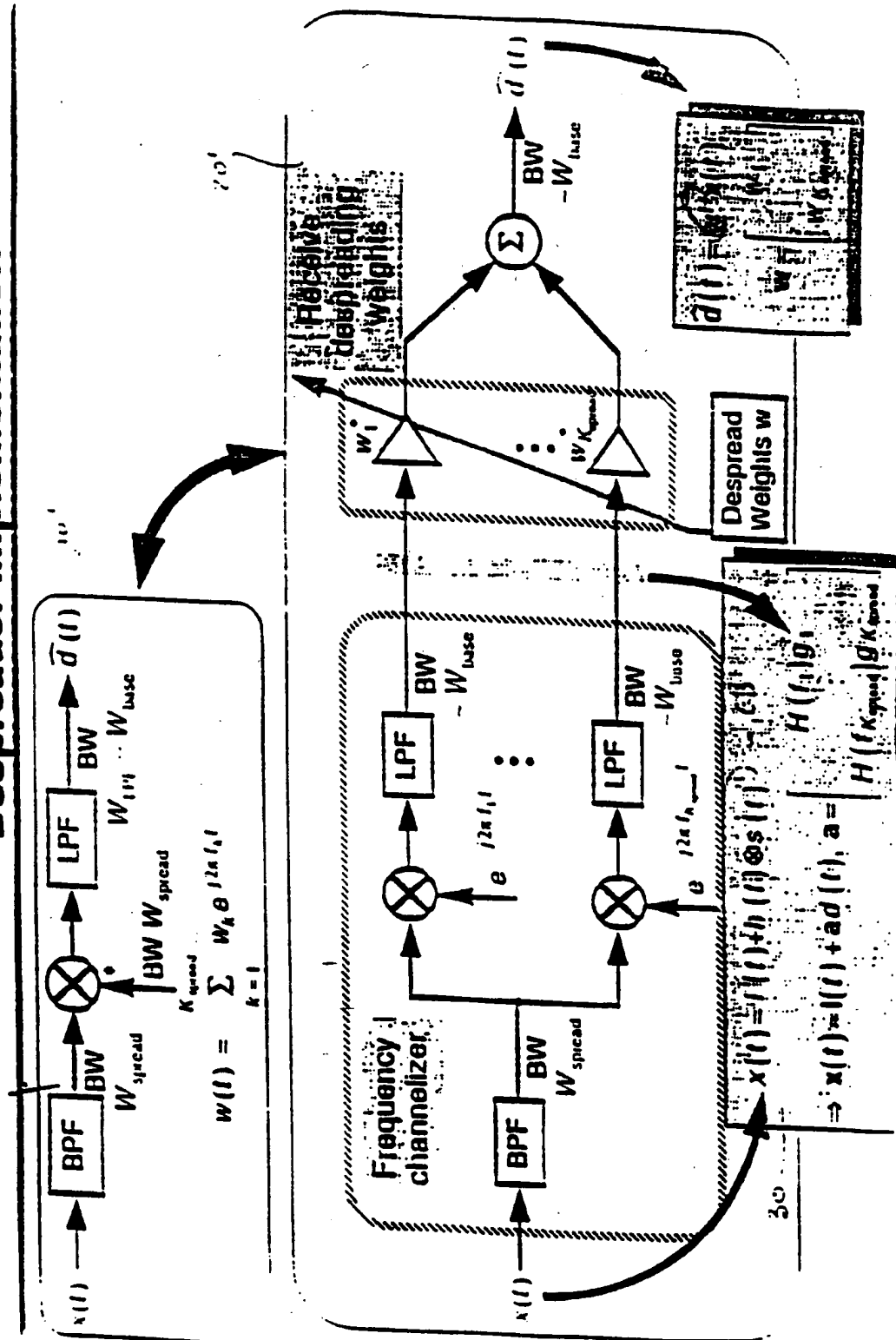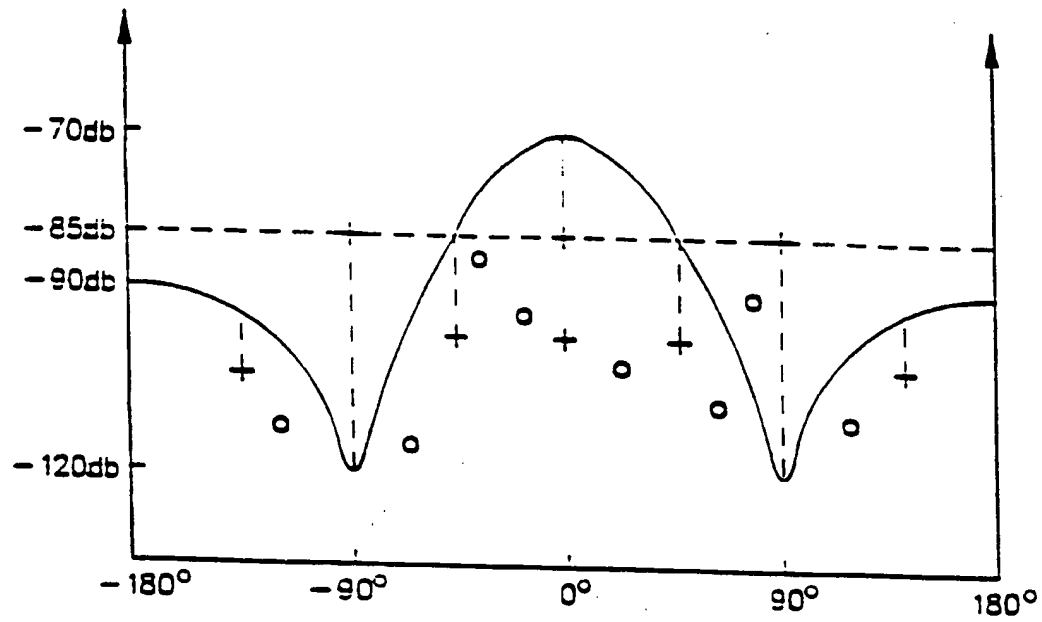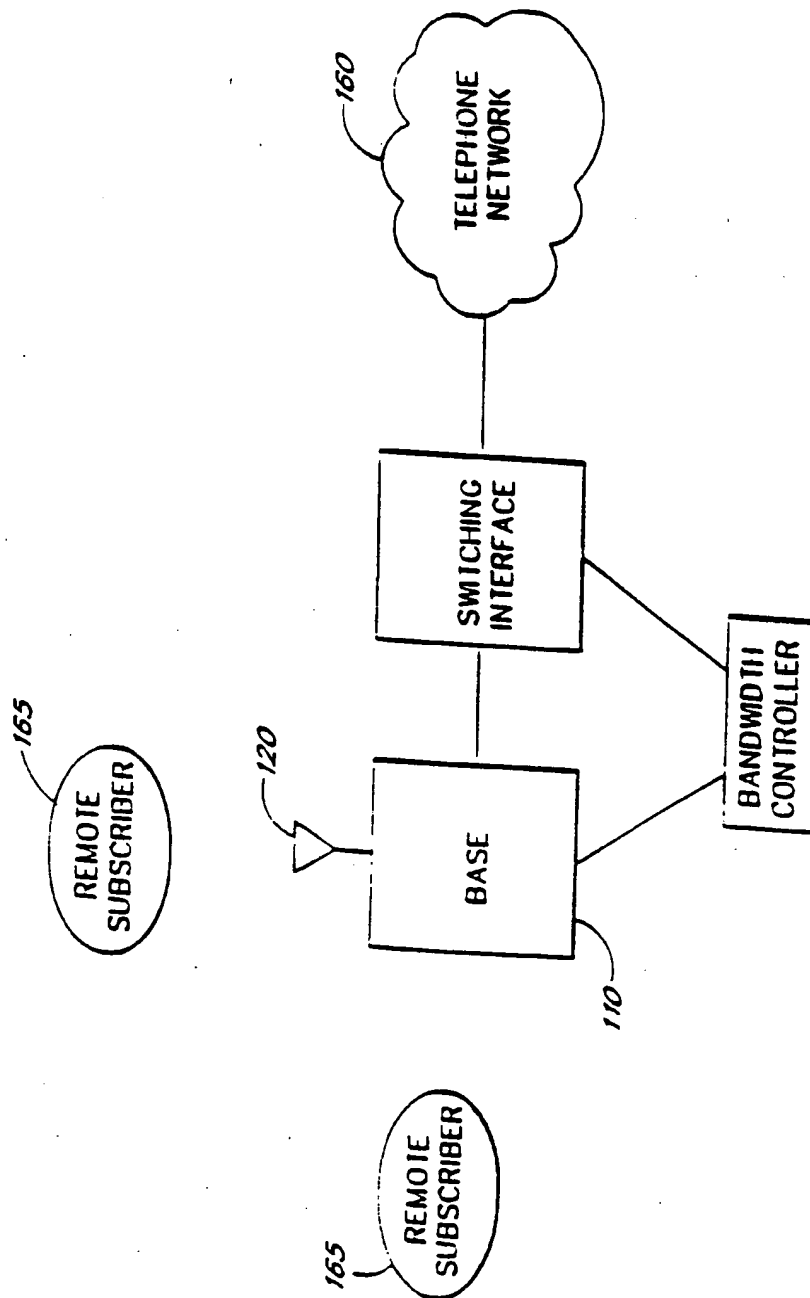
FIGURE 17

FIG. 18   Possible Operational Frequency Bands for PWAN

Base frequency	Lower RF band	Upper RF band
1850 MHz	1850-1855 MHz	1930-1935 MHz
1855 MHz	1855-1860 MHz	1935-1940 MHz
1860 MHz	1860-1865 MHz	1940-1945 MHz
1865 MHz	1865-1870 MHz	1945-1950 MHz
1870 MHz	1870-1875 MHz	1950-1955 MHz
1875 MHz	1875-1880 MHz	1955-1960 MHz
1880 MHz	1880-1885 MHz	1960-1965 MHz
1885 MHz	1885-1890 MHz	1965-1970 MHz
1890 MHz	1890-1895 MHz	1970-1975 MHz
1895 MHz	1895-1900 MHz	1975-1980 MHz
1900 MHz	1900-1905 MHz	1980-1985 MHz
1905 MHz	1905-1910 MHz	1985-1990 MHz

FIG. 19   *PWAN Airlink RF Band/Subband Organization*
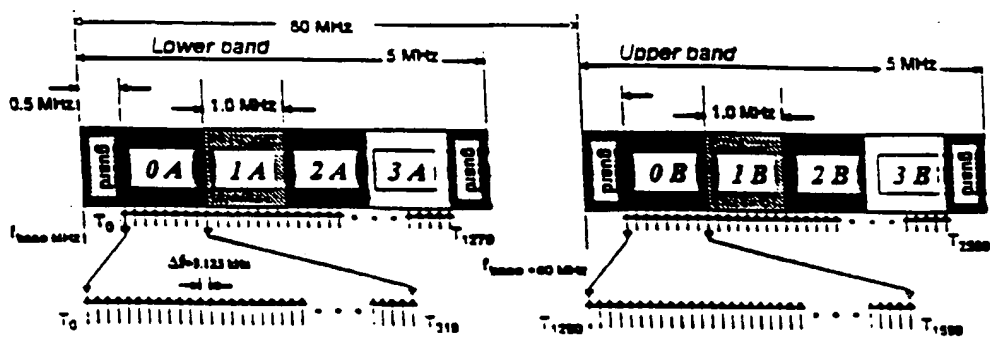
FIG. 20

Tones Within Each Subband

Subband pair designation		Tones
Subband pair 0	0 A	$(T_0, T_1, \ldots, T_{319})$
	0 B	$(T_{1280}, T_{1281}, \ldots, T_{1599})$
Subband pair 1	1 A	$(T_{320}, T_{321}, \ldots, T_{439})$
	1 B	$(T_{1600}, T_{1601}, \ldots, T_{1919})$
Subband pair 2	2 A	$(T_{640}, T_{641}, \ldots, T_{959})$
	2 B	$(T_{1920}, T_{1921}, \ldots, T_{2239})$
Subband pair 3	3 A	$(T_{960}, T_{961}, \ldots, T_{1279})$
	3 B	$(T_{2240}, T_{2241}, \ldots, T_{2559})$

FIG. 21 Traffic Partitions

		Traffic tones		

Traffic tones = 32 Traffic partitions

0	1	2	· · ·	30	31

1 Traffic partition = 72 Tones

0	1	2	3	· · ·	71	72
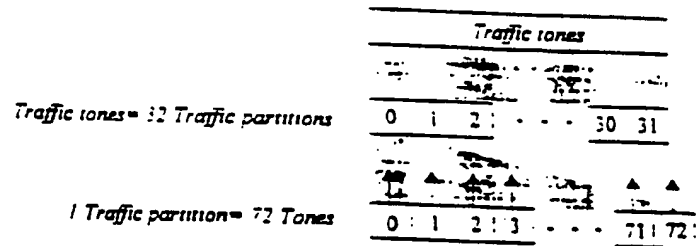
FIG. 22   Tone Mapping to the ith Traffic Partition

Tone index	Tone	Tone index	Tone	Tone index	Tone	Tone index	Tone
$P_i(0)$	T_{20i+1}	$P_i(18)$	$T_{20i+161}$	$P_i(36)$	$T_{20i+1281}$	$P_i(54)$	$T_{20i+1441}$
$P_i(1)$	T_{20i+2}	$P_i(19)$	$T_{20i+162}$	$P_i(37)$	$T_{20i+1282}$	$P_i(55)$	$T_{20i+1442}$
$P_i(2)$	T_{20i+3}	$P_i(20)$	$T_{20i+163}$	$P_i(38)$	$T_{20i+1283}$	$P_i(56)$	$T_{20i+1443}$
$P_i(3)$	T_{20i+4}	$P_i(21)$	$T_{20i+164}$	$P_i(39)$	$T_{20i+1284}$	$P_i(57)$	$T_{20i+1444}$
$P_i(4)$	T_{20i+5}	$P_i(22)$	$T_{20i+165}$	$P_i(40)$	$T_{20i+1285}$	$P_i(58)$	$T_{20i+1445}$
$P_i(5)$	T_{20i+6}	$P_i(23)$	$T_{20i+166}$	$P_i(41)$	$T_{20i+1286}$	$P_i(59)$	$T_{20i+1446}$
$P_i(6)$	T_{20i+7}	$P_i(24)$	$T_{20i+167}$	$P_i(42)$	$T_{20i+1287}$	$P_i(60)$	$T_{20i+1447}$
$P_i(7)$	T_{20i+8}	$P_i(25)$	$T_{20i+168}$	$P_i(43)$	$T_{20i+1288}$	$P_i(61)$	$T_{20i+1448}$
$P_i(8)$	T_{20i+9}	$P_i(26)$	$T_{20i+169}$	$P_i(44)$	$T_{20i+1289}$	$P_i(62)$	$T_{20i+1449}$
$P_i(9)$	T_{20i+11}	$P_i(27)$	$T_{20i+171}$	$P_i(45)$	$T_{20i+1291}$	$P_i(63)$	$T_{20i+1451}$
$P_i(10)$	T_{20i+12}	$P_i(28)$	$T_{20i+172}$	$P_i(46)$	$T_{20i+1292}$	$P_i(64)$	$T_{20i+1452}$
$P_i(11)$	T_{20i+13}	$P_i(29)$	$T_{20i+173}$	$P_i(47)$	$T_{20i+1293}$	$P_i(65)$	$T_{20i+1453}$
$P_i(12)$	T_{20i+14}	$P_i(30)$	$T_{20i+174}$	$P_i(48)$	$T_{20i+1294}$	$P_i(66)$	$T_{20i+1454}$
$P_i(13)$	T_{20i+15}	$P_i(31)$	$T_{20i+175}$	$P_i(49)$	$T_{20i+1295}$	$P_i(67)$	$T_{20i+1455}$
$P_i(14)$	T_{20i+16}	$P_i(32)$	$T_{20i+176}$	$P_i(50)$	$T_{20i+1296}$	$P_i(68)$	$T_{20i+1456}$
$P_i(15)$	T_{20i+17}	$P_i(33)$	$T_{20i+177}$	$P_i(51)$	$T_{20i+1297}$	$P_i(69)$	$T_{20i+1457}$
$P_i(16)$	T_{20i+18}	$P_i(34)$	$T_{20i+178}$	$P_i(52)$	$T_{20i+1298}$	$P_i(70)$	$T_{20i+1458}$
$P_i(17)$	T_{20i+19}	$P_i(35)$	$T_{20i+179}$	$P_i(53)$	$T_{20i+1299}$	$P_i(71)$	$T_{20i+1459}$

FIG. 23 Overhead Tone Mapping to Channels for the ith Subband Pair

Tones allocated to CLC/CAC in subband pair i (CLC/CAC$_{i,0}$)

index	tone	index	tone	index	tone	index	tone
0	T_{320i}	1	$T_{320i+20}$	2	$T_{320i+40}$	3	$T_{320i+60}$
4	$T_{320i+160}$	5	$T_{320i+180}$	6	$T_{320i+200}$	7	$T_{320i+220}$
8	$T_{320i+1280}$	9	$T_{320i+1300}$	10	$T_{320i+1320}$	11	$T_{320i+1340}$
12	$T_{320i+1440}$	13	$T_{320i+1460}$	14	$T_{320i+1480}$	15	$T_{320i+1500}$

Tones allocated to BRC/CAC in subband pair i (BRC/CAC$_{i,q}$)

index	tone	index	tone	index	tone	index	tone
0	$T_{320i+90}$	1	$T_{320i+110}$	2	$T_{320i+130}$	3	$T_{320i+150}$
4	$T_{320i+250}$	5	$T_{320i+270}$	6	$T_{320i+290}$	7	$T_{320i+310}$
8	$T_{320i+1370}$	9	$T_{320i+1390}$	10	$T_{320i+1410}$	11	$T_{320i+1430}$
12	$T_{320i+1530}$	13	$T_{320i+1550}$	14	$T_{320i+1570}$	15	$T_{320i+1590}$

Tones allocated to RSC/DCC in subband pair i (RSC/DCC$_i$)

index	tone	index	tone	index	tone	index	tone
0	$T_{320i+10}$	1	$T_{320i+30}$	2	$T_{320i+50}$	3	$T_{320i+70}$
4	$T_{320i+80}$	5	$T_{320i+100}$	6	$T_{320i+120}$	7	$T_{320i+140}$
8	$T_{320i+170}$	9	$T_{320i+190}$	10	$T_{320i+210}$	11	$T_{320i+230}$
12	$T_{320i+240}$	13	$T_{320i+260}$	14	$T_{320i+280}$	15	$T_{320i+300}$
16	$T_{320i+1290}$	17	$T_{320i+1310}$	18	$T_{320i+1330}$	19	$T_{320i+1350}$
20	$T_{320i+1360}$	21	$T_{320i+1380}$	22	$T_{320i+1400}$	23	$T_{320i+1420}$
24	$T_{320i+1450}$	25	$T_{320i+1470}$	26	$T_{320i+1490}$	27	$T_{320i+1510}$
28	$T_{320i+1520}$	29	$T_{320i+1540}$	30	$T_{320i+1560}$	31	$T_{320i+1580}$

FIG. 24
Division of Tone Space to Traffic and Overhead Tones
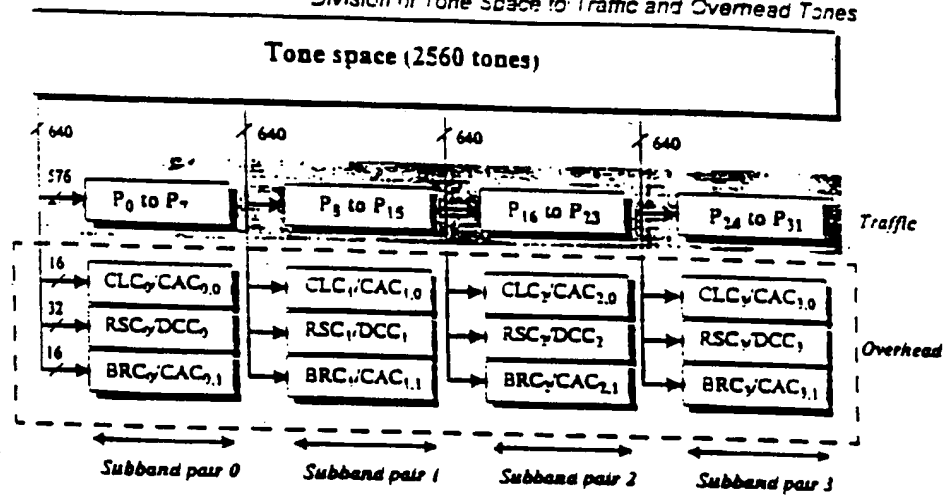
FIG. 25   Time Division Duplex for Base and RU Transmissions

- Base (forward) transmission
- RU (reverse) transmission
- Forward guard period
- Reverse guard period
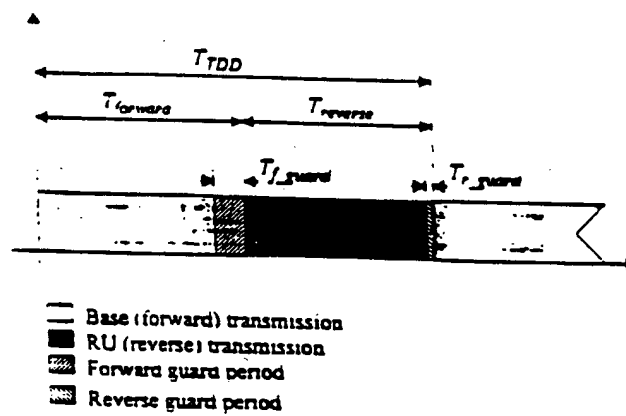
FIG. 26 *Details of Forward and Reverse Channel Time Parameters*

- Interburst guard time
- Base (forward) burst period
- RU (reverse) burst period
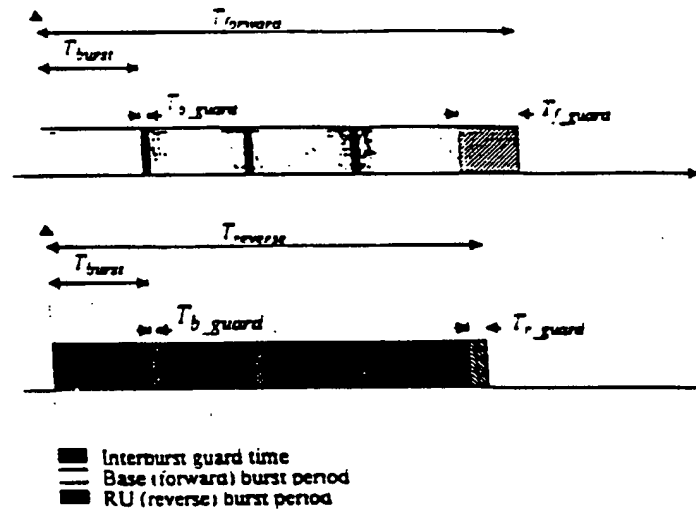
FIG. 27   TDD Parameter values

TDD parameter	Value (us)
$T_{forward}$	1610
$T_{reverse}$	1390
$T_{f\ guard}$	255
$T_{r\ guard}$	35
$T_{revisit}$	3000
T_{burst}	320
$T_{b\ guard}$	25

FIG. 28   *Physical Layer Framing Structure*
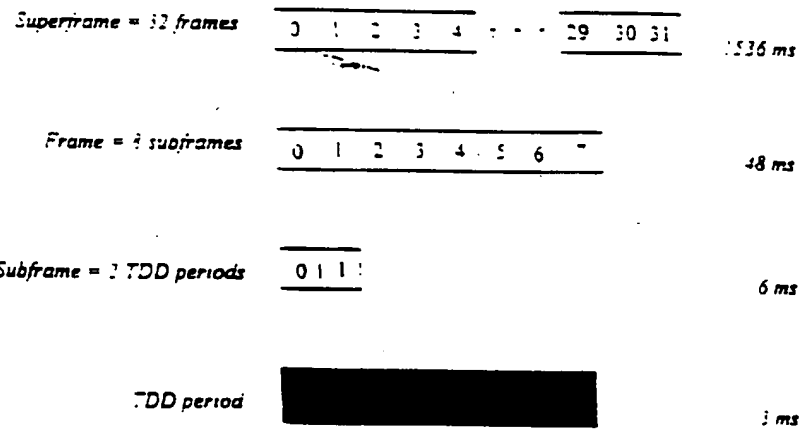
Superframe = 32 frames

| 0 | 1 | 2 | 3 | 4 | · · · | 29 | 30 | 31 |

1536 ms

Frame = 8 subframes

| 0 | 1 | 2 | 3 | 4 | 5 | 6 | 7 |

48 ms

Subframe = 2 TDD periods

| 0 | 1 | 1 |

6 ms

TDD period

3 ms

FIG. 29   Phase A Subband Pair Assignment within a Cell

N

Subband
Pair 1

Subband
Pair 2

Subband
Pair 3

FIG. 30   Phase-A Subband Pair Assignment across Cells

North-South Facing Sectors
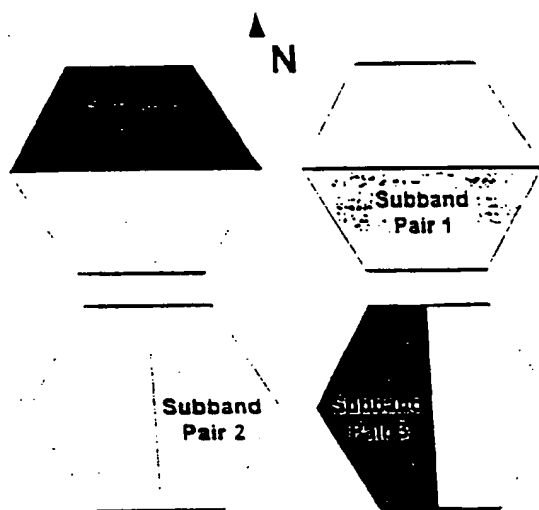
East-West Facing Sectors
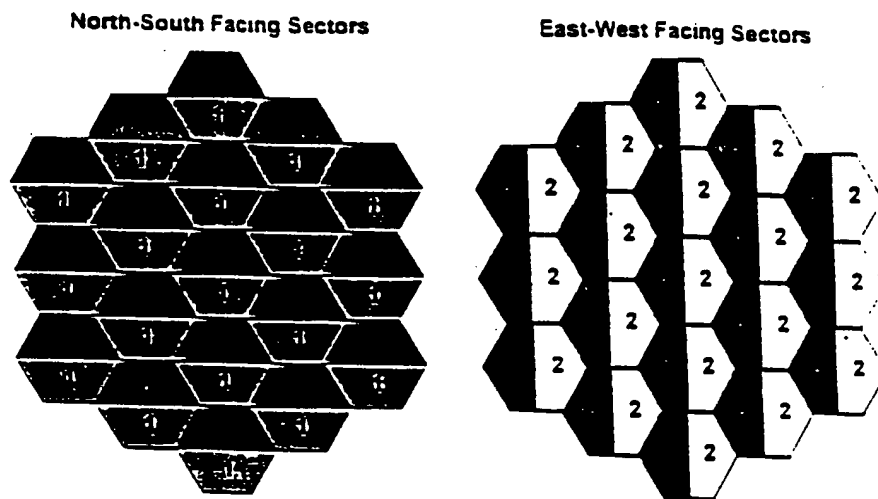
FIG. 31   Functional Block Diagram - Upper Physical Layer of Base
          Transmitter for High Capacity Mode
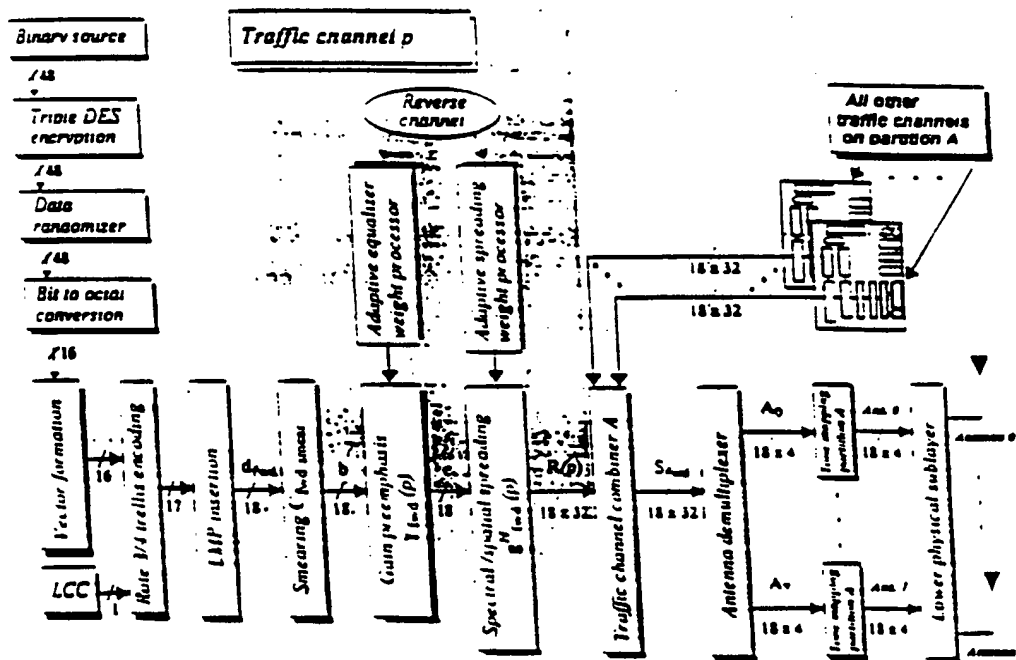
FIG. 32 Data Transformation Diagram - High Capacity Forward Channel Transmissions
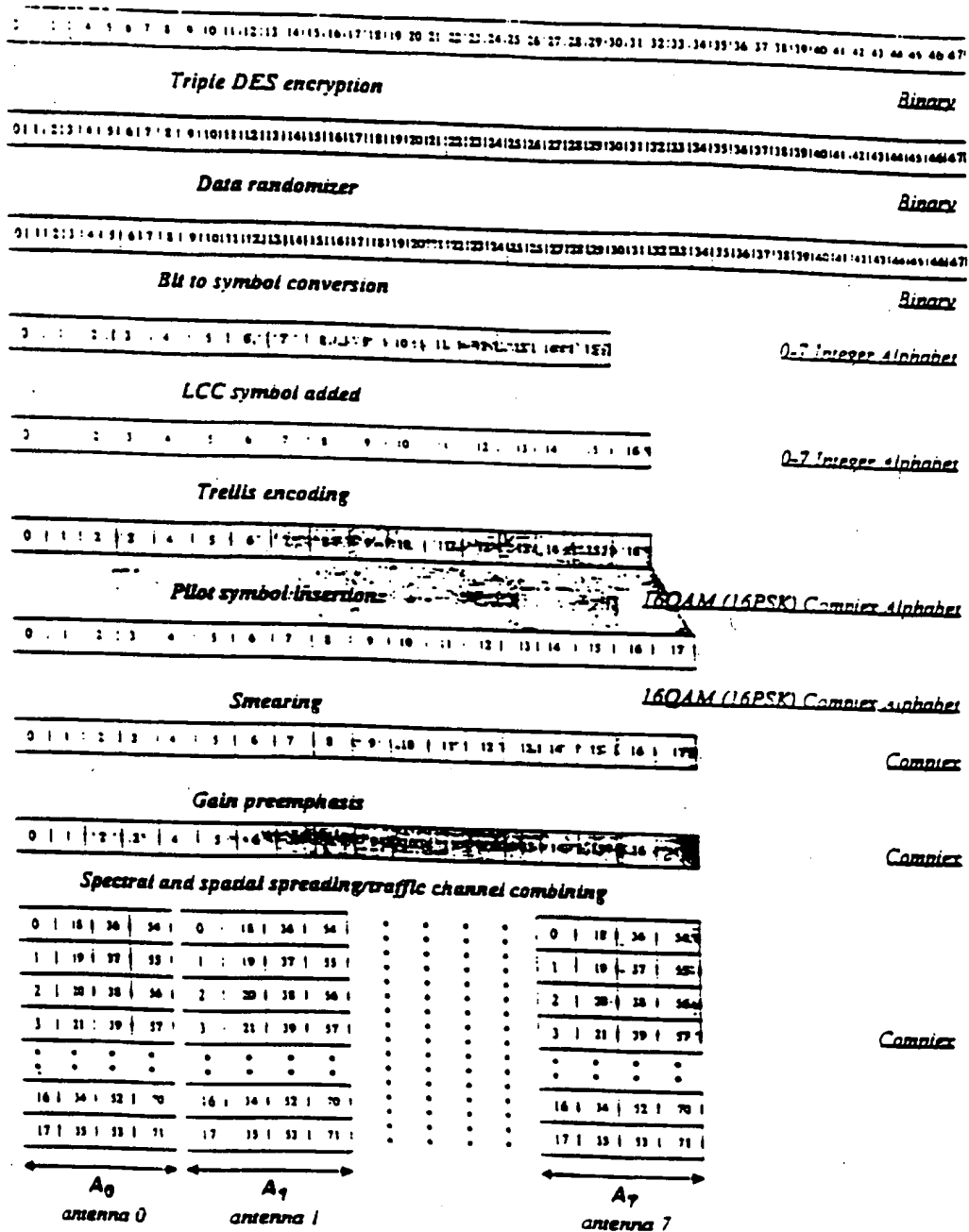
FIG. 33   Functional Block Diagram - Upper Physical Layer of Base
          Transmitter for Medium Capacity Mode
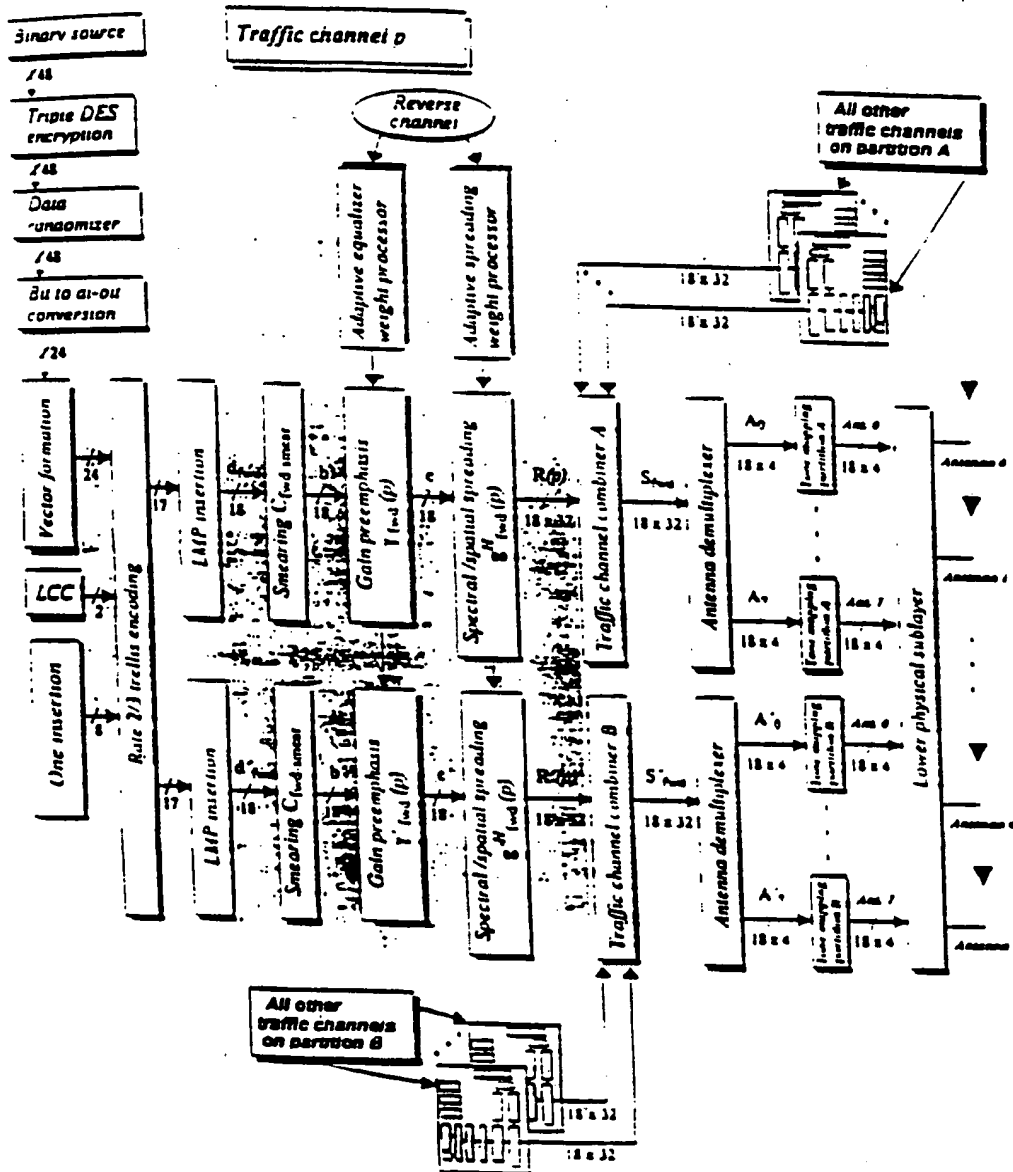
FIG. 34

Data Transformation Diagram - Medium Capacity Forward
Channel Transmissions
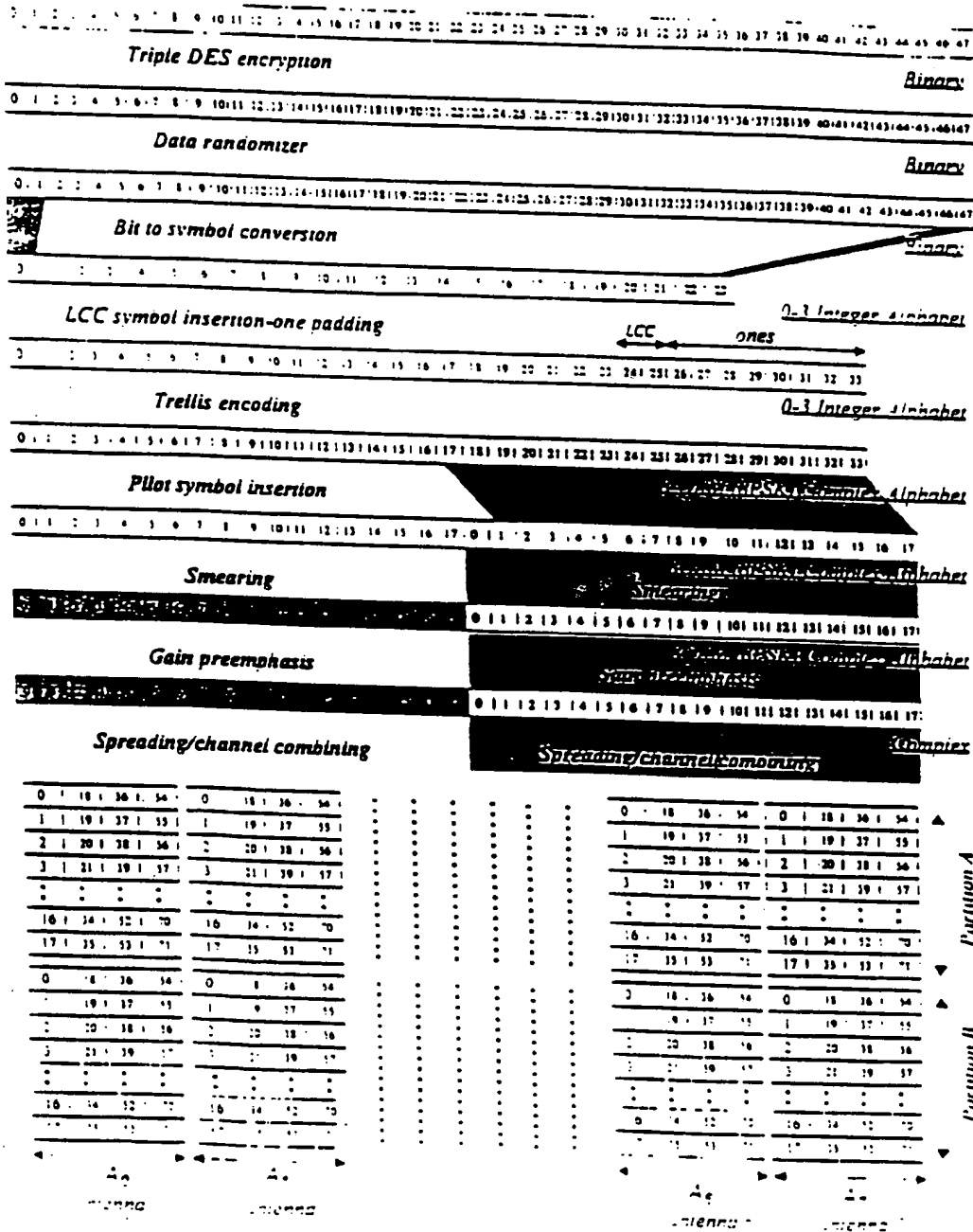
FIG. 35   Functional Block Diagram - Upper Physical Layer of Base
Transmitter for Low Capacity Mode

Note: Although not shown in the diagram, traffic channel combiners B
and C, combine all the traffic channels on their corresponding
traffic partitions
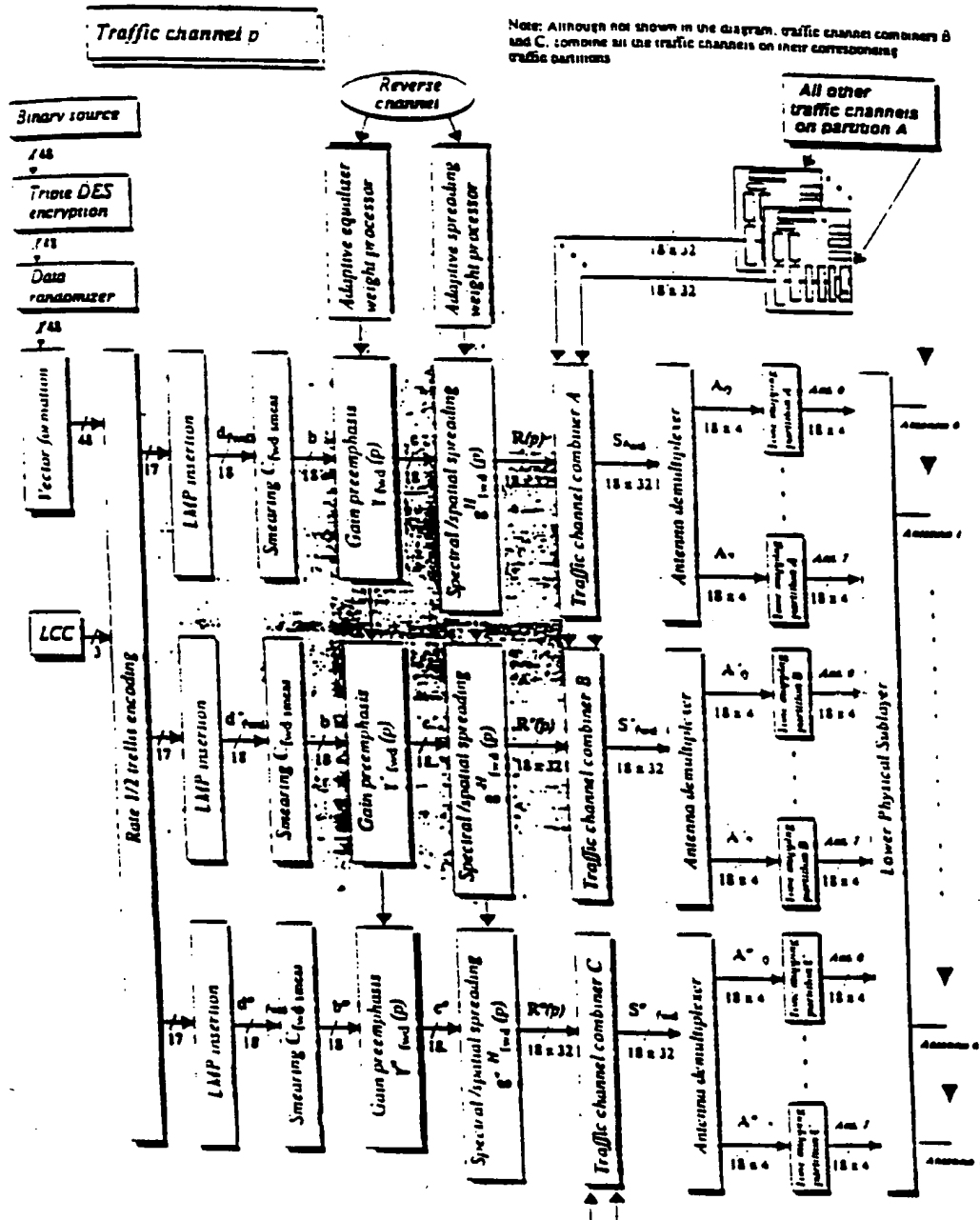
FIG. 36   Data Transformation Diagram - Low Capacity Forward Channel Transmissions
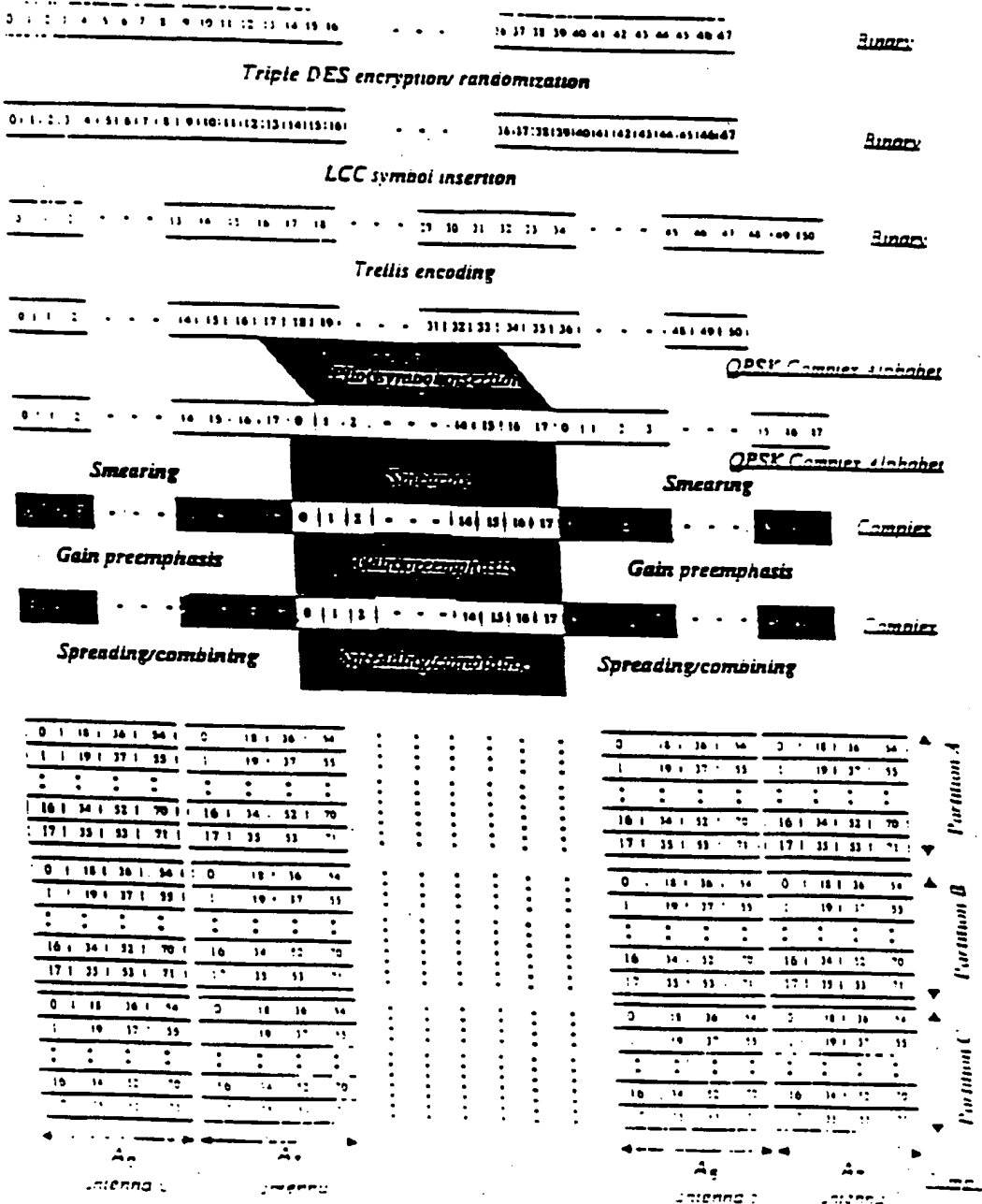
FIG. 37   Triple DES Encryption Algorithm
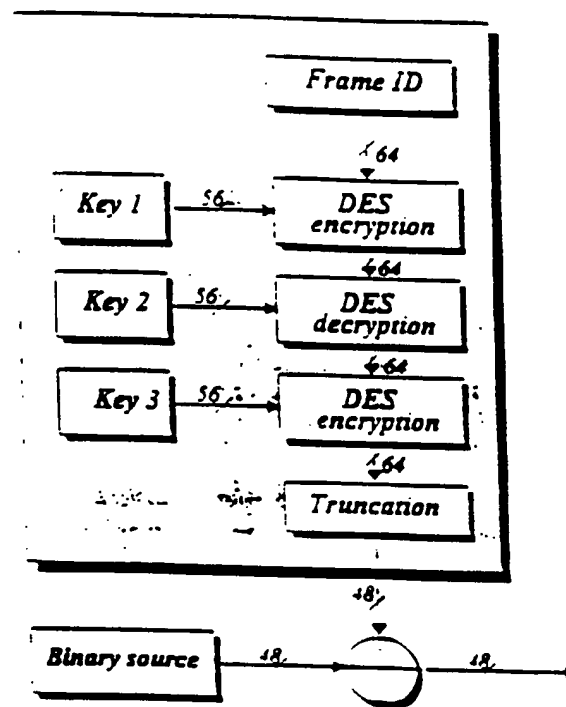
FIG. 38   Feed Forward Shift Register implementation of Rate 3/4, 16PSK
          Trellis Encoder for High Capacity Mode
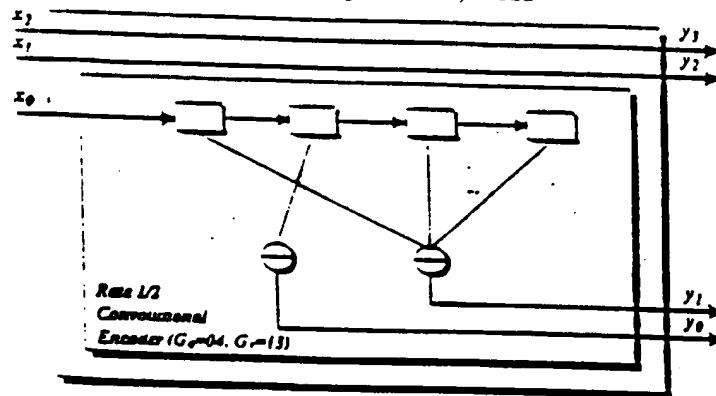
FIG. 39   Feed Forward Shift Register implementation of Rate 3/4
          16QAM Trellis Encoder for High Capacity Mode
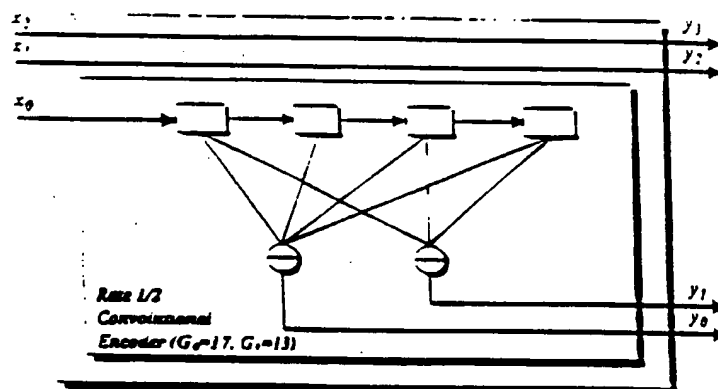
FIG. 40   Signal Mappings for Rate 3/4, 16QAM and 16PSK Trellis Encoding Schemes Employed in High Capacity Mode
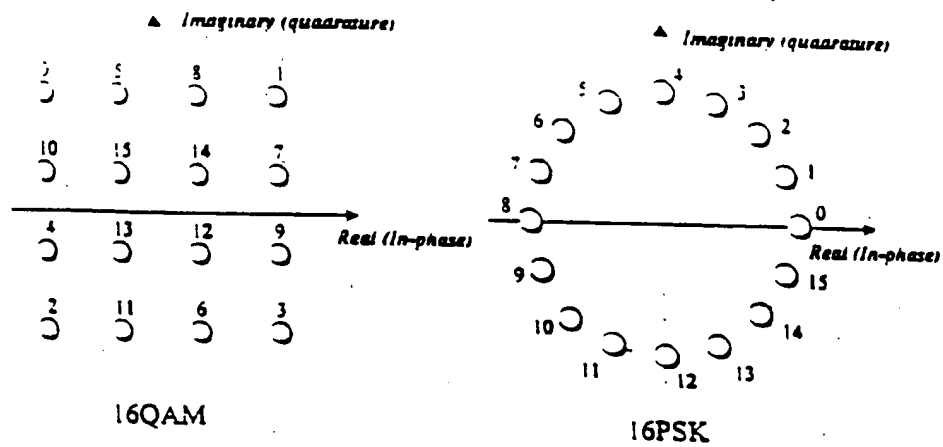
FIG. 41 *Signal Mappings for Rate 3/4, Pragmatic16QAM and 16PSK Trellis Encoding Schemes Employed in High Capacity Mode*

Output symbol	Output bits				Signal mapping (16QAM)		Signal mapping (16PSK)	
	Y_3	Y_2	Y_1	Y_0	In phase	Quadrature	In phase	Quadrature
0	0	0	0	0	$-3/\sqrt{10}$	$3/\sqrt{10}$	1.0	0.0
1	0	0	0	1	$3/\sqrt{10}$	$3/\sqrt{10}$	0.924	0.383
2	0	0	1	0	$-3/\sqrt{10}$	$-3/\sqrt{10}$	0.707	0.707
3	0	0	1	1	$3/\sqrt{10}$	$-3/\sqrt{10}$	0.383	0.924
4	0	1	0	0	$-3/\sqrt{10}$	$-1/\sqrt{10}$	0	1
5	0	1	0	1	$-1/\sqrt{10}$	$3/\sqrt{10}$	-0.383	0.924
6	0	1	1	0	$1/\sqrt{10}$	$-3/\sqrt{10}$	-0.707	0.707
7	0	1	1	1	$3/\sqrt{10}$	$1/\sqrt{10}$	-0.924	0.383
8	1	0	0	0	$1/\sqrt{10}$	$3/\sqrt{10}$	-1.0	0.0
9	1	0	0	1	$3/\sqrt{10}$	$-1/\sqrt{10}$	-0.924	-0.383
10	1	0	1	0	$-3/\sqrt{10}$	$1/\sqrt{10}$	-0.707	-0.707
11	1	0	1	1	$-1/\sqrt{10}$	$-3/\sqrt{10}$	-0.383	-0.924
12	1	1	0	0	$1/\sqrt{10}$	$-1/\sqrt{10}$	0	-1
13	1	1	0	1	$-1/\sqrt{10}$	$-1/\sqrt{10}$	0.383	-0.924
14	1	1	1	0	$1/\sqrt{10}$	$1/\sqrt{10}$	0.707	-0.707
15	1	1	1	1	$-1/\sqrt{10}$	$1/\sqrt{10}$	0.924	-0.383

FIG. 42

Feed Forward Shift Register Implementation of Rate 2/3, 8PSK
Trellis Encoder for Medium Capacity Mode
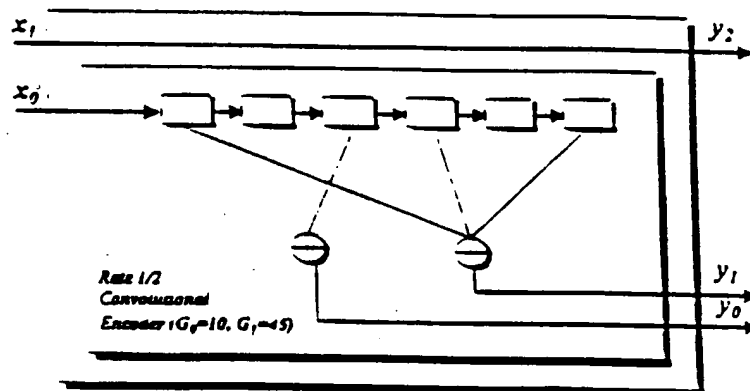
FIG. 43 Feed Forward Shift Register Implementation of Rate 2/3, 8QAM
Trellis Encoder for Medium Capacity Mode
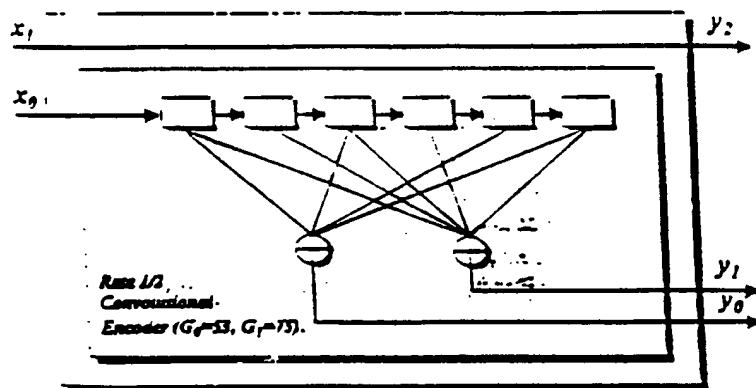
FIG. 44 Signal Mappings for Rate 2/3. 8QAM and 8PSK Trellis Encoding
Schemes Employed in Medium Capacity Mode
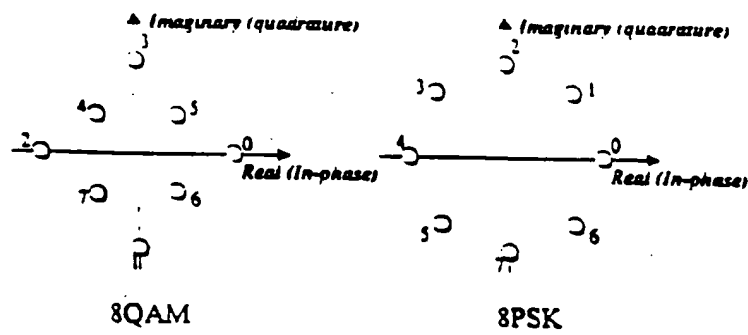
8QAM

8PSK

FIG. 45   Signal Mappings for Rate 2/3. 8QAM and 8PSK Trellis Encoding
Schemes Employed in Medium Capacity Mode

Output symbol	Output bits			Signal mapping (8QAM)		Signal mapping (8PSK)	
	y_2	y_1	y_0	In phase	Quadrature	In phase	Quadrature
0	0	0	0	1.21	0	1	0
1	0	0	1	0	-1.21	$1/\sqrt{2}$	$1/\sqrt{2}$
2	0	1	0	-1.21	0	0	1
3	0	1	1	0	1.21	$-1/\sqrt{2}$	$1/\sqrt{2}$
4	1	0	0	-0.518	0.518	-1	0
5	1	0	1	0.518	0.518	$-1/\sqrt{2}$	$-1/\sqrt{2}$
6	1	1	0	0.518	-0.518	0	-1
7	1	1	1	-0.518	-0.518	$1/\sqrt{2}$	$-1/\sqrt{2}$

FIG. 46   Feed Forward Shift Register implementation of Rate 1/2
           Convolutional Encoder for Low Capacity Mode
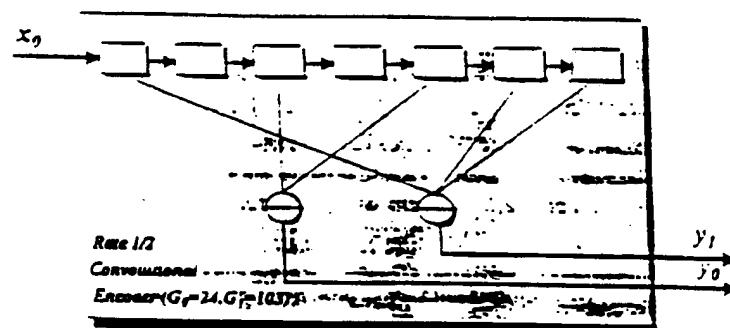
FIG. 47   Signal Mapping for Rate 1/2, QPSK Pragmatic Trellis Encoding
Scheme Employed in Low Capacity Mode
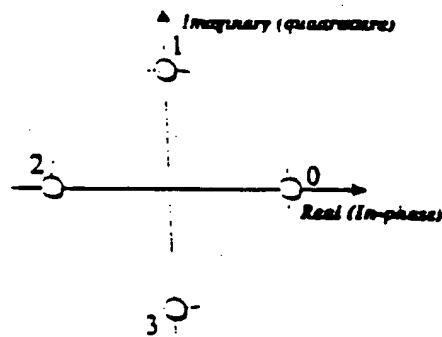
FIG. 48   Gray-Coded Mapping for Rate 1/2. QPSK Pragmatic Trellis
           Encoding Scheme Employed in Low Capacity Mode

Output symbol	Output bits		Signal mapping	
	Y_1	Y_0	In phase	Quadrature
0	0	0	1	0
1	0	1	0	1
2	1	0	-1	0
3	1	1	0	-1

FIG. 49 Base Mapping of Elements of Received Weight Vector to
Antenna Elements and Tones

w_0 ————————➤ (antenna element 0, tone 0)

w_1 ————————➤ (antenna element 0, tone 1)

w_2 ————————➤ (antenna element 0, tone 2)

w_3 ————————➤ (antenna element 0, tone 3)

w_4 ————————➤ (antenna element 1, tone 0)

w_5 ————————➤ (antenna element 1, tone 1)

w_6 ————————➤ (antenna element 1, tone 2)

w_7 ————————➤ (antenna element 1, tone 3)

.

.

.

.

w_{28} ————————➤ (antenna element 7, tone 0)

w_{29} ————————➤ (antenna element 7, tone 1)

w_{30} ————————➤ (antenna element 7, tone 2)

w_{31} ————————➤ (antenna element 7, tone 3)
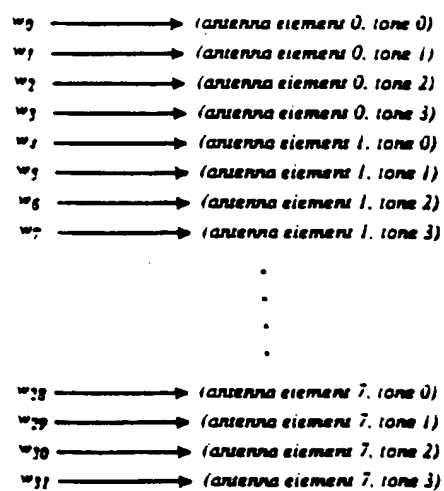
FIG. 51   QPSK Signal Mapping for the CLC Channel
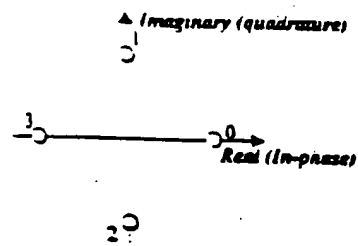
FIG. 50

Block Diagram Representation of CLC Physical Layer Format
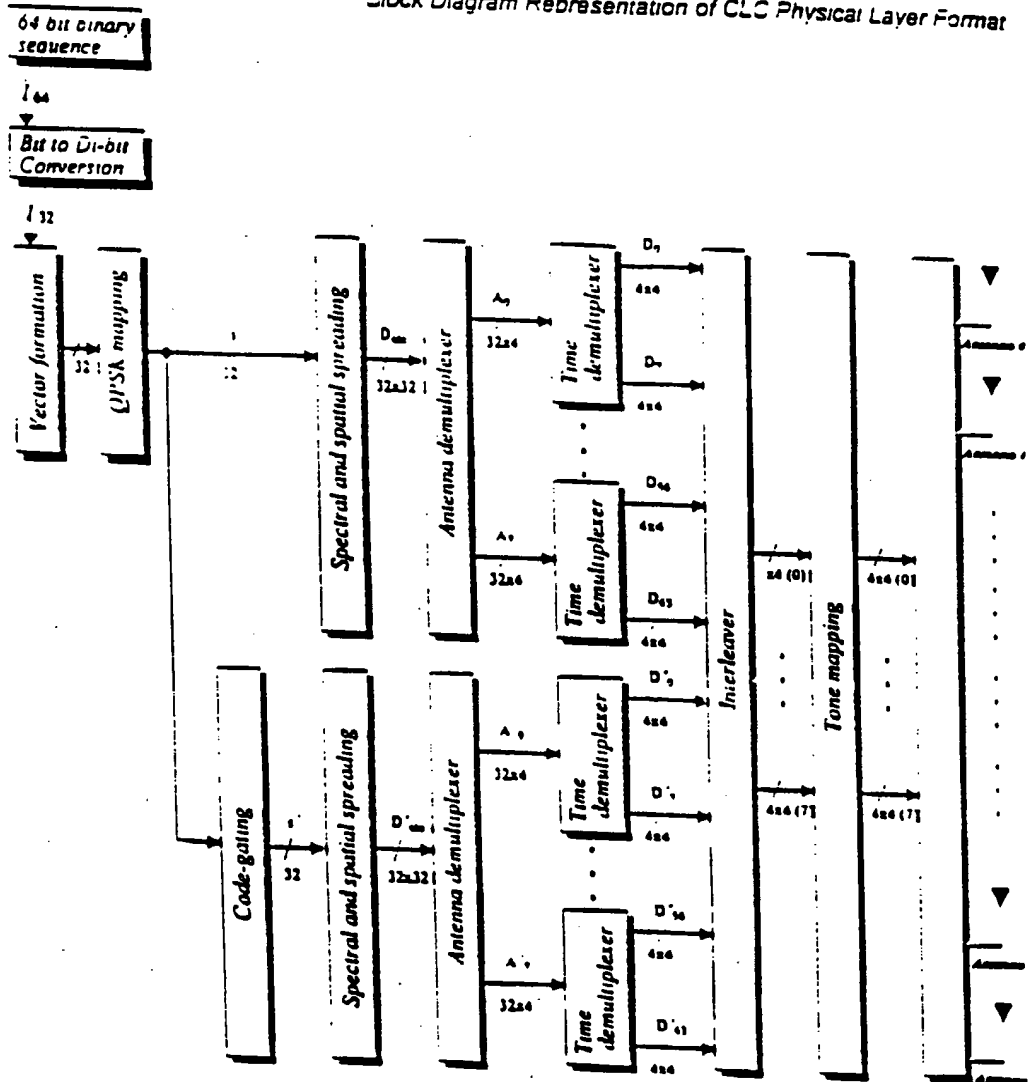
FIG. 51'   QPSK Signal Mapping for the CLC Channel

Symbol	Signal mapping	
	In phase	Quadrature
0	1	0
1	0	1
2	0	-1
3	-1	0

FIG. 52

The CLC Interleaving Rule

Antenna	Burst number															
	0	1	2	3	4	5	6	7	8	9	10	11	12	13	14	15
0																
1																
2																
3																
4																
5																
6																
7																

FIG. 53   Tone Mapping of (4 x 4) Interleaved Matrix Elements

		Column number			
		0	**1**	**2**	**3**
Row number	**0**	CLC,(0)ᵃ	CLC,(4)	CLC,(8)	CLC,(12)
	1	CLC,(1)	CLC,(5)	CLC,(9)	CLC,(13)
	2	CLC,(2)	CLC,(6)	CLC,(10)	CLC,(14)
	3	CLC,(3)	CLC,(7)	CLC,(11)	CLC,(15)

a. i is the subband pair index (0, 1, 2, or 3).

FIG. 54   Block Diagram representation of BRC Physical layer format.
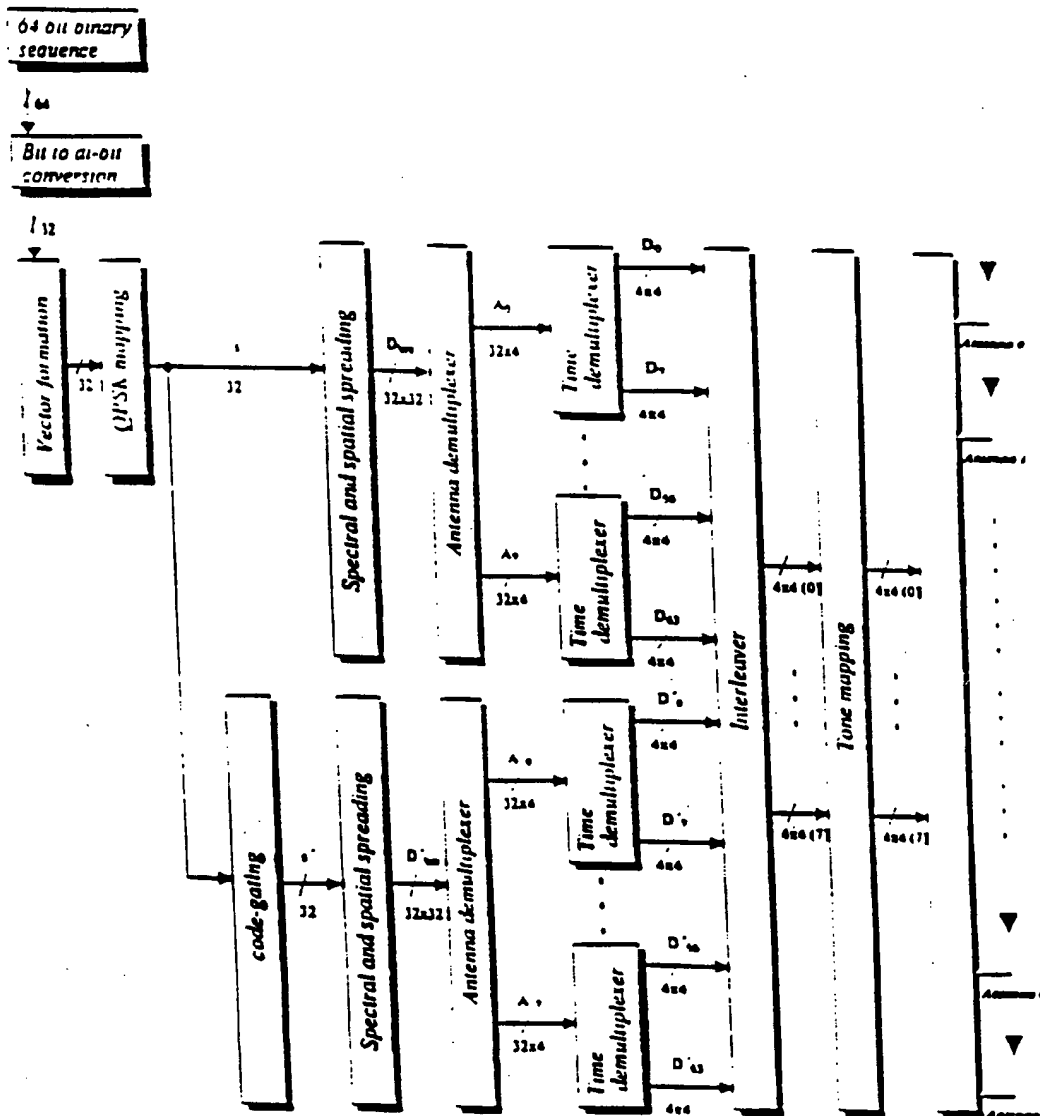
FIG. 55   Tone Mapping the (4x 4) Interleaved Matrix Elements

		Column number			
		0	1	2	3
Row number	0	BRC,(0)ᵃ	BRC,(4)	BRC,(8)	BRC,(12)
	1	BRC,(1)	BRC,(5)	BRC,(9)	BRC,(13)
	2	BRC,(2)	BRC,(6)	BRC,(10)	BRC,(14)
	3	BRC,(3)	BRC,(7)	BRC,(11)	BRC,(15)

a. i is the subband pair index (0, 1, 2, or 3). For the broadcast channel all the subband
pairs will be active at the same time.

FIG. 56 Broadcast Channel Beam Sweep

			Beam sweeping order									
0	15	16	17	18	19	0	1	2	3	4
1	5	6	7	8	9	10	11	12	13	14
2	0	1	2	3	4	5	6	7	8	9
3	10	11	12	13	13	14	15	16	17	18

FIG. 57   Functional Block Diagram - Upper Physical Layer of RU
           Transmitter for High Capacity Mode

Binary source

/48

Triple DES
encryption

/48

Data
randomizer

/48

Bit to octal
conversion

/16

Forward
channel

Adaptive spreading
weight processor
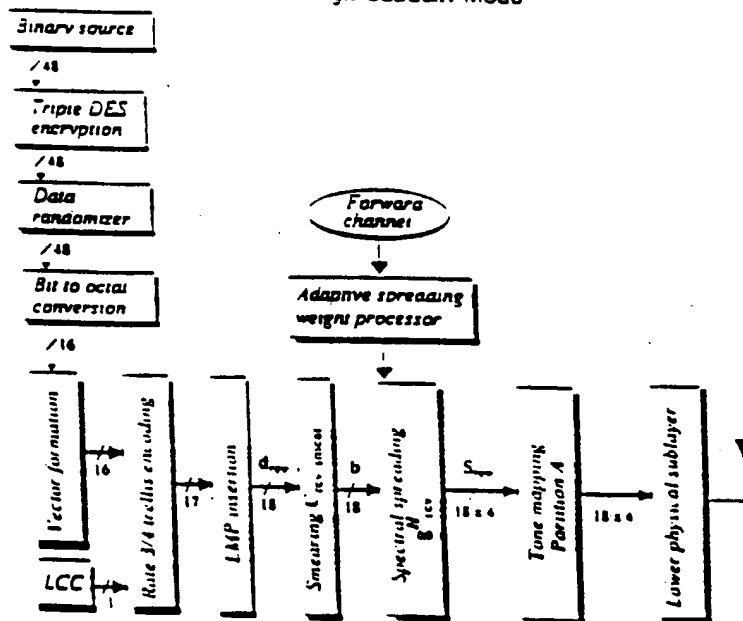
FIG. 58   Data Transformation Diagram - High Capacity Reverse Channel Transmissions

Triple DES encryption   *Binary*

Data randomization   *Binary*

Bit to symbol conversion   *Binary*

                                                                        0-7 Integer Alphabet

LCC symbol added   *0-7 Integer Alphabet*

Trellis encoding   *16QAM (16PSK) Complex Alphabet*

Pilot symbol insertion   *16QAM (16PSK) Complex Alphabet*

Smearing   *Complex*

4 Times spectral spreading   *Complex*
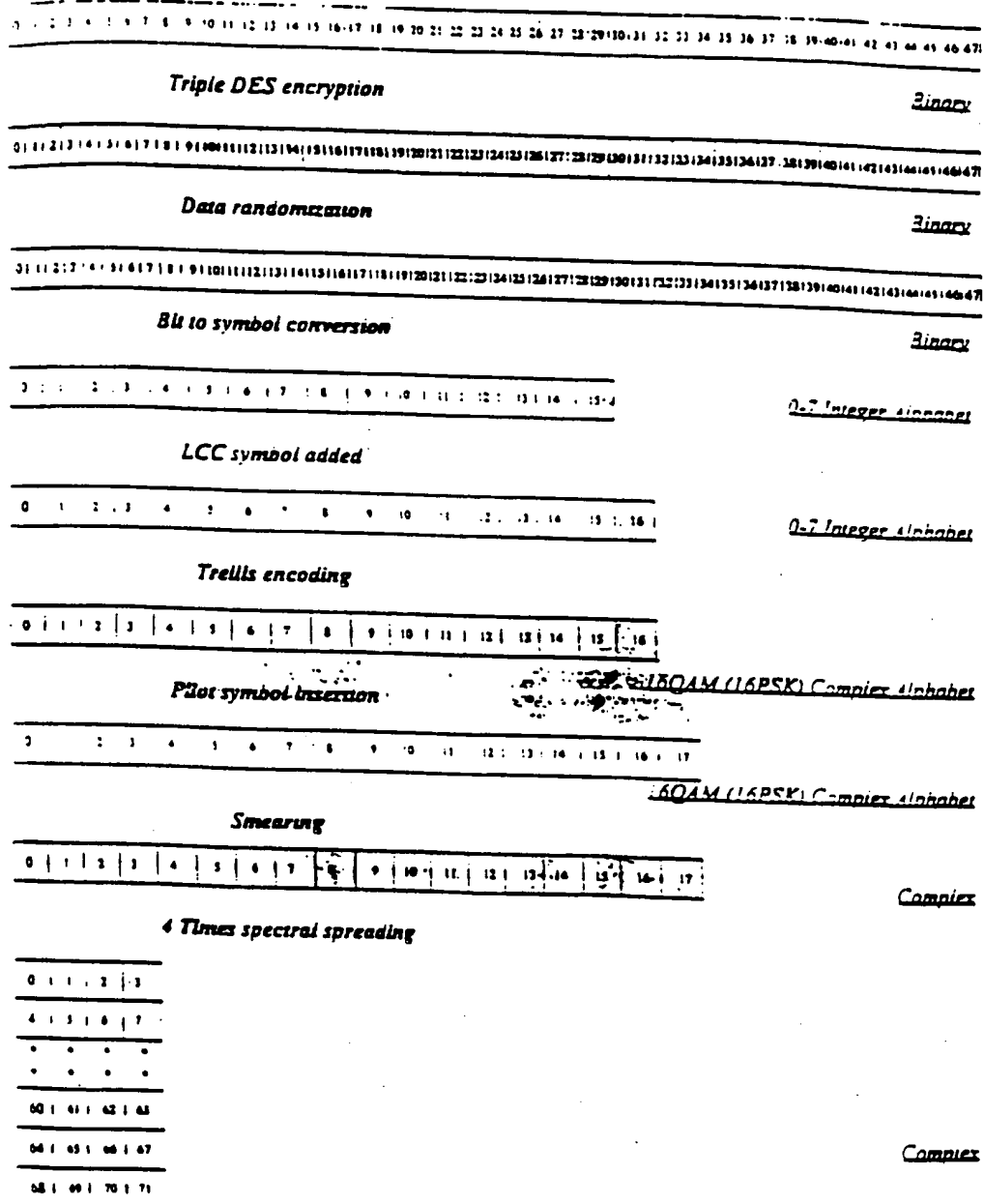
FIG. 59

Functional Block Diagram - Upper Physical Layer of RU
Transmitter for Medium Capacity Mode

FIG. 60
Data Transformation Diagram - Medium Capacity Reverse Channel Transmissions

Partition A

Partition B
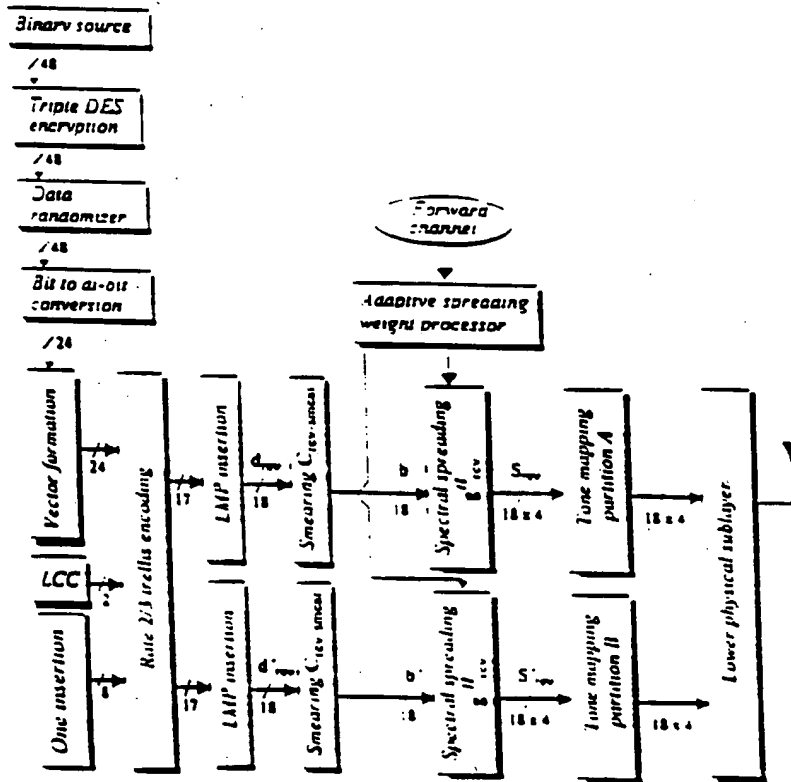
FIG. 61 Functional Block Diagram - Upper Physical Layer of RU
Transmitter for Low Capacity Mode
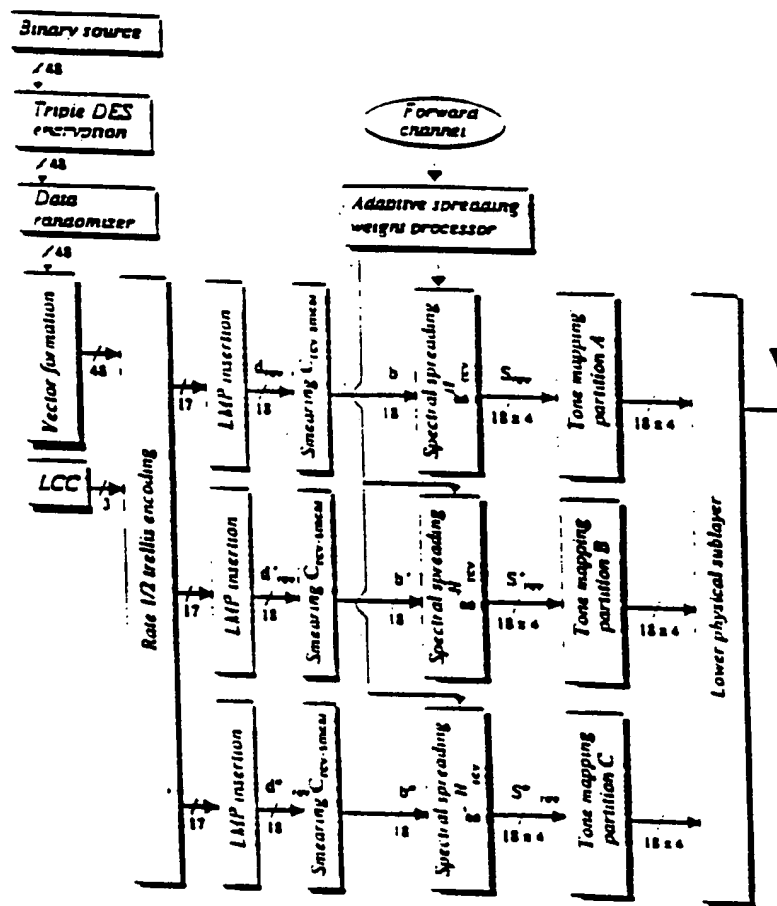
FIG. 62   Data Transformation Diagram - Low Capacity Reverse Channel Transmissions

Triple DES encryption

LCC symbol insertion-one padding

Trellis encoding

Pilot symbol insertion

Smearing   *Smearing*   *Smearing*

4 Times spreading   *4 Times spreading*   *4 Times spreading*

Partition A   Partition B   Partition C
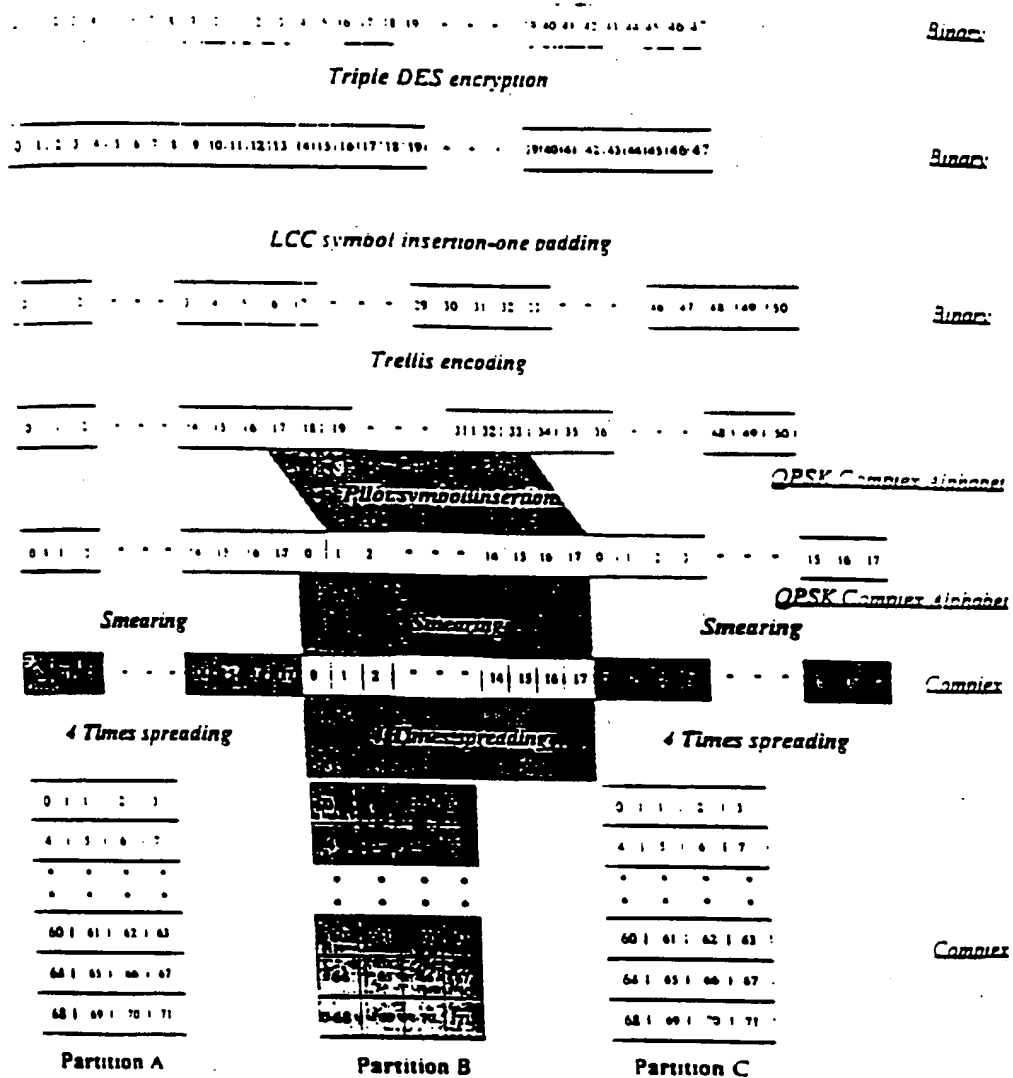
FIG. 63   RU Tone Mapping of Received Weight Vector Elements

w_0 ⟶ (tone 0)
w_1 ⟶ (tone 1)
w_2 ⟶ (tone 2)
w_3 ⟶ (tone 3)
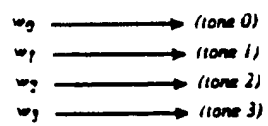
FIG. 64   Block Diagram Representation of CAC Physical Layer Format
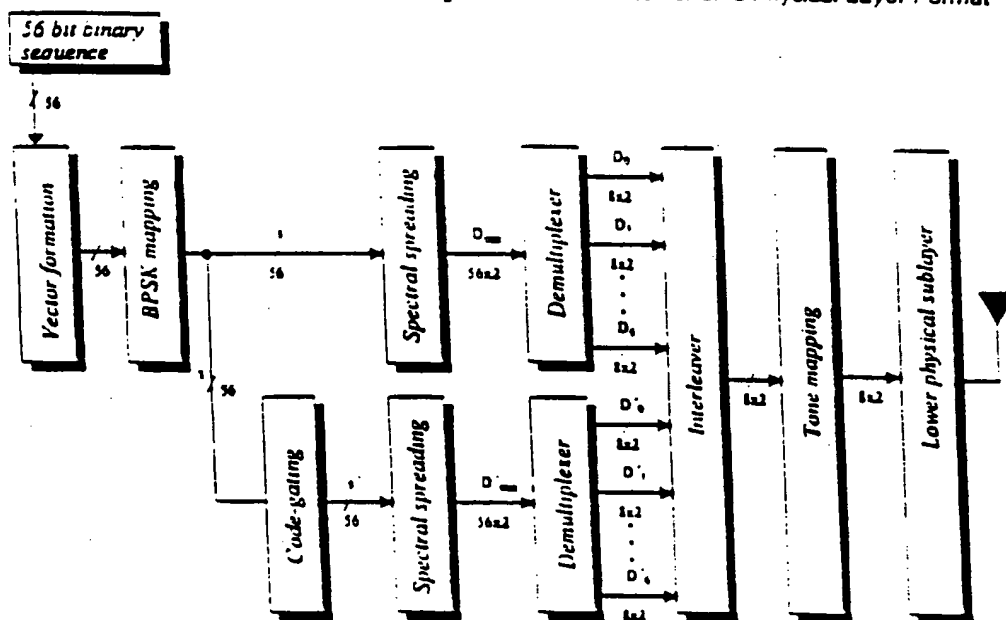
FIG. 65   BPSK Signal Mapping for the CAC Channel

Imaginary (quadrature)

Real (In-phase)
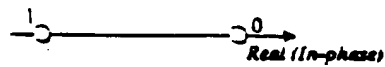
FIG. 65'   BPSK Signal Mapping for the CAC Channel

Bit	Signal mapping	
	In Phase	Quadrature
0	1	0
1	-1	0

FIG. 66 The CAC Interleaving Rule

Burst number													
0	1	2	3	4	5	6	7	8	9	10	11	12	13
Matrix D_0	D_1	D_2	D_3	D_4	D_5	D_6	D'_0	D'_1	D'_2	D'_3	D'_4	D'_5	D'_6

FIG. 67 Tone Mapping the (8 x 2) Interleaved Matrix Elements

		Column Number	
		0	1
Row Number	0	CAC$_{i,j}$(0)[a]	CAC$_{i,j}$(8)
	1	CAC$_{i,j}$(1)	CAC$_{i,j}$(9)
	2	CAC$_{i,j}$(2)	CAC$_{i,j}$(10)
	3	CAC$_{i,j}$(3)	CAC$_{i,j}$(11)
	4	CAC$_{i,j}$(4)	CAC$_{i,j}$(12)
	5	CAC$_{i,j}$(5)	CAC$_{i,j}$(13)
	6	CAC$_{i,j}$(6)	CAC$_{i,j}$(14)
	7	CAC$_{i,j}$(7)	CAC$_{i,j}$(15)

a. i is the subband pair index (0, 1, 2, or 3) and j is the
   CAC ID (0 or 1)

FIG. 68 Functional Block Diagram - Lower Physical Layer of Base Transmitter
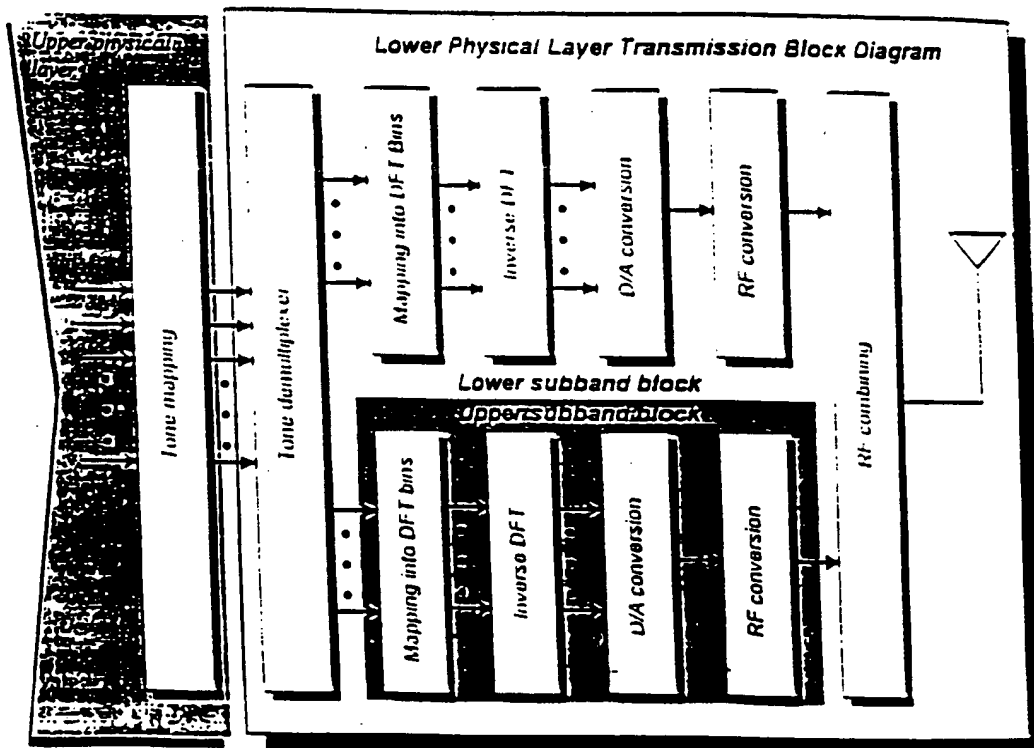
FIG. 69 Tone Mapping into DFT Bins

			Bin number		
			Bin 0 to Bin 95	Bin 96 to Bin 415	Bin 416 to Bin 511
DFT pair	0	lower		T_0 to T_{319}	
		upper		T_{1280} to T_{1599}	
	1	lower		T_{320} to T_{639}	
		upper	Unused	T_{1600} to T_{1919}	Unused
	2	lower		T_{640} to T_{959}	
		upper		T_{1920} to T_{2239}	
	3	lower		T_{960} to T_{1279}	
		upper		T_{2240} to T_{2559}	

FIG. 70   Tone Mapping into DFT Bins

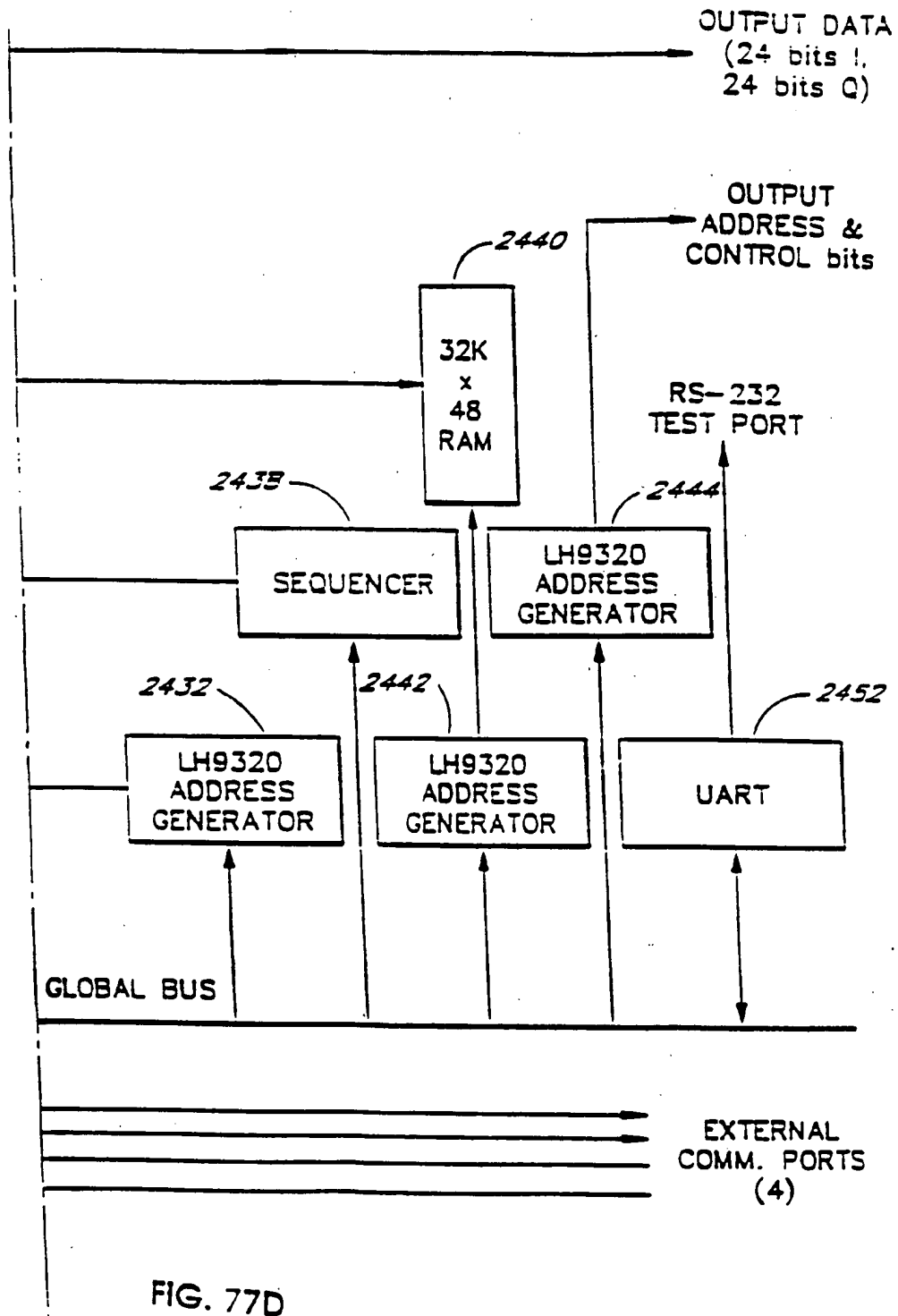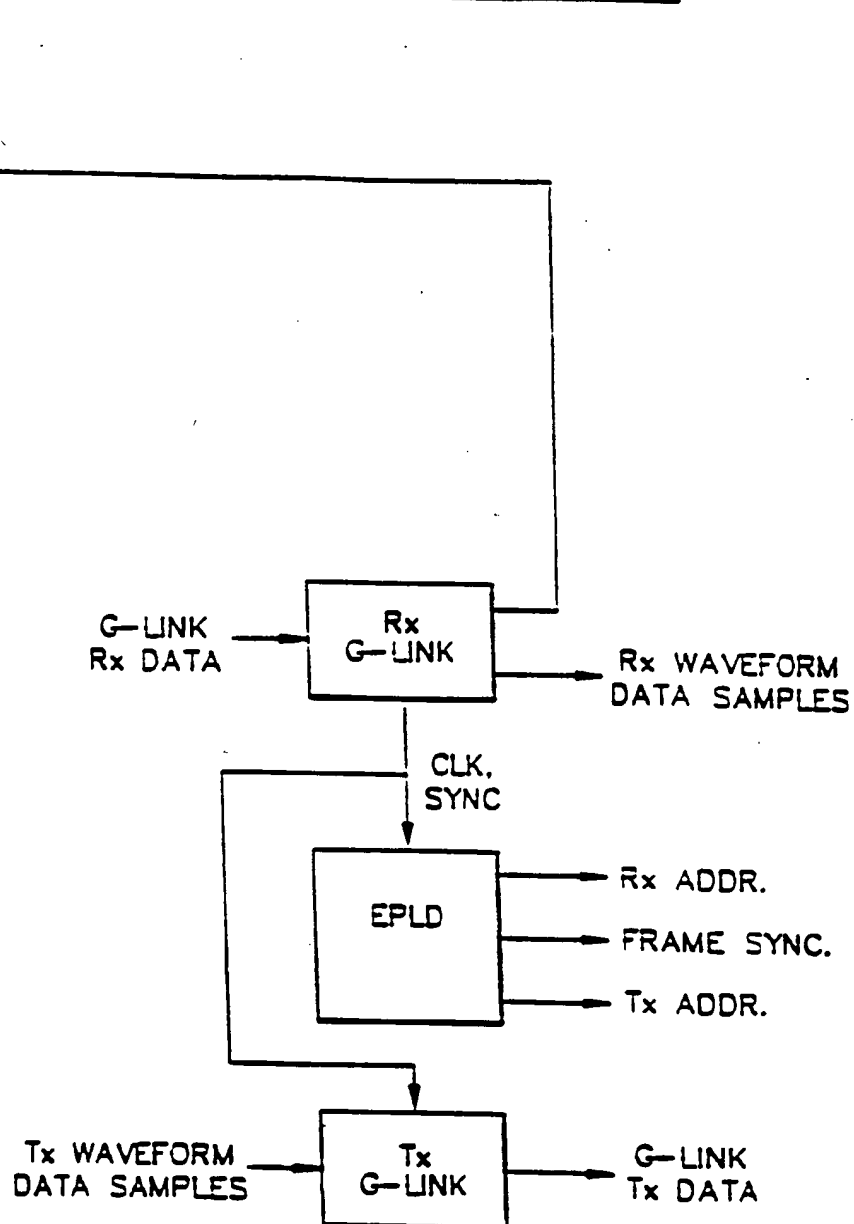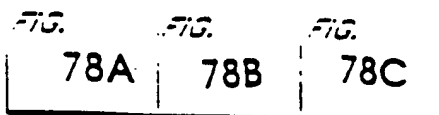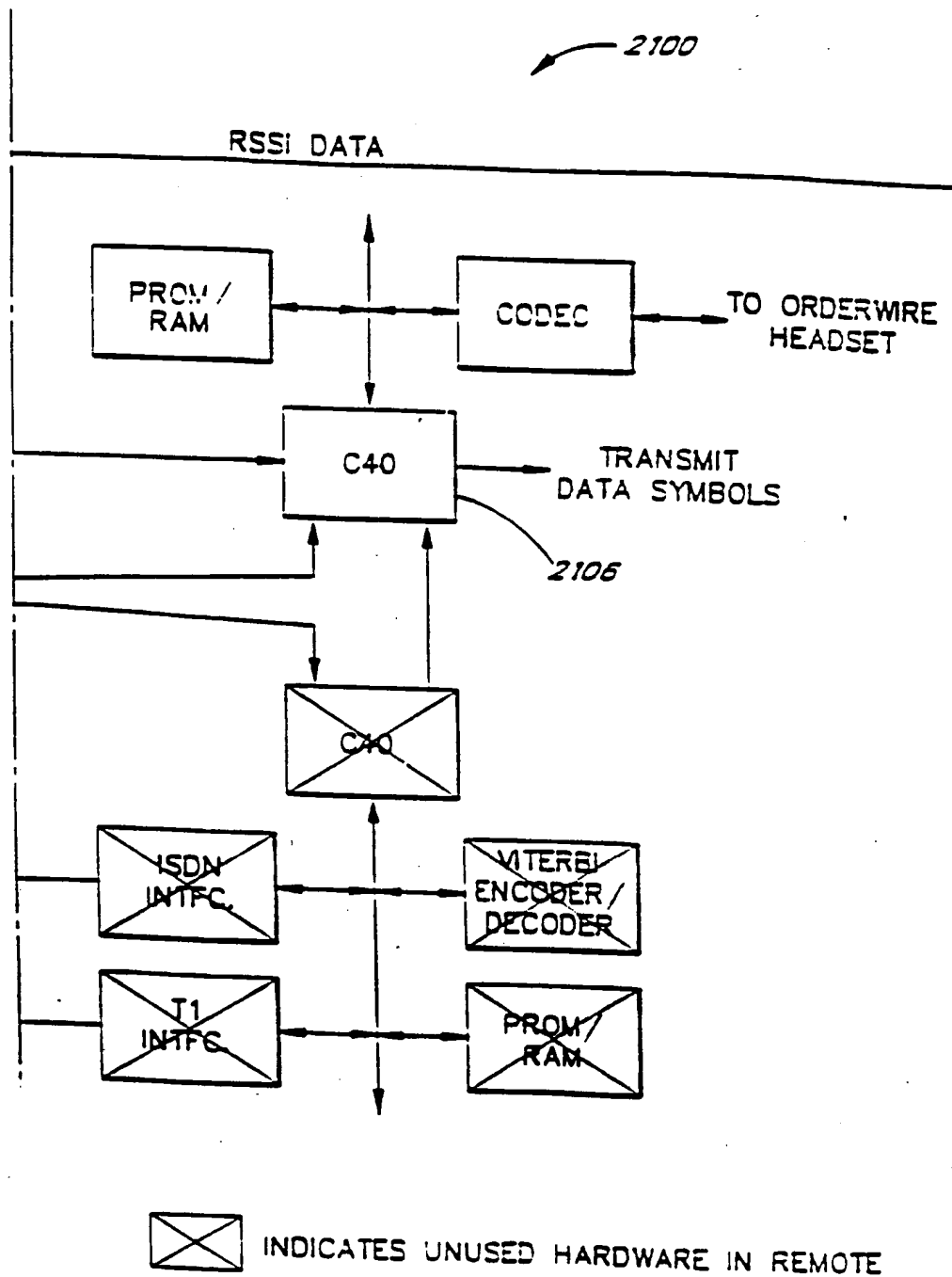FIG. 71

HIGH BANDWIDTH RADIO ACCESS STATION

FIG. 72

HIGH BANDWIDTH BASE STATION

FIG. 73

FIG. 74

FIG. 75

FIG. 75A

FIG. 75B

FIG. 75A

FIG. 75B

FIG. 76

FIG. 77A

SINE, COSINE LOOKUP TABLE

2402 — DOUBLE BUFFER

INPUT DATA
(24 bits I,
24 bits Q)

32K x 48 RAM | 32K x 48 RAM

INPUT ADDRESS & CONTROL bits

2408
FIFO
5048x48

RS-232 TEST PORT

2450
UART

2404
LH9320 ADDRESS GENERATOR

2454
128Kx32 RAM

2406
GLOBAL BUS

EXTERNAL COMM. PORTS (4)

LOCAL BUS

2460
512Kx8 BOOT EPROM

FIG. 77

FIG. 77A	FIG. 77B	FIG. 77C	FIG. 77D

FIG. 77B

FIG. 77C

OUTPUT DATA
(24 bits I,
24 bits Q)

OUTPUT
ADDRESS &
CONTROL bits

2440

32K
x
48
RAM

RS-232
TEST PORT

2438

2444

SEQUENCER

LH9320
ADDRESS
GENERATOR

2432

2442

2452

LH9320
ADDRESS
GENERATOR

LH9320
ADDRESS
GENERATOR

UART

GLOBAL BUS

EXTERNAL
COMM. PORTS
(4)

FIG. 77D

FIG. 78   *FIG.*   *FIG.*   *FIG.*

78A	78B	78C

G—LINK
Rx DATA → **Rx
G—LINK** → Rx WAVEFORM
DATA SAMPLES

CLK,
SYNC

EPLD → Rx ADDR.
→ FRAME SYNC.
→ Tx ADDR.

Tx WAVEFORM
DATA SAMPLES → **Tx
G—LINK** → G—LINK
Tx DATA

FIG. 78A

FIG. 78B

INDICATES UNUSED HARDWARE IN REMOTE

FIG. 78C

FIG. 79A

FIG. 79

FIG. 79B

FIG. 79D
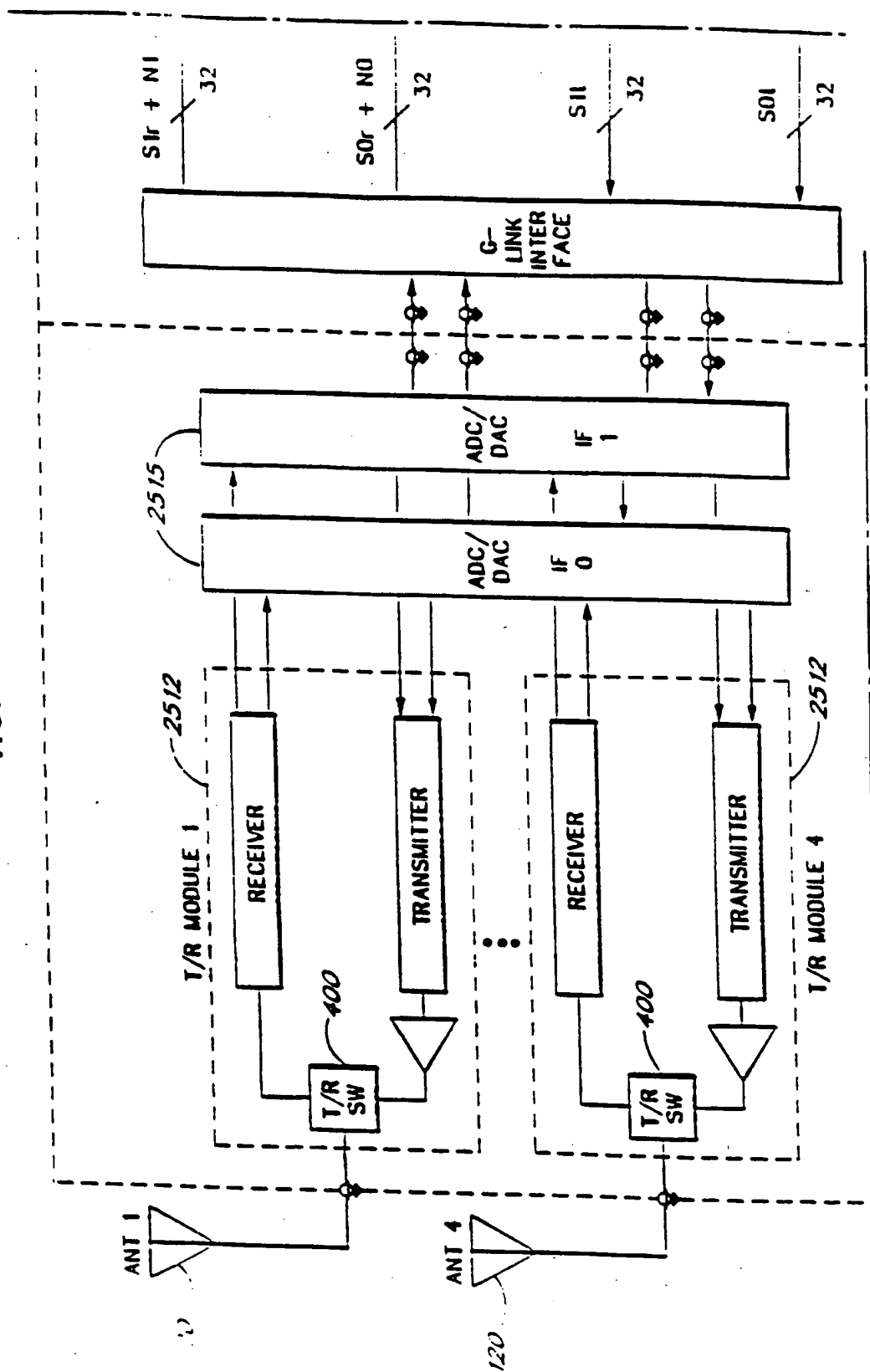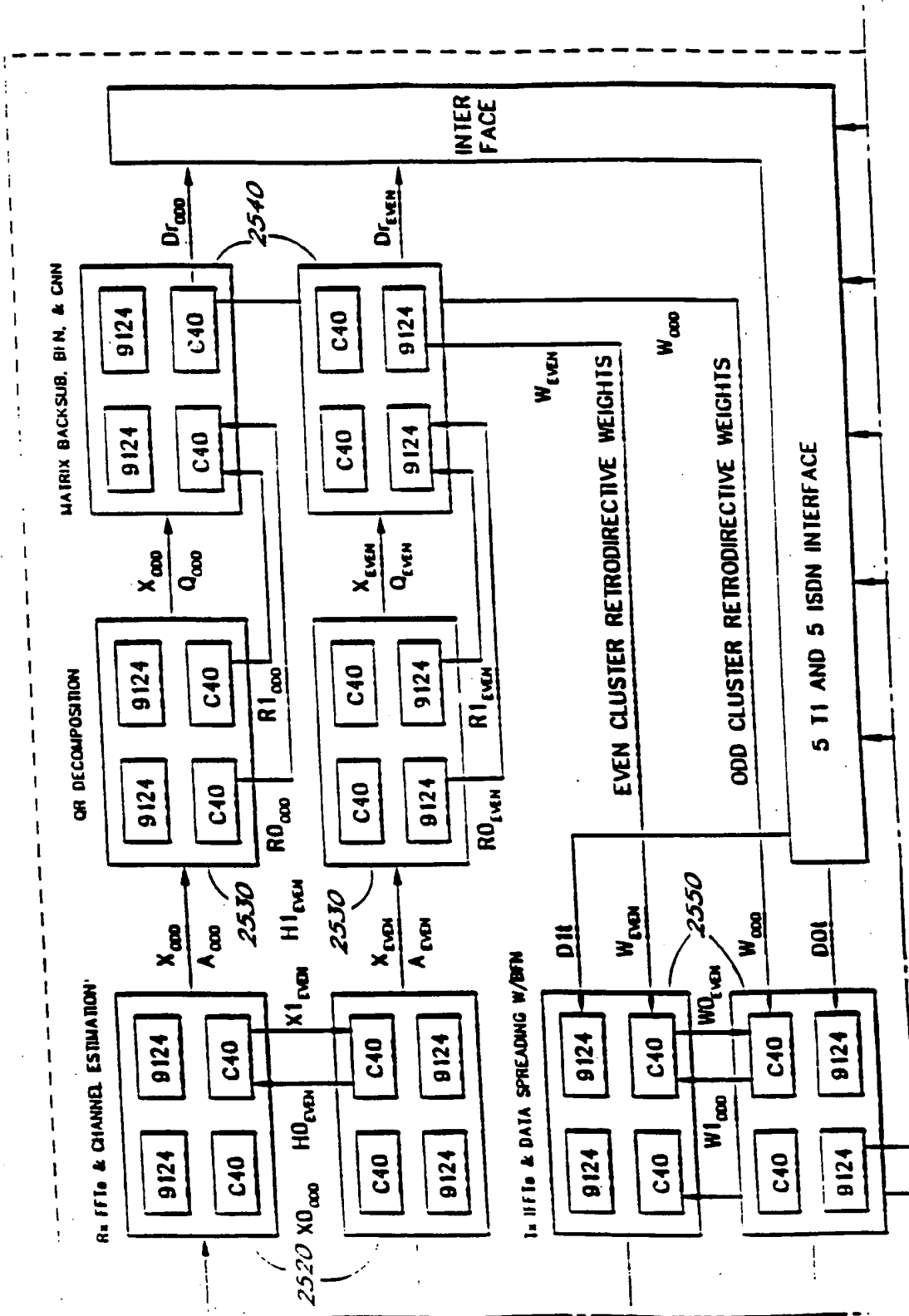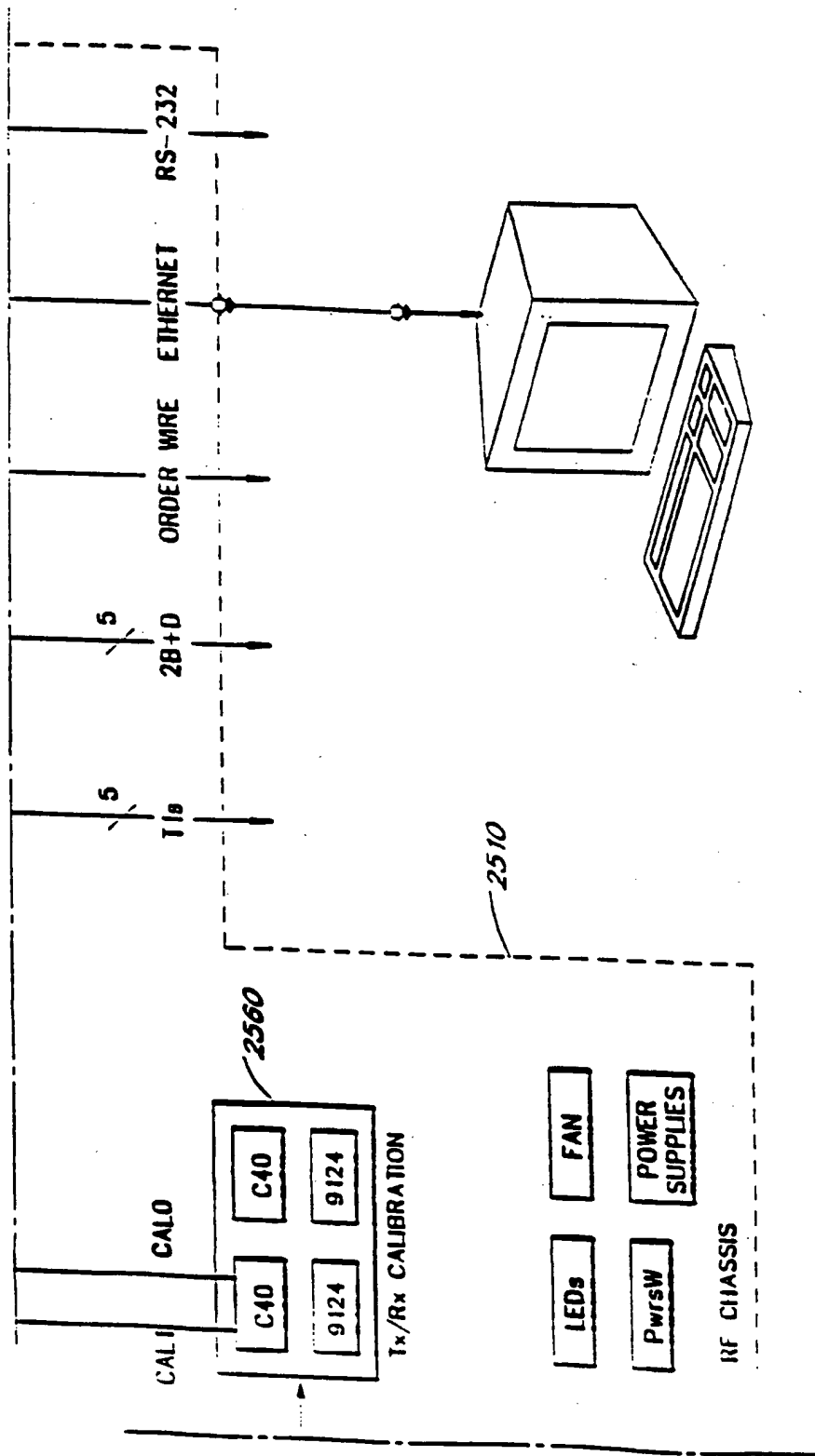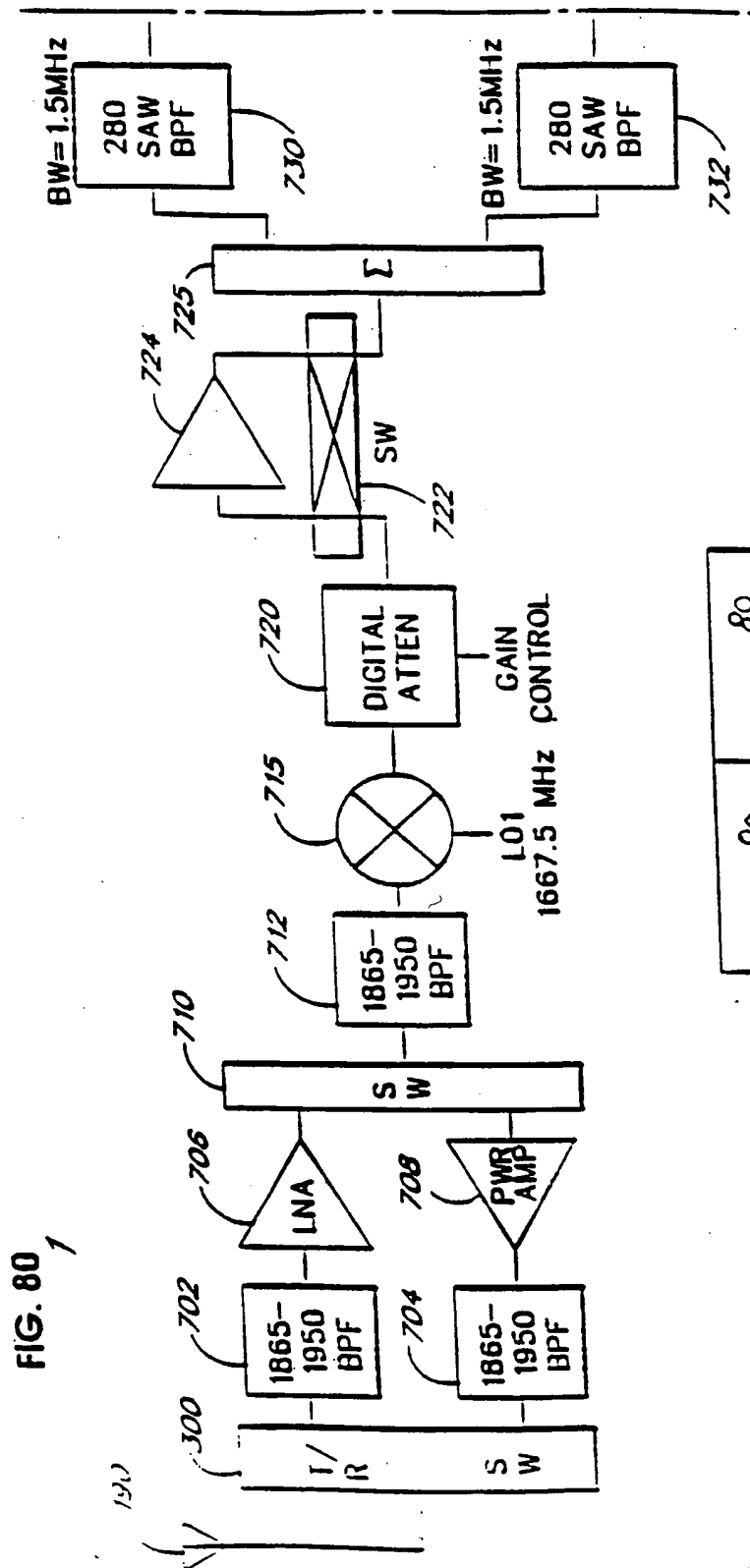
FIG. 80,1

FIG. 80 | FIG. 80
FIG. 1 | FIG. 2
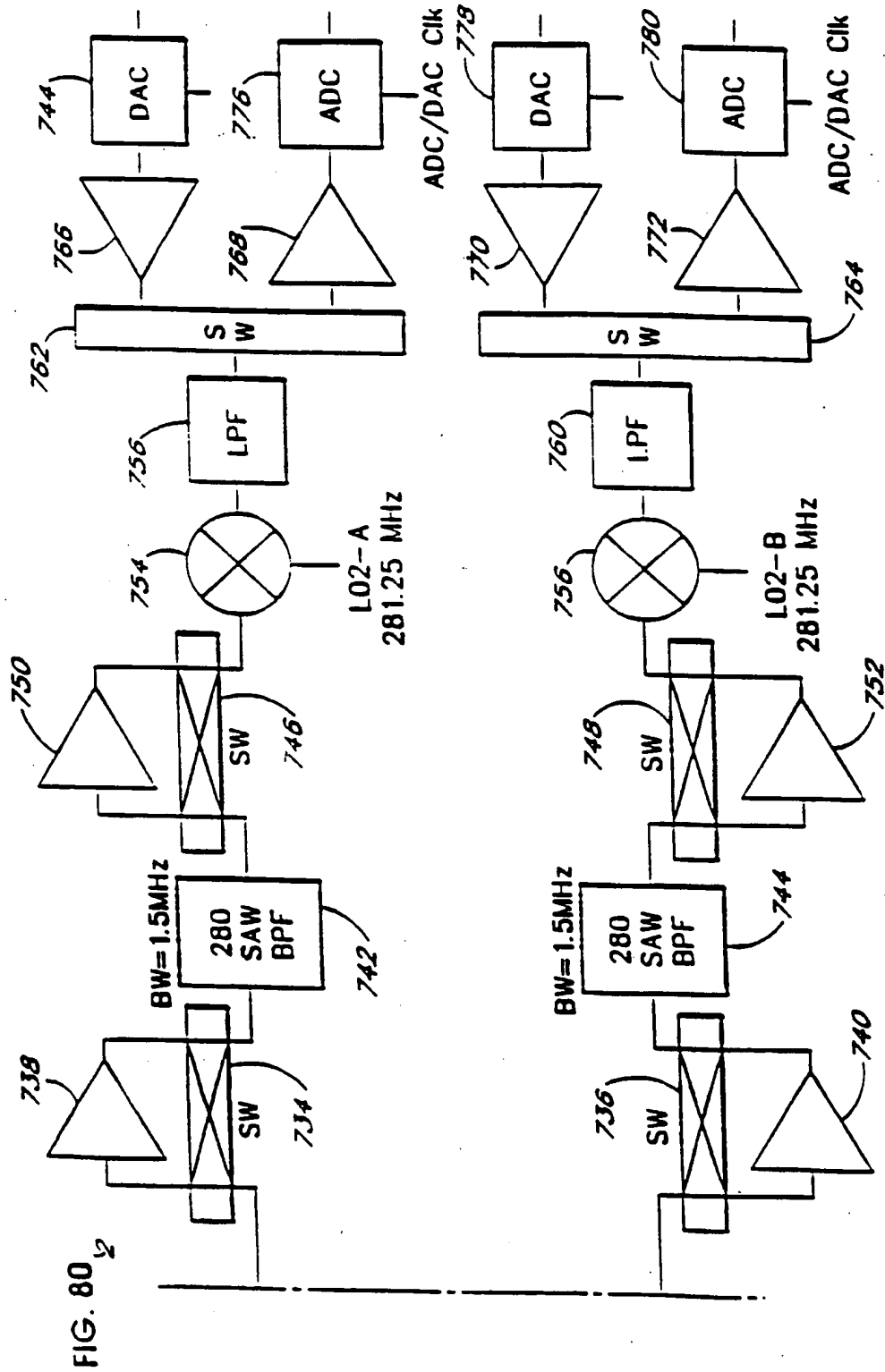
FIG. 80

FIG. 80A

FIG. 81₁

FIG. 81₂

FIG. 81

FIG. 81

FIG. 81A
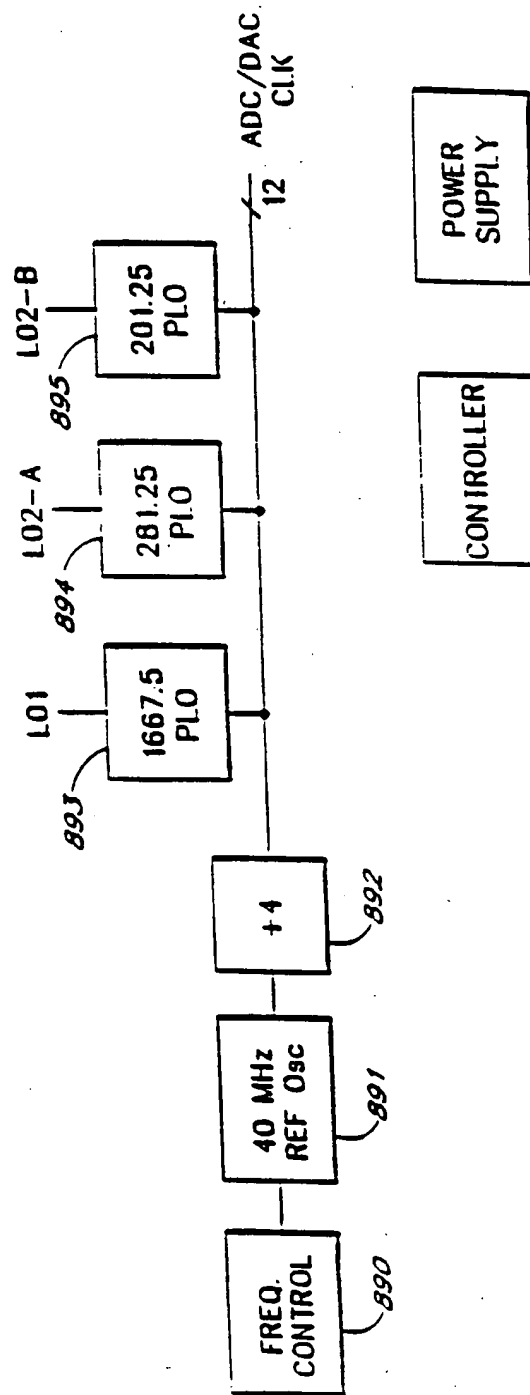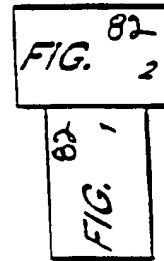
FIG. 82

FIG. 82 2

FIG. 83

FIG. 84A

BASE STATION

FIG. 84B

To DSP

Compute T Matrix

$R_x(p)T(p) = R_x$

$p = 1, 2$

106

104

RMGS Autocorrelation

$R_{xx} = \sum X X^*$

$R_{xx} = U^* \Delta_x U_x = A^*_x R_x$

Initial: $\Delta_x = \sigma I \quad U_x = I$

118

RMGS Autocorrelation

$R_{xx}(p) = \sum \Delta_x(p) \Delta^*_x(p)$

$R_{xx}(p) = U^*_x(p) \Delta_x(p) U_x(p)$

$= A^*_x(p) R_x(p)$

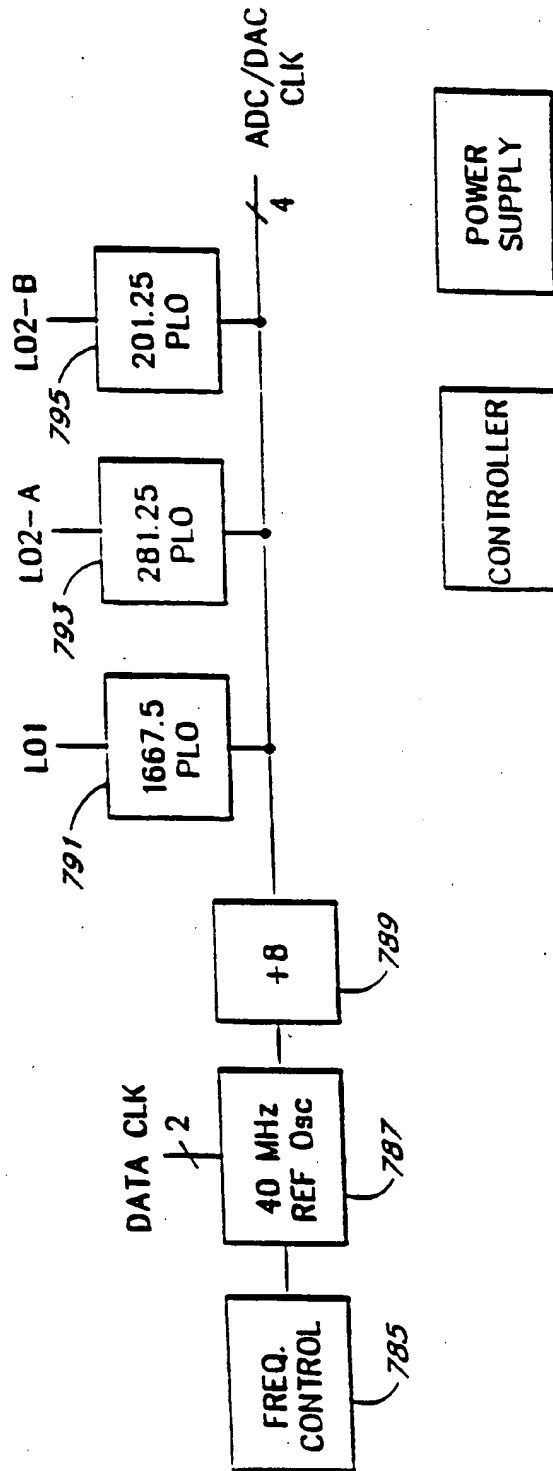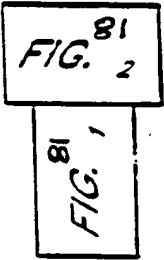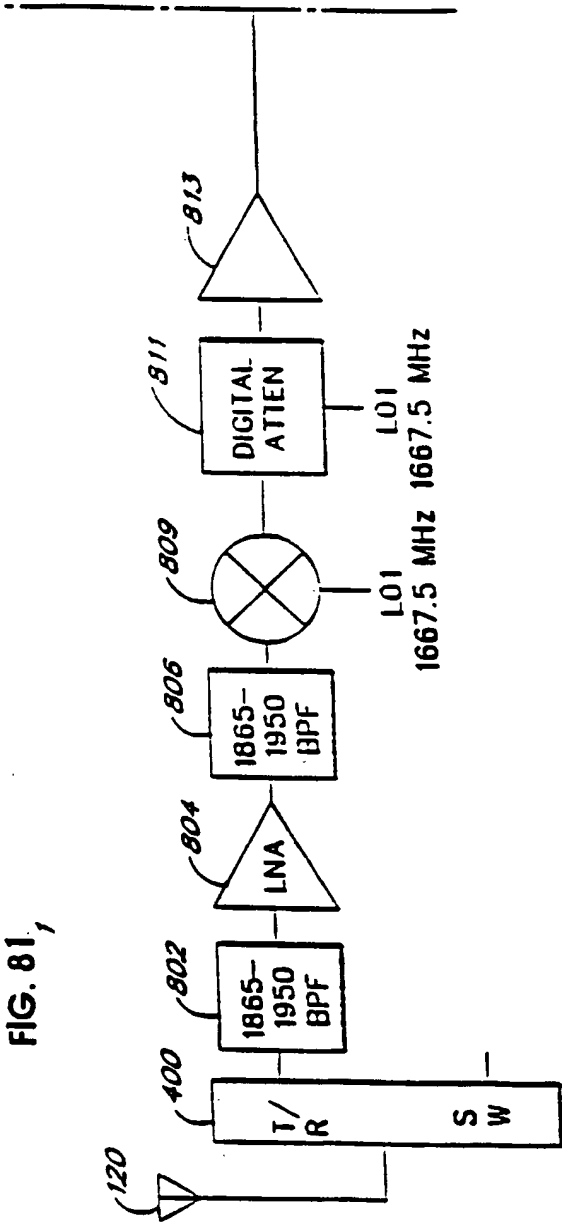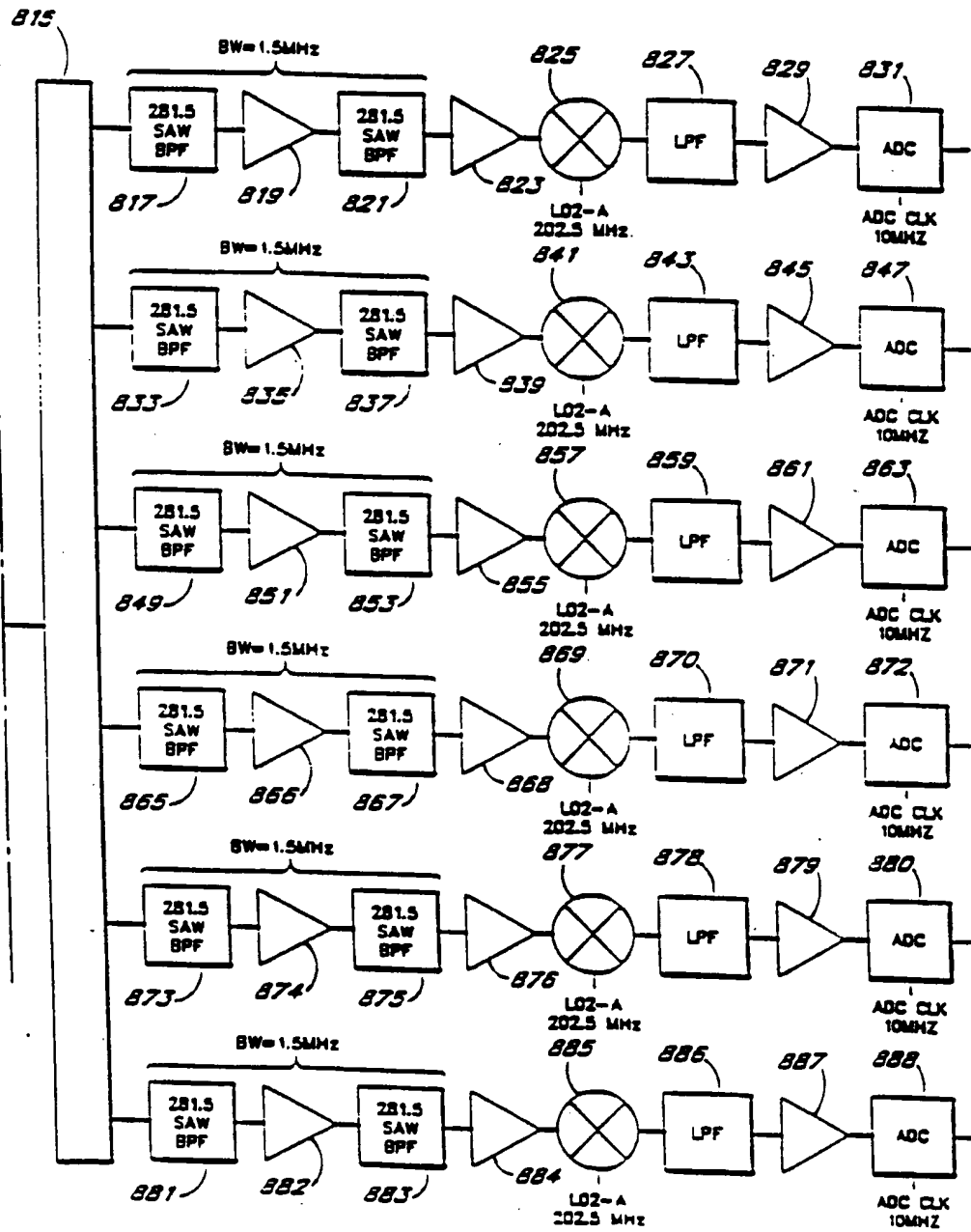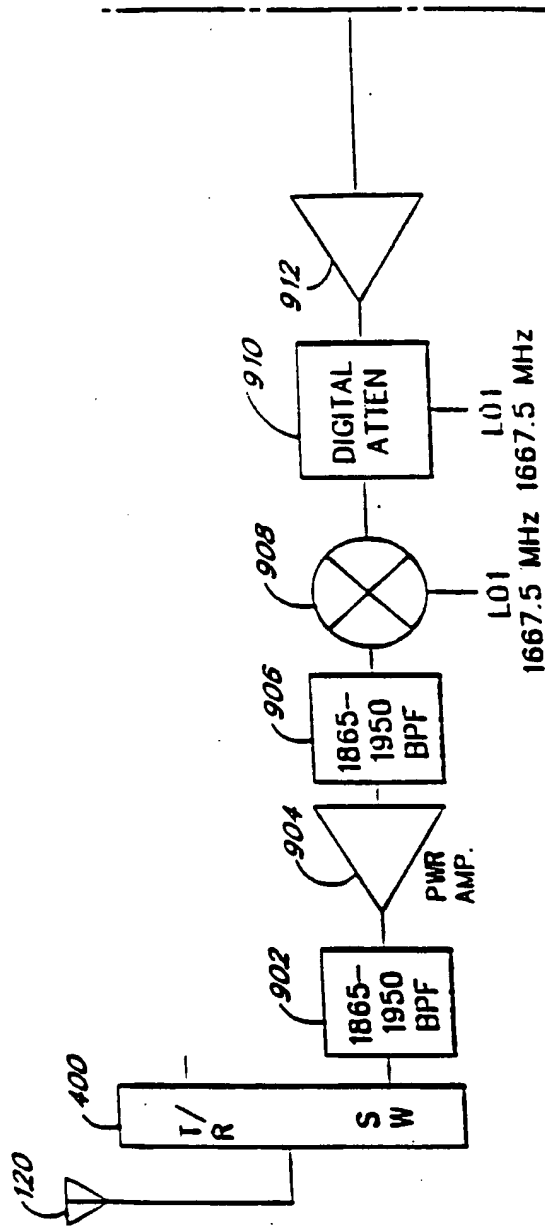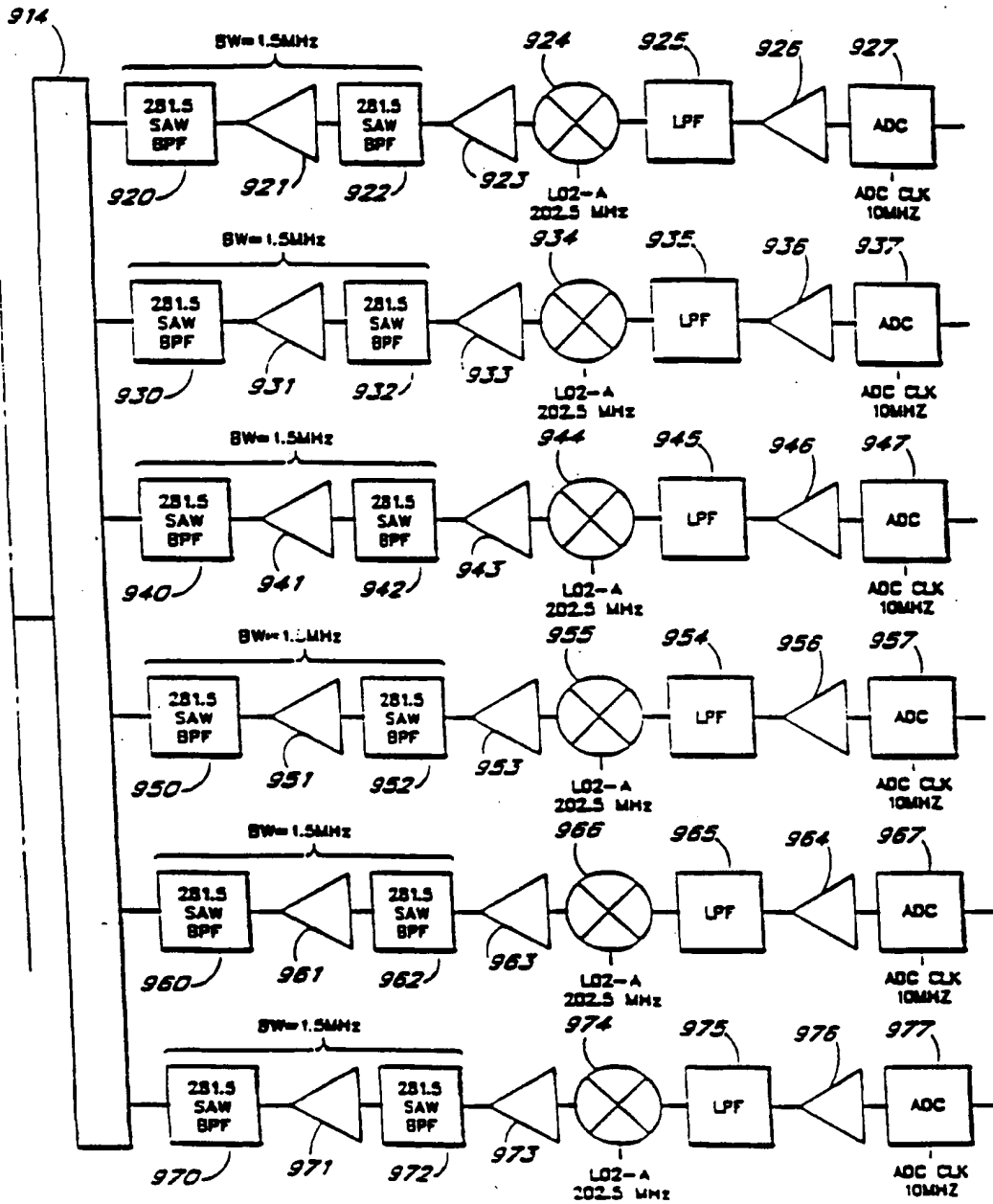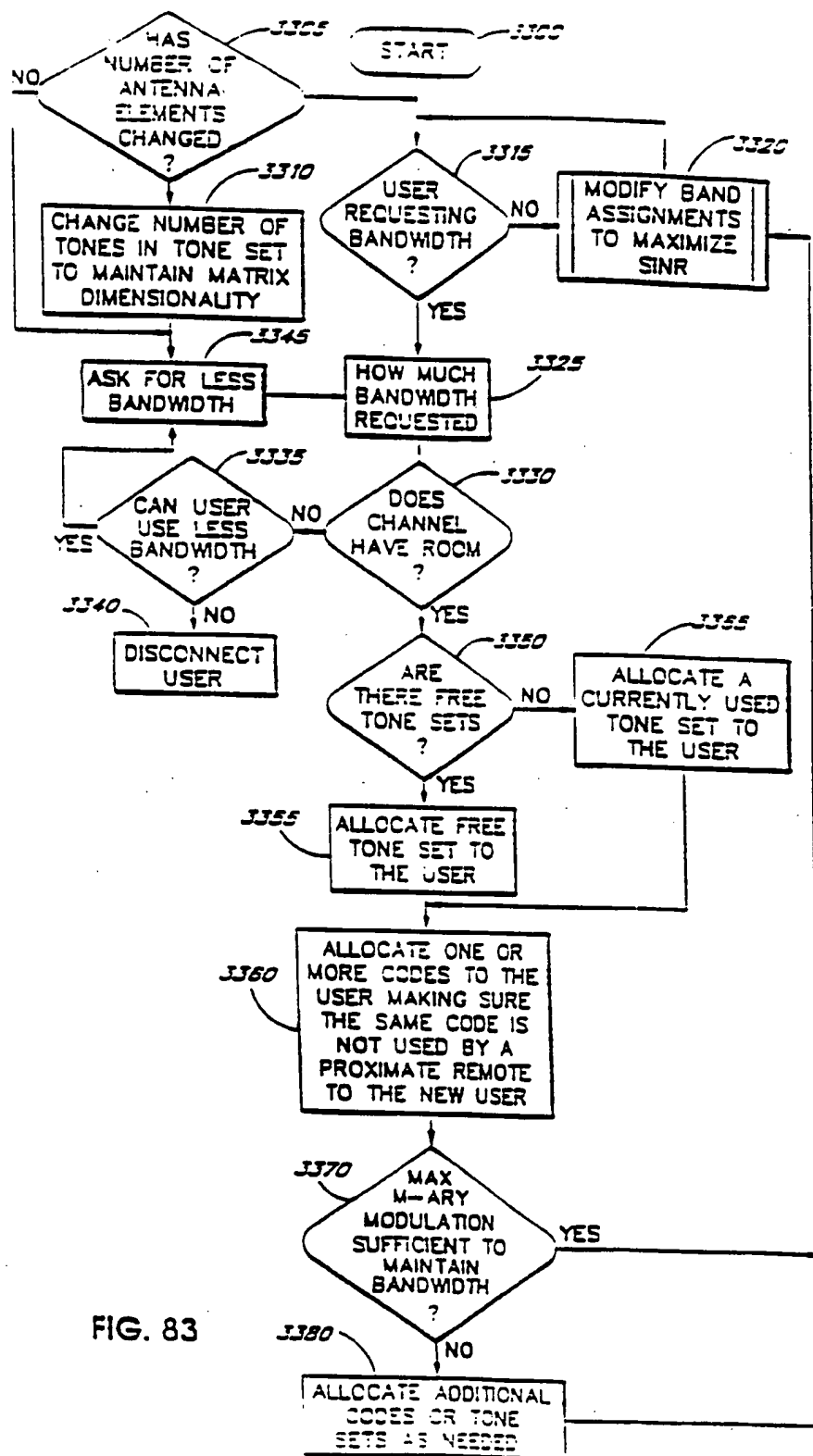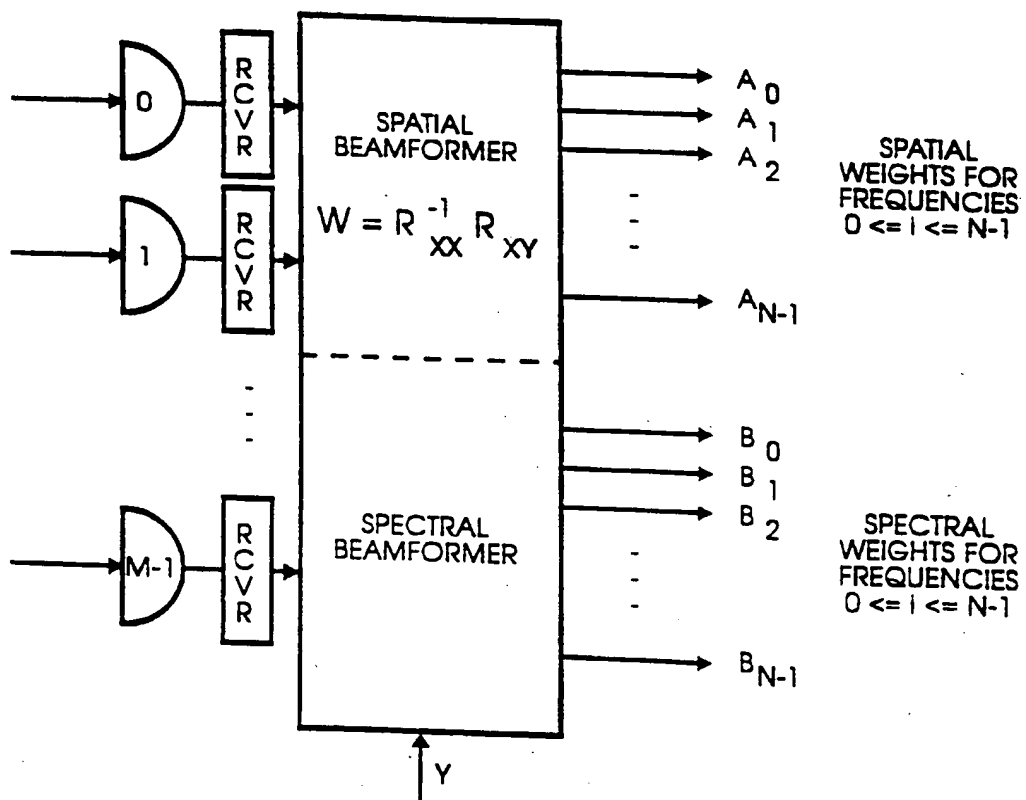Initial: $\Delta_x(p) = \sigma I \quad U_x(p) = I$

Subtract Emulated Packets

$\Delta_x(p) = X - Y_x(p)$

112

Select Ungated Packets

$X_i \quad i = 0, \ldots, 6$

108

from Input I/F
Total 2 CAC Channels to Process   102

X Vector   One of the two
Input   CAC Channel

$$X = \begin{bmatrix} z_{i,0}(0) & z_{i,0}(1) & \cdots & z_{i,0}(7) \\ z_{i,1}(0) & z_{i,1}(1) & \cdots & z_{i,1}(7) \\ \vdots & \vdots & & \vdots \\ z_{i,m}(0) & z_{i,m}(1) & \cdots & z_{i,m}(7) \end{bmatrix}$$

$i = 0, 1, \ldots, 15$

$$Y_x(p) = \begin{bmatrix} c_{i,0}(p)z_{i,max}(0) & c_{i,1}(p)z_{i,max}(0) & \cdots & c_{i,n}(p)z_{i,max}(0) \\ c_{i,0}(p)z_{i,max}(1) & c_{i,1}(p)z_{i,max}(1) & \cdots & c_{i,n}(p)z_{i,max}(1) \\ \vdots & \vdots & & \vdots \\ c_{i,0}(p)z_{i,max}(7) & c_{i,1}(p)z_{i,max}(7) & \cdots & c_{i,n}(p)z_{i,max}(7) \end{bmatrix}$$

110

Select i

$X_i \quad i = 7$

Apply Code Key

$Y_x(p) = C_i(p) \cdot X_i$

$i = 0, \ldots, 6$

114

$$C(p) = [C_0(p) \quad C_1(p) \quad \cdots \quad C_n(p)]$$

$$\begin{bmatrix} c_{0,0}(p) & c_{1,0}(p) & \cdots & c_{n,0}(p) \\ c_{0,1}(p) & c_{1,1}(p) & \cdots & c_{n,1}(p) \\ \vdots & \vdots & & \vdots \\ c_{0,k}(p) & c_{1,k}(p) & \cdots & c_{n,k}(p) \end{bmatrix}$$

116

CAC Code Key

$C(p), p = 1, 2$

From DSP

122

Select Ungated Packets

$X_i \quad i = 0, \ldots, 6$

from Input I/F
Total 2 CAC Channels to Process   120

X Vector   One of the two
Input   CAC Channel

$$X = \begin{bmatrix} z_{i,0}(0) & z_{i,0}(1) & \cdots & z_{i,0}(7) \\ z_{i,1}(0) & z_{i,1}(1) & \cdots & z_{i,1}(7) \\ \vdots & \vdots & & \vdots \\ z_{i,m}(0) & z_{i,m}(1) & \cdots & z_{i,m}(7) \end{bmatrix}$$

$i = 0, 1, \ldots, 15$

$$Y_x(p) = \begin{bmatrix} c_{i,0}(p)z_{i,max}(0) & c_{i,1}(p)z_{i,max}(0) & \cdots & c_{i,n}(p)z_{i,max}(0) \\ c_{i,0}(p)z_{i,max}(1) & c_{i,1}(p)z_{i,max}(1) & \cdots & c_{i,n}(p)z_{i,max}(1) \\ \vdots & \vdots & & \vdots \\ c_{i,0}(p)z_{i,max}(7) & c_{i,1}(p)z_{i,max}(7) & \cdots & c_{i,n}(p)z_{i,max}(7) \end{bmatrix}$$

124

Select Gated Packets

$X_i \quad i = 7, \ldots, 13$

Apply Code Key

$Y_x(p) = C_i(p) \cdot X_i$

$i = 0, \ldots, 6$

128

$$C(p) = [C_0(p) \quad C_1(p) \quad \cdots \quad C_n(p)]$$

130

CAC Code Key

$C(p), p = 1, 2$

From DSP